Active Driveline and Suspension Control to Improve Vehicle Handling

Nicholas James Cooper

Submitted in accordance with the requirements of the degree of Doctor of Philosophy

University of Leeds, School of Mechanical Engineering

September, 2006

Acknowledgements

I would like to thank my supervisor, Dr. Warren Manning, for all his help and guidance, especially due to the distance he had to travel to provide this supervision. I would also like to thank Professor David Crolla for providing the opportunity to come to the University of Leeds in the first place. I also want to thank Dr. Martin Levesley for taking over the administrative side of my supervision and providing help during the final stages of writing this thesis

A great contribution to my general welfare was provided by all the occupants who came and went from G54b. They provided a warm and friendly environment to work in and gave plenty of moral support and distractions to keep me going.

Finally I want to thank my family and friends who have provided endless support for me throughout, both morally and financially.

Publications

Cooper, N., W. Manning, et al. (2004). Study of the Integration of Roll Control and Torque Distribution. AVEC 2004, 7th Int'l Symposium on Advanced Vehicle Control, Arnhem, The Netherlands.

Cooper, N., W. Manning, et al. (2004). Integration of Active Suspension and Active Driveline to Improve Vehicle Dynamics. SAE Motorsports Engineering Conference and Exhibition, Dearborn, Michigan.

Cooper, N., W. Manning, et al. (2005). Integration of Active Suspension and Active Driveline to Ensure Stability While Improving Vehicle Dynamics. SAE 2005 World Congress, Detroit, Michigan.

Awards

"SAE 2005 Excellence in Oral Presentation Award", SAE 2005 World Congress

Abstract

This research focuses on the integration of roll moment distribution control and variable torque distribution control to improve vehicle handling and dynamics. A survey of the literature determines the current state of the art and directs the research toward undeveloped areas. The work is carried out with the racing environment in mind. The most promising control systems prove to be roll moment distribution and variable torque distribution. The control objectives are to both improve the driveability of the vehicle and ensure the stability. The driveability is measured by the ability to track a linear reference yaw rate. This aims to linearise the yaw rate response to the steering input and gives the driver predictable handling. Vehicle stability is determined by the sideslip behaviour of the vehicle, where the controllers aim to minimise the sideslip.

The testing is achieved by computer simulation. An eight degree of freedom non-linear vehicle model is developed to model the University of Leeds Formula Racing Car. Initially independent controllers are developed for both roll moment distribution and variable torque distribution to control the driveability and stability individually. The independent controllers are able to enhance the vehicle behaviour with respect to each of these goals. However, the roll moment distribution is more suited to the stability control while the variable torque distribution achieves the yaw rate tracking more effectively.

The independent controllers are combined to determine any interactions between them before a final integrated control strategy is developed. This integrated control strategy integrates the variable torque distribution driveability control and the roll moment distribution stability control to give a complete vehicle control strategy. The integrated controller shows improved yaw rate tracking as well as the ability to stabilise the vehicle at limit handling.

Table of contents

List of Figures and Tables

Nomenclature

a	distance from the centre of gravity to the front axle
A_f	frontal area
a_y	lateral acceleration
b	distance from the centre of gravity to the rear axle
C	control model
f	front (axle)
C_b	control boundary
c_{D_r}	coefficient torque distribution at the rear differential
c_I	integration controller coefficient
c_{K_d}	coefficient roll moment distribution
d_f	front scrub derivative
d_r	rear scrub derivative
D_ϕ	roll damping
e	error
E_{yaw}	sum of the absolute yaw rate error
F_x	longitudinal force
F_y	lateral force
F_z	vertical force
g	gravity
G	gain (controller)
h_a	height of the roll axis
h_{cf}	height of the front roll centre
h_{cr}	height of the rear roll centre
h_r	height of centre of mass above the roll axis
IR	suspension installation ratio

I_{xx}	roll moment of inertial
I_{xz}	roll-yaw inertial product
I_{zz}	yaw moment of inertial
I_{ω}	wheel rolling inertial
k	tyre longitudinal slip ratio
K	stability margin
K_{spring}	spring rate
K_{wheel}	wheel rate
K_{ϕ}	roll stiffness
$K_{antiroll}$	roll bar roll stiffness
$K_{\phi S}$	spring roll rate
$K_{\phi Tyre}$	tyre roll rate
m_b	body mass
m_f	front axle mass
m_r	rear axle mass
M_{tot}	total vehicle mass
P	plant model
r	yaw rate
R	reference model
r_{ω}	tyre rolling radius
t_f	front half track width
T_{in}	torque input
t_r	rear half track width
u	longitudinal velocity
$u_{desired}$	desired longitudinal velocity
u_{input}	input longitudinal velocity
u_0	initial longitudinal velocity
v	lateral velocity
α	tyre slip angle

β	body sideslip angle
Δ	difference/change in
δ_f	front axle steering angle (at the wheels)
ϕ	roll angle
μ	tyre/road friction coefficient
ρ	density of air
τ	time constant
ω	angular wheel velocity

Subscripts

cb	control boundary
d	derivative
f	front (axle)
fb	feedback
ff	feedforward
fl	front left (tyre)
fr	front right (tyre)
i	integral
inv	inverse
p	proportional
r	rear (axle)
ref	reference
rl	rear left (tyre)
rms	root mean square
rr	rear right (tyre)
x	longitudinal
y	lateral
z	vertical

Abbreviations

4WD	four wheel drive
ABS	anti-lock braking system
CG	centre of gravity
CVT	continuously variable transmission
FIA	Fédération Internationale de l'Automobile
IM	internal model (control)
LSD	limited slip differential
PID	proportional, integral, derivative (control)
RMD	roll moment distribution
SAE	Society of Automotive Engineers
SM	sliding mode (control)
TCS	traction control system
VDC	vehicle dynamics control
VTD	variable torque distribution

1. Introduction

Chapter 1 presents the introduction and background to this research. Vehicle dynamics controls are introduced along with the systems they operate on. The control evaluation methods are described before the aims and objectives of the research are stated. The chapter concludes with a brief summary and description of the contents of this thesis.

1.1. Background to Vehicle Dynamics Control

Advanced vehicle dynamics controls are becoming more common in automobiles. Initial controllers included anti-lock brakes and brake based active yaw controls. Now many more advanced vehicle dynamics controls are available. These include active steering and active suspension as well as active drivelines. All these control systems and strategies have different effects on the vehicle dynamics. Most are designed to promote safety and vehicle stability in evasive manoeuvres but they have different methods of creating the active control.

With all these systems available, current research is aimed at integrating all the active control systems into one package that creates a total vehicle dynamics control strategy. This research aims to create an integrated control strategy. The advanced controllers need to be effective under all vehicle operating conditions in the most demanding environments. The most demanding area of automotive operation is in racing. Racing cars are constantly being pushed to their limits and the performance requirements are very severe. Not only do the racing cars have to remain stable and on the track, but they have to extract every ounce of speed and handling performance available up to the absolute vehicle limit.

The active control systems in this research are developed with the racing environment in mind. The controllers will aim to expand the usable vehicle performance envelope and also maintain vehicle stability. To develop the controllers, they are simulated using vehicle models in MATLAB. This enables a quick development process and does not present the risks and dangers associated with real vehicle testing at the handling limits. The vehicle modelled is the University of Leeds

Formula Racing Car shown in Figure 1.1. The racing car is a high performance, single seat racing car that is designed and built by students at the University of Leeds. The car is used for the Formula SAE and Formula Student competitions in the USA and England each year. The data for the vehicle model was provided by the PhD research of Siegler [Siegler, 2002].

Figure 1.1 University of Leeds Formula Racing Car

In an actual vehicle, the driver is an integral part of the vehicle system and its dynamics. The driver affects the vehicle dynamics through the accelerator, brake pedal and steering wheel. These inputs are used to follow the desired path and maintain vehicle stability. The driver creates a closed loop system with the vehicle by determining the steering and pedal inputs from the observed vehicle dynamics. This is a very complex system which would require modelling human reactions to fully describe. Modelling human behaviour in this way is beyond the scope of this research. Instead, this research uses on an open loop system without modelling the driver reactions. The driver inputs are defined to give predetermined manoeuvres without feedback from the vehicle dynamics. This allows the results of the vehicle dynamics controllers to be observed without the interference from the dynamics of a driver model.

1.2. Application of Advanced Vehicle Dynamics Controls in Motorsport

Motorsport is the most demanding environment for vehicle performance. Racing teams are constantly trying to squeeze out any extra ounce of performance from their racing cars. Even small increases in performance lead to faster lap times which all add up at the end of a race. There are three main categories of racing cars: open-wheeled single seat racing cars like in Formula 1, production based saloon car racing like the British Touring Car Championships, and production based off road racing cars like the World Rally Championships. Each field of racing comes with its own different set of challenges. Formula 1 is arguably the most technologically advanced racing series with millions of pounds spent every year on researching new technology. The result of all the technology is increased speed. However, in the interests of safety, and more recently spectator interest, many restrictive rules have been introduced. A good example of this is active suspension. Active suspension gave a massive advantage to Nigel Mansell in his campaign for the 1992 championship. The FIA promptly banned active suspension as an unfair advantage and to limit the speed of the racing cars and promote safety. Formula 1 teams still spend enormous amounts of money researching new technologies but they are highly limited in what they can legally use and this rules out most advanced chassis control systems.

Saloon car racing by comparison has restrictive rules to limit and equalise the performance of the cars. The intentions of the restrictions are to allow the best driver to win and to prevent a team from "buying" the championship by simply spending money on exotic technologies that are out of reach for most teams. As a result, most teams have relatively small budgets and can not afford and are not allowed to have advanced vehicle dynamics control systems in the saloon racing cars.

Rally car racing lies in its own interesting position regarding regulations. Rally races are mostly run off-road on rough, low-grip surfaces. In addition to the off-road nature of the races, they run on special stages that the drivers only get to drive a limited number of times. The result being that, unlike Formula 1, where tenths and hundredths of a second can be the difference between winning and losing, driver consistency provides much more variability in stage times. Linked with the natural variability of the drivers is the fact that due to the low-grip environment, advanced control systems do not produce such obvious advantages that are not compensated for by the stage variability. With the relatively small gains available from advanced

control systems, vehicle speeds are not boosted to unsafe speeds, but a clear advantage can be gained over rival teams through the use of a well implemented control system. On the engineering development side, these off-road surfaces make it extremely difficult to define the vehicle state because of the very high frequency tyre load variations and the large sideslip angles and slip ratios that the tyres are operating under. It is extremely difficult to quantitatively simulate and design control systems to operate in such unknown conditions. As a result most control systems used on rally cars are designed to be subjectively tuned through testing.

The Formula SAE/Student competition does not prevent active control systems. The rules are in place to ensure safety, not to limit the technology or creativity of the design. However, due to the limited resources of the universities, not many teams use active control systems. Another consideration for vehicle dynamics control in Formula SAE/Student competition is the driver skill level. The drivers are all students and not many have professional racing experience. Providing a predictable racing car that is easy to drive is of great importance to give the drivers confidence. Therefore a well implemented vehicle dynamics control can give a competitive racing advantage as well as additional points in the design judging.

Like other developments in motorsport, any vehicle dynamics controls developed for the Formula SAE/Student racing car can be used in passenger cars. Even if the active controllers are not directly transferable, the research and development of the control algorithms and strategies can be used to aid the development of passenger vehicle control systems. Although the environment in which passenger vehicles operate is very different from that of racing cars, the objectives are still similar. In both cases it is desirable for the vehicle to have predictable, stable handling.

1.3. Advanced Vehicle Dynamics Control Systems

Vehicle dynamics controls are designed to improve the performance and stability of vehicles. They can be categorised by the systems they work on. The four main systems are the brakes, steering, driveline and suspension. The following is a brief overview of these four categories of controls.

1.3.1. Brakes

Active braking systems were the first active chassis controls to be developed and, due to the large influence they can have on vehicle behaviour, lots of research has been published on this subject. In the late 1970's ABS brakes were first offered on some luxury cars. ABS braking systems are brake control systems designed to maintain vehicle stability during braking by modulating the brake pressure to prevent wheel lockup. More recently dynamic yaw control systems have been developed to maintain vehicle stability by using the brakes to create yaw moments. An example of dynamic yaw control can be considered for a vehicle oversteering in a corner. The control system can monitor yaw rate, or a similar signal like body sideslip angle. When the control detects that the yaw rate is too high and the vehicle is oversteering, a contra-cornering yaw moment can be induced by the brakes. This can be done by applying the brake to the outside front wheel, as shown in Figure 1.2.

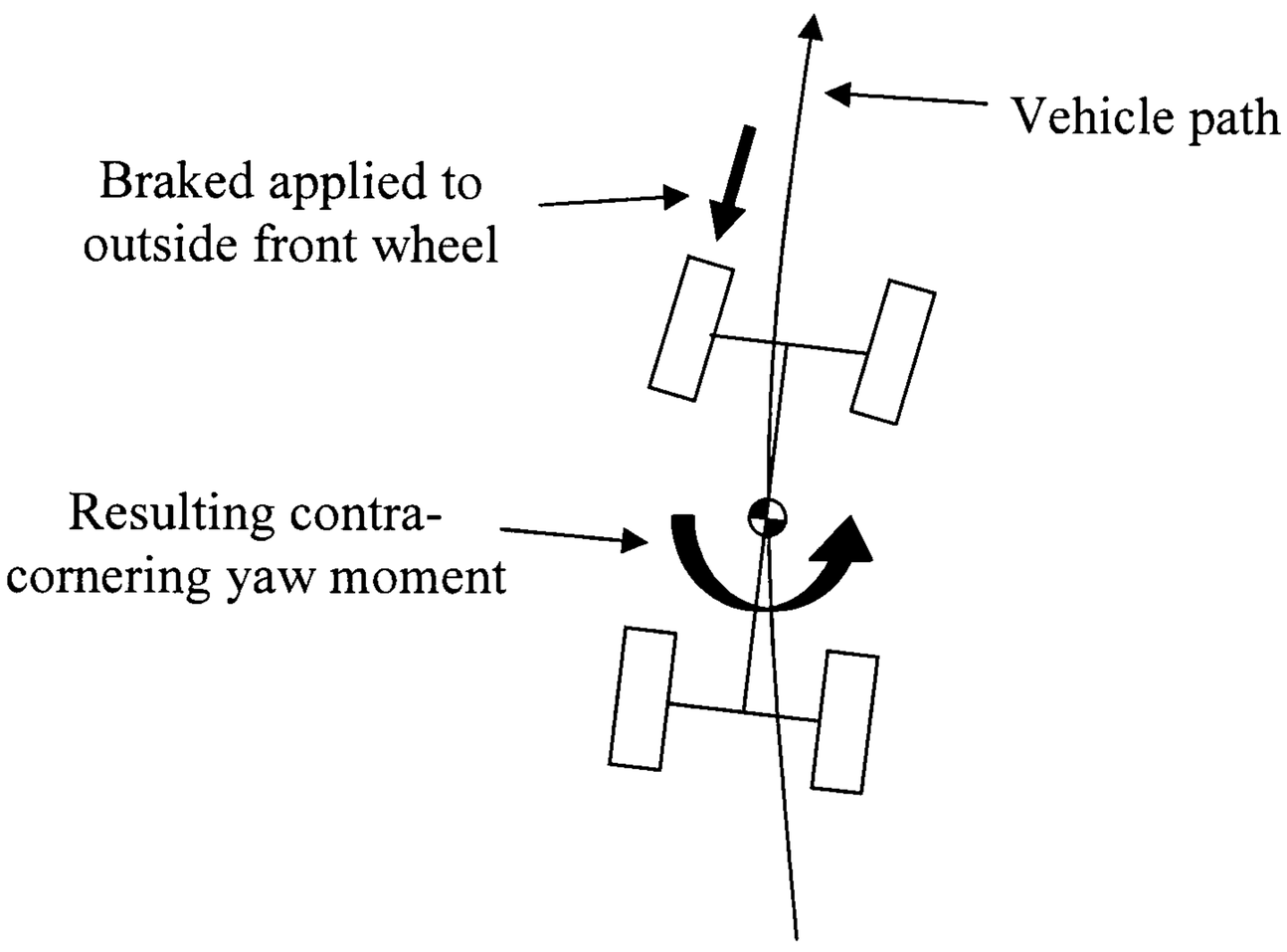

Figure 1.2 Brake based yaw control of an oversteering vehicle

Applying the brake in this situation has the combined effect of slowing the vehicle down as well as inducing the contra-cornering yaw moment. This can sometimes be tolerated in a passenger car but generally the resulting loss of speed is intrusive to the driver. In a racing car, loss of speed and the application of the brakes are definitely not desirable at all. For this reason, racing cars do not provide a good platform for vehicle stabilising controls based on braking systems.

1.3.2. Steering

Steering controls include active front steering and four-wheel steering. Active front steering is the control of a front steer angle that is additional to the inputs by the driver. A common example of active front steering is with an understeering vehicle. The controller determines the driver's desired path by measuring the driver inputs, e.g. steering wheel angle and vehicle speed, and compares a calculated yaw rate to the actual yaw rate. In an understeering vehicle the desired yaw rate will be greater than the actual yaw rate so the controller can actively augment the drivers input and add more front wheel steering angle to make the vehicle reach the desired yaw rate. Four-wheel steering uses active steering of the rear wheels as extra available inputs for the controller and can include either passive or active front steering. An example of four-wheel steering is to reduce the turning radius at low speed. At low speeds, the rear wheels can be steered in the opposite direction to the front wheels. The result is a very tight turning radius that aids the driver in tight parking manoeuvres. At high speeds, four-wheel steering can help reduce vehicle body sideslip angle in lane change manoeuvres. At motorway speeds the rear wheels can be steered in the same direction as the front wheels. This reduces the sideslip angle of the vehicle body and promotes vehicle stability.

Active steering is very effective during low-g manoeuvres when the tyres are well within their traction limits. However, as tyres approach saturation during high-g manoeuvres, their ability to create additional lateral forces greatly diminishes. However, since racing cars are constantly operating at the limits of their capabilities, active steering is not such a good choice for a motorsport application.

1.3.3. Driveline

There are two main types of driveline control that relate to vehicle handling. These are engine management systems and torque distribution systems. An example of an engine management system is traction control. Traction control is very similar to ABS except that it works during acceleration instead of braking. Like ABS, traction control monitors wheel slip, but during acceleration. If wheel slip is detected the control system reduces the power output of the engine. This can be done by reducing the throttle angle, limiting the fuel supply or selectively miss-firing spark plugs. This system is currently used in Formula 1 for launch control but is likely to be banned in

the near future. Although engine management systems are very effective, they do not directly affect the handling balance of the vehicle. Another problem is that the controller is taking power from the vehicle which is not an optimal solution. A more effective solution is to distribute the available power to the wheels in the most efficient way possible.

Torque distribution systems are control systems that can actively distribute power to the wheels. A major benefit over engine management systems is the ability to introduce yaw moments. Like dynamic yaw controls that use the brakes to stabilise vehicles during cornering, torque distribution systems can create yaw moments by changing the torque balance at the wheels. Consider the example of the oversteering vehicle that was discussed in Section 1.3.1. It can be seen that the vehicle can be stabilised without the penalty of reduced speed. Instead of applying the brakes, torque can be transferred from the outside wheel of the front axle and added to the inside front wheel, as shown in Figure 1.3. This would result in a contra-cornering yaw moment and stabilise the vehicle without changing the energy used to propel the vehicle forward.

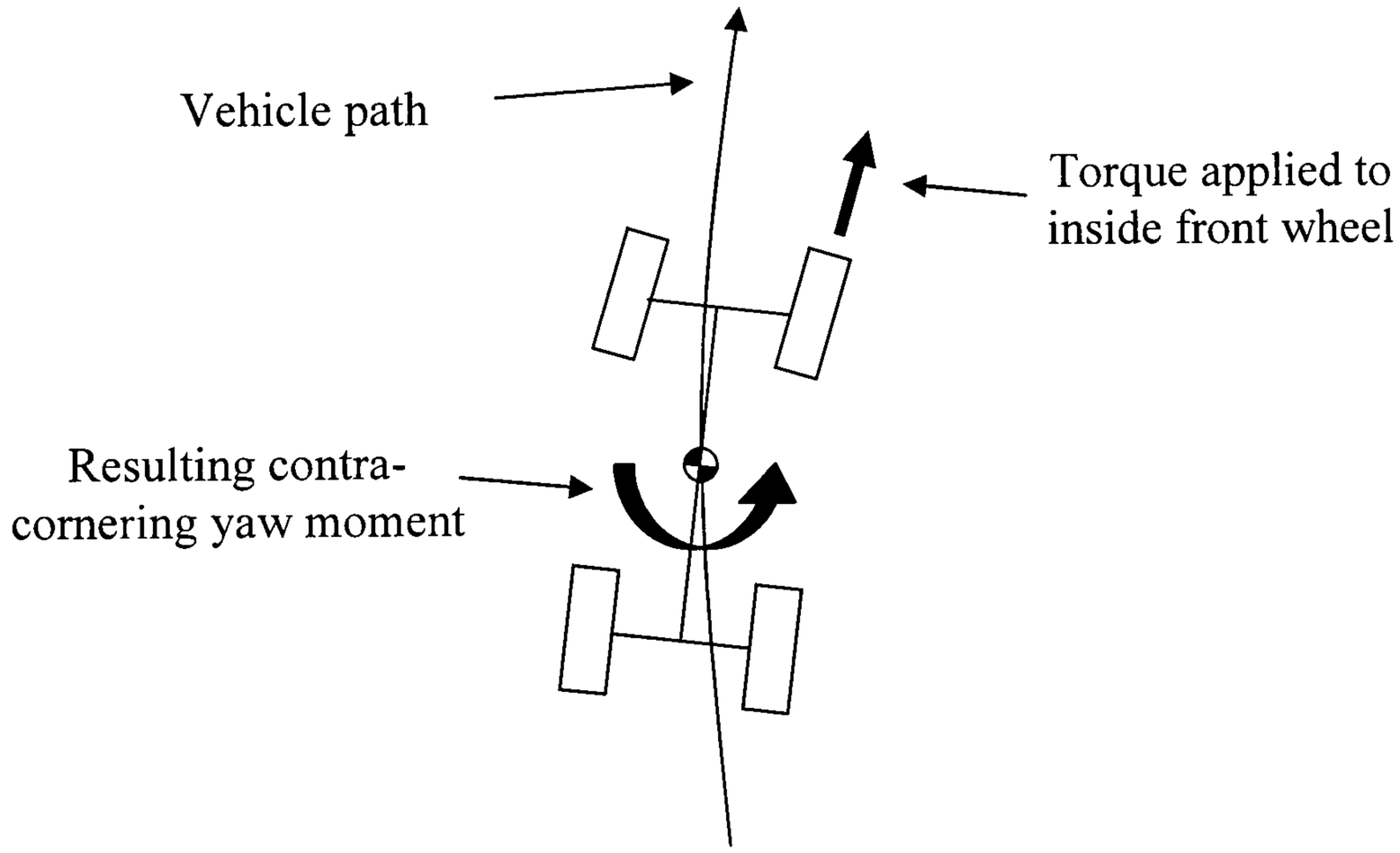

Figure 1.3 Driveline based yaw control of an oversteering vehicle

The only issue with torque distribution systems is that care must be taken not to adversely affect the lateral tyre dynamics by introducing longitudinal forces that can saturate the tyres. Also, there has to be torque input from the engine. If the interactions between the lateral and longitudinal tyre dynamics are considered, torque

distribution systems are well suited to racing cars since they can induce yaw moments without reducing vehicle speeds.

1.3.4. Suspension

Active suspension systems control the vertical wheel loads to enhance the ride and handling of vehicles. These systems have already received lots of attention in the racing environment. As mentioned in Section 1.2, the Williams Formula 1 team implemented active suspension in the 1992 season and won the championship. However, since it was considered an unfair advantage and speeds were becoming unsafe it was promptly banned. The technology developed in racing has filtered down in to consumer cars. By controlling the vertical wheel loads the attitude of the vehicle can be kept almost constant, practically eliminating heave, roll, and pitch. This results in very comfortable ride characteristics. Another effect of controlling wheel loads is improved handling. Since the ability of the tyres to create lateral and longitudinal force is proportional to the vertical load, the control system can distribute the vehicle load between the wheels to create the optimal lateral and longitudinal forces at each wheel. The disadvantage of a fully active suspension is the energy that the system requires. Active suspension systems use hydraulic actuators in place of conventional springs and dampers. For the system to work effectively the actuators have to be capable of creating large wheel displacements very rapidly. This of course requires a lot of energy and makes the system very expensive to add to passenger cars. In the racing environment cost is not as much of a problem as it is in consumer cars. The main difficulty is bypassing regulations against active suspension systems.

It has been found that most of the handling benefits of active suspension are found at low frequencies. Low bandwidth slow-active suspensions have been developed that do not have the energy requirements and associated costs of high frequency, fully active suspension. Slow-active suspension systems do not use high power, fast acting actuators and as a result are not able to react quickly to a rough road surface for ride comfort. However, they are able to react to load transfer. A common active suspension is load levelling suspension. This system usually controls the rear suspension to keep a vehicle level irrespective of the loading condition. Load levelling suspension has a fairly limited effect on vehicle handling. A more versatile slow-active suspension is active roll control. This system aims to eliminate body roll

during cornering. Body roll can be eliminated by actively controlled anti-roll bars or hydraulic actuators inline with a conventional suspension system. Either of these systems can transfer load from one side of an axle to the other. The benefit of active roll control is a subjective improvement in vehicle ride during cornering. To actually improve the vehicle handling in a roll control system, the roll moment must be actively distributed.

Roll moment distribution exploits the non-linear relation between vertical wheel load and lateral traction force. If there is a large load transfer across an axle the resulting ability to create lateral force will be less than if the load was evenly distributed. Using this concept an oversteering vehicle can be brought to a more neutral steering attitude in the following way. If the roll moment of the oversteering vehicle is transferred to the front there will be a greater load transfer at the front axle than the rear axle, as shown in Figure 1.4. This will result in the ability to generate lateral force being reduced at the front axle, due to larger lateral load transfer, while it is increased at the rear axle resulting in less oversteer.

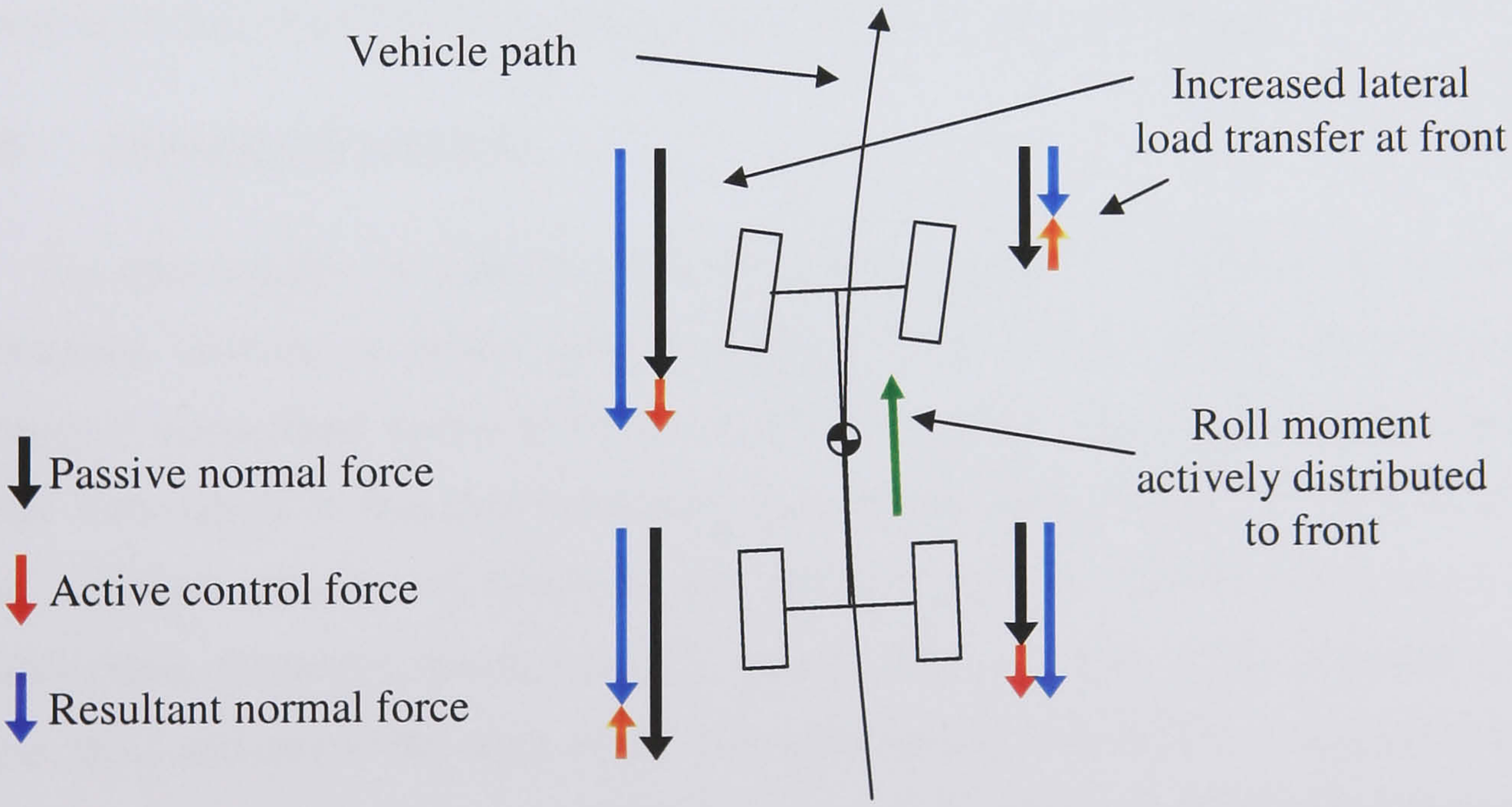

Figure 1.4 Active roll moment distribution in an oversteering vehicle

Roll moment distribution requires large lateral accelerations which are found during high-g manoeuvres. This makes it a good choice for the racing environment. It is also a subtle method of control that is more likely to be accepted by racing regulations than the high bandwidth, fully active suspension systems.

1.4. Control Integration

There are two types of control integration. The first is integrating controllers with similar goals to work together to achieve one common goal. For example, an integrated control can be developed with a brake based system and active suspension integrated together as a stability control. The purpose of integrating controllers in this way is to increase the effectiveness of the whole control system. This can involve increasing the operating range over which the controller is effective, increasing the ability of the control to affect the vehicle dynamics or providing an opportunity to optimise the control by giving the design engineer multiple systems to chose from. An example of optimisation would be minimising the required control actuator energy.

The second type of integration is the integration of controllers with different goals. For example, integrating a stability control with a driveability control. These two controllers aim to achieve different goals yet interact through the vehicle dynamics. The role of the integration strategy is to reinforce the positive interactions while minimising the negative interactions. This research will confront both types of integration task to provide an overall vehicle dynamics control strategy.

1.5. Controller Evaluation

The effectiveness of control systems must be evaluated by comparing the actively controlled vehicles to similar passive vehicles. Most control systems are tested in computer simulations before prototype vehicles are built. The designer must decide what manoeuvres to simulate to evaluate the vehicle. Most manoeuvres can be split into constant velocity manoeuvres and manoeuvres that include acceleration or deceleration. Common constant velocity manoeuvres are steady state cornering, step steer input and sinusoidal steer input. The same manoeuvres can be simulated while accelerating or decelerating. In addition to this, these manoeuvres can be performed on low friction or split friction surfaces.

The control strategies will be evaluated by simulating these manoeuvres with the driver in an open loop system. The results of these manoeuvres will be used to evaluate how well the controllers manage to follow the drivers desired vehicle path as well as describing the stability of the vehicle. The ideal controller would be able to precisely follow the driver's demands while maintaining vehicle stability. Of course the driver may demand a path that the vehicle is physically unable to follow. In these

cases the extent the controllers manage to keep following the drivers demands while maintaining stability is considered.

1.6. Aims and Objectives

The motivation behind this research is to expand the knowledge of active vehicle dynamics control. There has been a great deal of work already published on independent controllers and now the focus has turned to the challenge of integrating these independent control systems. The integration of roll moment distribution and variable torque distribution has not seen much research, yet it promises to be a powerful combination. The other facet of this research is the inclusion of the longitudinal dynamics in the control goal to track the drivers desired dynamics. Many vehicle dynamics controls are focused on maintaining vehicle stability at the expense of the longitudinal velocity and desired vehicle motion. This research aims to create a control strategy that preserves the drivers desired dynamics while maintaining the vehicle stability.

Unfortunately, the limited resources available for this research prevent actual vehicle testing. The results are obtained from vehicle simulations in the MATLAB/Simulink environment. There are inherent compromises involved in computer simulations. The computing capacity and simulation times require a model that includes all the critical vehicle dynamics while ignoring unrelated dynamics. Unfortunately, the vehicle system is a highly non-linear system that operates over a wide range of conditions. This requires a complex model, especially the tyre model. Although vehicle modelling at all levels of complexity has been well documented in the literature, many control algorithms require a simple or even linear model. Describing the control actuation, especially roll moment distribution which relies on the non-linear behaviour of the tyres, with a simple model may create some difficulties.

The aim of this research is to develop and simulate a control system to improve the driveability of a racing car while ensuring stability. The contribution is the integration of roll moment distribution and variable torque distribution to expand the performance envelope while tracking the drivers demands including both the lateral and longitudinal dynamics.

The following are benchmark objectives:

- Build a validated vehicle model. This will involve verifying results against current work in the Vehicle Dynamics group at the University of Leeds.
- Create drivability controls for variable torque distribution and roll moment distribution.
- Create stability controls for variable torque distribution and roll moment distribution.
- Develop combined drivability and stability controllers for torque distribution and roll moment distribution.
- Propose and evaluate fully integrated, multi-objective, drivability and stability controllers for torque distribution and roll moment distribution.

1.7. Thesis Outline

This thesis follows the following outline:

- Chapter 2 presents a critical review of the literature. The first section reviews the state of the art of roll moment distribution while the second section reviews torque distribution. Combined roll moment and torque distribution controllers are reviewed next before a summary of the literature is given. The chapter ends with a restatement of the aims and objectives of this research, obtained from reviewing the literature.
- Chapter 3 presents the vehicle modelling and validation. The level of model complexity required by the research is presented before a full eight degree of freedom model is developed in the MATLAB/Simulink environment. This model is validated against CarSim, a commercial vehicle dynamics package.
- Chapter 4 presents the vehicle dynamics control algorithms. The different control algorithms used in this research are described presenting their merits and disadvantages.
- Chapter 5 presents the independent controller tuning. Each control algorithm presented in Chapter 4 is developed into an independent controller for roll moment distribution driveability and stability control and variable torque distribution driveability and stability control. The gain selection and tuning process is described and presented for each independent controller.

- Chapter 6 presents a comparison of the independent controllers. All the independent driveability controllers are compared and all the independent stability controllers are compared to evaluate which controllers perform the best as driveability and stability controls. The chapter concludes with a comparison of combined controllers created from the most effective independent controllers.
- Chapter 7 presents the development and results of the multi-objective integrated control strategy. An initial integrated control strategy developed for a paper presented at the 2005 SAE World Congress is presented [Cooper, 2005]. A final integrated control strategy is developed and compared to the initial strategy as well as the passive vehicle and independent controls
- Chapter 8 presents the final conclusions of this research and concludes with recommendations for areas of future research.

2. *Literature Review*

Chapter 2 presents a critical review of the literature. The first section reviews the state of the art of roll moment distribution while the second section reviews torque distribution. Combined roll moment and torque distribution controllers are reviewed next before a summary of the literature is given. The chapter ends with a restatement of the aims and objectives of this research, obtained from reviewing the literature.

2.1. Roll Moment Distribution Control

High bandwidth, fully active suspensions have proved very successful in the racing environment, however they require large amounts of energy and expensive hardware. More economic active suspension systems are active roll bars that are used in roll control and roll moment distribution. Roll control aims to limit or prevent body roll. Non-rolling vehicles perform better in ride and it is generally accepted that they subjectively have better handling [Sharp, 1992]. The reasons for the handling benefits are unclear, however benefits from roll control might be realised in the suspension design. Sharp suggests that if the vehicle does not roll, the suspension geometry and kinematics can be simplified and optimised to operate around the zero roll position. However, a more sophisticated control, on which this thesis concentrates, is roll moment distribution. Roll moment distribution has been shown to affect the handling of a vehicle through oversteer/ understeer balance, which makes it more beneficial in the racing environment.

Roll moment distribution takes advantage of the load transfer during cornering due to lateral acceleration and the non-linear characteristics of tyres. Considering a single axle during straight driving, if the centre of gravity is on the central longitudinal axis then the vertical load distributed on each tyre of the axle will be equal. As the vehicle corners the lateral load transfer will take load from the inside tyre and transfer it to the outside tyre. Since the amount of lateral force available from a tyre is non-linear with respect to the vertical load, the outside tyre will gain less lateral traction force than the inside tyre loses. The result is a relative reduction in the total available lateral traction force from the axle. Anti-roll bars affect the amount of

load transfer across an axle. The stiffer the anti-roll bar the more load is transferred across the axle.

If both axles are considered together, anti-roll bars can change the understeer/oversteer balance of the vehicle by introducing yaw moments. Consider a vehicle equipped with an anti-roll bar on the front axle. During cornering there will be a large load transfer across the front axle and only a small load transfer across the rear axle. The result will be a relative loss of lateral traction force at the front axle. This loss of lateral force at the front axle will result in a contra-cornering yaw moment and an understeer behaviour for the vehicle. The front of the car will drift wide from the corner, or to keep the same path, larger slip angles would be required to compensate for the reduced lateral force. The reverse is true as well. If the anti-roll bar is equipped on the rear axle there will be a large load transfer across the rear axle during cornering resulting in a relative loss of lateral force at the rear causing a pro-cornering yaw moment and oversteer.

Roll moment distribution is actively controlled by changing the roll stiffness at each axle. The two common methods of varying the roll stiffness are active anti-roll bars and active suspension. Both of these systems are applied as low bandwidth, slow acting systems which limits the amount of energy they consume, especially compared to full active suspension. The active suspension systems commonly proposed for roll moment distribution are slow-active hydro-pneumatic systems not the high energy consumption systems used in fully active suspension. These systems generally consist of springs inline with hydraulic pistons at each wheel that can directly vary the load on each wheel with cutoff frequencies around 0.5 Hz [Cech, 2000]. For anti-roll bar based systems there are two common methods to create an active anti-roll bar. The first method is to split an anti-roll bar in the middle and insert a rotary actuator. This rotary actuator would twist the ends of the anti-roll bar relative to each other to transfer the load from one wheel to the other. The second method to create an active anti-roll bar is to place a linear actuator between the anti-roll bar end and the wheel arm. Cech shows that a single actuator on an anti-roll bar would enable load to be transferred across the axle.

2.1.1. Roll Angle Control

A simple and popular control method to control the roll angle is by either directly measuring the roll angle or indirectly by measuring the lateral acceleration. However, since these controllers aim to control the roll angle for ride improvements, most do not control the roll moment distribution and rely on the subjective improvement to the handling. A few papers do use roll moment distribution. Roll moment distribution is acknowledged by [Lang, 1991]. In this paper roll control is developed based on lateral acceleration. Lang mentions that by changing the roll stiffness ratio between the front and rear of a vehicle the oversteer/understeer behaviour can be affected. However, the roll control does not actively control roll moment distribution.

Roll angle based control is used in [Constantine, 1994] to improve handling and stability in emergency manoeuvres. Three control strategies are developed, two using roll angle and one using lateral acceleration and yaw rate. The roll angle control schemes will be described here while the lateral acceleration and yaw rate strategy is discussed in Section 2.1.3. The first control, called Semi Active Bang Bang Roll Control or SABB, uses roll angle to switch the roll stiffness between two states, a normal setting and a firm setting with double the normal roll stiffness. This strategy is a simple roll control and does not control the roll moment distribution.

The second controller using roll angle described by Constantine is Active Roll Control with Lateral Handling Augmentation, or ALAT. ALAT uses a PID control based on roll angle to determine the total anti-roll moment. Once the anti-roll moment has been calculated there is a three state logic control based on steer angle and brake input to determine the roll moment distribution. If the steering wheel input is less than 10 degrees then the roll moment is distributed 75% to the front and 25% to the rear. The front bias distribution used is based on passive vehicle simulation where tighter cornering was realised by a front bias roll stiffness. However, as speed increases so does vehicle understeer which is countered by changing the roll distribution. If the steering wheel angle is greater than 10 degrees and there is no brake input then the roll moment is distributed 25% to the front and 75% to the rear. In the third state, if the steering wheel angle is greater than 10 degrees and there is braking the roll moment distribution is based on the total roll moment. If the total roll moment is 1.1 times the nominal roll moment then the roll moment is distributed 25% to the front and 75% to the rear. This is the case in most avoidance type manoeuvres. However, if

the total roll moment is 0.9 times the nominal roll moment then the roll moment is distributed 75% to the front and 25% to the rear. In between 1.1 and 0.9 times the nominal roll moment the distribution of the roll moment is linearly varied between 25% in the front to 75% in the front.

These control strategies proposed by Constantine are designed to aid obstacle avoidance in emergency manoeuvres. They are tested in a constant steer angle test in a 0.4g corner but the main evaluation is with an avoidance manoeuvre test. The criterion for this test is the longitudinal distance required for the vehicle to move 4.57m (15ft) laterally during a braking while steering manoeuvre. The shorter the required longitudinal distance the better the control. The manoeuvre is simulated just below the stability limit of the vehicle. This stability limit is determined by the lock up of three wheels. All the simulations are run to complete vehicle stop without regard to returning the vehicle to normal driving. For the constant steer angle test the ALAT controller reduces understeer while keeping it positive leading to a more neutral handling vehicle. However, the understeer coefficient is more consistent and does not vary as much with lateral acceleration. It is noted that despite creating more neutral handling vehicles the trajectories are degraded compared to the nominal vehicle. In the 0.4g corner the controlled vehicles had larger radius corners but with less steering angle input. This is due to the increased roll stiffness which creates larger lateral load transfers and results in less lateral tyre force.

The ALAT controller performs better in the braking while steering avoidance test. In this test the ALAT controller cuts the longitudinal distance needed to move 15ft laterally by 13% compared to the nominal vehicle. This is due to a faster response time. The yaw rate and lateral acceleration for the ALAT controlled vehicle reach their peak values much faster. This increased response can be attributed to improved management of the tyre normal forces due to roll stiffness distribution. Another point to note is that the difference between the front and rear slip angles remains positive and close to zero. This means that it would be easy to steer into another manoeuvre. The results from this paper are interesting and show insight into how to speed up the vehicle response time. By distributing the roll moment to the rear, the front axle grip can be increased to make the vehicle respond faster. However, since the avoidance manoeuvre used for the test ends with a stopped vehicle it is difficult to evaluate how effective the controls would be in a racing environment.

In a follow on paper to Constantine, Kahrs to develops the SABB controller [Kahrs, 1995]. In this paper, Kahrs is investigating the dynamics of a sport utility vehicle unlike the passenger car used in Constantine. This results in the Front Semi Active Bang Bang or FSABB control. At roll angles greater than 0.5 degrees, the control doubles the front roll stiffness promoting vehicle stability by distributing the roll moment towards the front axle as well as controlling roll. Both the SABB and FSABB controllers are compared to the passive vehicle. The FSABB controller gives an improved vehicle trajectory and controls the vehicle oscillations with a quicker settling time. The reason for the quick settling time is the front biased roll stiffness distribution that has less of an oversteer characteristic. Since the heading angle change is less for the same driver input with FSABB the correction to come back to the original heading is also less. It seems as though the benefits of the FSABB control are a result of increasing the understeer tendency and stabilising the vehicle. This is not the ideal method of control in a racing environment where a faster response and more cornering power are desired as well as stability. As a side note, it is interesting to note that the SABB controller was considered a performance degradation by Constantine yet when the simulated vehicle is changed and the test and evaluation criterion are changed Kahrs finds the SABB controller to be an improvement on the passive vehicle.

Lateral acceleration and roll angle based control strategies are generally not effective in controlling the roll moment distribution. They are used to eliminate roll which does create some subjective handling benefits. Roll moment distribution, on the other hand, is used to actively control the vehicle balance yet lateral acceleration or roll angle on its own does not reflect the state of vehicle balance. Another input is needed to determine if a vehicle is oversteering or understeering for a driveability control system to be effective. In both Constantine and Kahrs, the roll moment distribution was based on fixed values that changed based on logic controls from other parameters. To affect vehicle balance, the goal of active roll moment distribution, the input into the control scheme must carry information on the state of the vehicle understeer/oversteer balance.

2.1.2. Sideslip Angle and Tyre Slip Angle Control

Sideslip angle and tyre slip angle difference are ways of evaluating the state of the vehicle understeer/oversteer balance. Both sideslip angle and tyre slip angle difference are very similar and can be related to each other by including or excluding the steer angle of the wheels. [Hwang, 1995] describes a roll moment distribution stability control based on the difference between the front and rear tyre slip angles, which he calls 'α^*'. Hwang calculates the tyre slip angles, and therefore 'α^*', using the steer angle, yaw rate and speed as well as wheelbase, which are readily measurable. The control is a proportional control of the inverse of 'α^*' multiplied by the lateral acceleration. The result is that for positive values of 'α^*' multiplied by the lateral acceleration the roll moment is biased towards the rear. The controller is tested in a braking and steering test and compared against a passive vehicle and a simple roll control without dynamic roll moment distribution control. The passive vehicle is the least stable with the roll controlled vehicle showing a marked improvement but the roll moment distribution shows the best performance. This demonstrates that even without roll moment distribution, roll control can still promote stability. The controller is also compared to a vehicle with a distribution of 90% roll moment at the front that shows the most stable response. However, this is misleading since a vehicle with almost all of the roll stiffness at the front would probably suffer handling problems like general understeer. So even though it might appear to perform better than the vehicle with active roll moment distribution, the roll moment distribution controller probably proves to be a better all round performer.

Another paper that uses the difference in tyre slip angles to control vehicle stability is [Ottgen, 2002]. The controller is a roll angle based PID control with the roll moment distribution proportional-integral control based on '$\Delta\alpha$', which Ottgen defines as the difference between the absolute values of the front and rear tyre slip angles. The controller is developed with a simple model then tested on a more complex model. The simulated results from the simple model show that the controlled vehicle is more neutrally balanced in a step steer test and follows a tighter trajectory compared to the passive vehicle. Or, for the same trajectory less steering angle is required and the controlled vehicle has more potential to create additional lateral forces. The controller also reduces the peak roll angle as well as cancelling the steady state roll and roll angle oscillations. When used with the complex vehicle model the

results are not as dramatic. The controlled vehicle shows more stability than the passive vehicle, with a faster response and slight understeer throughout the manoeuvre. The faster response and reduced roll angle of the controlled vehicle creates a more predictable behaviour. Unfortunately, the only test given is a step steer evaluation which does look very promising but data from other test procedures would be beneficial.

Body sideslip angle based roll control is explored in [Abe, 1992] to reduce the sideslip angle and maintain stability. An anti-roll moment is applied to eliminate body roll that is proportional to the lateral acceleration. To determine the distribution of the active roll moment to the front and rear axles, a phase plane approach is used. The control decides how to distribute the roll moment based on which quadrant the vehicle state lies and whether there is a spin or drift component to the vehicle motion. The distribution is adjusted by half the hypothetical roll moment caused by the acceleration of vehicle velocity times either the front or rear axle sideslip angle. This acceleration can be considered driftout or spinout acceleration. The control is evaluated with a single sine steer test at constant speed and then while braking. For the constant speed test the phase plane trajectories show that the controlled vehicle reduces the spin and drift components and results in a manoeuvre with a smaller slip angle. During the braking test the control keeps the vehicle stable due to the roll moment being biased to the front axle while the uncontrolled passive vehicle becomes unstable and spins out

Sideslip angle and tyre slip angle are effective in characterising vehicle behaviour and providing effective roll moment distribution controls. However, they are difficult to measure in an actual vehicle and as a result most controls of this type require an observer or estimator to determine the body sideslip or tyre slip angles.

2.1.3. Yaw Rate Control

The vehicle state can also be determined by observing yaw rate. [Constantine, 1994] uses yaw rate to control roll moment distribution and stabilise the vehicle. The other roll angle based controls discussed in this paper have been outlined in Section 2.1.1. The yaw rate based control is called Active Roll Control with Stability Augmentation, or ASTAB. The control determines the total active roll moment to cancel out the roll based on the lateral acceleration. The distribution of the active roll

moment is then determined to be inversely proportional to the ratio of front to rear lateral acceleration, calculated using the yaw rate. So when the rear lateral acceleration is large relative to the front, more roll torque is distributed to the front increasing understeer and vice versa. The ASTAB controller is evaluated in the same manner as the SABB, FSABB and ALAT controllers previously reviewed with a steady state cornering test and emergency braking and steering obstacle avoidance test. ASTAB keeps the understeer closer to neutral than SABB but does not keep a consistent, flat profile like ALAT. However, like the SABB and ALAT controllers, the trajectory of the ASTAB vehicle is degraded compared to the passive vehicle in a step steer test, but with less steer angle required to generate a 0.4g corner. The ASTAB controller has the worst trajectory in the obstacle avoidance test. This implies that the ASTAB vehicle has third wheel lock up on worse trajectories and at lower steering angles than the static vehicle. The controlled vehicle has a higher yaw rate and lateral acceleration response only at the very end of the manoeuvre when the vehicle has almost stopped. The benefit of the ASTAB vehicle comes when the sideslip angle is observed. The sideslip angle is greatly reduced compared to the passive vehicle, up to 60% at the peak values. With a lower sideslip angle the vehicle remains more controllable. Again, it is difficult to determine the actual effectiveness and usability of ASTAB since the test is run to vehicle stop.

In Kahrs' follow on paper to [Constantine, 1994], a second controller, called the Yaw Rate Controller or YAWRC, is created based on yaw rate [Kahrs, 1995]. The interesting concept discussed in this paper is the control of the total roll damping rate as well as the roll damping distribution front to rear based on yaw rate. The controller is a two state controller and starts with an initial 56% rear bias for the roll damping. The purpose of this is to increase to oversteer tendency to create a faster response time. When the yaw rate increases to 11 deg/s the total roll damping is doubled and distributed 70% to the front. The front bias and increased damping are designed to promote stability and reduce any oscillations by giving the vehicle an understeering tendency. To prevent chatter, YAWRC switches back to the soft setting when the yaw rate drops below 9.0 deg/s instead of 11 deg/s. The YAWRC controller is evaluated in a single lane change manoeuvre and shows improvement over the passive vehicle with better damped yaw oscillations. However, it is not apparent if the response time is quicker. It appears that the YAWRC vehicle follows the same trajectories and shows the same response as the passive vehicle until after the lane change. A benefit

to this control system is that the hardware required is controllable dampers which are already available.

A common way of implementing a yaw rate based control is to use a reference yaw rate tracking control to improve handling. A reference yaw rate is calculated and then compared to the actual yaw rate to create an error signal. [Everett, 2000] uses this approach using the vehicle speed and steering angle to calculate the reference yaw rate and error signal. A proportional controller is used on the error signal to control the roll moment distribution while the total anti-roll moment is proportional to the lateral acceleration. The control scheme is tested with a severe ramp steer test. Compared to a roll control with constant roll moment distribution, the active roll moment distribution controller was able to follow the larger steady state reference yaw rate much closer. However, this was the limit of the benefits from the controller. There was no improvement to the transient behaviour of the vehicle. This is probably because a large lateral load transfer is required to make the control effective which takes time to build up. At high lateral accelerations the vehicle yaw rate is not able to match the reference yaw rate due to non-linear tyre characteristics that are not accounted for in the reference model. The vehicle does settle into a safe understeering behaviour when these high lateral acceleration conditions occur and overall the control produces a more neutral vehicle behaviour.

Two yaw rate based control strategies are developed in [Williams, 1995] to improve handling and stability. Both strategies use a reference yaw rate tracking control. The reference yaw rate for both controls are calculated using speed and steering angle. The first control is similar to a sliding mode control but it is developed with a linearised system. A yaw rate tracking problem is presented with the tracking error becoming the control signal. Due to the system and the linearisation, a solution only exists if the tracking error signal is between -1 and 1 so a saturation function is created which resembles a sliding mode control to keep the tracking error signal bounded. Due to the complexity of this control scheme the full vehicle state must be available as input. The second control system is more simple. It is an intuitive non-linear control. Again it is a yaw rate tracking control. The error signal is given by the difference in the reference yaw rate and the measured yaw rate. If the yaw rate is greater than the desired yaw rate, the roll moment is biased to the front axle to promote understeering behaviour and vice versa.

Williams evaluates the controls with a simulated step steer test. The complex controller is evaluated with both a high gain and a low gain. The results show that in all three control strategies the actual yaw rate does follow the desired yaw rate in the steady state. The high gain, complex control reaches the desired yaw rate the fastest with the low gain, complex control the slowest but still faster than the passive vehicle. The simple control lies in between the two complex controls and none of the controls show any overshoot or oscillations. It is noted that initially there is a large yaw rate error build up for all three controls due to the slow response time of the dynamics compared to the steering input and the fact that load transfer must be present for roll moment distribution to have any effect. Another point made is that the controllers all have similar response time since they all initially saturate the roll moment to the rear axle.

The simple control is also evaluated with a 90 degree corner at 30mph actual vehicle test. The complex controls can not be evaluated in a vehicle due to the requirement of full vehicle state input. The control is compared to the passive vehicle as well as a roll controlled vehicle with different static roll moment distributions, varying from 100% at the front axle to 100% at the rear axle. Since the vehicle path is fairly well controlled by the test procedure, the yaw rate does not vary much between the different vehicle configurations. However, a difference is evident in the required steering input. The passive vehicle is the worst performer with large steering inputs required while the roll moment distribution controlled vehicle shows the best steering profile. A peculiar feel is noted in the roll moment distribution controlled vehicle. This is the controller helping to initiate the manoeuvre by transferring the roll moment to the rear axle. The vehicle never oversteers but drivers not trusting the control system did not find this sensation comfortable. To solve this problem the control is modified to limit the amount of roll moment available to the rear axle at any given time. However, it is not obvious what the results of this modification are on the performance of the vehicle since no data is presented.

Another reference yaw rate tracking control scheme is described in [Elbeheiry, 2001]. In this paper an active roll moment distribution system using active roll bars is combined with active front steering to promote stability in emergency manoeuvres. The roll control is provided by a proportional lateral acceleration control that is modified with a proportional reference yaw rate tracking control. The reference yaw rate is calculated by a two degree of freedom bicycle model with a non-linear tyre

model provided by a neural network. The control is evaluated in a braking and steering test on a high and low friction surface. The vehicle is equipped with an ABS braking system, this system is not described in detail but maintains the longitudinal slip ratio of the tyres at 0.1. The roll moment control combined with active front steering provides the best performance as expected. The active steering control is most effective in reducing the yaw rate error at the beginning of the manoeuvre while the roll moment control performs best toward the end of the manoeuvre. The reason for this is that the roll moment control needs lateral load transfer to be effective. Conversely, the active steering can affect the lateral forces at the beginning of the manoeuvre while the tyres are not saturated. Unlike the data from the high-μ test, the data for the individual controls was not given from the low-μ test. As a result the effects of roll moment distribution control on low friction surfaces is not obvious.

Yaw rate based controls are effective at determining the vehicle state and balance. They are able to do this without complicated sensors or estimation algorithms. These two attributes make yaw rate control a good option for the designer. Many of the yaw rate based controllers use models that are designed to promote stability in emergency manoeuvres. Not much emphasis is put on improving the response time and increasing the performance envelope of the vehicle before limit handling conditions are experienced.

2.1.4. Other Controls

There are many other ways of implementing a roll moment distribution control. The following section describes a few of these alternative control strategies.

The longitudinal acceleration and wheel speed are used as the control signals in [Tobata, 1993]. Tobata introduces a roll moment distribution control in conjunction with active suspension designed for ride comfort. The roll moment control is designed to operate strictly in combined braking and cornering or accelerating and cornering manoeuvres, which explains the choice of control variables. The longitudinal deceleration is used as the control signal for the roll moment control in a braking and cornering manoeuvre. When deceleration is sensed, the control increases the roll moment distributed to the front, promoting understeer and stabilising the vehicle. This control is tested with a manoeuvre where the driver lifts off the accelerator during cornering. The control maintains the yaw rate at a fairly constant level whereas

vehicles with a passive roll moment distribution show an initial two fold increase in yaw rate which either converges back to the initial yaw rate or keeps increasing depending on the static roll moment distribution. These results are confirmed with a vehicle test. The vehicle with roll moment distribution control is stabilised and shows less variation in the vehicle cornering path although it does follow a wider radius path than the uncontrolled vehicles.

Tobata's control for cornering and accelerating is based on wheel speeds. The difference in wheel speed between the two wheels of the driven rear axle is used as the control variable. An increase in the speed difference of the wheels of the rear axle shows that the inner rear wheel is beginning to slip due to reduced vertical force. At this point the roll moment is distributed towards the front of the vehicle to promote stability and increase the vertical tyre force on the inner rear wheel. The roll moment control suppresses changes in vehicle behaviour, promotes understeer and helps smooth acceleration while cornering. Not much detail beyond these qualitative evaluations is given in the paper and the effects of the control in other manoeuvres is not discussed.

Wheel movement based controls are proposed by [Cech, 2000] to improve comfort and safety. A slow active hydraulic suspension and active roll bars are used to develop an anti-roll and an active roll strategy. The active roll control strategy only uses the slow active hydraulic suspension. The sum of the wheel loads of the rear axle control a proportional gain for the load difference at the rear axle. Likewise, the same is true at the front. The outputs of these proportional gains are compared and the difference determines the control of the front suspension. The active roll comes from lateral acceleration. The rear suspension is controlled by this lateral acceleration signal after being filtered and the phase is matched to the suspension. Ride and handling evaluations are carried out and the anti-roll control and the active roll control are compared to a passive vehicle. The ride evaluation shows that the active roll control shows improvement over the passive vehicle but the anti-roll control is a minor degradation of performance. The handling performance is evaluated with an anti-phased road impulse disturbance during cornering. The anti-roll control does show performance improvements over the passive vehicle but the active roll control still shows the best performance. Unfortunately, only these ride biased handling tests are presented so the true effect these controls have on the handling performance of a vehicle is not shown.

2.1.5. Roll Moment Distribution Control Summary

Roll control based purely on lateral acceleration or roll angle is easy to implement and provides many benefits to the ride characteristics of a vehicle. Connected to the benefit in the ride characteristics is a qualitative benefit in handling as shown by [Constantine, 1994]. To realise the full benefits of roll moment control the distribution between the front and rear axles must be actively controlled. Not only must the roll moment be distributed actively but the control must be based on a vehicle parameter that can describe the handling state of the vehicle. The two common parameters used are sideslip angle and yaw rate. [Abe, 1992]] gives one example of sideslip angle control using a phase plane plot to maintain vehicle stability. The sideslip angle and sideslip rate are controlled to minimise the disturbance to the vehicle. Yaw rate control is also a popular way of controlling the vehicle since it is easy to measure, unlike sideslip angle controllers that require a sideslip estimator. A reference yaw rate tracking control is a common way of implementing the yaw rate control. An example is given by [Williams, 1995]. Although yaw rate controllers aim to follow a reference vehicle, they are generally implemented for path tracking and to limit the yaw rate and maintain stability rather than increase the limit performance.

2.2. Torque Distribution Control

Active driveline controls include engine management systems and torque distribution systems. Engine management systems regulate the power output of the engine to prevent the wheels from slipping. These systems can positively affect vehicle stability in straight line and cornering tests [Park, 1999], and have been used both in consumer cars and in racing cars. A disadvantage of engine management systems is the reduction in available power to the wheels and the lack of control over the distribution of the power. Torque distribution systems aim to address these two problems. These control systems actively distribute the engine torque to the wheels in the most efficient way possible. By actively distributing torque to different wheels, yaw moments can be created to affect the handling of the vehicle.

Torque distribution systems can create yaw moments indirectly or directly. Indirect yaw moments can be created by changing the torque distribution from front to rear. If a vehicle has an understeering tendency, torque can be transferred away from the front axle toward the rear axle. The effect of this torque transfer is that more

of the rear tyres available traction force will be used in the longitudinal direction and they will have less capacity to create lateral forces. At the same time the front tyres will be able to create more lateral forces for the opposite reason. The result is a pro-cornering yaw moment. The yaw moments available through this indirect method are not very large and only become effective when the tyres are close to saturation [Motoyama, 1993].

Yaw moments can also be created directly by distributing torque between the left and right wheels. Consider again the case of an understeering vehicle. If torque is taken from the inside tyre and transferred to the outside tyre a pro-cornering yaw moment is created [Doniselli, 1994]. This induced yaw moment does not rely on the lateral and longitudinal coupling of tyre forces, it is directly created. As a result, yaw moments can be created in all driving situations from low-g manoeuvres to high-g limit cornering. However, controlling the torque distribution to create yaw moments is not trivial during high-g manoeuvres for the very reason that the longitudinal and lateral tyre dynamics are coupled [Pacejka, 1997]. Consider the case of an understeering vehicle near the limits of traction. A pro-cornering yaw moment could be induced by transferring torque across the front axle, adding torque to the outside tyre and removing it from the inside tyre. If the lateral and longitudinal tyre dynamics were not coupled this would be fine. However, adding the torque to the outside tyre would increase the tyres demand for longitudinal traction. The result would be a reduction in the available lateral traction of the tyre. This reduction of lateral traction at the front axle could create even more understeer [Everett, 2001]. This has to be considered when designing controllers to work in limit handling manoeuvres.

The simplest method of torque distribution is a passive limited slip differential. In this case there is no active control beyond the initial tuning of the hardware. Most limited slip differentials are viscous coupling devices [Lugner, 1987]. To actively control the torque distribution active differentials with clutches are needed. These differentials can be progressively adjusted from fully open to fully locked. Three devices are described in [Hutchkoetter, 2004]. The first example is a locking differential that is controlled by an electromagnetic pilot clutch. The second locking differential uses hydraulic pressure to lock the differential while the third uses an electric motor. [Liu, 2002] also describes some locking differentials. He provides examples of differentials between the wheels on the same axle as well as locking differentials between the two axles in 4WD and on demand systems.

In the last few years there have been a number of developments in torque distribution hardware. A system has been developed with a CVT around a conventional differential to transfer torque across the axle more efficiently [Ikushima, 1995]. Torque vectoring is described by [Wheals, 2004]. Torque vectoring is the process of changing the magnitude and direction of the torque transmitted by a differential. The system developed has an electric motor that can bias torque to either wheel. Another system is developed by [Park, 2004] that consists of three clutches. One on each of the half-shafts and one clutch in the differential. By locking the centre clutch and releasing one of the half-shaft clutches, torque can be directed to a specific wheel or split between the wheels in any ratio regardless of speed or torque transmitted. This hardware configuration also allows fully locked differentials for off road use. A future technology for torque distribution is the independent wheel torque control [Esmilzadeh, 2001]. This concept is being developed for electric vehicles. The idea is to have a separate, controllable motor at each wheel. Due to the conceptual nature of this hardware configuration and its absence from the motorsport environment, it will not be considered in this thesis. However, the control concepts can still be used with a more conventional vehicle. The only limitations are that these controls are designed with separate controllable wheel motors in mind. This means that the individual wheel torque is easily measured and it is able to be controlled much more precisely than in a conventional drivetrain [Sakai, 2000].

2.2.1. Wheel Slip Control

Wheel velocity feedback control is developed to prevent wheel slip in [Sakai, 2000]. The goal of this controller is to increase the wheel inertia during wheel slip to prevent rapid increases (spinning) or decreases (lockup) in rotational velocity of the wheels. The controller is an internal model control that uses wheel velocity feedback to control individual wheel motors to effectively increase the equivalent wheel inertia. This control is evaluated in a split-μ acceleration test with an actual vehicle. The slip ratio of the uncontrolled vehicle increases rapidly while in the controlled vehicle the increase is five times slower. The controller is also evaluated in a braking while cornering test. Results show that the controlled vehicle demonstrates stable performance where the uncontrolled vehicle spins out. Although the rapid growth of the slip ratio is regulated, this controller does not control the absolute slip ratio which

can still exceed the stable limit. Another drawback to this control is that it is designed with electric motors in mind that can react quickly and precisely to demands for changes in torque. A conventional drivetrain would not have a fast enough response time to use this control strategy.

[Kaelani, 2002] develops a traction control based on wheel slip using a proportional-integral-derivative (PID) control with fuzzy logic. The objective of the controller is to keep wheel slip below 10%. Kaelani argues that while PID controllers are very cost effective for linear system control, they are not suitable for high order non-linear systems control. For this reason, fuzzy logic is introduced to the control. The basic control measures vehicle speed and compares it to the wheel speed. If slip is detected the control cuts engine power then uses the braking system to control the slip. The PID control is the main control and fuzzy logic is used to improve the responsiveness and recovery from noise. The results show that the wheel slip is maintained below 10% but the addition of fuzzy logic does not affect the performance very much. However, the type of tests used to evaluate the controllers and the actual results are not given much detail in the paper. Due to this, not much can be determined apart from the qualitative description.

A torque distribution control is developed by [Doniselli, 1994] using wheel slip. The control is designed to enhance driveability and active safety for a front wheel drive vehicle using an active differential. Ten different differential configurations are discussed with regards to the amount of power they dissipate and the amount of active control they are able to provide. The control scheme is designed with two objectives, first to maximise steady state lateral acceleration and second, to minimise the response time to a step steer input. The control sets the required difference in the longitudinal slips at the driven front wheels. The slips are measured by comparing the vehicle speed and the wheel speeds. To maximise the steady state lateral acceleration the best performance benefit would be realised if the two tyres had approximately the same slips. However, due to the difficulty in measuring the lateral slip of a tyre the control only takes longitudinal slip in to account. Since the outside tyre has a greater normal force on it due to lateral load transfer a higher amount of longitudinal force can be tolerated to get to the same slip ratio. This reduces the understeer tendency of the vehicle since the outer tyre has more longitudinal force which creates a pro-cornering yaw moment. To make sure that the control does not promote an oversteering behaviour the yaw rate of the vehicle is measured and compared to a

reference yaw rate based on speed and steer angle. To minimise the response time to a step steer input a linear model formulation is used. A vehicle state feedback loop and steering wheel input feedforward loop is used. The feedback loop is used to tune the transient behaviour while the steady state is controlled by the feedforward loop.

Doniselli then evaluates the front wheel drive control strategy against a passive vehicle and also compares the different differential configurations. During a step steer test at a velocity of 40 m/s the response time is four times faster while maintaining the same steady state response. During a lane change manoeuvre the yaw rate response is well damped and the steering input required by the driver is much less than in the passive vehicle. A power on cornering manoeuvre is also used to evaluate the control. It is noted that the controlled vehicles manage to maintain a closer path to the steady state model. The vehicle with torque distribution control via ABS maintains the closest path to the steady state model, however in the process a lot of energy is dissipated and the vehicle slows down. The better performing differential is the controlled active differential which does use some power, but uses it for traction. Finally the control scheme is quickly compared to other control strategies. There is not much detail in this section but it is briefly said that this control resembles a proportional yaw rate tracking control and that a control based on lateral and longitudinal accelerations shows a lot of potential. Also a proportional-derivative yaw rate tracking control looks promising but should be studied further to avoid negative effects of road induced disturbances.

A proportional-integral control based on wheel slip is developed by Park to prevent wheel slip and maximise traction forces [Park, 1999]. The throttle angle is regulated to limit wheel slip. The control calculates the slip ratio from lateral velocity, steering angle and yaw rate and uses a lookup table to determine the target slip ratio. The variable slip ratio control is based on the idea that as the lateral force increases the slip ratio should be decreased to provide a more capability for lateral acceleration. This target slip ratio is then used to generate a target vehicle speed. The target vehicle speed and the wheel speeds are used as inputs to the proportional-integral controller along with the drivers throttle angle to determine the required throttle angle. The controller is evaluated on slippery surfaces against a fixed slip ratio controller and a passive vehicle. In an accelerating while cornering test the low μ surface begins after 2.0 seconds. When the vehicles encounter the low μ surface they all slide wide compared to a vehicle on a high μ surface. The passive vehicle slides out of control

while the fixed slip ratio controlled vehicle maintains stability. However, the variable slip ratio vehicle retains stability and follows the original vehicle path best. It gains this lateral force advantage at the cost of losing some traction force and travels 4 meters less than the fixed slip ratio vehicle in 10 seconds. This could be an acceptable trade off for a consumer vehicle. A lane change manoeuvre is also tested on a low μ surface. The variable slip ratio vehicle requires less steer angle input compared to the fixed slip ratio controller. The controller was also tested for robustness by varying the tyre characteristics. It is found that although the system performance is dependent on the tyre characteristics, the controller still manages to work when the tyre characteristics are altered from the nominal values. Also, over this range of tyre characteristics the variable slip ratio controller always manages to create larger yaw rates than the fixed ratio controller which allows better cornering performance.

[Lyon, 1994] is a paper of particular interest since it describes the design and development of a traction control system in a Formula 1 racing car to control wheel slip. The control strategy is a rotating cylinder, injection cutoff engine control. A closed loop PID control is developed based on a slip goal value. The slip goal is determined from a map of vehicle speed and throttle position and compensated for depending on a driver selectable wet/dry switch, a gear dependent curve and the lateral acceleration. This creates a slip goal lookup map that can be tuned with great precision. The wheel slip is calculated from the front wheel speed and rear wheel speed. The difference between this actual slip and the slip goal is the error signal that is fed into the PID control. The controller gains are stored in maps as functions of vehicle speed, throttle position and gear. The output of the control is the percentage reduction in wheel torque which is converted into the appropriate injection cutoff pattern.

Once the vehicle began running in testing and races, telemetry data and driver feedback were used to tune the control and revealed new insights. Due to having two drivers with different styles and preferences the control had to be tuned differently for each driver and track as well as the conditions of the track. Another realisation was the difference between good and bad slip. Driver feedback showed that near total elimination of slip is not the proper goal, especially on wet tracks. The desired slip goal changes with the vehicle speed with 12-15% slip desirable at low speeds and less than 2% slip at high speeds. Also, it is the relative difference in front and rear wheel rotational speeds that give the car its characteristic feel in yaw. During corner exit the

slip response has to be able to detect the yaw attitude of the vehicle to avoid unnecessary slip reduction. If the driver is in his comfort zone of yaw attitude he might exceed the control threshold throttle setting. In this situation control intervention is not desired. To prevent this, the throttle threshold is used to predict when less intervention is preferred even if slip is detected. The control is also modified to cope with situations when single wheel spin occurs. Single wheel spin is rarely found to be the cause of vehicle oversteer requiring system intervention. Rather, single wheel spin is largely a function of differential lockup or unusual tyre road contact, i.e. impact with a curb. The solution is a multiplicative factor on the rear wheel average speed when there is a significant speed difference between the rear wheels.

This paper provides valuable insight into the development of a control system used in a racing environment. Obviously, a simple, easily to tune and calibrate system is chosen to minimise the risks associated with a complicated "smart" scheme. Another obvious difference lies in the goals of the control system. The control is being designed for one specific person and is tuned to fit their exact preferences not only for themselves but for each different track. This means that a simple control that is controlled by mapped relations is best. The mapping can be fine tuned and easily adjusted to custom tailor the exact feel of the vehicle. This is not practical for development on a production vehicle where the drivers are not professional race drivers and the same control system has to be used under all road conditions for all drivers. Again the difference in driving skill is exhibited when Lyon describes the fact that on corner exit large amounts of slip can be tolerated by the driver if he is in his "comfort zone". Control strategies for consumer vehicles are primarily designed with safety in mind. This results in strategies that provide neutral handling characteristics but in any emergency situation always default to an understeering characteristic without much concern for a loss in vehicle velocity.

It seems as though wheel slip control is particularly suited to engine control strategies. The advantage of engine control is that it is easily implemented in modern engines where the only requirement for a control is software development with minimal hardware requirements. Another benefit is that the control is realised through engine power reduction which saves energy rather than active differentials or brake controlled systems that only dissipate energy. However, one problem in implementing wheel slip control strategies is the difficulty in actually measuring the wheel slip.

Another concern is that although these controls do affect the lateral and yaw behaviours of vehicles, a more effective and precise solution to vehicle control is through more efficient torque distribution rather than reducing torque.

2.2.2. Sideslip Angle Control

Another vehicle stability control is sideslip angle control. [Abe, 1998] and [Abe, 1999] use sideslip control to maintain vehicle stability by minimising the sideslip angle and claim that it is better than yaw rate control. The reasoning is that the ratio of steady state sideslip gain to yaw rate gain increases with a decrease in the cornering power of the rear tyres. If the cornering power of the rear tyre is reduced the negative value of sideslip angle to generate some definite yaw rate increases. So when yaw rate reference model following is used as a control it yields a larger sideslip response when the vehicle is subjected to the deterioration of the rear tyre characteristics. However, when a sideslip reference model following control is used the vehicle yaw rate and lateral acceleration gains are restricted with the deterioration of the rear tyre characteristics due to low friction, large sideslip angle and load transfer under braking. Because of this, a reference model following sliding control is proposed.

The reference model is a linear two degree of freedom vehicle model. The sideslip error between the reference model and the actual vehicle is the control input. One of the most challenging aspects of sideslip control schemes is the measurement of the sideslip. A common method to estimate the sideslip is through pseudo integration of lateral acceleration and yaw rate. However, this method leads to significant error through the integration of the sensor signals. Abe therefore uses the lateral forces calculated by an on board tyre model in the integration to avoid error in the sideslip estimation. Although sideslip estimation is potentially limited by the knowledge of the road friction in the tyre model, Abe finds that the sideslip can be estimated precisely in severe handling manoeuvres as well as on low friction surfaces. In all the simulated manoeuvres, single wave sine steer, lane change and braking while turning, the passive vehicle spins out of control while the controller keeps the vehicle stable. The yaw rate and lateral acceleration as well as the sideslip angle are reduced and the controller maintains vehicle stability.

A sideslip angle phase plane approach is used in [He, 2004]. An integrated controller is developed with torque distribution and active steering. The controller

aims to improve yaw rate tracking with a sliding mode active steering control and maintain stability with torque distribution. The torque distribution control is a proportional, phase plane control based on the sideslip angle and its rate of change. A stable region on the phase plane is defined by running vehicle simulations at zero steer angle and constant speed but with varying initial conditions for the sideslip angle and its rate of change. The error signal into the proportional control is defined as the distance from the vehicle state to the stable boundary. This gives a stabilising control without using excess amounts of energy and control interference when its not required. The integrator is a ruled based control that gives priority to the controllers based on the vehicle stability. Although the work is interesting for the description of the sliding mode active steering control and the sideslip angle phase plane approach to torque distribution the results given do not separate the actions of the two controls, they concentrate on the different interactions between active front steering and active rear steering with the torque distribution.

Although the control schemes developed by Abe are effective and present a powerful argument for using sideslip control, they use braking forces to control the vehicle motion and they are evaluated using decelerating manoeuvres where use of the brakes is already occurring. The control strategies need to be evaluated with torque distribution hardware to determine the effectiveness for this research. The control presented by He does use torque distribution and looks promising but it needs to be explored as an individual controller.

2.2.3. Yaw Rate Control

Abe develops a control strategy based on a reference model yaw rate tracking control in [Abe, 1996]. A sideslip control scheme is tried initially, it sets the sideslip angle to zero. However, it is found that this is not a very good control scheme for direct yaw control. As a result, a feedforward yaw rate control is developed that aims to maintain vehicle stability by tracking a reference yaw rate. Both direct yaw moment control and four wheel steering controllers are developed and compared. The reference yaw rate is calculated using steering angle and vehicle speed and a first order lag. Both control schemes improve the vehicle response compared to the passive vehicle reducing the sideslip as well as controlling the yaw rate to closely match the model. The direct yaw control also performs better than the four wheel steering since

it requires less work load from the rear tyres. To further improve the control, yaw rate feedback is added. Again the direct yaw control performs the best, with the four wheel steering better than the passive vehicle. The direct yaw control is able to closely follow the reference yaw rate due to the addition of feedback signal. Again although these controls can be adapted for use with a torque distribution system, the disadvantage to these control strategies is the use of brakes as the controlled hardware.

A fuzzy control is developed by [Tahami, 2004] for an independent wheel motor reference yaw rate tracking stability control. Again, the control of independent electric wheel motors is not the hardware configuration in this research but the control strategy is still interesting. The control uses fuzzy logic to track the reference yaw rate which is determined from a linear model and uses a correction term. The correction term is provided by a trained feedforward neural network. A final addition to the control is another fuzzy controller based on wheel slip and wheel angular acceleration used to keep the wheel slip in a stable region. The results show that the estimators used to estimate the wheel slip and vehicle speed are accurate enough for the application and the neural network can provide an accurate reference yaw rate. The vehicle is tested with a simulated braking while turning manoeuvre. The controller manages to track the reference yaw rate and also reduces the sideslip angle. As mentioned before, this work is of interest for the development of the fuzzy controllers and neural network however, the concept of individual wheel motors is still untested in a high performance environment.

[Kuriki, 1998] uses yaw rate feedback and acceleration feedforward to control an active front differential in a two wheel drive vehicle. The objective of the control is to provide more precise vehicle control through the steering system by reducing changes in the vehicle behaviour caused by acceleration and deceleration. The longitudinal acceleration and the lateral acceleration are used to determine the torque split with yaw rate feedback. The control is evaluated in acceleration and deceleration while cornering tests and shows improved performance and stability in both tests. In the acceleration and cornering test the turning radius is regulated much better providing an improved trajectory. Not only is the trajectory improved but the tyre side forces are used more efficiently. The hardware for this control is an active differential with an accelerator mechanism. The accelerator mechanism consists of a planetary gear set and two clutches and is used to provide more torque to the outer wheel during

accelerating manoeuvres. This stabilises the vehicle since the outer wheel has more normal load and can produce more longitudinal and lateral force and it delays the saturation of the inner wheel.

An all wheel drive torque distribution control is developed by [Matsuno, 2000] to improve stability on low μ surfaces and handling performance on high μ surfaces. The control includes ABS, traction control and a brake based vehicle dynamics control (VDC). The torque distribution control is through an active centre differential. The normal distribution is 36% of the torque to the front wheels and 64% to the rear but this is actively controlled by a clutch that locks or unlocks the centre differential to maintain stability. The control includes a μ estimator. When the detected friction is high the torque is biased towards the rear but as the friction decreases more torque is given to the front wheels. The main stability control is based on yaw rate. The control uses reference model tracking yaw rate feedback to determine the stability of the vehicle. When understeer is detected the transfer torque is decreased and during oversteer it is increased to improve stability. For low speed manoeuvring the transfer torque is decreased to reduce running drag and improve steering feel. The centre differential control also communicates with the ABS, TCS and VDC to insure that there are no conflicts. The μ estimator is integral to the control system. The estimator determines μ by comparing the identified value of tyre cornering stiffness with a reference value on a high μ surface. The total control system is evaluated on wet asphalt with an acceleration while turning test. The controlled vehicle follows the best trajectory while the passive vehicle follows a tight trajectory as well but spins out of control. This control seems to be very effective however, there is not much detail given beyond qualitative descriptions of the different aspects of the control.

Active differentials are also used by [Motoyama, 1993]. The effect of front/rear torque distribution is compared to right/left torque distribution during an accelerating while turning test. It is found that the front/rear torque distribution scheme can influence the handling behaviour. The effects are not large when the lateral accelerations are small but become noticeable at higher lateral accelerations. With a forward distribution of driving torque the front tyres' force generating capabilities saturate before the rear tyres' leading to an understeer characteristic. The opposite is true with a rear bias torque distribution which results in an oversteering characteristic and leads to spinout behaviour. This is an indirect way of controlling the handling behaviour. In comparison, a right/left torque distribution more directly controls the

yaw moment. By distributing the torque to one side of the vehicle, larger, direct yaw moments can be induced from lower lateral accelerations.

Motoyama uses reference yaw rate tracking, proportional-derivative feedback to control the right/left torque distribution with the aim of keeping a neutral steer characteristic. The centre differential is set to a 50% front/rear distribution while both front and rear differentials distribute the torque between the left and right wheels by the same ratio. The control is first evaluated in a computer simulation. During steady state cornering tests the control is capable of maintaining a much more neutral characteristic. However, at the turning limit the vehicle shows a sudden instability as the vehicle goes beyond the limits of the controller. The control is then evaluated in a test vehicle. The sudden behaviour change shown in the simulation is not present in the vehicle test. The vehicle displayed stable, predictable yaw rate behaviour with the modelled neutral behaviour throughout the testing, however no sideslip angle data is presented. It is determined that the reason for this discrepancy was that the driver model in the simulation was not capable of accurately emulating a real driver.

[Ikushima, 1995] also uses active differentials for right/left torque distribution in a reference yaw rate tracking feed back control aimed at improving manoeuvrability and stability. The active differential consists of a conventional differential with a continuously variable transmission around it to distribute torque between the left and right wheels. This configuration is more energy efficient than other types of active differentials that use clutches or brakes. The controller compares the actual yaw rate with the reference yaw rate and applies a proportional-integral controller to minimise this error signal. The control is evaluated with accelerating while cornering, decelerating while cornering and lane change manoeuvres. During the accelerating while cornering test the vehicle critical lateral acceleration is increased by about 0.5 m/s^2. This is because the vehicle shows a more neutral behaviour and the lateral force balance between the wheels is more evenly distributed so the tyres are used more efficiently. During the decelerating while cornering test the controlled vehicle again helped maintain a more neutral behaviour. The passive vehicle shows significant oversteer "tuck-in" behaviour while the controlled vehicle remains stable and controllable with a much more consistent yaw rate. During the lane change manoeuvre the controlled vehicle shows faster response and less yaw rate required to complete the same manoeuvre. The steering angle input also shows that the required driver input is less in the controlled vehicle compared to the passive vehicle. For all

the manoeuvres the controller reduced the sideslip angle and lateral acceleration slightly as would be expected.

Yaw rate based control is effective with torque distribution. The controllers are able to create direct yaw moments to match the vehicle yaw rate to the reference yaw rates. Matching the reference yaw rates keeps the controlled vehicles closer to the desired trajectories of an ideal reference vehicle. To make these controllers work a reference model is required to create the reference yaw rate, usually a simple vehicle model based on steering angle and velocity. The controllers were also mainly stability controllers. The manoeuvres tested were limit handling manoeuvres in which the passive vehicles would lose control so the controllers would try and limit the yaw rate to maintain vehicle stability. There was not much emphasis on trying to expand the vehicle performance envelope, rather a focus on enforcing or regaining vehicle stability where a passive vehicle would spin out of control. There is potential for yaw rate tracking controllers to expand the performance envelope, especially since torque distribution optimises the use of the available torque which can help control the sideslip angle. Unfortunately, the effect of the controllers on the sideslip angle was not presented in many of these papers.

2.2.4. Yaw Rate and Sideslip Angle Control

One of the most popular control schemes uses both yaw rate and sideslip angle to control the vehicle handling behaviour. Unfortunately, many of the control schemes described use the braking system to induce the active yaw moments. Brake based systems are popular due to the fact that the hardware is already in many vehicles with ABS braking systems and because most control strategies are designed with safety in mind so the side effect of reduced speed is not a big disadvantage. On the other hand, driveline based systems usually require additional hardware and are more suited to controls that improve tracking performance and driveability. These papers have still been reviewed due to the absence of papers using torque distribution. Also, the control strategies are still interesting and could be used in a torque distribution control scheme.

An interesting approach to direct yaw control is taken by [van Zanten, 1996]. He develops a stability control that aims to minimise errors in vehicle motion relative to a reference model. The controller is a cascade control with two loops, an outer feedback

loop to control the vehicle motion and an inner feedback loop to control the wheel slips. The reason for the two loops is to separate the high inertia, low frequency body dynamics from the low inertia, high frequency wheel dynamics to improve accuracy and efficiency in the controller. The outer loop controller uses a linear reference model to determine the reference yaw rate and sideslip behaviour. Since sideslip angle is difficult to measure directly an observer is used to estimate sideslip angle, lateral velocity, tyre slip angles, lateral forces, normal forces and resultant forces. The vehicle model is then linearised about the operating point so the optimal tyre slips can be found using the Riccati method.

Once the optimal tyre slips have been determined the inner feedback loop determines the brake actuation to achieve them. The inner loop is split into two controllers, a brake slip controller and drive slip controller. The brake slip controller is a PID control. It uses a wheel velocity estimator to calculate the road friction and determine the brake actuation required. The drive slip controller also uses a PID control based on the average driven wheel velocity to determine the engine output torque while a proportional-integral control is used to determine the brake actuation to transfer torque across the axle. The results are obtained by simulating a lane change manoeuvre and an increasing velocity constant radius cornering manoeuvre. The controlled vehicle maintains stability and manages to control the yaw rate. The sideslip angle is also reduced and kept more linear relative to lateral acceleration. The simulation results are also verified with an increasing steer angle real vehicle slalom test. Even though the brake system is used to control the vehicle, this paper shows that, although it may be undesirable to use estimators, it is possible to make them work.

In [Horiuchi, 1998] and [Horiuchi, 1999] a yaw rate and sideslip control is developed. Nonlinear predictive control is used to create a reference state trajectory tracking control. The reference state trajectory consists of the longitudinal and lateral velocities and the yaw rate. The yaw rate is calculated from steering wheel angle and vehicle speed while the lateral velocity is defined by setting the sideslip angle of the vehicle to zero. The controller is evaluated with a step steer test, sinusoidal steer test and braking on a split-μ surface. The paper also develops an active steering control and an integrated control and compares the three different control strategies but unfortunately does not present data for a passive vehicle. Compared to the active rear steering controller the torque controller is better. The phase plane response shows a

more stable behaviour for the torque controller but not as controlled as the integrated controller. The torque controller reduces the sideslip angle and the yaw rate compared to the steering control. Compared to the integrated control, the sideslip angle is larger on the torque controller but the yaw rate is very similar. The tyre work load is also evaluated. It is interesting to note that the peak tyre workload for the torque control is very similar to the integrated control and better than the active steering. The drawback of this controller is that it is designed with the full vehicle state being available to the controller. This is not practical for implementation where it is difficult to accurately measure the full vehicle state.

[Shino, 2000] develops a wheel torque distribution, reference yaw rate tracking and sideslip control. A two degree of freedom model defines the reference behaviour of the vehicle. State feedback is used by the reference model to create a yaw rate and sideslip angle error signal for the controller. A steering angle feedforward compensator is used with the state feedback controller. The feedforward control is designed to make the sideslip angle become zero and follow a reference yaw rate. The reference yaw rate is determined with a first order delay system from the steering angle. The reference model tracking feedback control is used to compensate for external disturbances and uncertainties in the system. The controller is evaluated with a J-turn test and lane change manoeuvre. During the J-turn test the feedforward controller on its own managed to significantly reduce the sideslip angle, but with the feedback compensator added the sideslip angle was almost entirely eliminated. When tested on a wet road the controller did not manage to perform as well but still reduced the error between the desired yaw rate and the actual yaw rate as well as reducing the sideslip and stabilising the vehicle. In the lane change manoeuvre similar results are obtained. The vehicle without control becomes unstable while the controlled vehicle remains stable. Although this controller seems effective, especially in wet conditions without a friction estimator, it requires the knowledge of the vehicle state, particularly the sideslip angle. The means of measuring this are not discussed and it remains unknown how this system would be implemented in a vehicle.

A further paper is presented by Shino [Shino, 2002] that uses the same basic controller. Again the means of measuring the sideslip are not detailed. This paper deals with the integration of various active steering controls with variable torque distribution however it does show results for the variable torque distribution on its own. Again, the same variable torque distribution control is used with feedforward

and feedback compensators where the rear wheel torques are used to induce controlling yaw moments. The controller is evaluated in two stability oriented tests, side wind disturbance and split-μ braking. In the side wind disturbance test the controlled vehicle shows a larger sideslip angle but a smaller yaw rate response than the passive vehicle. This suggests that wheel torque control is good at yaw rate control but not as good at suppressing sideslip. In the split-μ braking test the wheel torque controller does not perform very well. Although it successfully reduces the yaw rate this is accomplished by sacrificing braking performance. The wheel torque controller does not look as promising in this paper. This shows how changing the evaluation method can greatly affect the perceived performance of a control strategy.

[Ghoneim, 2000] develops a yaw rate feedback stability control that is developed into a full state feedback control if the sideslip angle is available. The yaw rate feedback control is a proportional-derivative, reference model tracking control that is expanded to incorporate sideslip angle in the full state feedback control. The control is evaluated with a lane change manoeuvre test. The lateral deviation from the ideal path is the lowest with the full state feedback controller, which has half the deviation of the yaw rate controller and a quarter of the passive vehicle deviation. The yaw rate response shows that the full state controller has a faster response time and manages to create the yaw moment to get the vehicle back on the desired path quicker than the other vehicles. However, the maximum yaw rates for the controlled vehicles are both about the same. The sideslip response shows that the full state controller limits the maximum sideslip to create a more steerable vehicle while the yaw rate controlled vehicle does also reduce the maximum sideslip. It is interesting to note that the full state feedback controller produces the largest lateral accelerations and therefore the largest roll angles. As expected the full state feedback controller shows improvement over the yaw rate feedback control. However, both these control strategies use the brake systems to induce the active yaw moments.

Kin develops a yaw rate and sideslip control to enhance stability and steerability which uses a sideslip estimator [Kin, 2002]. The β estimator uses steer angle, yaw rate and wheel speeds as well as longitudinal and lateral acceleration sensors. The slip ratio of the tyres are used to estimate the coefficient of friction. This is then used along with the other sensor signals and tyre data maps to estimate the sideslip angle. The estimation of both μ and β is shown to be very accurate during driving on snowy, wet and dry surfaces. The torque distribution controller uses three wheel braking to

stabilise the vehicle. This corresponds to always controlling the rear wheel torques and one front wheel, the outer front wheel in an oversteer situation and the inner front wheel during understeer. The sideslip angle is used to control the wheel slips. The sideslip is also used in combination with the yaw rate to determine the understeer/oversteer state of the vehicle, which determines the amount of yaw moment control required. The control is evaluated in a J-turn test and a double lane change test. The J-turn test is conducted on both a wet surface and a snowy surface. During both of these tests the controller manages to maintain stability and steerability while the passive vehicles spin out of control. The results for the double lane change test are very similar. In both tests the controller manages to keep a more linear relationship between yaw rate and steering angle.

[Mokhiamar, 2002] develops a sliding mode sideslip control for three different configurations, direct yaw moment control with active rear wheel steering, direct yaw moment control with active front wheel steering, and direct yaw moment control with active front and rear wheel steering. The goal of these controls is to maximise stability and responsiveness. Mokhiamar claims that from a stability point of view, due to non-linear tyre characteristics, sideslip control is more effective than yaw rate control for direct yaw moment control. He references Abe's work [Abe, 1999] to validate this, which is reviewed in Section 2.2.2. However, he continues on to develop a sliding control for yaw rate as well as for sideslip. The reason for adding the yaw rate controller is for the active steering, which is integrated with the wheel torque control to improve responsiveness. The sideslip angle control is realised with a β estimator, which is based on a simple tyre model as well as yaw rate and vehicle speed. The different control methods are evaluated with a single sine steer test. In this test the passive vehicle spins out and loses control. For the four different control cases, wheel torque control and three different wheel torque and active steering controls, the vehicle remains stable. The wheel torque control does not reduce the sideslip angle as much as the combined control systems but the yaw rate response is very similar in both cases. The lateral acceleration is smoother in the wheel torque controlled vehicle but it reaches higher values to complete the same manoeuvres. Unfortunately, the evaluation of these control schemes is only done with one test and the wheel torque control is achieved with the brakes.

A vehicle dynamics controller with the aim of improving path tracking and preventing rollover is developed by Chen [Chen, 2002]. This controller consists of

three parts, yaw rate following, sideslip angle reduction and rollover prevention. The yaw rate following part is based on a reference yaw rate that is found in a nonlinear look up table based on steering angle and vehicle speed. The control is a simple proportional control that is activated when the yaw rate error and yaw rate error percentage reach their thresholds. The sideslip reduction part is a proportional-derivative control that, like the yaw rate following part, is only activated outside normal driving conditions. The control is activated when the sideslip and the product of the sideslip and its derivative reach their thresholds. The rollover prevention is a proportional control based on lateral acceleration but activated when lateral load transfer reaches a threshold. One interesting part of this paper is in the evaluation of the control system. As well as the usual steady state and double lane change tests, Chen introduces a fishhook manoeuvre test. This test consists of a right turn followed immediately by a steady state left hand turn. This test is very effective in determining the ultimate stability of the vehicle. A conventional direct yaw control was compared with the active yaw control with the rollover prevention system. Unfortunately, the only measures of performance presented are percent improvement in path error and lateral load transfer ratio. Both systems performed relatively well in the steady state and double lane change manoeuvres but during the fishhook test the conventional control was not able to match the performance of the rollover prevention control. Unfortunately, the system is a brake based system that is used for accident prevention. As a result the general handling of the vehicle is not improved, only limit manoeuvre stability is considered.

A multiple sliding mode stability controller is developed by [Kwak, 2000]. The controller uses a reference model to give a desired yaw rate and sideslip angle. The multiple sliding mode control consists of two sliding surfaces, the first is defined by the sideslip error and the second is defined by the yaw rate error. Two tests are used to evaluate this controller on a low friction surface while braking, the step steering test and a lane change manoeuvre. The controller manages to follow the desired yaw rate and sideslip very closely while the passive vehicle spins out and loses stability. Although this multiple sliding mode control is interesting, not much detail is given and the braking system is used to stabilise the vehicle.

Park uses a linear quadratic regulator as the basis for a control system [Park, 2000]. The controller uses yaw rate and sideslip as inputs with the target of improving vehicle stability. To determine the sideslip a μ estimator and a β estimator are used. A

brush type tyre model is used to estimate μ, which in turn is used to determine tyre forces which are required by the model based β estimator. A linearised reference model is used by the state feedback control to calculate the necessary active yaw moment to match the reference yaw rate while reducing the sideslip to zero. There is also a feedforward component to the control that is based on the steering angle. The μ and β estimators work well when the tyre slip ratios are small. However, due to the simple tyre model, as the slip ratio increases the estimators loose accuracy, especially on low friction surfaces. The evaluation of the control scheme shows that although the estimators loose accuracy with increasing slip ratios they perform well enough for the controller. The controller is evaluated in a J-turn test and a slalom test. In the J-turn test the controlled vehicle follows the desired yaw rate and sideslip angle maintaining vehicle stability while the sideslip of the passive vehicle increases and diverges causing a loss of control. The slalom test results are similar with the passive vehicle becoming unstable and loosing control while the active vehicle manages to follow the desired yaw rate and sideslip angle successfully. Again, these results are good but the braking system is used to generate the active yaw moment.

These combined input sideslip angle and yaw rate controllers show very good results. They manage to stabilise the vehicles in limit manoeuvres and track the reference yaw rates. The sideslip angle is generally minimised in the controllers while the yaw rate is compared to a reference signal to make the vehicles track a reference yaw rate. However, it seems as though the yaw rate tracking is not used to improve the responsiveness of the vehicle and enhance the handling performance; it is only used to reduce the vehicle yaw rate when instability occurs. This is also usually done with brake based systems rather than torque distribution control.

2.2.5. Other Controls

Jung develops a different control scheme. In [Jung, 2000 a] and [Jung, 2000 b] a combination of lateral acceleration and yaw rate, which he calls 'Ψ', is used to determine the vehicle state for a stability controller. The control is a proportional reference model tracking control where the desired 'Ψ' is calculated using steering wheel angle and vehicle speed. The controller is evaluated with an acceleration while cornering test and a split-μ start test. In the accelerating while cornering test the controlled vehicle shows more stability and follows the desired path much closer than

the passive vehicle. However, it achieves this by retarding the vehicle acceleration. In the split-μ start test the controller keeps the vehicle on the desired straight path while the passive vehicle is unable to maintain stability and spins out. Although this method of combining yaw rate and lateral acceleration shows promise as a control variable, the implementation of it with brakes does not give a good idea of its capability in a torque distribution controller.

The β-method is developed by [Shibahata, 1993] to promote stability. The β-method (sideslip angle) is a way of defining the stability and behaviour of a vehicle, especially in non-linear transient handling and acceleration manoeuvres. The vehicle characteristics are determined from plotting sideslip verses yaw moment. This diagram shows curves of constant front steering angle plotted on a diagram that shows the stabilising yaw moment verses the sideslip angle. The basic stability is determined from the stabilising yaw moment and the stabilising yaw moment inclination. When the inclination of the yaw moment is positive the vehicle converges to a stable state, but when it is negative the vehicle is partially divergent if the stabilising yaw moment is positive or divergent and unstable if it is negative. The β yaw moment diagram shows that as the sideslip angle increases the stabilising yaw moment inclination decreases resulting in a decline in vehicle stability as the cornering limits are approached. If a β yaw moment diagram is created for an accelerating and a decelerating vehicle it is found that the stabilising yaw moment increases during acceleration while is decreases during deceleration. This increase or decrease in stabilising yaw moment during steady state cornering with acceleration or deceleration is proportional to the lateral acceleration.

Shibahata goes on to create a direct yaw moment control that uses the wheel traction and braking forces. A four wheel drive vehicle with a fixed front to rear torque distribution is used for the evaluation of the control strategy. The distribution between the right and left wheels is based on the longitudinal and lateral accelerations. The results show that the controlled vehicle, during acceleration and braking while cornering tests, comes close to matching the turning radius of a non-accelerating vehicle. The reason for this is a more efficient use of the lateral tyre force. This paper proposes a very useful method for evaluating vehicle behaviour, the β-method.

A wheel load based torque distribution control is proposed by [Abe, 1987]. The goal is to create a vehicle behaviour that is insensitive to acceleration and power off

braking as well as increase the lateral acceleration capabilities. The control distributes the traction forces to the front and rear axles proportionally to the axle loads. The traction forces at the rear axle are also distributed to the right and left wheels proportionally to their respective wheel loads. However, the front wheel traction forces are distributed evenly at a constant 50:50 ratio. By controlling the rear traction forces the front wheels should always reach the tyre saturation limits first resulting in safer understeer limit behaviour. By distributing the traction force between the wheels in proportion to the wheel loads the tyres should be able to work to their limits and be used in a more balanced manner. The results of cornering while accelerating and power off cornering tests show that the controlled vehicle has increased stability. The steer angle required to create lateral acceleration is reduced and made more linear. Unlike the passive vehicle, the controlled vehicle no longer exhibits oversteer in power off cornering. The overall characteristic of the controlled vehicle has become a stable, understeering behaviour.

A different approach is taken by [Ono, 2006]. This control strategy aims to minimise the workload of each tyre and make them all equal. A hierarchical control structure is used where the first layer determines the vehicle target resultant force and moment based on an error signal from a reference model, the second layer distributes the vehicle target resultant force and moment to individual target tyre forces and the third layer controls the individual wheel motions to achieve the target tyre forces. The base of the control is a tyre grip margin estimator based on self aligning torque and the normalised longitudinal tyre force. Using the tyre grip margin the friction rate of each tyre is calculated. It is this friction rate that the controller is trying to reduce and equalise among the four tyres. A large optimisation problem is set up and solved to determine the magnitude and direction of the target tyre forces. This approach to optimise the tyre forces is very interesting and aims to maximise the vehicle performance. Unfortunately, although the optimisation problem is presented, it is extremely complex and there is not much information on creating the reference vehicle motion or how to achieve the target tyre forces with the tyres.

2.2.6. Torque Distribution Control Summary

Wheel slip control has seen quite a lot of development but through control of the engine rather than the differentials. These controls can create yaw moments and affect

the vehicle handling through an indirect method. Controlling the torque distribution directly induces yaw moments. To control the handling of the vehicle through torque distribution the vehicle state must be measured. The two main vehicle state parameters measured are yaw rate and sideslip angle. Most control strategies use one or both of these parameters to create an error signal. Sideslip angle control is primarily used as a stability control as shown by [Abe, 1999]. The problem with sideslip angle based controllers is that the sideslip angle is difficult to measure directly so an estimator must be used. Yaw rate controllers usually use a reference model control like [Motoyama, 1993]. The yaw rate is easier to measure compared to sideslip angle and the controls can be used to track the vehicle path more directly. These path tracking controllers are mainly used with the ultimate goal of promoting stability. They rarely actively try to expand the overall performance envelope of the vehicle. Combined sideslip angle and yaw rate controllers combine the benefits of both individual control strategies. The sideslip angle control can be used to stabilise the vehicle while the yaw rate control can guide the vehicle on the desired path. An example of this is developed by [Chen, 2002]. However, these controllers have only been used with brake based control systems and need to be re-evaluated with torque distribution control systems.

2.3. Combined Roll Moment Distribution and Torque Distribution Control

Combined control of roll moment distribution and torque distribution should provide the benefits of both control schemes. However, combining the two control systems has to be done with care. The two systems can augment each other in some situations but can also work against each other, for example by saturating the tyres. Integration of the two systems must be done carefully with consideration of the interactions between both control strategies.

The most obvious interaction of the two control systems is through the wheel load. Roll moment distribution affects the wheel loads of the vehicle and can reduce or increase the cornering potential of an axle. However, torque distribution controls require the necessary wheel load to realise the active torque demands. If the roll moment distribution system reduces the wheel load while the torque distribution wants to increase the torque at that same wheel then the two systems will work against each other and potentially produce performance worse than a passive,

uncontrolled vehicle. One example of this negative interaction is when trying to promote understeer. To promote understeer, the roll stiffness of the front axle is increased to create a large lateral load transfer and reduce the cornering power of the front axle compared to the rear. With torque distribution to promote understeer the torque should be transferred from the outside front wheel to the inside front wheel. However, the inside front wheel is becoming unloaded due to the increased roll stiffness which makes the torque distribution ineffective.

2.3.1. Sideslip Control

Smakman develops a combined wheel torque and roll moment distribution control in [Smakman, 2000 a] and [Smakman, 2000 b]. Smakman uses braking, not traction, forces to create the active yaw moments to stabilise the vehicle. Although the braking system is used they still provide a useful example of the integration of these two control schemes. It is found that roll moment distribution does not work at low lateral accelerations but the potential to generate yaw moments increases as lateral acceleration increases. However, as the cornering limit is approached less RMD can be used before one wheel loses contact with the road surface. For brake intervention, single wheel control is used for simplicity. It is found that braking the rear inner wheel creates the most effect pro-cornering moment while braking front outer wheel creates the most effective contra-cornering moment. While the contra-cornering yaw moment available increases with lateral acceleration, the pro-cornering yaw moment is relatively independent of the lateral acceleration with less absolute yaw moment available.

Both individual controllers are stability controllers based on the sideslip angle phase plane. A stable region is defined in the phase plane which acts as the control boundary. If the vehicle state leaves the stable region then control intervention is required to stabilise the vehicle. An error signal is defined as the distance between the current vehicle state and the control boundary in the phase plane. When the two systems are integrated they still both aim to stabilise the vehicle, the integration strategy is just used to determine when it is most desirable for each system to be active. The integration strategy is designed to limit the undesirable interaction of the brake system with the longitudinal vehicle dynamics. This is accomplished by initially using roll moment distribution to stabilise the vehicle. The brake intervention is only

added when the wheel load control reaches the limits of actuation, when one tyre loses contact with the road surface.

The controller is evaluated with an increasing amplitude sinusoidal steer test and is compared to a stand alone brake control. The integrated controller shows very similar performance to the brake control when comparing the sideslip angle, yaw velocity and lateral acceleration. The difference becomes apparent when the vehicle speed is observed. The integrated controller is able to wait longer before applying the brake intervention which results in less deceleration. Although this paper is a good example of the integration of wheel load control and brake intervention, the interactions of the two systems will not be the same when a torque distribution system is analysed with roll moment distribution.

2.3.2. Yaw Rate Control

Hac presents an integrated control based on a reference yaw rate tracking controller [Hac, 2002]. Hac uses brake intervention and roll moment distribution as well as active front and rear wheel steering to improve vehicle stability and emergency handling. A similar approach is taken to Smakman. First the individual controllers are evaluated to determine how effective they are over the range of vehicle states. Maps of yaw moment control authority are created for each control system that give the yaw moment available for any given steering angle and control input. Next the integrated controller is developed.

The controller is divided into two levels. The first level is a supervisory vehicle level controller. This controller consists of the reference yaw rate tracking control used to determine the overall active yaw moment required. The reference yaw rate is determined from the steering angle, vehicle speed and brake and throttle inputs. The second level of the controller then determines how to create the total active yaw moment from the separate control systems. This second level controller takes into account the quickness of response, level of obtrusiveness, compatibility with driver intentions and the required active yaw moment compared to the available control input of each control for the given vehicle state. Unfortunately, the cost function or decision algorithm to determine the distribution of total stabilising yaw moment to the individual control systems is not detailed beyond this description of the input criteria.

The evaluation of the integrated controller was conducted on a snowy surface and was designed to reduce the use of the brake control system. The most significant improvements are found during a double lane change test where the brake intervention time is reduced by 69%. The smallest improvement is found during a sinusoidal steer test where the improvement is a 23% reduction in time the brake control system is used. Again this paper presents positive results but uses the brake system for wheel torque control. Another disadvantage is the lack of detail presented in the second level of the controller regarding the control algorithm used to actually determine the distribution of the active yaw moment requirements to the individual control systems.

Interactive multi-objective programming (IMOP) is proposed as an integration method by [Mastinu, 1995]. IMOP is a method to help and guide the control system in deciding how to distribute the control objective between multiple systems. The control systems that Mastinu investigates are torque distribution via an active differential, active roll moment distribution, active four wheel steering and sky-hook damper active suspension. These controllers are integrated to improve ride and handling. IMOP consists of two stages that are iterated to find the optimal setup. In the first stage the initial individual control strategies are defined as proportional controls based on a reference model yaw rate. The exception being the active suspension, which uses skyhook damping. Once the individual control strategies are defined, their gains are tuned in the second stage where appropriate trade off among conflicting requirements are defined.

Within this second stage there are four steps. The first step is the exploratory step where the individual controls are evaluated and minimised separately with respect to the different objectives. A matrix of correlation coefficients can be constructed in which the correlations between the different objectives can be observed. The next step is the formulation step. Here the multi-objective problem is constrained into a single objective problem and solved for a suitable combination of constraints that can be chosen from the results of the exploration step. The search step is then used to find the efficient solutions to the optimisation problem using numerical techniques. The fourth step is the evaluation step where the solutions are examined and used to innovate new control designs and create the exploratory step in the next iteration. The integrated controller is evaluated with many different manoeuvres and shows improvement over the passive vehicle. Unfortunately, it is not obvious how much of this improvement is

due to just the roll moment distribution and torque distribution since the results are not separated for this combination of control systems.

Everett proposes an integrated control using active roll bars and an active rear differential in [Everett, 2000 b]. The controller is designed to improve the vehicle handling on-road without compromising off-road ability. It is based on a reference model following yaw rate control where the reference yaw rate is calculated using vehicle speed, steering angle and lateral acceleration. The integrated strategy uses a hyperbolic bias curve based on the rate of change of the yaw rate to decide which active control is used to create the active yaw moment. During steady state cornering when the yaw acceleration is very small, roll moment distribution is used to create the active yaw rate. As the yaw acceleration increases, the integrated controller uses the hyperbolic bias curve to progressively switch the control action to the torque distribution. This limits the energy used by the active differential and minimises the steady state roll angle. The control is evaluated with a step steer test, sine steer test, and braking and accelerating while cornering tests. Unfortunately, the controller is not evaluated against a passive vehicle but results show that the reference yaw rate is followed more closely with the active rear differential integrated with the roll control as opposed to the roll control on its own. It is also noted that eliminating the torque distribution control during the steady state does not significantly affect the vehicle performance.

The yaw rate based integrated controllers use reference models just like the independent controllers. An error signal is created and a corrective yaw moment is determined and the controllers allocate the corrective action to the different control systems. Roll moment distribution is used initially but as the corrective action required increases, torque distribution is brought in. This is to minimise the interference with the longitudinal vehicle dynamics. Again, most of the controllers are stability controllers, they are not trying to stretch the handling boundaries. They only try to stabilise the vehicle.

2.3.3. Yaw Rate and Sideslip Angle Control

An integrated stability control is designed by [Kitajima, 2000]. This control system consists of roll moment distribution, traction control and vehicle dynamic control as well as active four wheel steering. The vehicle dynamic control is a brake

based stability control. It uses a reference yaw rate tracking, proportional control as well as a proportional sideslip control using a phase plane approach. The purpose of the four wheel steering is to reduce the sideslip angle by a reference model based control so lateral velocity is minimised. The roll moment distribution is designed to minimise the roll angle and uses a PID control based on the roll angle. Finally, the traction control is a wheel slip based proportional control. The goal is to keep the wheel slip within a specified range.

Two types of integration are studied, feedforward integration and H_∞ integration. The feedforward integration strategy takes each vehicle objective and assigns it to a specific controller and makes that the main objective of the controller. Once the controllers are assigned their main objectives the inputs from other controllers are considered disturbances. Next a decoupling matrix was designed from step response results. The decoupling matrix is used to modify the un-coordinated control signals to achieve a feedforward decoupled control response. The H_∞ integration method measures the front steering angle and regards it as a disturbance input whose effect is to be rejected by the control signal. This way the front steering angle is used as feedforward control information. The control tries to minimise a cost function that includes sideslip, yaw rate error, roll angle and the control inputs.

Both of these integration methods are evaluated with a J-turn, fishhook manoeuvre (a turn in one direction immediately followed by a steady state corner in the other direction), braking while cornering and a sinusoidal steering test. Both controllers are evaluated and compared to a passive vehicle and a controlled vehicle with uncoordinated controls. The results show that the uncoordinated controlled vehicle performs only slightly better than the passive vehicle but both integration schemes improve on this performance by reducing the sideslip angle. However, the feedforward integration method fails to work properly. Each controller considers the other control inputs as disturbances without regard to evaluating whether or not they are positive or negative disturbances. It is suggested that further improvement could possibly be attained by introducing a gain scheduled decoupling matrix that would help determine if the controller interactions were good or bad. The best performance comes from the H_∞ integrated controller however, it does not always show a clear performance benefit over the other vehicles.

2.3.4. Combined Control Summary

The combined torque distribution and roll moment distribution controls follow the same type of control strategies as the individual controls. Sideslip angle control, as implemented by Smakman, is used to maintain vehicle stability. In this case a phase plane approach is used to control both the roll moment and torque distribution. The strategy is to use the roll moment control initially and only add the torque control when it is needed. This limits the intrusive nature of the torque control. Yaw rate controllers tend to be model tracking stability controllers. These controllers determine an ideal yaw rate and create an error signal between the model yaw rate and the actual yaw rate. Everett uses a yaw rate model based control. Unlike Smakman the method of determining control system dominance is based on the rate of change of the yaw rate. If the rate of change is large, the manoeuvre would require the more powerful torque distribution control to stabilise the vehicle. A controller using both yaw rate and sideslip signals is developed by Kitajima. The integration method used measures the potential effects of each control and then uses an algorithm to prioritise them to get the optimal solution. The integration of the different control systems is usually based on assigning control system priority for the same control goal. The individual controllers are evaluated and assigned regions of vehicle behaviour where they are effective. The integrated control then uses an algorithm or cost function to decide when each individual control system should be used. There are not many examples of integration strategies that have algorithms that decide between different overall control goals or objectives.

2.4. Literature Critical Review

Control strategies based on roll angle and lateral acceleration can be very similar since roll angle is proportional to lateral acceleration. The controls using either of these inputs are generally used for roll angle control. Lateral acceleration has been used for torque distribution but not as the only input into the controller. Roll control using roll angle or lateral acceleration can have subjective improvements in vehicle handling and enable suspension designers to optimise the handling at zero body roll. However, no judgement can be made on the understeer/oversteer behaviour of the vehicle without other input signals. As a result, control strategies based primarily on

roll angle and lateral acceleration can be effective in improving ride but are not suited to handling control.

Wheel slip or wheel speed controls fall into a similar category as roll angle and lateral acceleration controllers. They lack the ability to fully describe understeer and oversteer. Controls using wheel slip or wheel speed are primarily used for traction control. Traction control detects a loss of traction at a wheel and reduces the power to the wheel to prevent the wheel from spinning. This type of control can prevent power oversteer in low friction conditions but since there is no information on the understeer/oversteer balance of the vehicle there can be no informed decision to create corrective yaw moments. Another disadvantage is that the controls generally reduce the power output at the engine rather than intelligently distributing the torque. This potentially slows the vehicle down unnecessarily. However, the main difficulty is the implementation of these controls since it is difficult to accurately measure the wheel slip or the speed of a slipping wheel. There are methods to estimate the free rolling wheel speed but actual direct measurement is still very difficult.

One way of determining the understeer/oversteer balance of a vehicle is through the sideslip angle. A vehicle with no sideslip angle will be neutrally balanced. Both roll moment distribution and torque distribution controllers can be created with sideslip angle as their inputs. Sideslip angle has also been used with combined roll moment and torque distribution controllers. A common way of implementing a sideslip angle control strategy is to reduce it as much as possible or contain it within prescribed bounds. An extension of a simple sideslip angle control strategy is to create a phase plane control strategy that maintains the vehicle state within boundaries on a sideslip verses sideslip rate phase plane plot. This is a very effective way of controlling the stability of a vehicle since a vehicle with small sideslip angles will be stable and controllable. It is also possible, although less common, to have a sideslip reference model following control. A consideration with sideslip angle control is that when sideslip angle is blindly minimised it can degrade the yaw rate performance. Generally, when sideslip angle is reduced the yaw rate is also reduced which tends to prevent the vehicle from following the desired path. Another problem with sideslip angle control strategies is the difficulty in measuring the sideslip angle. There is no direct way of measuring sideslip angle. It can be calculated from the lateral acceleration but errors are introduced through integration. The sideslip angle can be

determined with an estimator. These estimators use on-board tyre models and friction estimators and have produced adequate results in some cases.

Yaw rate based control strategies avoid the use of an estimator while still providing information on the understeer/oversteer balance of the vehicle. Like sideslip angle controllers, yaw rate based control strategies can be effectively created for roll moment and torque distribution as well as combined controllers. However, unlike sideslip angle, yaw rate is easily measured with readily available sensors. The understeer/oversteer balance of the vehicle is captured by comparing the actual vehicle yaw rate to a reference yaw rate. This requires a reference model. Reference models are usually simple to implement but do introduce a potential for misguided controls. Generally, reference models are linear models that are used to try and push the vehicle to have a predictable linear handling response. Using a reference yaw rate tracking control basically creates a tracking control that tries to keep the vehicle on the path that a perfectly linear vehicle would follow. In trying to match the behaviour of a linear vehicle, yaw rate controls also tend to manage the sideslip angle as well. The sideslip angle is not reduced to zero but tends to be smaller than in an uncontrolled vehicle. For this reason yaw rate controls are generally used as stability controls and limit the yaw rate behaviour. However, not much work has focused on trying to expand the performance limits of a vehicle. This presents an opportunity to use yaw rate as a good input for driveability control strategies to expand the handling envelope of a vehicle.

To get the benefits of both yaw rate control and sideslip control they can be used together in a single control strategy. One way of doing this is by using a phase plane approach. A phase plane plot can be created with yaw rate verses sideslip angle. Another approach is to use a two layer control strategy. One of the signals will be used as a supervisor control that determines the overall state of the vehicle. This supervisor control then determines the specific strategy for the second layer control which operates on the other input signal. Both of these strategies can be implemented on roll moment or torque distribution controls as well as on combined controllers. However, possibly the best implementation of a control strategy using both yaw rate and sideslip angle is to create a combined or integrated yaw rate based driveability tracking control and a sideslip angle based stability control. The control strategy can create a desired yaw moment input to track a desired path or stabilise the vehicle depending on the vehicle state and then determine how to realise that yaw moment

through roll moment distribution or torque distribution. This has been done in some of the literature but not for combining roll moment distribution and variable torque distribution with the aim of actually expanding the performance limits of a vehicle.

The effects of roll moment distribution are only available at high lateral accelerations with load transfer. This makes it a good candidate for a stability control during limit manoeuvres. As a stability controller a good strategy would be to use a sideslip angle phase plane approach. To control the vehicle at the lower lateral accelerations torque distribution is more effective. A torque distribution feedforward control based on driver inputs could be effective to improve response and turn initiation. Once the vehicle response is improved a control to help direct the vehicle path is required. A reference yaw rate tracking control could keep the vehicle on the drivers desired path and expand the limit performance. The torque distribution could do this while the roll moment distribution keeps the vehicle stable.

Vehicle handling at the limit is highly non-linear and controlling its behaviour is difficult with strategies designed for linear systems. The complex non-linear models can also be linearised for use with linear control strategies, although this can involve very complex mathematics. As such, PID controls can be effective since non-linearities can be handled through adaptive control using gain maps or gain scheduling. Internal model control also provides a good strategy since the internal models can have varying levels of complexity to suit the application. Another popular control strategy is sliding mode control. Here the sliding surface can be defined to maintain stable vehicle behaviour. An innovative approach to vehicle control and maximising performance is through optimising the tyre workload. There has not been much work in this area due to the complexity of estimating the tyre state however, tyre state estimators are becoming more accurate. The integration of control strategies lends itself to rule based strategies or fuzzy logic because of the complex non-linear vehicle behaviour. In integration strategies without fuzzy logic, complex optimisation of cost functions based on performance metrics are required.

2.5. Literature Review Conclusions

The following conclusions are drawn from the literature.

- Control inputs must be able to determine the understeer/oversteer balance of the vehicle, for example sideslip angle and yaw rate.

- Sideslip angle can be used to determine the stability of the vehicle, however, it requires an estimator since sideslip angle is difficult to measure.
- Sideslip angle controllers usually degrade the yaw rate performance.
- Yaw rate can be used in driveability controllers but requires a reference model to determine the understeer/oversteer balance of the vehicle.
- Reference yaw rate tracking controllers tend to reduce the sideslip angle as well, which is desirable.
- Many yaw rate controllers aim to mimic linear handling but do not try and expand the performance limits of the vehicle.
- Roll moment distribution is only effective when there are large lateral load transfers in the vehicle.
- Torque distribution can be used over a wide range of manoeuvres but may cause secondary effects through tyre force saturation at high lateral loads.
- Simple combinations of roll moment distribution and torque distribution controllers can result in degraded vehicle performance through controller induced tyre saturation due to interfering interactions of the control demands.
- Roll moment distribution and variable torque distribution have individually been combined with active steering and other control strategies but rarely with each other and not to actively increase the performance envelope of the vehicle.
- Fuzzy logic or rule based controllers provide good integration strategies to deal with the highly non-linear integration of vehicle controls.
- Optimisation strategies can be used with cost functions to integrate controllers

2.6. Aims and Objectives

The aim of this research is to develop and simulate a control system to improve the driveability of a racing car while ensuring stability. The contribution is the integration of roll moment distribution and variable torque distribution to expand the performance envelope while tracking the drivers demands including both the lateral and longitudinal dynamics.

The following are benchmark objectives:

- Build a validated vehicle model. This will involve verifying results against current work in the Vehicle Dynamics Group at the University of Leeds.
- Create drivability controls for torque distribution and roll moment distribution.
- Create stability controls for torque distribution and roll moment distribution.
- Develop combined drivability and stability controllers for torque distribution and roll moment distribution.
- Propose and evaluate fully integrated multi-objective drivability and stability controllers for torque distribution and roll moment distribution.

3. *Vehicle Modelling*

Chapter 3 presents the vehicle modelling and validation. The level of model complexity required by the research is presented before a full eight degree of freedom model is developed in the MATLAB/Simulink environment. This model is validated against CarSim, a commercial vehicle dynamics package.

3.1. Introduction to Vehicle Modelling

Vehicle modelling is used to save time and money. A vehicle model can be used to simulate a vehicle's behaviour without requiring an actual vehicle. This can be useful in the conceptual development stage of design when building prototypes to test every different design possibility would be time consuming and prohibitively expensive. Vehicle models can also be used in the mature phases of vehicle design when investigating potentially dangerous manoeuvres. Accident avoidance and evasive manoeuvres, where rollover or vehicle damage are possible, can be simulated without the need to risk test driver safety or damage expensive prototypes.

A basic vehicle model is the linear bicycle model. This is a linear two degree of freedom model that treats each axle (front and rear) as a single tyre instead of two individual tyres [Milliken, 1995]. The two degrees of freedom are lateral velocity and yaw rate which are created through changes to the steer angle while the longitudinal velocity is kept constant. Although this model is a simple representation of a vehicle it still produces a good characterisation of vehicle behaviour since passenger cars generally operate in the linear handling regime. The linear handling regime of vehicle behaviour is characterised by small slip angles and low lateral accelerations. As the tyre slip angles increase the resulting lateral forces saturate and depart from their initial linear characteristics. Actual vehicles also experience increasing load transfer as the lateral acceleration increases. This load transfer affects the normal forces on the tyres and therefore the lateral forces they create. As the normal force increases the lateral force increases in an increasingly non-linear fashion. However, within the linear handling region steady state behaviour can be observed with step steer manoeuvres while insight into the transient handling behaviour of vehicles can be

observed through the understeer/oversteer characteristics [Crolla, 1991]. Another use of the linear bicycle model is as a reference model. Linear bicycle models can be compared to more complicated vehicle models to determine how far they are from an ideal linear vehicle behaviour.

To accurately model vehicle behaviour beyond the linear regime, the basic linear bicycle model can be extended by modifying the tyre model and adding additional degrees of freedom. The tyres provide the medium through which most of the forces acting on the vehicle are transferred. Therefore, the accuracy of the tyre model plays a key role in the accuracy of the vehicle model. Tyres are generally linear under small slip angles, slip ratios and normal loads, however during high-g cornering manoeuvres large slip angles, slip ratios and high and low loading occur on tyres. The initial relationship between tyre slip angle and lateral force is linear. As the slip angle increases the tyre saturates and the resulting gains in lateral force decrease non-linearly. If tyre slip ratio is also modelled it shows a similar non-linear characteristic. Initially, the longitudinal force is linearly dependent on tyre slip ratio but saturates at higher slip ratios. The tyre shows an even more non-linear behaviour under combined slip, with the initial linear portion of the curve becoming smaller at large slips. Likewise, as the normal force on the tyre increases the tyre becomes more non-linear and saturates. A common non-linear tyre model is the Pacejka "Magic Formula" tyre model [Pacejka, 1997]. This tyre model is an empirical model based on curve fitting the tyre model to experimental data. The empirical tyre models tend to be more accurate than physical models derived theoretically. This is because of the complexity of tyres and the number of different variables associated with modelling a tyre. The draw back to the empirical tyre model is that extensive testing of a tyre set is required to accurately describe the tyre. This testing is costly and results in a model for only one specific tyre.

Additional degrees of freedom can be added to increase the model accuracy and explore specific behaviours. The most obvious extension to the linear bicycle model is to include the longitudinal degree of freedom. This allows investigations into the accelerating and braking manoeuvres to be modelled. Adding the longitudinal degree of freedom creates non-linearities by introducing cross coupling with the lateral and yaw motion. However, just adding the longitudinal degree of freedom is usually not enough. To properly investigate accelerating and braking behaviour, the wheel spin degree of freedom is required. Modelling the wheel spin dynamics allows the

calculation of the tyre slip ratio which can be used with the tyre model to determine the longitudinal wheel forces.

As the vehicle accelerations increase modelling load transfer becomes more important to describe the changing normal forces on the tyres. Load transfer can be calculated by steady-state approximations using the lateral and longitudinal accelerations without any additional degrees of freedom [Sharp 2000]. However, to include the dynamic behaviour of these load transfers, roll and pitch need to be modelled. With the two degree of freedom model the vehicle is treated as a point mass. To model roll and pitch, the vehicle can be separated in to a body mass and two axle masses, one for the front axle and one for the rear axle [Crolla, 1991]. The last major vehicle body degree of freedom is vertical acceleration, or heave. This is found in vehicle ride models to evaluate ride comfort and bounce but is not as necessary in some racing car modelling where the tracks are relatively smooth [Siegler, 2002]. Beyond the six vehicle body degrees of freedom, more degrees of freedom can be added to model and analyse specific components. Many vehicle models are created in multi-body dynamics packages, like Adams, with lots of degrees of freedom describing the relationships between suspension or driveline components. However, these additional degrees of freedom rarely have a large impact on the overall vehicle handling behaviour, they are generally used to analyse the interactions of the various modelled components.

3.2. Model Selection and Assumptions

The aim of this research is the control of the limit handling behaviour of race cars. This will be achieved by controlling the yaw and sideslip motion using roll moment distribution and variable torque distribution during high-g manoeuvres. This requires a vehicle model with more detail than the linear bicycle model, which only describes yaw and lateral motion in the linear regime. The limit handling manoeuvres used to evaluate the control strategies result in large accelerations and tyre slips requiring the non-linear Pacejka tyre model. The tyre model includes the ability to model not only slip angles but also longitudinal slip ratios and combined slip. This is necessary since variable torque distribution uses torque inputs at the wheels to create longitudinal tyre forces through slip ratios that modify the yaw moment of the vehicle. This control action occurs during cornering manoeuvres where combined slip will occur.

Modelling the tyre slip ratios created by varying the torque directed to a wheel requires the wheel spin degree of freedom to be included for each driven wheel. This allows the variable torque distribution control action to be translated into slip ratios and tyre longitudinal forces, which result in vehicle yaw moments. Since longitudinal forces are being created by the tyres, the longitudinal degree of freedom must be added to the vehicle model. Not only does this allow the effects of the changing longitudinal tyre forces to be properly modelled, it also allows the investigation of accelerating and braking manoeuvres.

The other control system researched is roll moment distribution. Roll moment distribution relies on altering the roll stiffness at the front and rear axles to control the normal forces on the tyres. This changes the tyre's ability to create lateral and longitudinal forces through the non-linear tyre model. Controlling the roll stiffness changes the roll dynamics of the vehicle, which requires the roll degree of freedom in the vehicle model. The pitch degree of freedom also affects the normal forces on the tyres. Vehicle pitch is important in modelling race cars with aerodynamic aids and ground effects where the distance from the ground greatly affects the amount of downforce created. Pitch dynamics are also important in softly sprung cars with low damping or during ride evaluations. However, the vehicle modelled for this research does not have any aerodynamic aids and is stiffly sprung with high damping. Also, although the evaluation manoeuvres in this research are run with non-constant velocities, longitudinal accelerations are kept small enough that the body pitch dynamics do not greatly affect the tyre normal forces. It is adequate to simply model the longitudinal load transfer using a quasi-static approximation [Sharp, 2000].

Vertical acceleration, or heave, is the final body degree of freedom to model. Heave is usually used to measure passenger comfort in ride evaluations on uneven road surfaces. It is not modelled in this research since the emphasis is on handling evaluations and it is assumed that the simulations are run on an ideal flat surface with a constant coefficient of friction. Without uneven road inputs the heave motion of the vehicle will be minimal and consequently is not of interest in a handling evaluation.

The other assumptions in the model are an ideal engine and drivetrain that produce ideal torque inputs to the torque control devices. This eliminates the very complex engine dynamics that have no noticeable effect on vehicle handling. Also, to simplify the model, no compliance in the chassis, suspension or steering components is

modelled. The final assumption is that no aerodynamic lift or down forces act on the vehicle.

3.3. Eight Degree of Freedom Non-Linear Vehicle Model

The eight degree of freedom non-linear vehicle model is an extension of the linear bicycle model. This model consists of eight degrees of freedom, the longitudinal, lateral, yaw and roll motions as well as the four wheel spin degrees of freedoms and Pacejka non-linear tyres. The coordinate system used by the vehicle model is the SAE standard coordinate system and is shown in Figure 3.1.

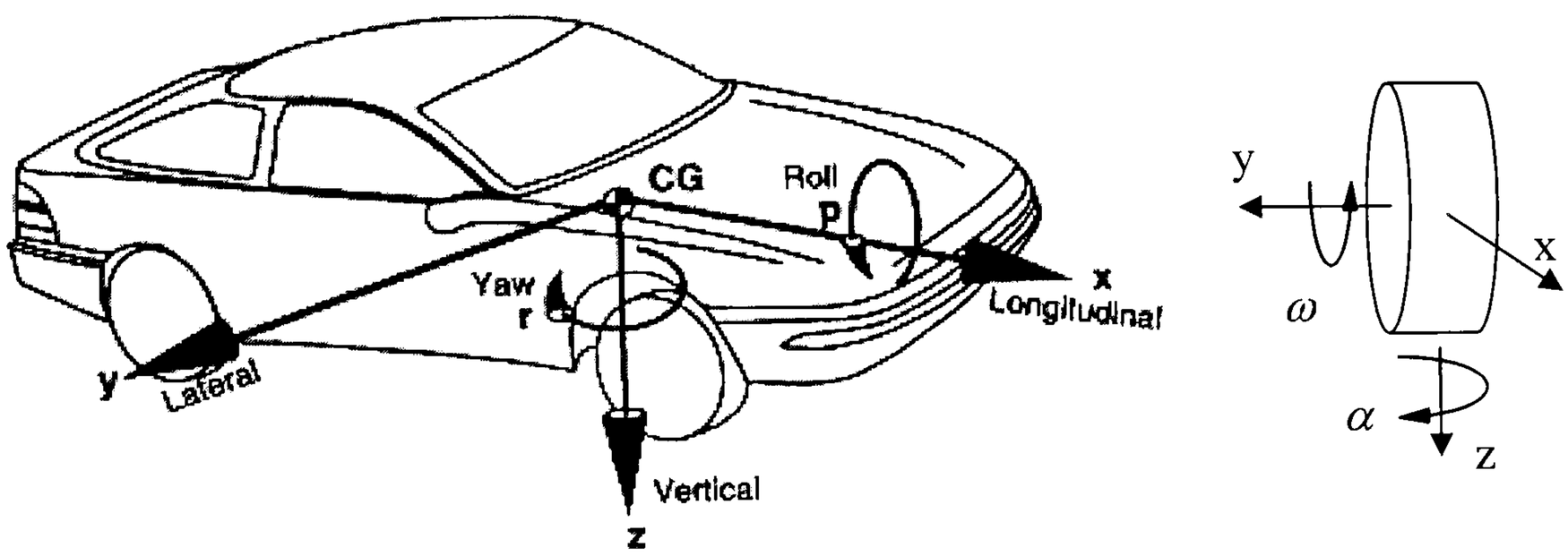

Figure 3.1 Vehicle and wheel coordinate system [He, 2004]

With the vehicle coordinate system defined, the vehicle model takes the form of the block diagram shown in Figure 3.2.

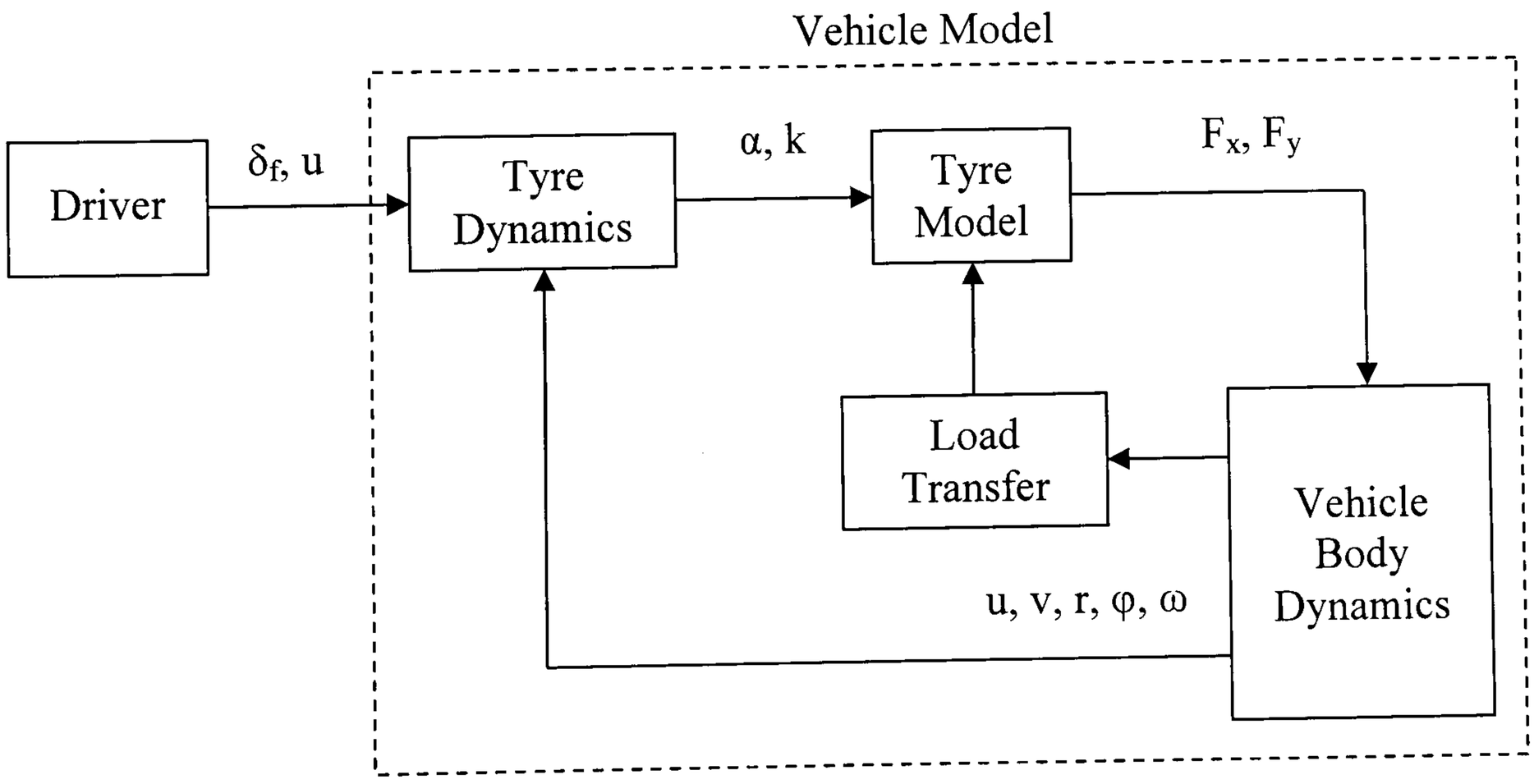

Figure 3.2 Vehicle block diagram

3.3.1. *Vehicle Body Equations of Motion*

The equations describing the balance of forces on the vehicle body are similar to the equations for the bicycle model with the addition of the longitudinal and roll degrees of freedom as shown in Equations (3.1) to (3.4) [Crolla, 1991].

$$M_{tot}\left(\dot{u}-vr\right)=\sum F_x-\frac{1}{2}\rho A_f C_d u^2 \tag{3.1.}$$

$$M_{tot}\left(\dot{v}+ur\right)+m_b h_r\ddot{\phi}=\sum F_y \tag{3.2.}$$

$$I_{zz}\dot{r}+I_{xz}\ddot{\phi}=aF_{yf}-bF_{yr}+t_f\left(F_{xfl}-F_{xfr}\right)+t_r\left(F_{xrl}-F_{xrr}\right) \tag{3.3.}$$

$$\left(K_\phi-m_b g h_r\right)\phi+D_\phi\dot{\phi}+I_{xx}\ddot{\phi}=d_f F_{yf}+d_r F_{yr}-m_b h_r\left(\frac{\sum F_y}{M_{tot}}\right) \tag{3.4.}$$

The nomenclature for these equations is given in the diagrams and the Notation section at the beginning of this thesis. The longitudinal dynamics are predominantly determined by the longitudinal tyre forces. Likewise the lateral dynamics are dominated by the lateral tyre forces with the roll dynamics only playing a minor role in Equation (3.2). The yaw rate in Equation (3.3) is once again dominated by the lateral tyre forces and the yaw moments they create. The longitudinal forces do not contribute as much since the left and right tyres of an axle are usually balanced. The roll dynamics in Equation (3.4) are again dominated by the lateral forces and the roll stiffness. The front and rear scrub derivatives, d_f and d_r, give secondary effects and are defined by the following equations:

$$\begin{aligned} d_f &= h_{cf}-h_a \\ d_r &= h_{cr}-h_a \end{aligned} \tag{3.5.}$$

A graphical representation of the vehicle parameters can be found in Figure 3.3. The blue arrows show forces while the red arrows show velocities. The green arrow shows the direction of motion of the wheel.

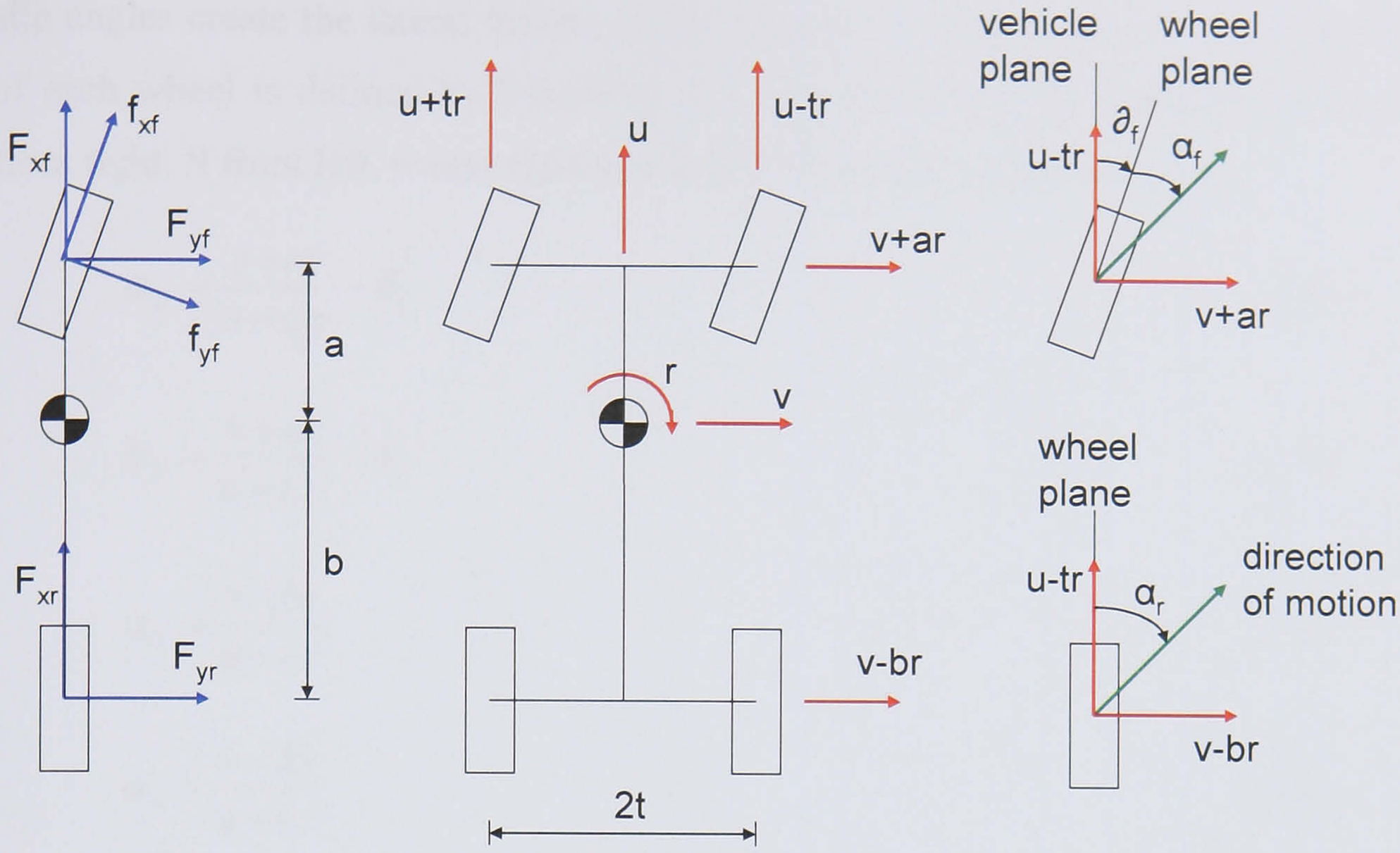

Figure 3.3 Diagram of vehicle parameters

3.3.2. Tyre Model and Dynamics

The tyre model is a non-linear transient "Magic Formula" Pacejka tyre model [Pacejka, 1997]. The required inputs are the vertical load on the tyre, the lateral slip angle and longitudinal slip ratio. For simplification, the camber has been set to zero. This simplification is based on the suspension and tyres modelled. The suspension is relatively stiff and does not allow much wheel travel. This in turn results in minimal camber change due to the working suspension movement. In addition, small changes in the tyre camber angle do not noticeably change the tyre behaviour. With both of these considerations in mind changes in camber angle are not modelled.

Most vehicle handling research focuses on manoeuvres where the vehicle changes direction. The driver input that leads to the vehicle changing directions is through the steering wheel, which turns the front wheels and creates slip angles at the tyres. These

slip angles create the lateral forces, which change the vehicle motion. The slip angle of each wheel is defined by Equations (3.6) to (3.9) where the subscript fr denotes front right, fl front left, rr rear right and rl rear left and δ_f is the steer angle.

$$\alpha_{fr} = \frac{v + ar}{u - t_f r} - \delta_f \tag{3.6.}$$

$$\alpha_{fl} = \frac{v + ar}{u + t_f r} - \delta_f \tag{3.7.}$$

$$\alpha_{rr} = \frac{v - br}{u - t_r r} \tag{3.8.}$$

$$\alpha_{rl} = \frac{v - br}{u + t_r r} \tag{3.9.}$$

The lateral force generated by the slip angle at four different normal forces is shown in Figure 3.4. Due to the sign convention adopted in this research and described at the start of Section 3.3, a positive slip angle will create a negative lateral force.

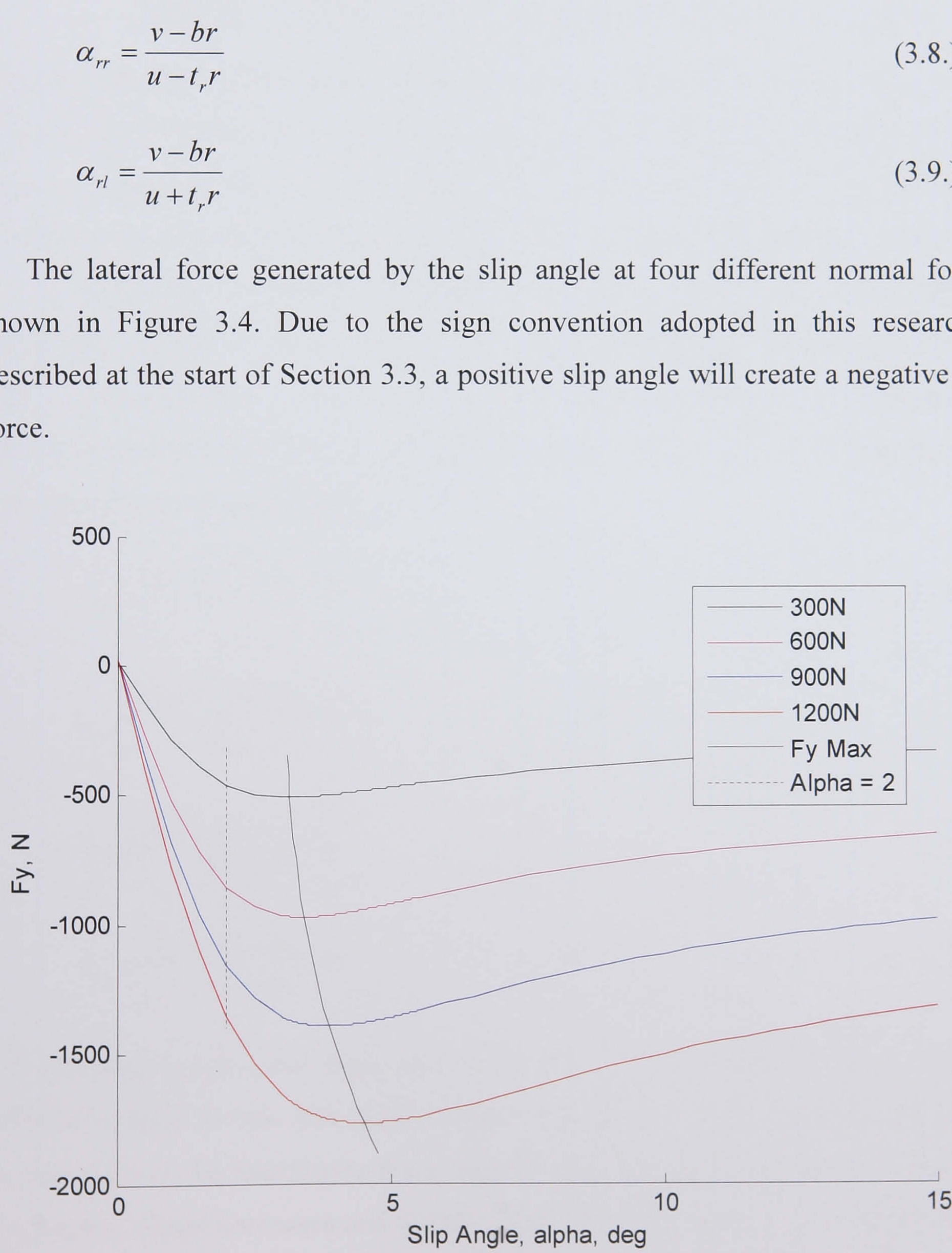

Figure 3.4 Lateral force as a function of slip angle for increasing normal force

The plot shows that as the normal force increases two things happen. First, for a constant slip angle as the normal force increases, the gain in lateral force decreases. So a tyre with double the normal force will generate less than double the lateral force. For example, Table 3.1 shows the lateral forces at a slip angle of 2.0 degrees.

Normal Force (N)	300	600	1200
Lateral Force (N)	460	854	1350
Normalised Force	1.53	1.42	1.13

Table 3.1 Lateral force at a constant slip angle of 2.0 degrees

The second observation is that as the normal force increases, the slip angle at which the maximum lateral force occurs also increases. The tyre can tolerate a larger slip angle at larger normal forces, or presented in another way, a larger slip angle is required to get the maximum potential out of the tyre as the normal force increases.

To change the longitudinal behaviour of the vehicle the driver uses the brakes or accelerator. Either of these controls will input an additional torque into the wheel trying to speed it up or slow it down creating longitudinal slips. It is these slip ratios that create the tyre forces that allow acceleration and braking. The longitudinal slip ratio at each wheel is given by:

$$k_{fr} = \frac{(u - t_f r) - (\omega_{fr} r_\omega)}{u - t_f r} \tag{3.10.}$$

$$k_{fl} = \frac{(u + t_f r) - (\omega_{fl} r_\omega)}{u + t_f r} \tag{3.11.}$$

$$k_{rr} = \frac{(u - t_r r) - (\omega_{rr} r_\omega)}{u - t_r r} \tag{3.12.}$$

$$k_{rl} = \frac{(u + t_r r) - (\omega_{rl} r_\omega)}{u + t_r r} \tag{3.13.}$$

The resulting longitudinal force due to the slip ratio is shown in Figure 3.5 at four different normal forces. The similar trends can be seen in the longitudinal tyre force as were seen in the lateral tyre force. Again, with increasing normal force the gain in longitudinal force decreases and the slip ratio where the maximum longitudinal force occurs also increases. However, the effects are not as dramatic as they where with the

lateral force, as shown in Table 3.2. This results in a more linear behaviour in the longitudinal tyre dynamics with respect to the normal force.

Normal Force (N)	300	600	1200
Longitudinal Force (N)	395	787	1560
Normalised Force	1.32	1.31	1.30

Table 3.2 Longitudinal force at a constant slip ratio of 0.1

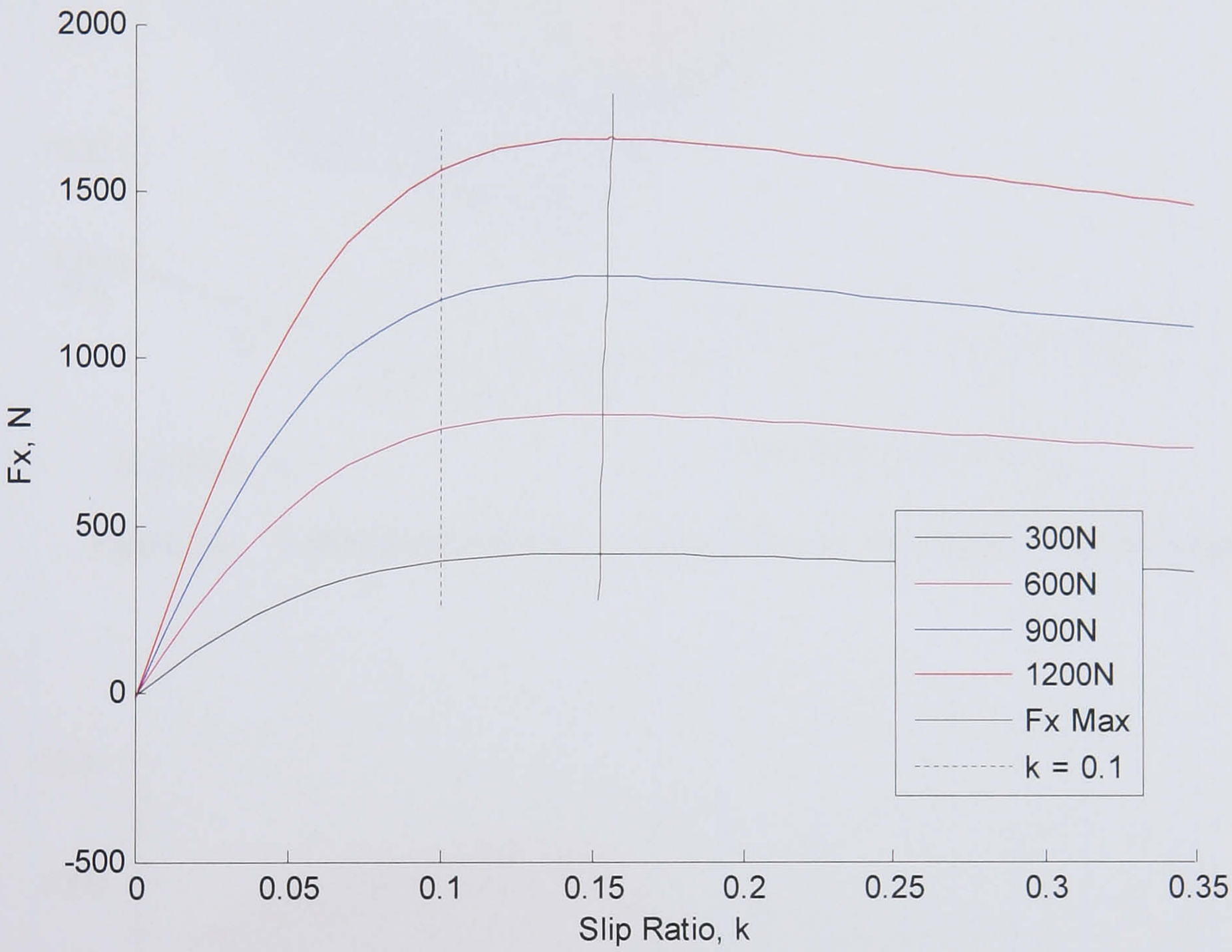

Figure 3.5 Longitudinal force as a function of slip ratio for increasing normal force

When both steering and torque input are given to a wheel a combined effect of slip angle and slip ratio is observed. The combined tyre properties from the Pacejka "Magic Formula" tyre model can be seen in Figure 3.6 and Figure 3.7. The lateral force and the longitudinal force given by the tyre is plotted against the longitudinal slip ratio and the slip angle. The effects of combined slip degrading the overall performance can be seen. If a tyre is at a constant slip angle, as the slip ratio increases the lateral tyre force generated decreases. The same is true of a tyre at constant slip ratio. If the slip angle increases while the slip ratio is constant the longitudinal force decreases.

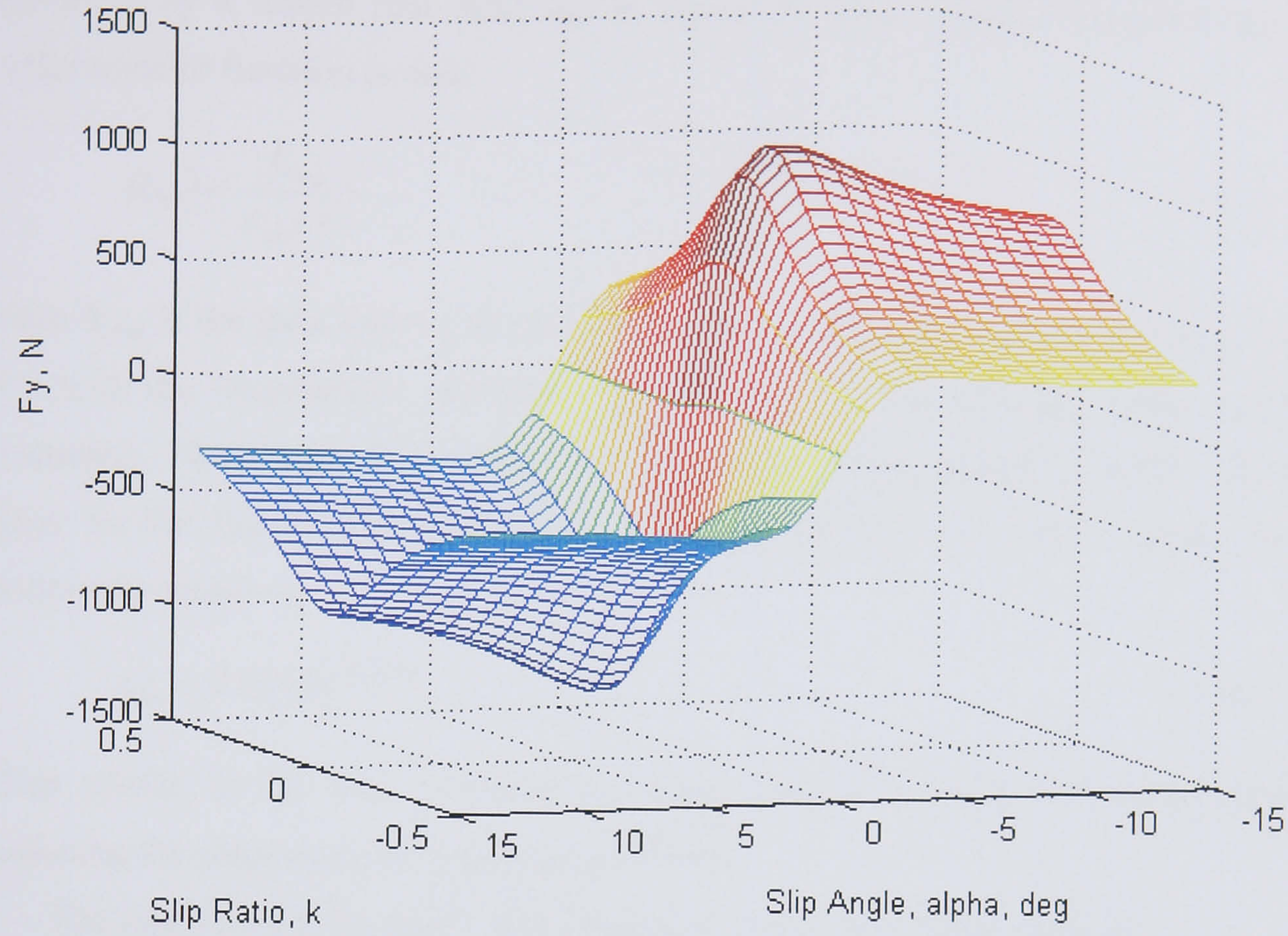

Figure 3.6 Lateral tyre force as a function of slip ratio and slip angle

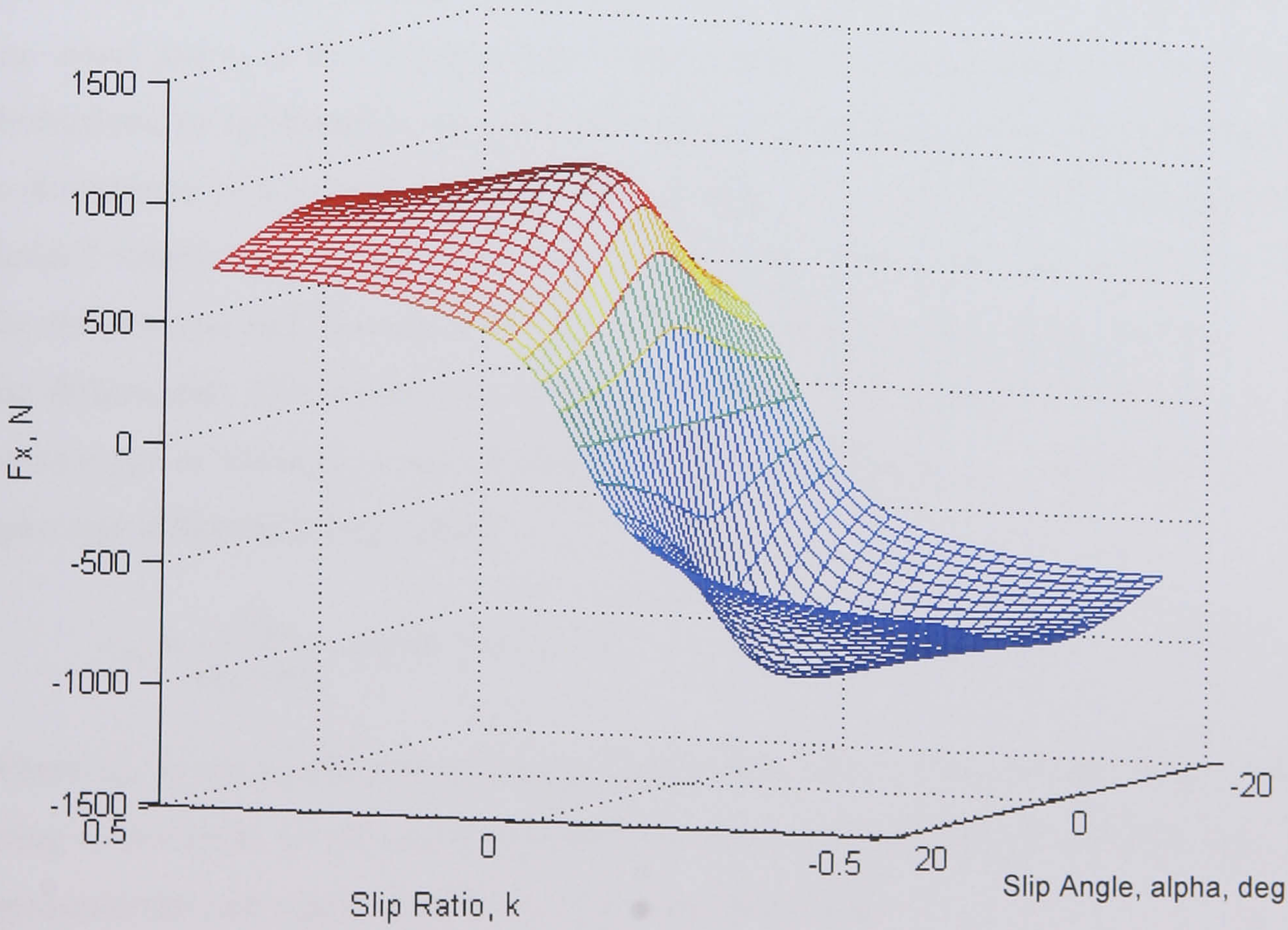

Figure 3.7 Longitudinal tyre force as a function of slip ratio and slip angle

A tyre lag is included on the longitudinal and lateral tyre forces. This can be modelled by a simple first order lag as shown by [Hou, 2001]. The following first order transfer function is used:

$$H(s) = \frac{K_{lag}}{\tau_{lag} s + 1} \tag{3.14.}$$

Here K_{lag} is the gain and τ_{lag} is the time constant. The same transfer function is used for both the longitudinal and lateral tyre forces but with different gains and time constants. The longitudinal gain is 1.0 and the lag time constant is 0.001 while the gain for the lateral tyre force lag is 0.75 and the time constant is given by the following equation:

$$\tau_{lag} = 0.0163 e^{-0.0253u} \tag{3.15.}$$

This results in the time constant becoming smaller at higher velocities, thereby reducing the response time [Samsundar, 1999].

The equation for the wheel spin dynamics of each individual wheel is:

$$I_\omega \dot{\omega}_\omega = T_{in} - F_x r_\omega \tag{3.16.}$$

where T_{in} is the input torque from either engine or brakes, I_ω is the rolling inertia of the wheel and r_ω is the rolling radius of the wheel. The input torque to each wheel is determined by splitting the overall torque through the differentials. The overall torque is determined by a velocity control that determines the torque required to maintain the desired vehicle speed as described in Section 3.3.4. This torque is then split through the differentials and directed to the wheels with a coefficient of torque distribution for the differential. This coefficient is either determined by an open differential for the passive car or through a control algorithm. The equation for the torque split for the open rear differential is given by:

$$c_{D_r} = \frac{\omega_{rr}}{\omega_{rr} + \omega_{rl}} \text{ where } 0 \le c_{D_r} \le 1 \tag{3.17.}$$

Where c_{Dr} is the coefficient of torque distribution with 1 representing all the torque going to the right wheel and 0 representing all the torque going to the left wheel. rr represents the rear right wheel and rl is the rear left wheel.

3.3.3. Roll and Load Transfer Equations

The roll stiffness is determined from the tyre stiffness, the spring stiffness and the suspension geometry [Milliken, 1995]. The front wheel rate is given by:

$$K_{wheel_f} = K_{spring_f} IR_f^{\,2} \tag{3.18.}$$

where $K_{springf}$ is the front spring rate and IR_f is the front installation ratio (the ratio of spring movement to wheel movement) of the suspension. The rear wheel rate is calculated in the same way but with the rear spring rate and rear installation ratio. The front spring roll rate at the wheel and the front tyre roll rate at the wheel are given by:

$$K_{\phi S_f} = \frac{1}{2} K_{wheel_f} t_f^{\,2} \tag{3.19.}$$

$$K_{\phi Tyre_f} = \frac{1}{2} K_{tyre} t_f^{\,2} \tag{3.20.}$$

Again the rear roll rates will be calculated in the same way but with the rear track width, wheel rate and tyre rate. Finally the front roll rate is determined by:

$$K_{\phi_f} = \frac{K_{\phi Tyre_f}\left(K_{\phi S_f} + K_{antiroll_f}\right)}{K_{\phi Tyre_f} + K_{\phi S_f} + K_{antiroll_f}} \tag{3.21.}$$

where $K_{antirollf}$ is the roll stiffness of the front roll bar. Again the rear roll rate is calculated in the same way and can be used to determine the roll moment distribution given by:

$$c_{Kd} = \frac{K_{\phi_f}}{K_{\phi_f} + K_{\phi_r}} \tag{3.22.}$$

Although there are no pitch or heave degrees of freedom in the model, the vertical load on the tyres is dependent on load transfer due to roll and lateral and longitudinal accelerations. The load on each tyre is defined as:

$$F_{zfr} = \frac{1}{2}\left(\frac{bM_{tot}g}{a+b} - \frac{M_{tot}h\dot{u}}{a+b}\right) + 2\phi K_{\phi f} t_f \tag{3.23.}$$

$$F_{zfl} = \frac{1}{2}\left(\frac{bM_{tot}g}{a+b} - \frac{M_{tot}h\dot{u}}{a+b}\right) - 2\phi K_{\phi f} t_f \tag{3.24.}$$

$$F_{zrr} = \frac{1}{2}\left(\frac{aM_{tot}g}{a+b} + \frac{M_{tot}h\dot{u}}{a+b}\right) + 2\phi K_{\phi r} t_r \tag{3.25.}$$

$$F_{zrl} = \frac{1}{2}\left(\frac{aM_{tot}g}{a+b} + \frac{M_{tot}h\dot{u}}{a+b}\right) - 2\phi K_{\phi r} t_r \tag{3.26.}$$

Aerodynamic drag and lift are not taken into account on the tyre load.

3.3.4. Longitudinal Velocity Driver Model

There is also a longitudinal velocity controller, which acts as a driver model to maintain the desired speed profile of the vehicle during the test manoeuvres. The speed controller is a proportional, integral (PI) control given by the following equation:

$$\begin{aligned} throttle &= G_{pt}(u_{desired} - u) + G_{it}\int(u_{desired} - u)dt \\ u_{desired} &= u_0 + u_{input} \end{aligned} \tag{3.27.}$$

Here *throttle* is a signal that multiplies the maximum available engine torque to give the torque available to be distributed to the wheels. It is limited by a saturation function to values between -1.0 and 1.0 to include both braking and accelerating. G_{pt} and G_{it} are the proportional and integral gains and $u_{desired}$ is made of an initial velocity, u_0, and an input velocity, u_{input}, that can be a step or ramp function.

3.4. Model Validation

The vehicle model is coded in the Matlab and Simulink environment. To validate the vehicle model, it is compared to a model in the CarSim environment with the same vehicle dataset provided from the University of Leeds Formula Student race car [Siegler, 2002]. A problem with validating the Matlab model to a commercially developed vehicle dynamics package like CarSim is that there is no control over how CarSim operates and what degrees of freedom are used. More importantly, the method used to model the tyre is not well documented. This lack of knowledge and control over the CarSim vehicle model is particularly frustrating when trying to determine the reasons for any inconsistencies.

Since the vehicle model is a continuous loop, a point must be chosen to break the loop and begin describing it. The tyres are the start of the dynamic system in the vehicle model. They are also the most complex part of the vehicle system to model

and if the tyre forces are modelled correctly then all the vehicle motions are simply mathematical manipulations of these forces. For this reason the outputs of the tyre model will be considered first. Then the validation will look at the body motions and end with the inputs to the tyre model. The tyre model used in CarSim is basically a modified linear tyre model. There is a cornering stiffness map for the vertical force on the tyre that gives a mapped cornering stiffness for a given vertical force. However, given a steady state vertical force it appears that the lateral force just has a linear relationship to the steer angle. This is a much simpler tyre model than the full non-linear Pacejka tyre model used in the Matlab model.

The first comparison will be of the lateral tyre forces given in Figures 3.8-3.10 and Tables 3.3-3.5. In the tables, the C denotes the CarSim data while the M denotes the Matlab model. The manoeuvre represented is a constant velocity step steer at three different velocities and steer angles. The step steer manoeuvre is chosen to validate the vehicle model and tune the tyre lag since the transient as well as the steady state behaviour is represented. The data from CarSim is not very smooth. This is due to the data sampling rate which is set by the software. As shown in the figures and tables, the steady state values of lateral force of the Matlab model match the results from the CarSim simulations.

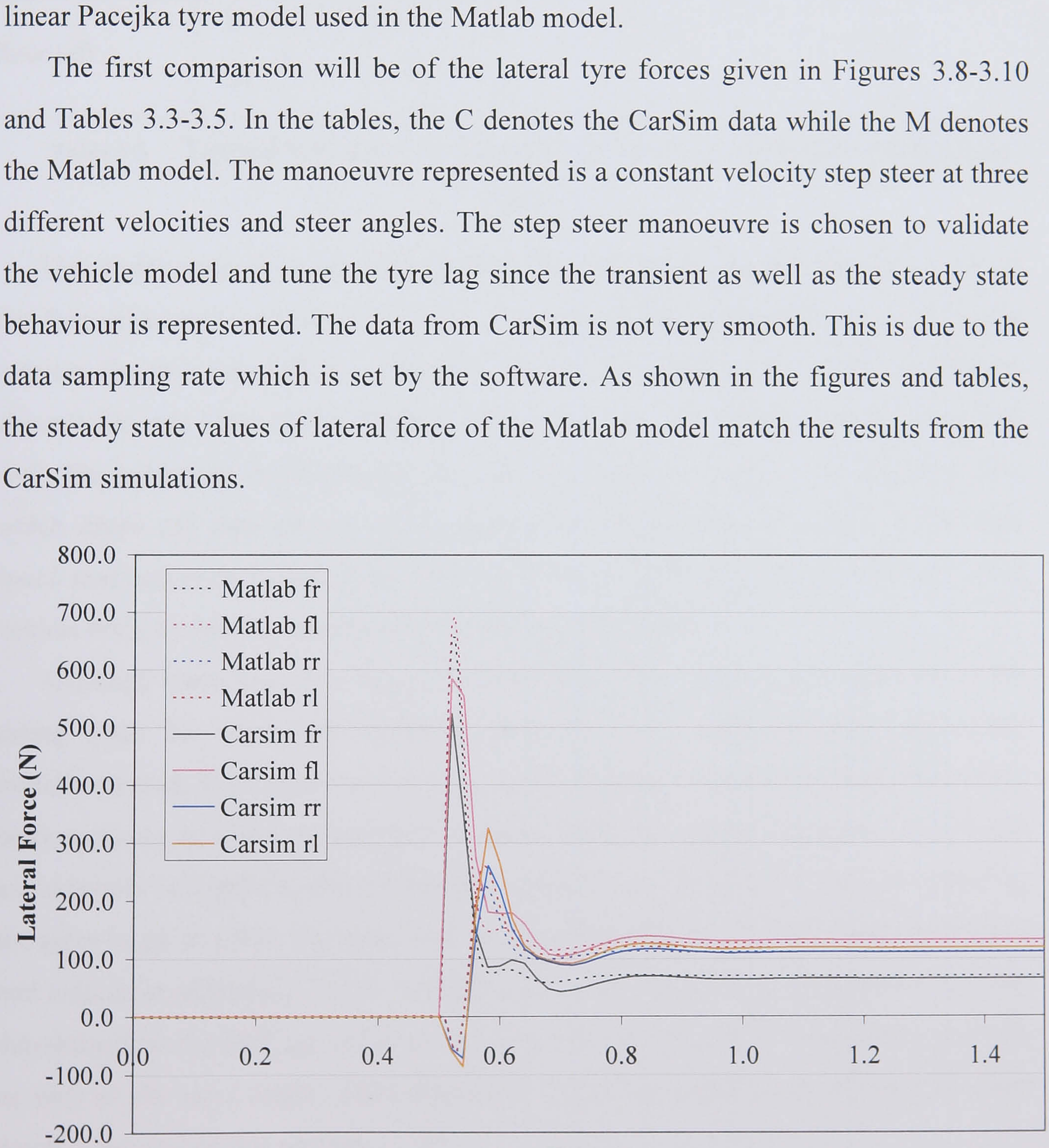

Figure 3.8 Lateral tyre force for a 6.94 m/s, 3.0 deg step steer

Tyre	C/M	Overshoot Ratio	Steady State (N)	Steady State Error (%)
Front right	C	7.06	65	7.7
	M	8.37	70	
Front left	C	3.42	132	3.8
	M	4.45	127	
Rear right	C	1.34	111	0.0
	M	1.04	111	
Rear left	C	1.73	119	0.0
	M	1.18	119	

Table 3.3 Lateral tyre force transient properties for a 6.94 m/s, 3.0 deg step steer

The steady state error is generally less than 4% except for the right front tyre in the first manoeuvre where it is 7.7%. Also, the transient response is very similar between the two simulations. Although there are not enough data points to properly observe the rise time in the CarSim simulations, the overshoot percentages match well. The behaviour is characterised by an initial spike in the front tyre lateral forces, which drops off then slowly builds again. This is particularly evident in the high speed manoeuvre in Figure 3.10. This is due to the difference in the relatively slow vehicle body dynamics compared to the quicker tyre dynamics.

Although there is a tyre lag, it is quite small due to the quick reactions of the racing tyres. So, observing Equations (3.6) and (3.7), when the front wheels are initially steered, δ_f increases and the slip angles increase more rapidly than the vehicle body motions, u, v and r, leading to a spike in the slip angle. This spike in the slip angle results in a spike in the lateral force. However, as the lateral forces generated by the tyres begin to affect the body motion, the vehicle body dynamics take precedence and reduce the slip angle. As the vehicle reaches the steady state the lateral forces are determined by the balance of lateral velocity and yaw rate in the slip angle equations as well as the steer angle. The calculation of the slip angles is considered in more detail at the end of this section.

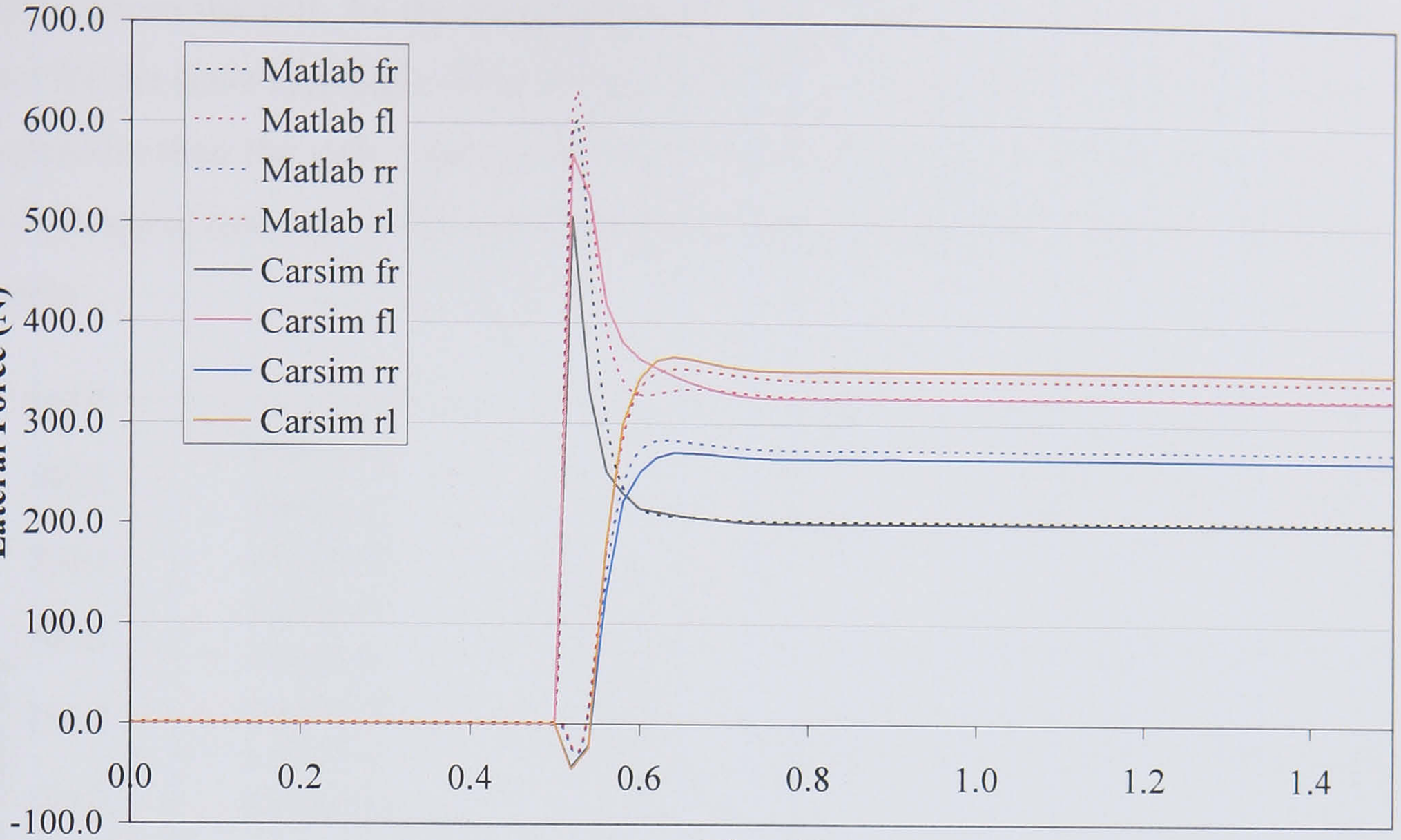

Figure 3.9 Lateral tyre force for a 13.89 m/s, 2.0 deg step steer

Tyre	C/M	Overshoot Ratio	Steady State (N)	Steady State Error (%)
Front right	C	1.52	201	1.0
	M	1.97	203	
Front left	C	1.51	226	0.4
	M	1.79	227	
Rear right	C	0.02	265	3.4
	M	0.03	274	
Rear left	C	0.04	352	2.6
	M	0.03	343	

Table 3.4 Lateral tyre force transient properties for a 13.89 m/s, 2.0 deg step steer

The subsequent second rise in lateral force, seen in the higher speed manoeuvre in Figure 3.10, is caused by the roll dynamics and lateral load transfer. The roll and lateral dynamics are the dynamics of the body which has a large inertia compared to the tyres. Due to this large inertia the roll and lateral dynamics are slower than the tyre dynamics. The body motions depend on the tyre forces building up and working through the tyres, suspension and body, which creates the body lateral accelerations

which induce the roll. As the outside tyres become loaded they produce more lateral force for the same slip angle. This is why the left tyre lateral forces build up to greater magnitudes than the right tyres as the manoeuvre progresses. This is most evident in the high speed manoeuvre since the low speed manoeuvres do not create as much load transfer.

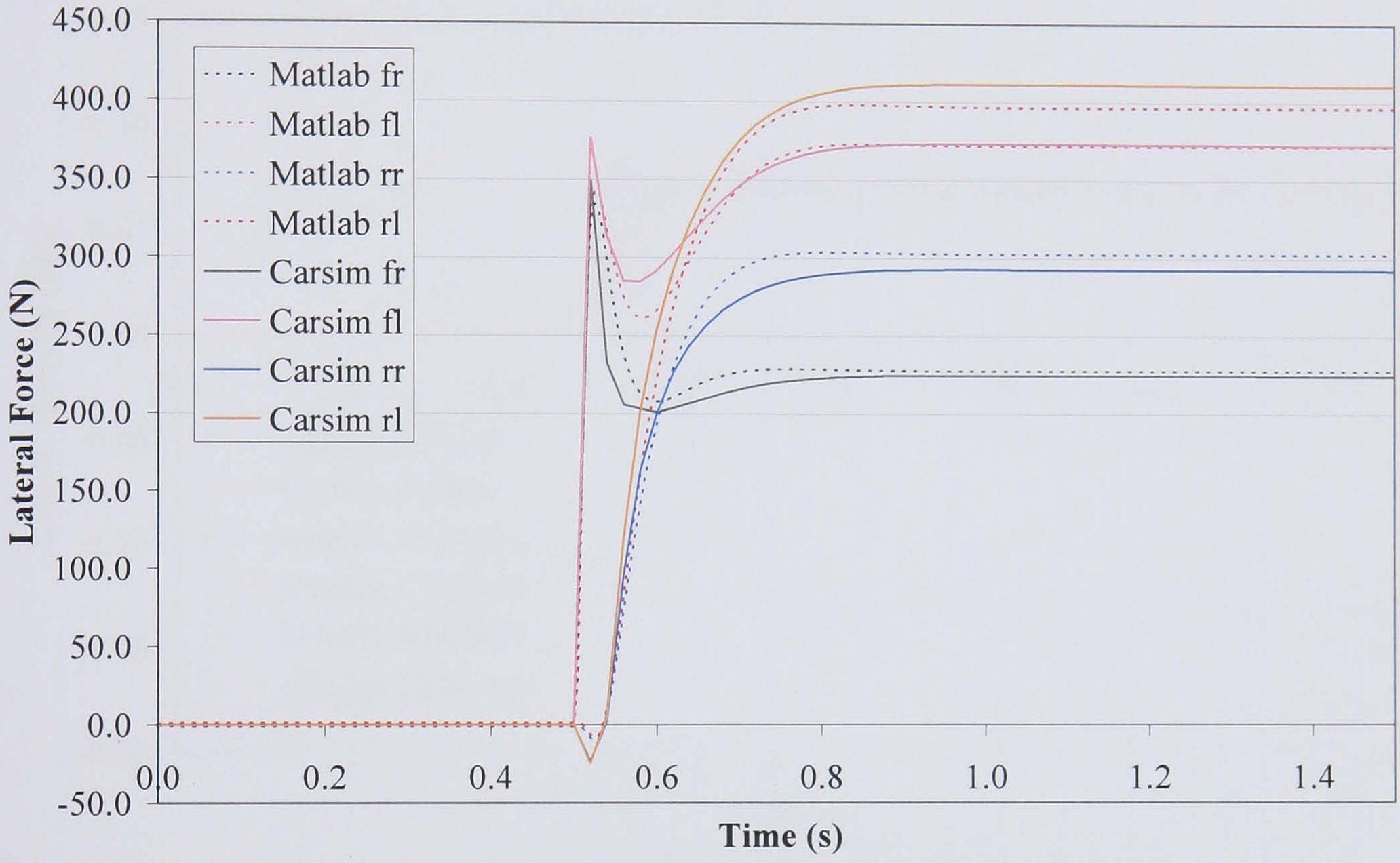

Figure 3.10 Lateral tyre force for a 20.83 m/s, 1.0 deg step steer

Tyre	C/M	Overshoot Ratio	Steady State (N)	Steady State Error (%)
Front right	C	0.56	224	1.3
	M	0.48	227	
Front left	C	0.01	372	0.0
	M	0	372	
Rear right	C	0	292	3.4
	M	0	302	
Rear left	C	0	410	3.2
	M	0	397	

Table 3.5 Lateral tyre force transient properties for a 20.83 m/s, 1.0 deg step steer

The vehicle body motion follows from the tyre forces. Figures 3.11-3.13 and Tables 3.6-3.8 show a comparison of lateral velocity, yaw rate and roll angle for three constant velocity step steer manoeuvres. All the manoeuvres are run at a steer angle of 1.5 degrees but with varying velocities, 6.94 m/s, 13.89 m/s and 20.83 m/s which correspond to 25 km/h, 50 km/h and 75 km/h respectively.

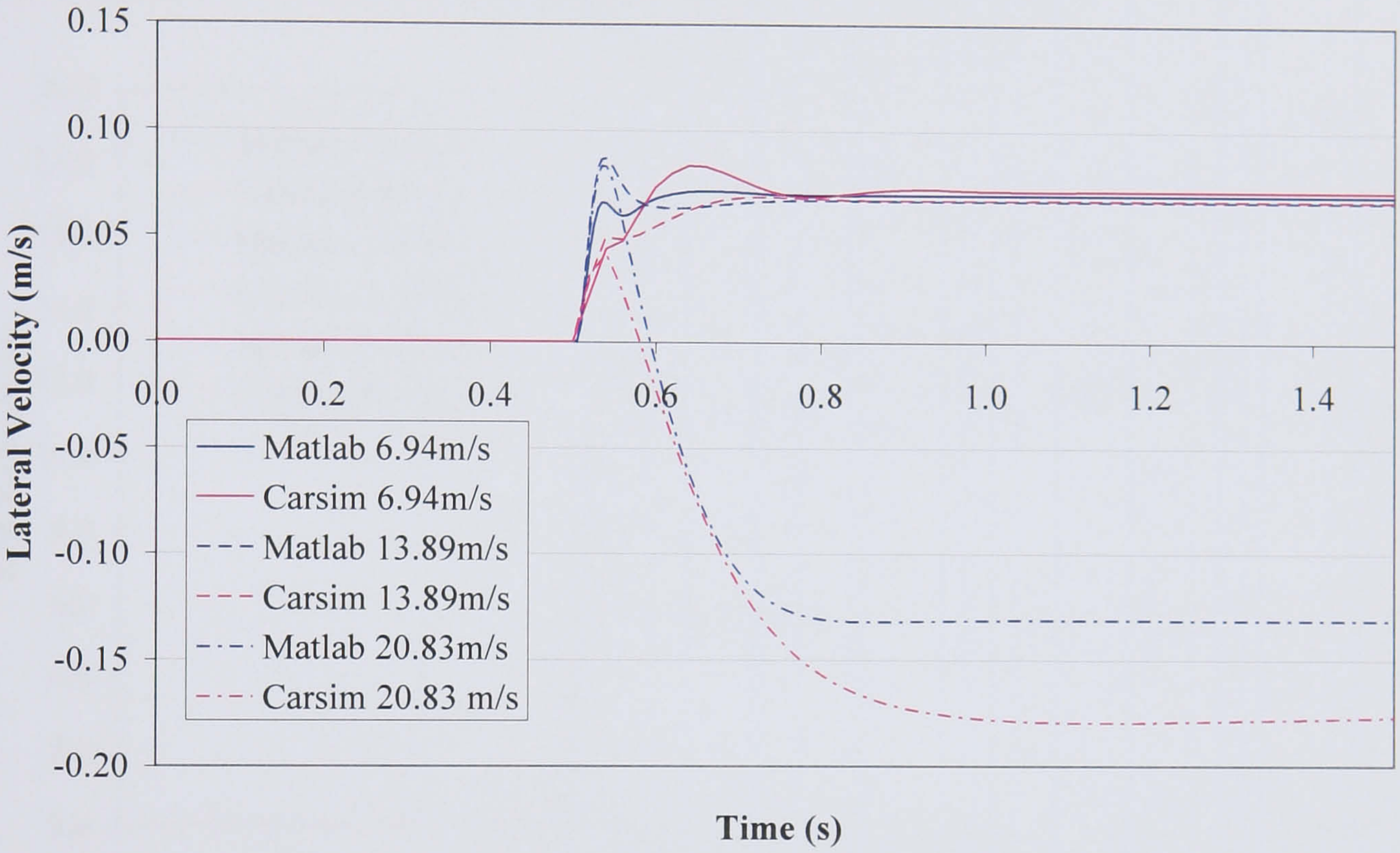

Figure 3.11 Lateral velocity for a 1.5 degree step steer

Velocity (m/s)	C/M	63% Rise Time (s)	Overshoot (%)	Steady State Error (%)
6.94	C	0.05	16.2	2.6
	M	0.02	2.3	
13.89	C	0.04	1.8	0.5
	M	0.02	29.4	
20.83	C	0.20	1.3	26.0
	M	0.16	0.6	

Table 3.6 Lateral velocity transient properties for a 1.5 degree step steer

The vehicle motions of the Matlab model follow the trends and behaviour of the CarSim model. The yaw rate results, shown in Figure 3.12, not only follow the behaviour but also match the steady state values with an overshoot present at the low speed manoeuvres being damped out as the speed increases. This undamped

overshoot comes from the same behaviour found in the lateral tyre forces. In Figure 3.8 the lateral forces show undamped behaviour due to the yaw rate and lateral velocity fighting for dominance in determining the slip angle. The front and rear tyre forces oscillate out of phase causing oscillations in the yaw rate as seen in Equation (3.3). However, in the high speed manoeuvre shown in Figure 3.10 the lateral force is well damped which results in well damped behaviour in the yaw rate.

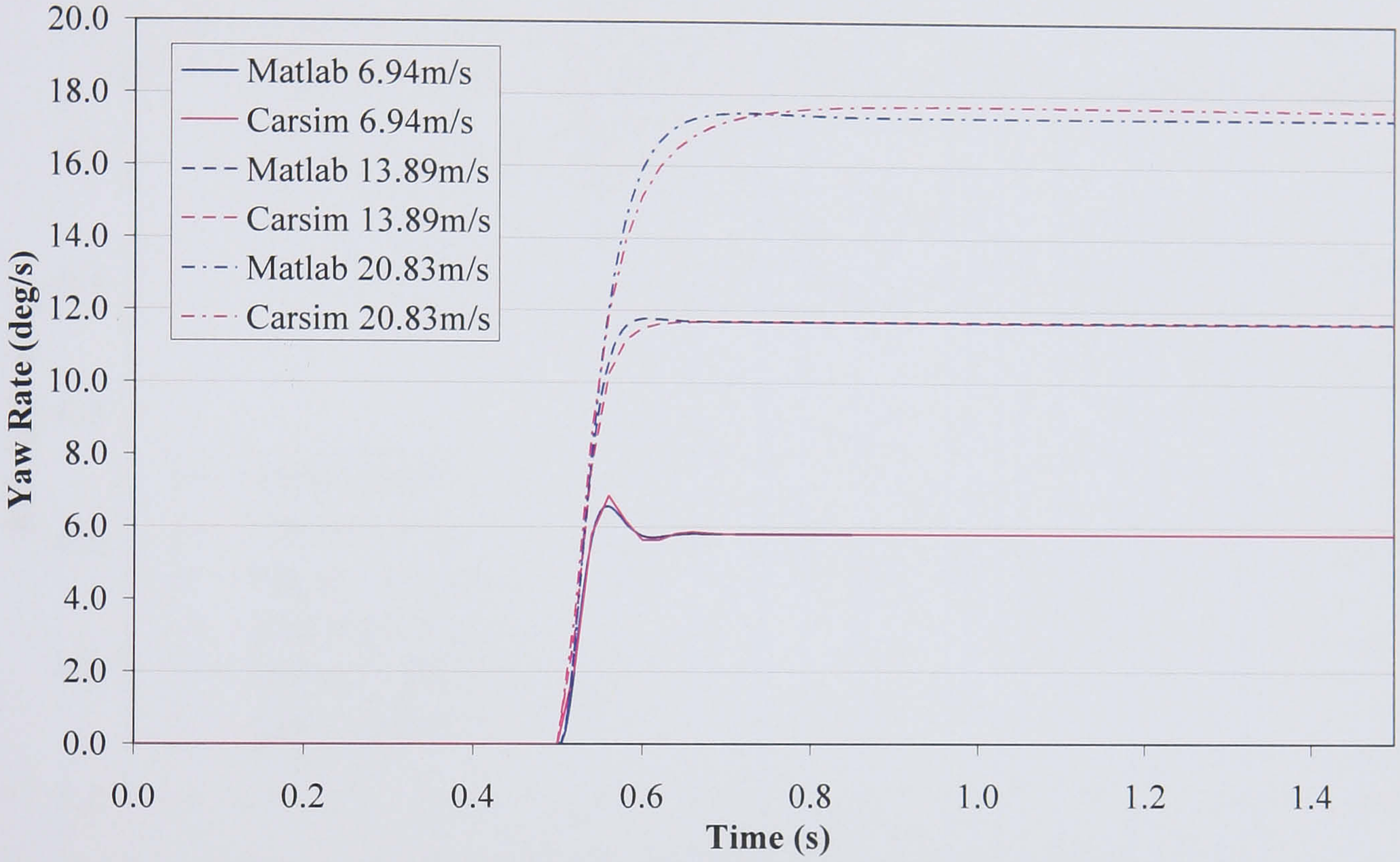

Figure 3.12 Yaw rate for a 1.5 degree step steer

Velocity (m/s)	C/M	63% Rise Time (s)	Overshoot (%)	Steady State Error (%)
6.94	C	0.03	18.2	0.0
	M	0.03	13.3	
13.89	C	0.04	0.1	0.2
	M	0.04	0.7	
20.83	C	0.06	0.4	1.4
	M	0.05	0.6	

Table 3.7 Yaw rate transient properties for a 1.5 degree step steer

The lateral velocities and roll angles do not match as well as the yaw rate. The steady state error of the roll angle is consistently around 12% while the lateral velocity steady state error increases as lateral acceleration increases. This is due to the

small differences in the tyre models and the resulting lateral tyre forces. Any small differences in the tyre forces become compounded when they are integrated to derive the vehicle body motions and result in steady state offsets. These errors are especially prevalent in calculating the roll angle, which requires integrating the tyre forces twice. Despite the larger steady state errors, they still follow the same behaviour with very similar rise times.

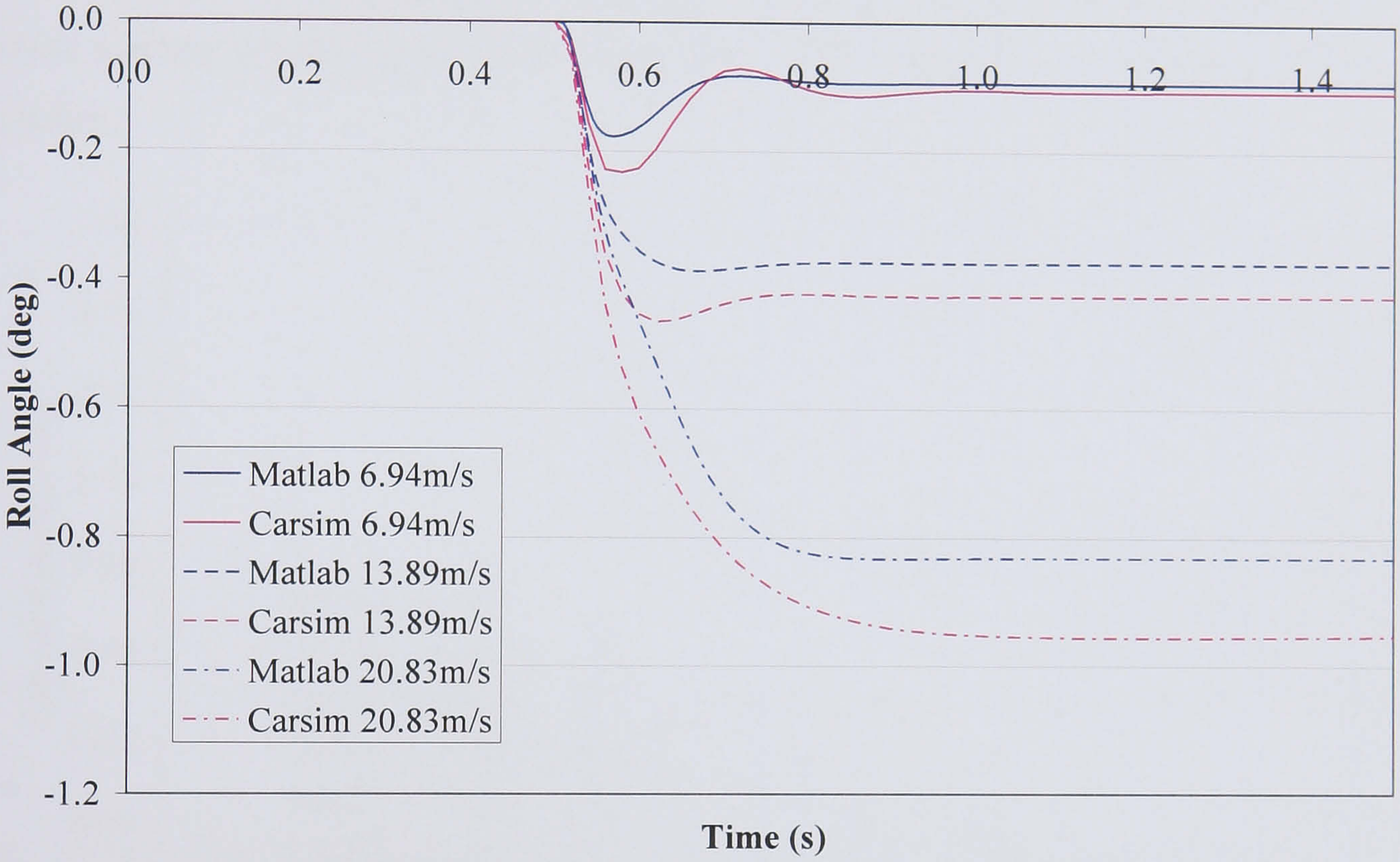

Figure 3.13 Roll angle for a 1.5 degree step steer

Velocity (m/s)	C/M	63% Rise Time (s)	Overshoot (%)	Steady State Error (%)
6.94	C	0.04	120.7	12.4
	M	0.04	92.0	
13.89	C	0.05	9.5	12.1
	M	0.05	3.5	
20.83	C	0.10	0.3	12.8
	M	0.12	0.2	

Table 3.8 Roll angle transient properties for a 1.5 degree step steer

Both the lateral velocity and roll angle also show similar oscillation behaviour to the yaw rate. At low speed they oscillate more than at high speed where they are better damped. This again comes from the lateral tyre forces, which oscillate more at

low speeds. Lateral velocity is proportional to the sum of the lateral forces and roll angle also comes from a balance of the lateral forces and their sum as described in Equations (3.2) and (3.4). Also, since the vehicle body motions are all cross coupled, oscillations in one motion will contribute to oscillations in the other motions.

A further comparison of the vehicle behaviour at different steer angles is shown in Figures 3.14-3.16 and Tables 3.9-3.11. Again, lateral velocity, yaw rate and roll angle are shown but the simulations were carried out at a constant velocity of 13.89 m/s while varying the step steer input magnitude from 1.0 degree to 2.0 degrees and 3.0 degrees.

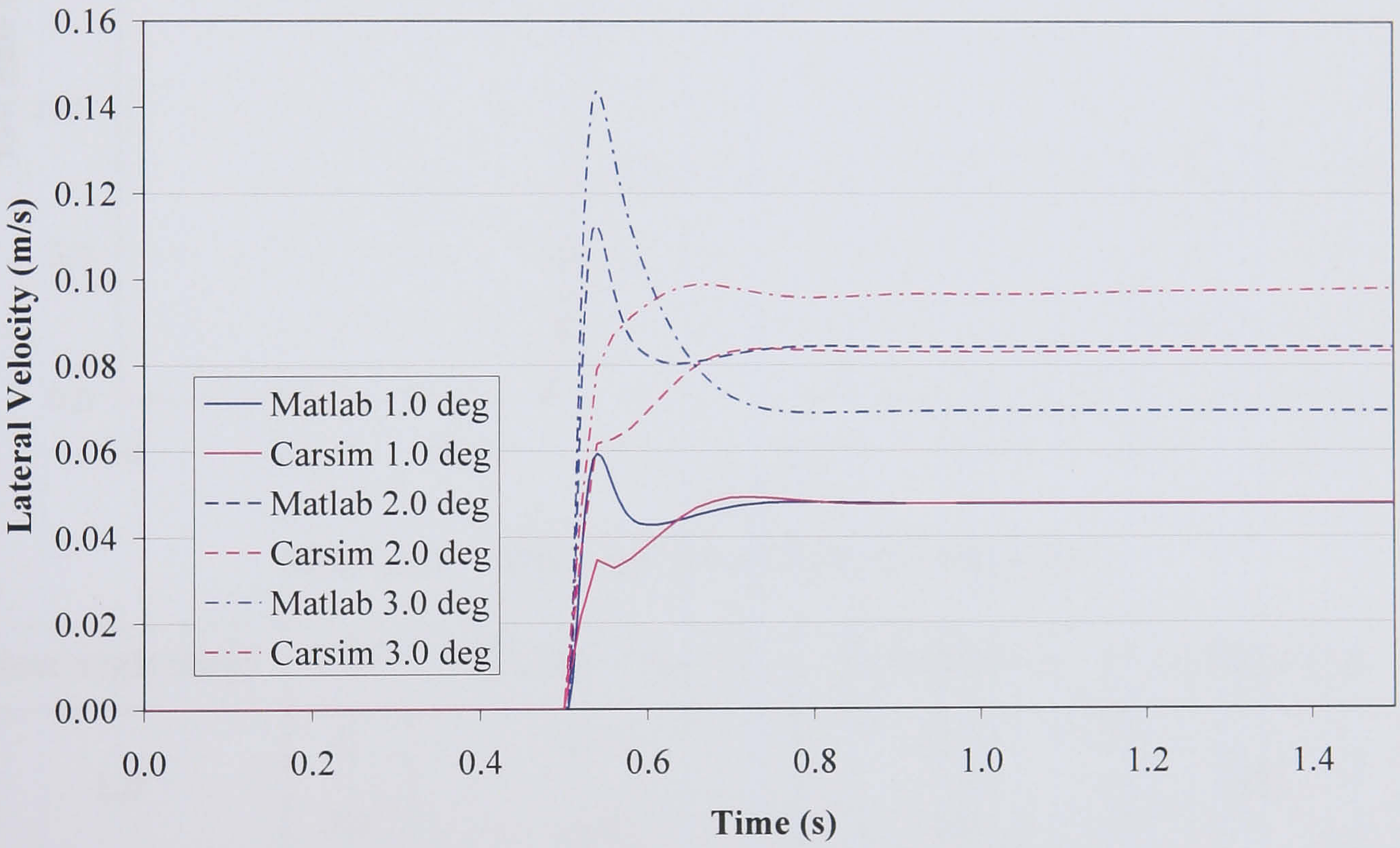

Figure 3.14 Lateral velocity for a 13.89 m/s step steer

Steer angle (deg)	C/M	63% Rise Time (s)	Overshoot (%)	SS Error (%)
1.0	C	0.04	3.0	0.0
	M	0.02	0.7	
2.0	C	0.04	0.5	1.2
	M	0.02	33.9	
3.0	C	0.03	1.0	29.1
	M	0.01	107.5	

Table 3.9 Lateral velocity transient properties for a 13.89 m/s step steer

Again the vehicle behaviour of the Matlab model closely correlates to the CarSim model. Unlike the previous set of result taken at different velocities, these results show similar levels of damping for the different steer angles. The oscillatory behaviour is less dependant on the steer angle than the vehicle velocity.

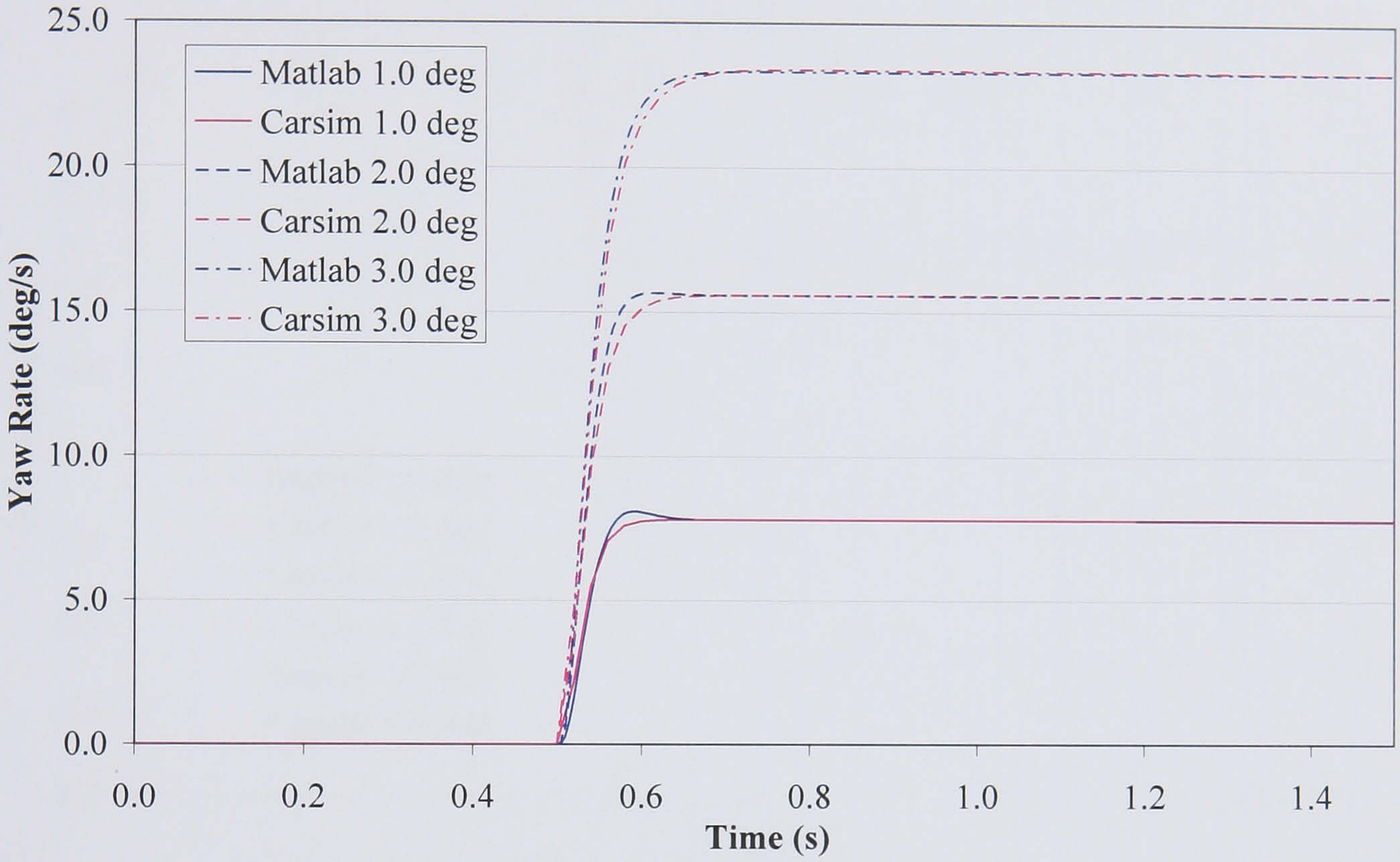

Figure 3.15 Yaw rate for a 13.89 m/s step steer

Steer angle (deg)	C/M	63% Rise Time (s)	Overshoot (%)	SS Error (%)
1.0	C	0.04	0.1	0.0
	M	0.04	3.6	
2.0	C	0.04	0.2	0.0
	M	0.04	0.7	
3.0	C	0.05	0.3	0.0
	M	0.05	-	

Table 3.10 Yaw rate transient properties for a 13.89 m/s step steer

The yaw rate behaviour is very similar to the previous set of results with the behaviour matching well with 0% offset and matching rise times. The roll angle data is also similar to the previous set of results with a 12% offset but matching rise times due to differences in the tyre model that get compounded during integration. This offset is also present in the lateral velocity data, which again varies more at the high

steer angles, up to 30% in these simulations. This is due to a saturation of the tyre model as the manoeuvres become more extreme. The linear nature of the CarSim tyre model does not adequately describe the tyre dynamics of high-g manoeuvres and results in the differences in the lateral velocity behaviour.

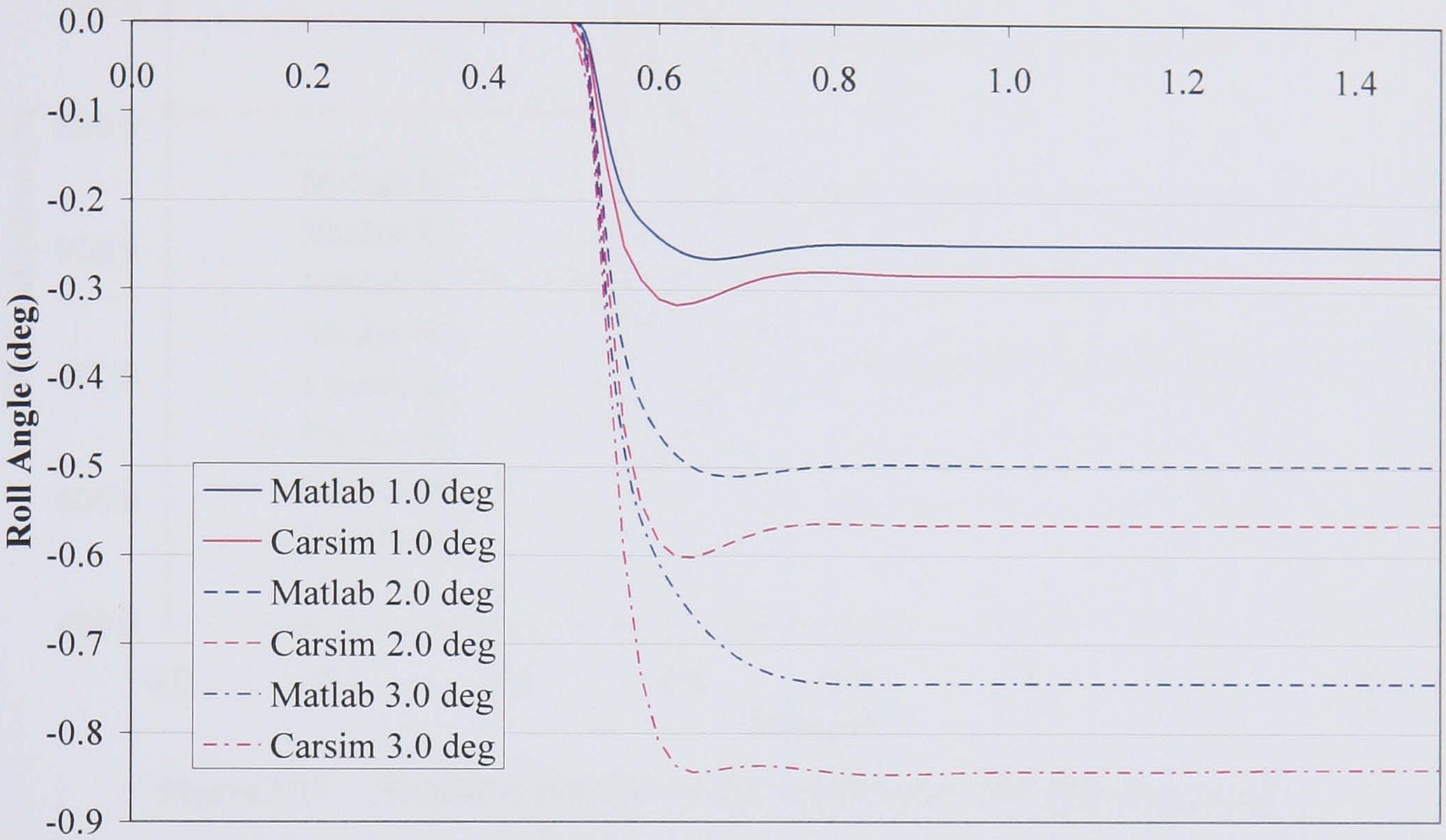

Figure 3.16 Roll angle for a 13.89 m/s step steer

Steer angle (deg)	C/M	63% Rise Time (s)	Overshoot (%)	SS Error (%)
1.0	C	0.04	12.2	12.1
	M	0.05	6.5	
2.0	C	0.05	6.6	11.9
	M	0.05	2.6	
3.0	C	0.06	0.7	11.5
	M	0.06	0.2	

Table 3.11 Roll angle transient properties for a 13.89 m/s step steer

The correlation of the vehicle motion carries over to the vertical forces. Figures 3.17-3.19 and Tables 3.12-3.14 show the vertical tyre forces from the same three manoeuvres depicted in Figures 3.8-3.10, namely step steer manoeuvres at three different velocities and steer angles. Again the steady state response of the tyres closely matches between the Matlab model and CarSim model with less than 5%

steady state error. This is despite the differences in the steady state roll angle on which the normal forces are very dependant as shown in Equations (3.23) – (3.26).

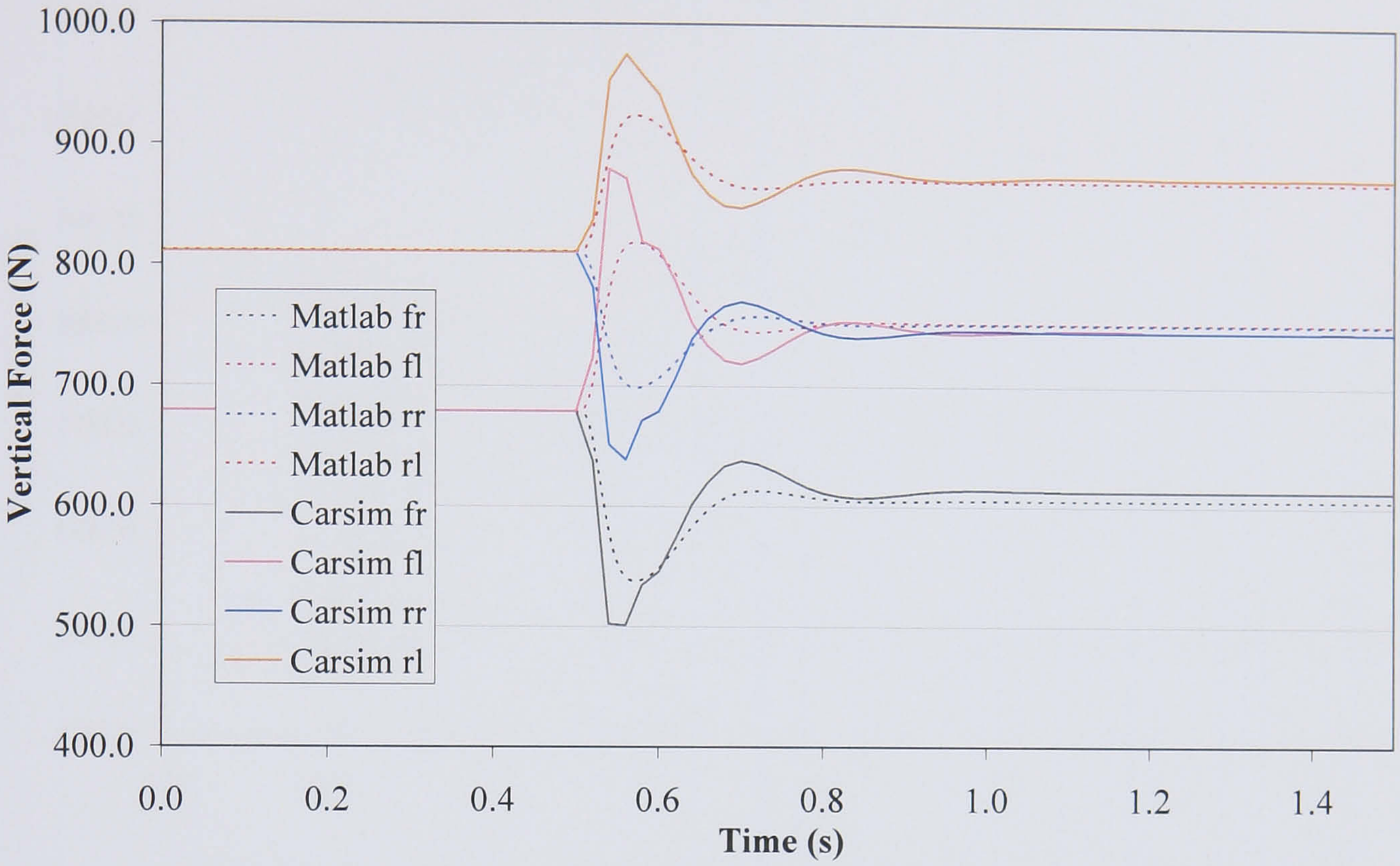

Figure 3.17 Vertical tyre force for a 6.94 m/s, 3.0 deg step steer

Tyre	C/M	63% Rise Time (s)	Overshoot (%)	Steady State Error (%)
Front right	C	0.02	18.4	1.3
	M	0.03	11.2	
Front left	C	0.02	9.7	0.8
	M	0.03	16.9	
Rear right	C	0.02	14.3	0.8
	M	0.03	7.1	
Rear left	C	0.02	11.6	0.3
	M	0.03	6.2	

Table 3.12 Vertical tyre force transient properties for a 6.94 m/s, 3.0 deg step steer

The transient behaviour also matches well with the rise times. Again, there are more oscillations at lower speed, which come from the undamped roll angle at low speed, as shown in Figure 3.13, but there is also some variation in the behaviour.

There appears to be a step in the initial rise in the CarSim model that is more damped in the Matlab simulation.

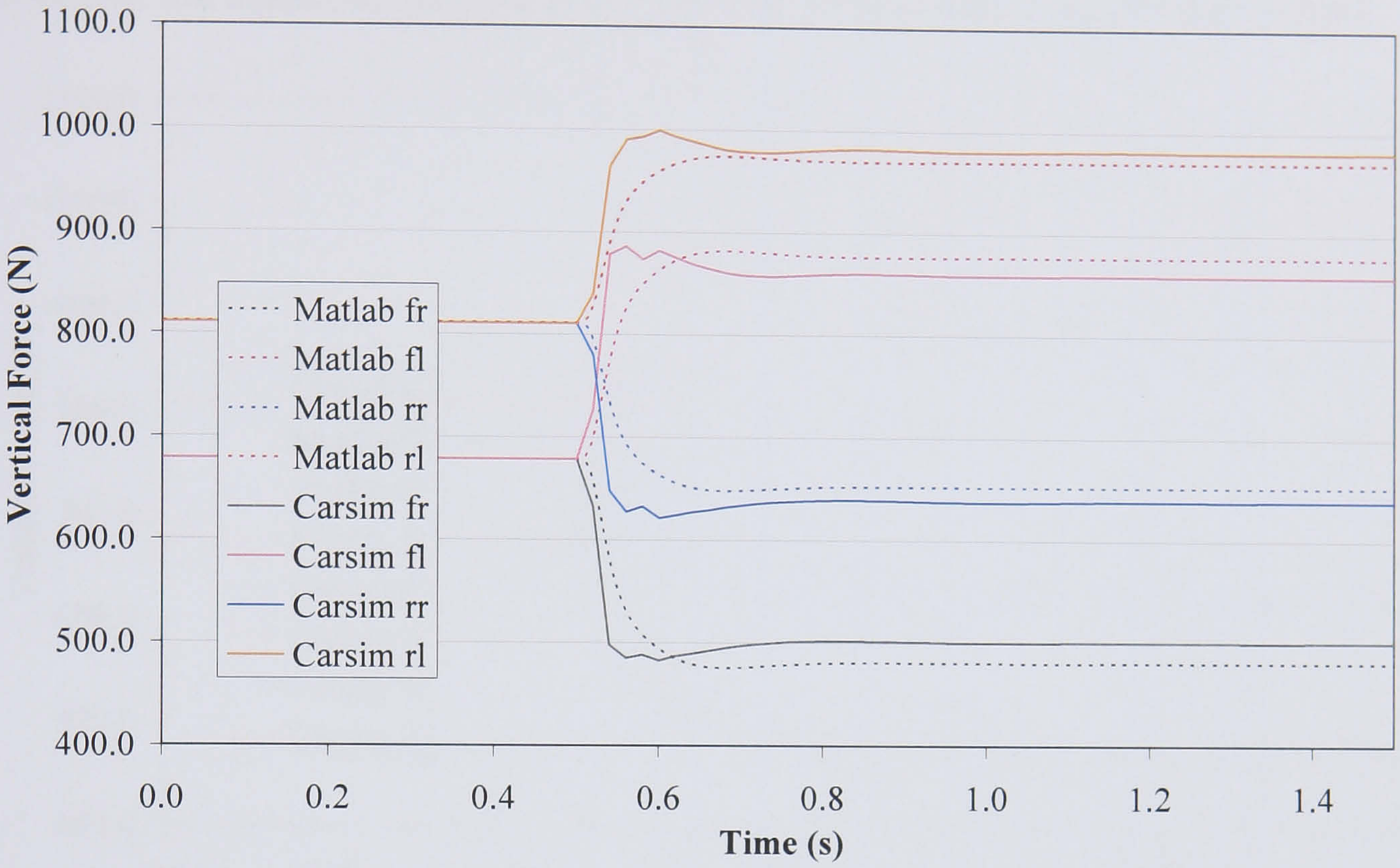

Figure 3.18 Vertical tyre force for a 13.89 m/s, 2.0 deg step steer

Tyre	C/M	63% Rise Time (s)	Overshoot (%)	Steady State Error (%)
Front right	C	0.03	3.6	4.0
	M	0.05	1.0	
Front left	C	0.03	3.2	2.1
	M	0.05	0.7	
Rear right	C	0.03	2.8	2.0
	M	0.05	0.6	
Rear left	C	0.03	1.9	1.0
	M	0.05	0.4	

Table 3.13 Vertical tyre force transient properties for a 13.89 m/s, 2.0 deg step steer

The source of this step is the same as the source of the spike in the lateral tyre forces. The vehicle body dynamics lag the tyre dynamics. In the initial phase of the step steer the tyre dynamics are dominant and determine the resulting vehicle behaviour. However, as the manoeuvre progresses, the vehicle body motions start

come to life and with their greater mass and inertia, they take precedence. The result is a manoeuvre with two distinct phases with different characteristics. Initially the tyre dynamics will determine the behaviour before the vehicle body dynamics take control.

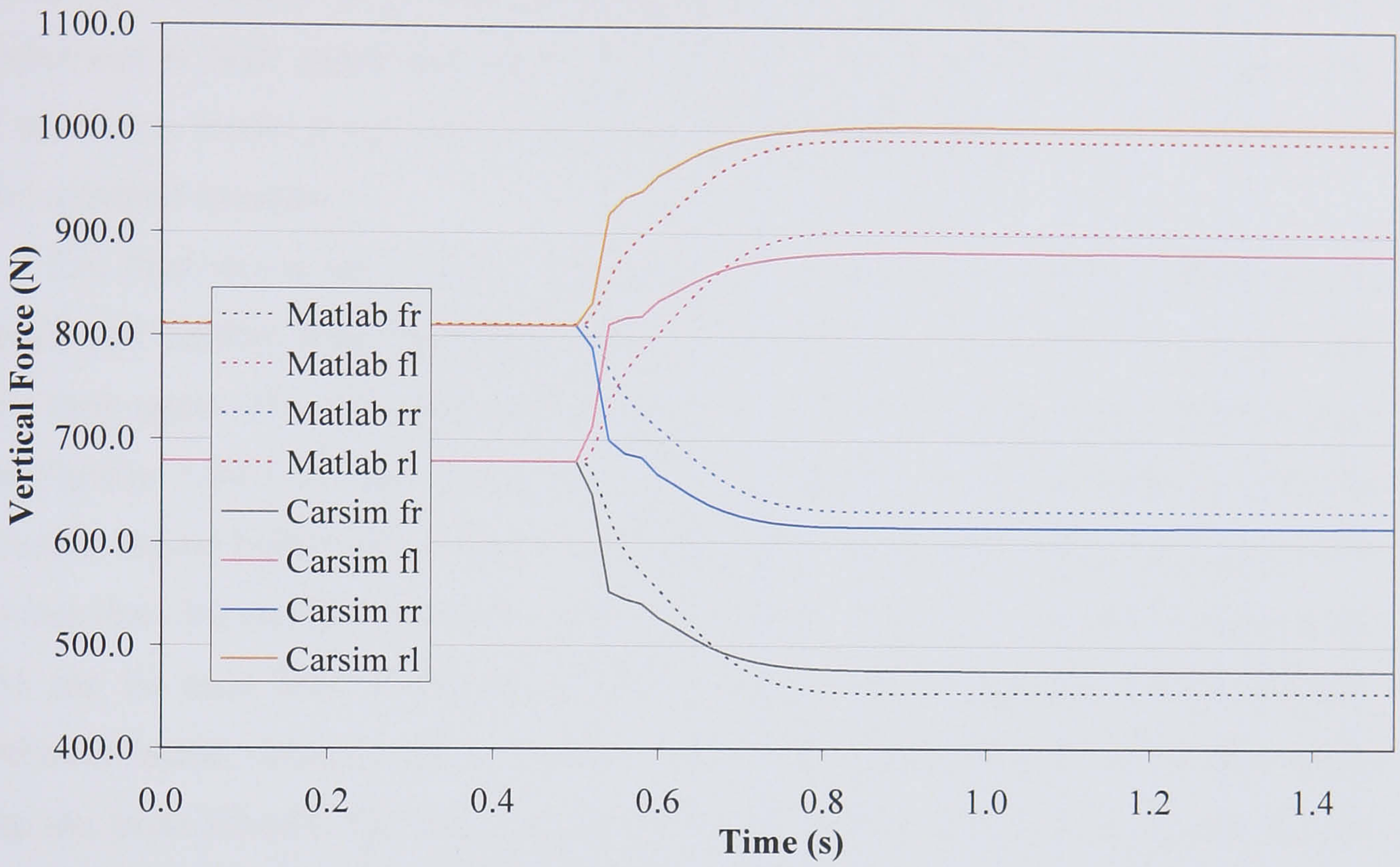

Figure 3.19 Vertical tyre force for a 20.83 m/s 1.0 deg step steer

Tyre	C/M	63% Rise Time (s)	Overshoot (%)	Steady State Error (%)
Front right	C	0.04	0.2	4.4
	M	0.12	0.2	
Front left	C	0.04	0.1	2.3
	M	0.12	0.1	
Rear right	C	0.04	0.2	2.4
	M	0.12	0.0	
Rear left	C	0.04	0.0	1.3
	M	0.12	0.0	

Table 3.14 Vertical tyre force transient properties for 20.83 m/s 1.0 deg step steer

Another potential source of any inconsistencies between the Matlab model and CarSim model is the tyre model. Not only does the CarSim model only use a linear tyre model modified for vertical force but it is also unclear how the tyre lag is

modelled. The Matlab model uses a first order lag to model the tyre lag. However, it has been suggested in some literature that the tyre lag is better modelled with a second order lag function [Heydinger, 1991]. Here it is argued that the tyre, which is normally modelled as a first order system, has an underdamped second order behaviour at high speed that can not be modelled by a first order system. Since the CarSim tyre model is not well documented this could be a source of any differences in the transient responses.

The final step in the vehicle model loop is the slip angle calculation. With the slip angle and vertical force the tyre model can calculate the lateral tyre forces and start the loop again. The slip angles follow from the vehicle body motions and are shown in Figures 3.20-3.22 and Table 3.15-3.17. They show a good correlation with the CarSim model both in the transient and steady state behaviours. The steady state error is less than 2% and the rise times match very well except in the low speed manoeuvre. As can be seen from Equations (3.6) – (3.9), they are dependant on the balance between lateral velocity and yaw rate, with the additional influence of the steer angle for the front wheels. The slip angles show very similar behaviour to the lateral tyre forces, which should be the case since they are a major input into the tyre model.

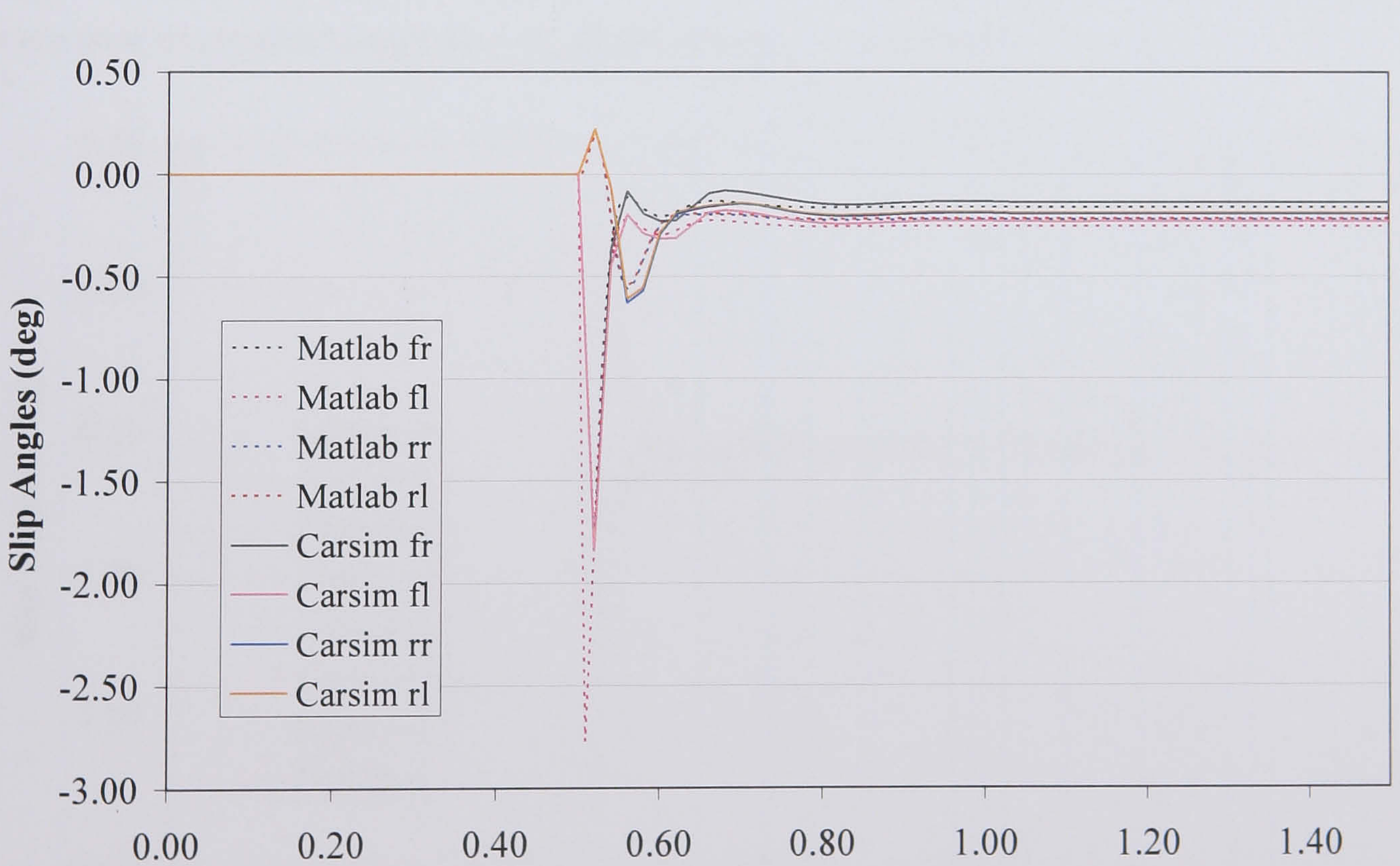

Figure 3.20 Slip angles for a 6.94 m/s, 3.0 deg step steer

Tyre	C/M	63% Rise Time (s)	Overshoot (%)	Steady State Error (%)
Front right	C	0.01	1210	14.3
	M	0.01	1640	
Front left	C	0.01	700	8.7
	M	0.01	1010	
Rear right	C	0.04	215	10.0
	M	0.04	155	
Rear left	C	0.04	189	15.8
	M	0.04	145	

Table 3.15 Slip angle transient properties for a 6.94 m/s, 3.0 deg step steer

At all three different speeds, the front slip angles start with an initial negative spike. The reason for the overshoot percentages not matching very well is that the CarSim data was not taken at a very high frequency and some of the very fast initial dynamics might have been missed. This very fast initial spike occurs because the slip angles are mainly influenced by the steer angle. The vehicle body dynamics do not have time to create enough yaw or lateral velocity to offset the steer angle.

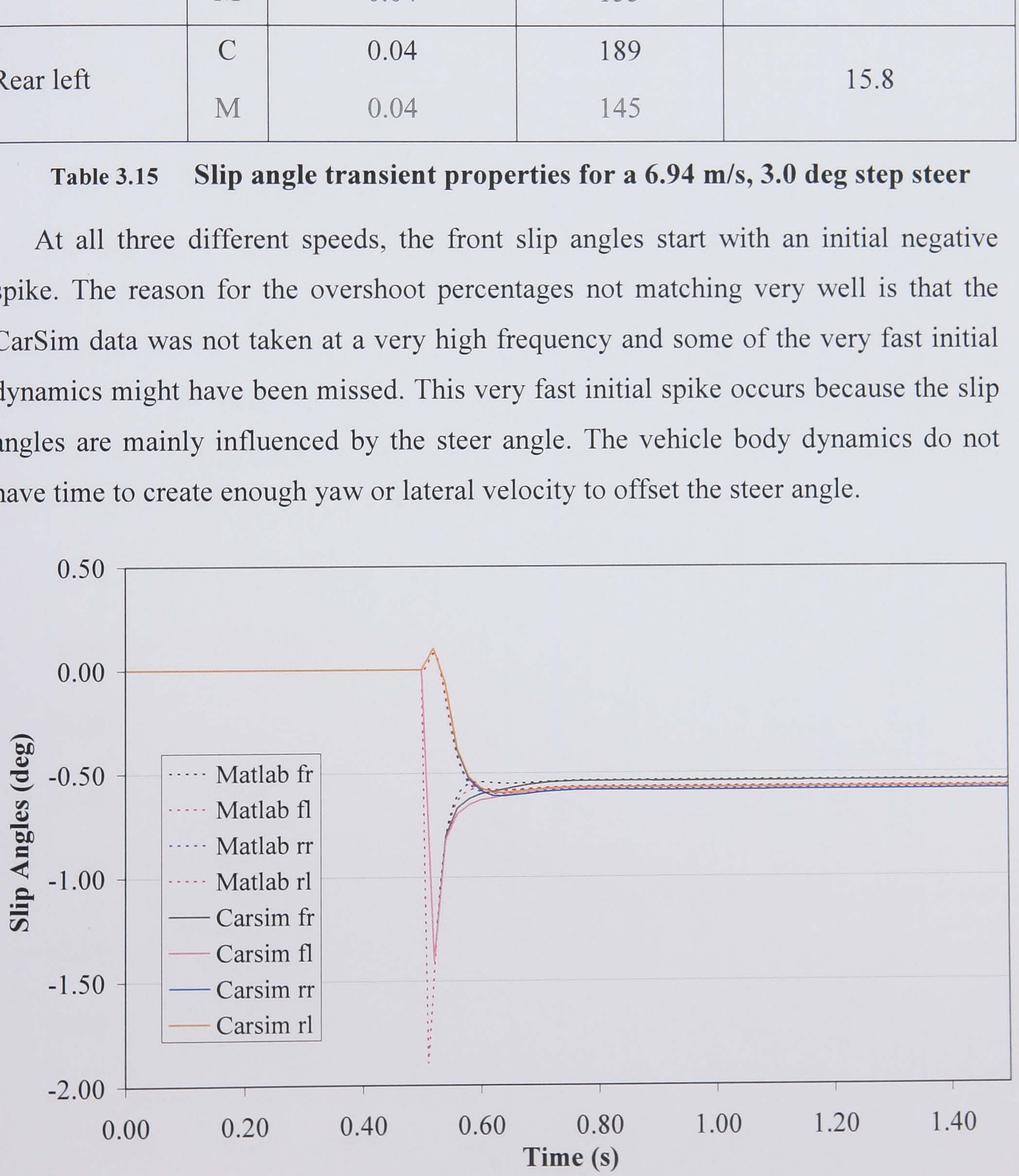

Figure 3.21 Slip angles for a 13.89 m/s, 2.0 deg step steer

Tyre	C/M	63% Rise Time (s)	Overshoot (%)	Steady State Error (%)
Front right	C	0.01	159	0.0
	M	0.01	252	
Front left	C	0.01	143	1.7
	M	0.01	233	
Rear right	C	0.06	5.2	0.0
	M	0.06	3.5	
Rear left	C	0.06	5.3	0.0
	M	0.05	3.5	

Table 3.16 Slip angle transient properties for a 13.89 m/s, 2.0 deg step steer

The balance of the yaw and lateral velocity in the numerator of the slip angle equations (Equations (3.6) – (3.9)) determines the slip angles after the initial step steer. For a forward moving vehicle, the denominator is almost always going to be positive since the yaw term will be over powered by the longitudinal velocity. The yaw rate is always positive in these manoeuvres as seen in Figure 3.12 and Figure 3.15. So the changes in the slip angles come from the lateral velocity.

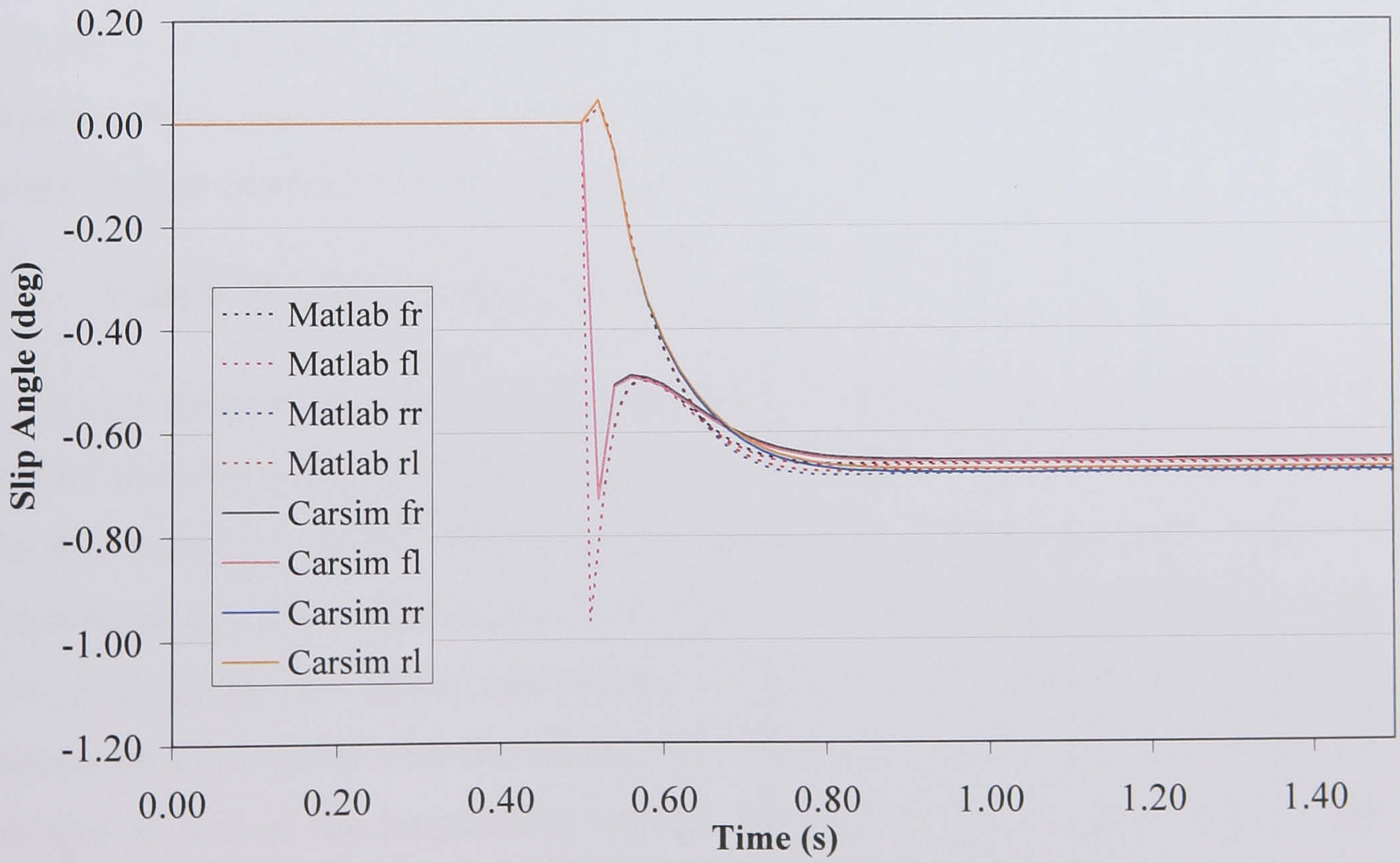

Figure 3.22 Slip angles for a 20.83 m/s, 1.0 deg step steer

Tyre	C/M	63% Rise Time (s)	Overshoot (%)	Steady State Error (%)
Front right	C	0.01	10.6	0.0
	M	0.01	47.0	
Front left	C	0.01	10.6	0.0
	M	0.01	47.0	
Rear right	C	0.10	-	0.0
	M	0.10	-	
Rear left	C	0.10	-	1.5
	M	0.10	-	

Table 3.17 Slip angle transient properties for a 20.83 m/s, 1.0 deg step steer

For the rear slip angles, the lateral velocity is positive and initially takes precedence before the yaw rate builds up and overpowers it creating a negative slip angle. As the velocity increases, the lateral velocity becomes negative as well and adds to the negative rear slip angle. The front slip angles are not affected as much by the positive lateral velocity since the steer angle term is more dominant. However, as the yaw rate and lateral velocity build up they offset the steer angle and reduce the front slip angles. As the velocity increases the lateral velocity becomes negative after an initial positive trend. This then adds to the steer angle sending the slip angles more negative. Once again, the low speed oscillations in the lateral velocity and yaw rate create similar oscillations in the slip angles.

3.5. Vehicle Modelling Conclusions

In this chapter the vehicle model has been presented. First, the background to vehicle modelling was presented including linear models. Next, the assumptions to the full nonlinear model were discussed before introducing the eight degree of freedom model. The eight degrees of freedom are longitudinal and lateral velocity, yaw, roll and the four wheel spin degrees of freedom. The equations for the vehicle motion were presented with the description of the load transfer. The tyre model was detailed as well as the longitudinal velocity controller. After the full vehicle model equations were presented the model was validated against CarSim, a commercial vehicle dynamics simulation package. The Matlab model that was developed matched

the behaviour of the CarSim model. The important factor in validating the vehicle model is matching the tyre forces. Vehicle dynamics is a well understood subject with the equations of motion defined by simple dynamics. The errors in model validation must come from parameter differences and tyre modelling differences. Since the vehicle parameters are fairly well known the main focus in model validation surrounds modelling the tyre forces. These tyre forces matched up well and resulted in a good correlation of the vehicle motion.

4. Control Algorithms and Evaluation

Chapter 4 presents the vehicle dynamics control algorithms. The different control algorithms used in this research are described presenting their merits and disadvantages.

4.1. Introduction to Control Algorithms

The objective of this research is to improve the handling dynamics of a racing car through active controls. This includes extending the limits of handling performance and also controlling and stabilising the vehicle as it approaches or goes beyond these limits. Researching the limit handling of the vehicle requires a non-linear model, which means standard linear control methods and analysis may not be directly applicable. Non-linearities in the vehicle may cause unexpected behaviour that is difficult for linear methods to describe [Schwarzenbach, 1992]. The non-linear vehicle models may also be too complex to use with the linear methods and linearisation or simpler models may be required. Another option is to use non-linear or adaptive control methods with the complex vehicle models.

The main vehicle states that are used as control parameters and characterise handling performance are the yaw rate and sideslip angle. Although lateral acceleration is also commonly used as a benchmark of vehicle handling, it does not provide as much insight into the handling balance of the vehicle and as such is not well suited to be used as a control parameter. The objectives of the controllers are therefore to optimise the yaw rate and sideslip angle to increase the limit handling boundaries and driveability while maintaining vehicle stability.

The optimal sideslip angle control will aim to minimise the sideslip angle. As the vehicle sideslip angle increases the lateral loads on the tyres also increase. As the tyre loads increase, the additional available forces from the tyres decrease. The tyres get closer to saturating and become less responsive to driver inputs. This results in a vehicle that is less controllable. If the sideslip angle is minimised the potential to create tyre forces in response to driver steering inputs will remain, resulting in a more controllable vehicle.

Yaw rate control is not as simple as minimising or maximising the yaw rate. The optimal yaw rate is directly related to the driver inputs. Driving in a straight line requires zero yaw rate while an accident avoidance manoeuvre would require a much larger yaw rate. Therefore, a reference model is required to generate the desired yaw rate based on the driver inputs. Non-linear systems, like vehicles, are difficult to predict; however systems with a linear response are predictable. If the vehicle response could be linearised it would create a more predictable vehicle that would simplify and decrease the driver work load. By using a linear reference model the vehicle behaviour will be pushed toward a more predictable behaviour. Not only would the behaviour be more predicable but the non-linearites in vehicles tend to reduce overall handling performance. For example, the tyre forces can saturate and produce less grip. If a linear reference model is used, the control systems can work to eliminate these non-linearities and increase the performance envelope of the vehicle while making it more predictable and easier to drive. However, yaw tracking controls do not guarantee stability. Even with a controlled yaw rate it is possible that a vehicle can have large lateral velocities and accelerations, which are very undesireable.

The requirements of the vehicle control are to track a reference yaw rate created by a linear model and to minimise the sideslip angle. One way of matching the vehicle yaw rate to the reference yaw rate is by using a driver input based feedforward control, which will improve vehicle responsiveness by introducing a phase advance and limiting the gain drop off at high frequencies, as well as a feedback path to minimise the yaw rate error. However, the stability control will generally require a vehicle state based feedback control to maintain stability and controllability at the vehicle handling limits. Stability controls aim to limit and minimise the sideslip angle, not to follow a reference behaviour where feedforward control is most effective. Since the vehicle dynamics are cross coupled, increasing the yaw rate will tend to increase the sideslip angle. This makes it very difficult to have a single control strategy to accomplish the entire control objective. A two stage control or integrated strategy will be required to control both yaw rate and sideslip angle. For this reason independent controllers with a single objective of controlling yaw rate or sideslip angle separately are developed initially. Once effective independent controllers have been developed they will be combined and integrated into an overall vehicle control strategy.

The performance of the controllers will be evaluated with simulated vehicle test manoeuvres. Steady state cornering tests are useful for the general characterisation of the vehicle dynamics, including understeer and oversteer characteristics. However, limit handling behaviour is highly dynamic and requires transient manoeuvres to evaluate the control strategies. These include step steer tests, increasing amplitude sinusoidal steering tests and these same tests while accelerating and decelerating. Another key feature to test is the control robustness. Performing the same tests on low friction surfaces will expose an ineffective controller.

4.2. Independent Control Algorithms

The controllers are initially developed as stand alone, independent controllers. The objective of the independent controllers will be to control either roll moment distribution or variable torque distribution for driveability or stability. Each algorithm presented here will be evaluated in Chapter 5. The independent controllers will not control both RMD and VTD with a single controller. This would require two controllers with a switching mechanism or an integrated control, which would be categorised as a combined or integrated controller. Likewise, the driveability and stability will not be controlled by the same controller for the same reason. The combined controllers are simple combinations of the independent controllers and do not have their own algorithms while the integrated control algorithms are presented in Section 4.3.

The goal of the independent algorithms presented is to take an error signal and try to minimise it. For a driveability control this error signal is usually the difference between the actual vehicle yaw rate and the reference yaw rate. The stability controls will generally be based on the sideslip angle, which the control will try to minimise. However, it is also possible to use a reference model to create a reference sideslip angle.

4.2.1. Proportional, Integral, Derivative Control

Proportional, Integral, Derivative (PID) control is a simple control strategy that consists of three parts that work to minimise an error signal. It is an appropriate benchmarking tool as it addresses key control objectives of response time, damping and steady state error minimisation. The error signal along with its integral and

derivative are each multiplied by a separate gain and summed to create the control signal, as shown in the block diagram in Figure 4.1. The weighting of the three components in the control determine the overall behaviour of the control strategy. It is a very flexible control algorithm due to the tuneable nature of the gains. However, these same gains can lead to poor controller performance if they are improperly set. Unfortunately, many of the PID control tuning methods, like the Ziegler-Nichols method, work well for process controls where the desired plant state is relatively static but are not suited to the highly variable dynamics found in automotive control applications where manual tuning may be required.

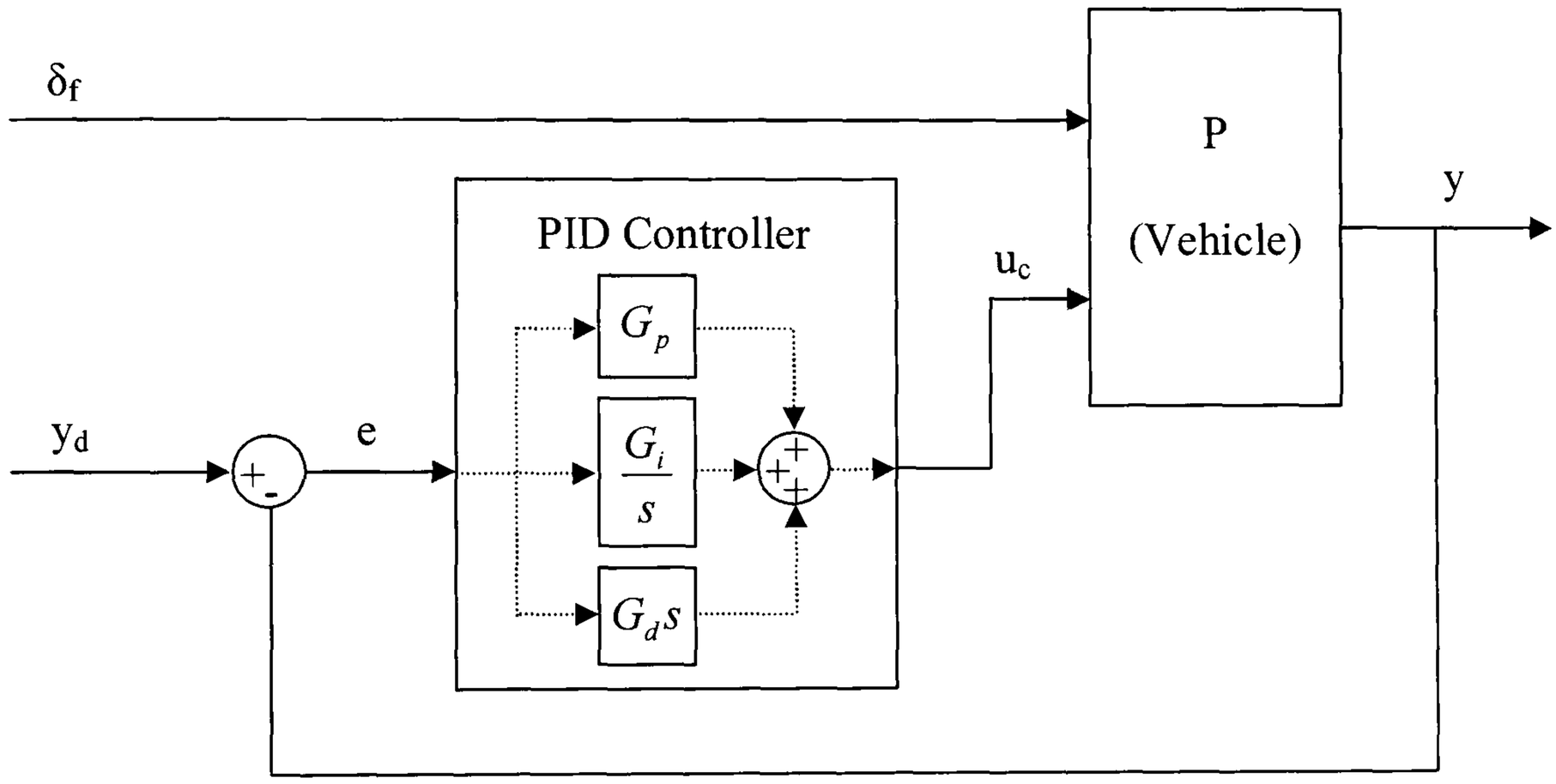

Figure 4.1 Generic PID controller block diagram

To get the transfer function of the controller, the plant can be separated into two plants with separate inputs, as shown in Figure 4.2. The first plant has steering angle as the input while the second plant has the control input. If the plant is assumed to be linear then the sum of these two separated plants will be equal to the original plant by the principle of superposition. In reality, the plant is not linear but this concept can be used to get the linear transfer function. The other modification that is required is the addition of a reference model, based on the steering angle, to determine the desired state output and error signal. The resulting transfer function is:

$$\frac{y}{\delta_f} = \frac{P_1 + P_2 C_{PID} R}{1 + P_2 C_{PID}} = \frac{s^2 R P_2 G_d + s\left(P_1 + R P_2 G_p\right) + R P_2 G_i}{s^2 P_2 G_d + s\left(1 + P_2 G_p\right) + P_2 G_i} \qquad (4.1.)$$

Splitting the plant into two separate transfer functions, P_1 and P_2, also allows the controller to act on the minimum phase part of the plant, P_2, while the driver input acts on the non-minimum phase part, P_1. This simplifies the control dynamics and can be easily done since P_1 only appears in the numerator of the transfer function.

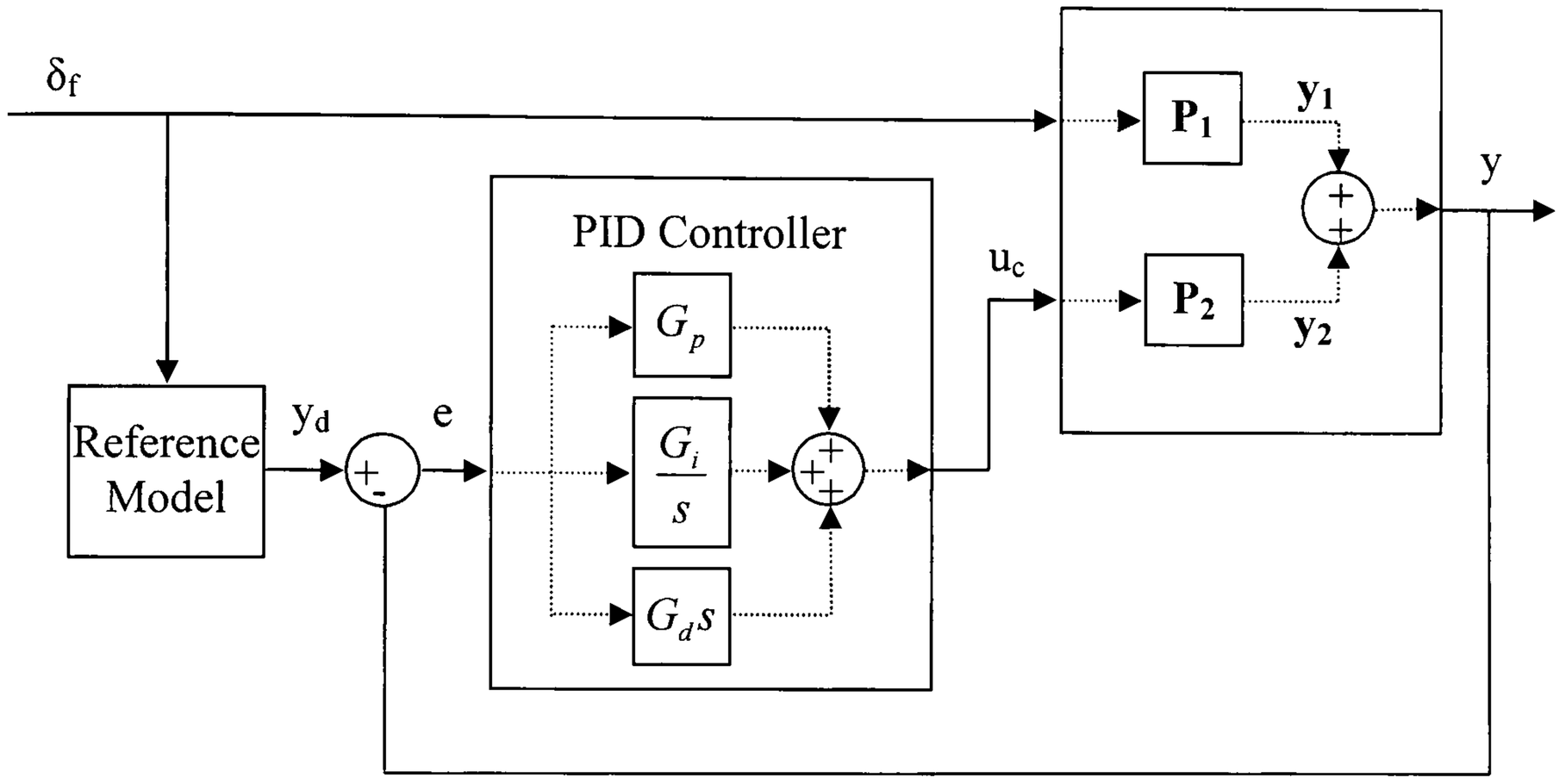

Figure 4.2 PID controller block diagram with separated plant inputs

The first part is the proportional control. The proportional control is just a proportional gain on the error signal as shown:

$$K = G_p e \tag{4.2.}$$

Here K is the resulting proportional control input, e is the error signal and G_p is the proportional gain. The result is that the larger the error the greater the control action. To remove any steady state error an integral term can be added to the control algorithm as shown:

$$K = G_p e + G_i \int e \cdot dt \tag{4.3.}$$

Here G_i is the integral gain. The integral term works on the sum of the error signal trying to equalise the positive area with the negative area under the plot of the error signal and therefore remove any steady state error. However, the integral term would not work to damp out any oscillations in the error signal. A sinusoidal error signal with equal positive and negative area would not be greatly affected by the addition of

an integral term in the control algorithm. To damp out oscillations in the error signal a derivative term needs to be added:

$$K = G_p e + G_i \int e \cdot dt + G_d \dot{e} \qquad (4.4.)$$

where G_d is the derivative gain. The derivative term works on the rate of change of the error signal. So an error signal with large fluctuations will create a large control action, which will work to damp out the system behaviour.

PID controllers are very simple and allow fine tuning. All the controller needs is an error signal and some simple mathematical manipulation. The difficulty in implementing this control algorithm is the gain selection. With linear systems there are many analysis methods that can be used for gain selection. These include the use of zero-pole placement and root locus maps, bode diagrams, Nyquist plots, Nichols plots and many more techniques including the Ziegler-Nichols method [Schwarzenbach, 1992]. However, determining the optimal gains in a non-linear system can be difficult. The techniques just mentioned are difficult to use on complex non-linear models. If the system is linearised they can be applied more easily. However, any system linearisation is only going to be valid around the point of linearisation. This can be effective with a stable plant but in a highly dynamic system like a racing car, the system state can vary widely requiring lots of linearised models. This means the gain selection process can revert back to a tedious and time consuming trial and error process where the entire dynamic range of the system is explored through numerous test cases to find the optimal gains. Trying to find these optimal gains for the complete range of the system performance can also involve large compromises. The system behaviour can vary widely and one set of gains that are effective over the entire range can be difficult to find. Another drawback to PID control is that unless the goal is to drive the error signal to zero a reference model is required. At this point the controller is only as good as the reference model it is using and if the reference model is a linear model it can prescribe a behaviour that is beyond the limits of the non-linear vehicle. Finally, the PID controller is a pure feedback controller. There is no feedforward component to anticipate the required control inputs.

Adaptive Control

One method available to avoid the compromises in gain selection is to use adaptive control. Adaptive control can be used to adapt controller gains by the gain modifier block which bases the gain selection on the current vehicle state, as shown in the block diagram in Figure 4.3. It can be used with a PID controller by using adaptive gains for the proportional, integral and derivative parts of the control algorithm instead of using three set gains.

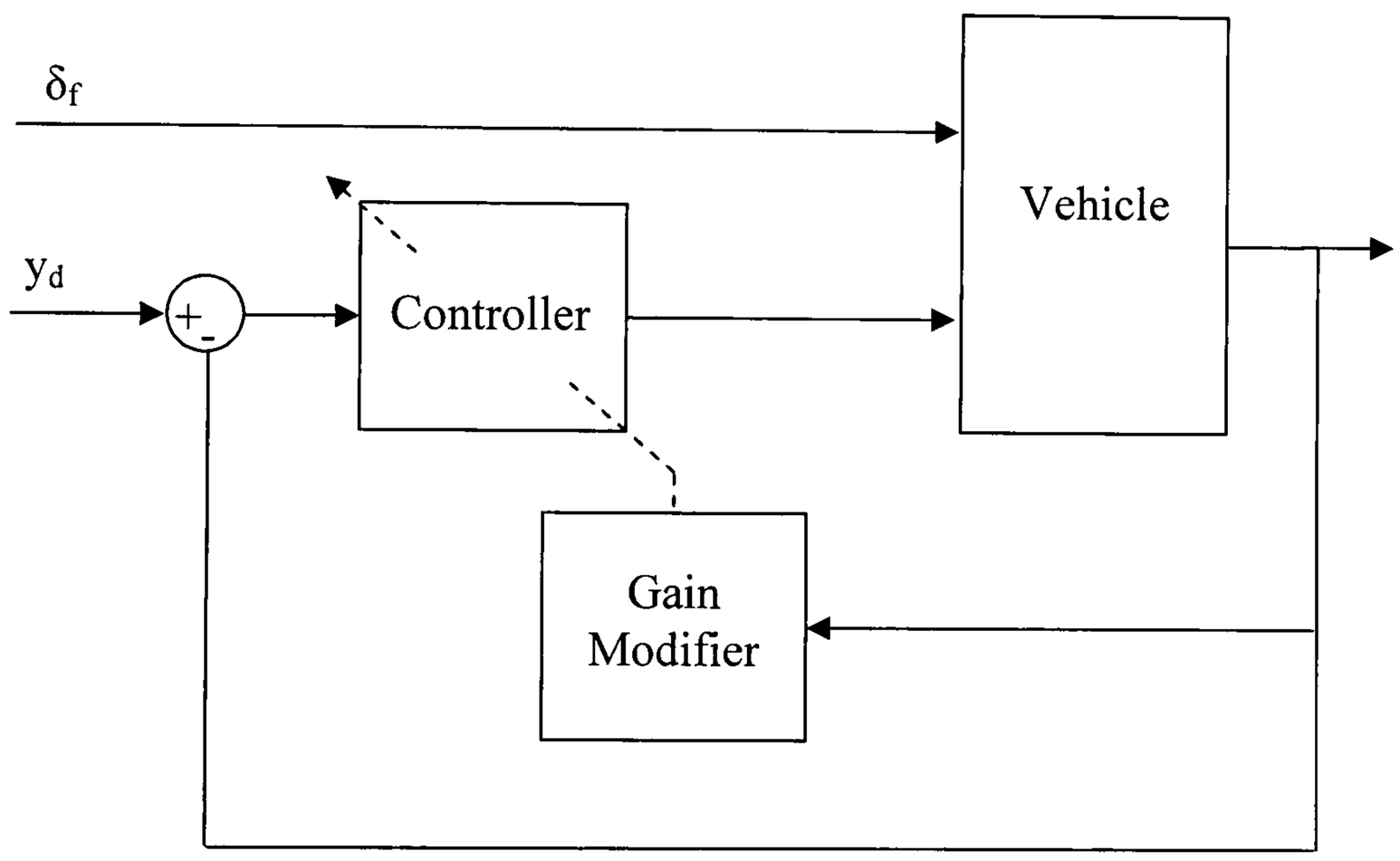

Figure 4.3 Model reference adaptive control block diagram

In [Lyon, 1994], the PID control is an adaptive control with gains mapped throughout the different system states where different behaviours are observed. This allows the gains to be optimised and tuned to any operating condition and results in a finely tuned controller. This is particularly useful in a vehicle control that operates in the highly non-linear range at limit handling. Although vehicle behaviour is qualitatively similar in the non-linear range where oversteer and understeer are still observed, the quantitative vehicle states at the limit can vary widely depending on the specific vehicle manoeuvre. Adaptive gains can give flexibility to controls and extend their useful range of performance. Obviously, having mapped gains or gain scheduling allows an infinite degree of tuneability in the control algorithm but a method is still needed to determine the gain maps. Once again, this can be extremely

time consuming and involves a large number of tests over the whole dynamic range of the system that is being controlled.

4.2.2. Phase Plane Control

The stability of a system can be analysed through a phase plane representation of its states. A phase plane is a plot of a state derivative vs. the state. The dynamic behaviour of a system can be represented by a phase curve plotted on the phase plane. Phase curves progress from left to right above the x-axis and from right to left below it. They cross the x-axis at a perpendicular angle and any steady state points of the system lie on the x-axis since points off the x-axis have a non-zero derivative. Stable systems will be represented by a spiral that ends up on the x-axis while unstable systems will diverge from the x-axis in a spiral. Systems which are critically stable will end in limit cycle shown by a closed curve rotating around the x-axis. Examples of these systems are shown in Figure 4.4.

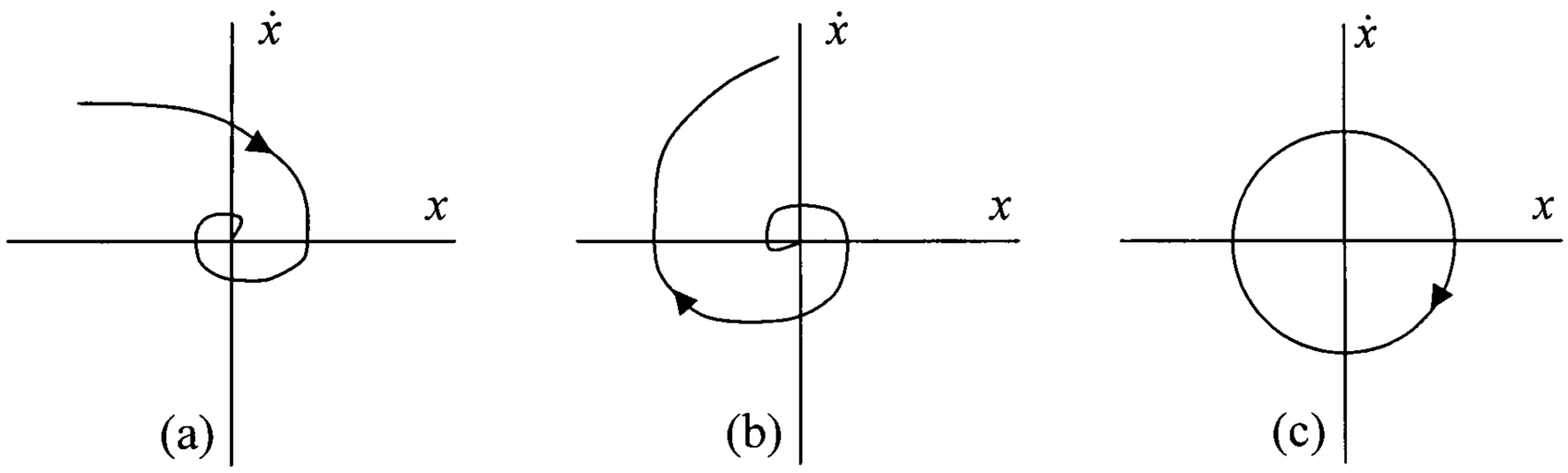

Figure 4.4 Stable (a), unstable (b), and critically stable (c) phase curves

The block diagram of a phase plane control is shown in Figure 4.5. The system state and its rate of change are used in a feedback loop with the controller. If the same assumptions are made with the plant model that where given in Section 4.2.1 where it can be separated into two plants then the transfer function is given by:

$$\frac{y}{\delta_f} = \frac{P_1}{1 - P_2 C_{pp}} \tag{4.5.}$$

where P_1 is the plants response to the steering angle, P_2 is the response to the control signal and C_{pp} is the phase plane controller.

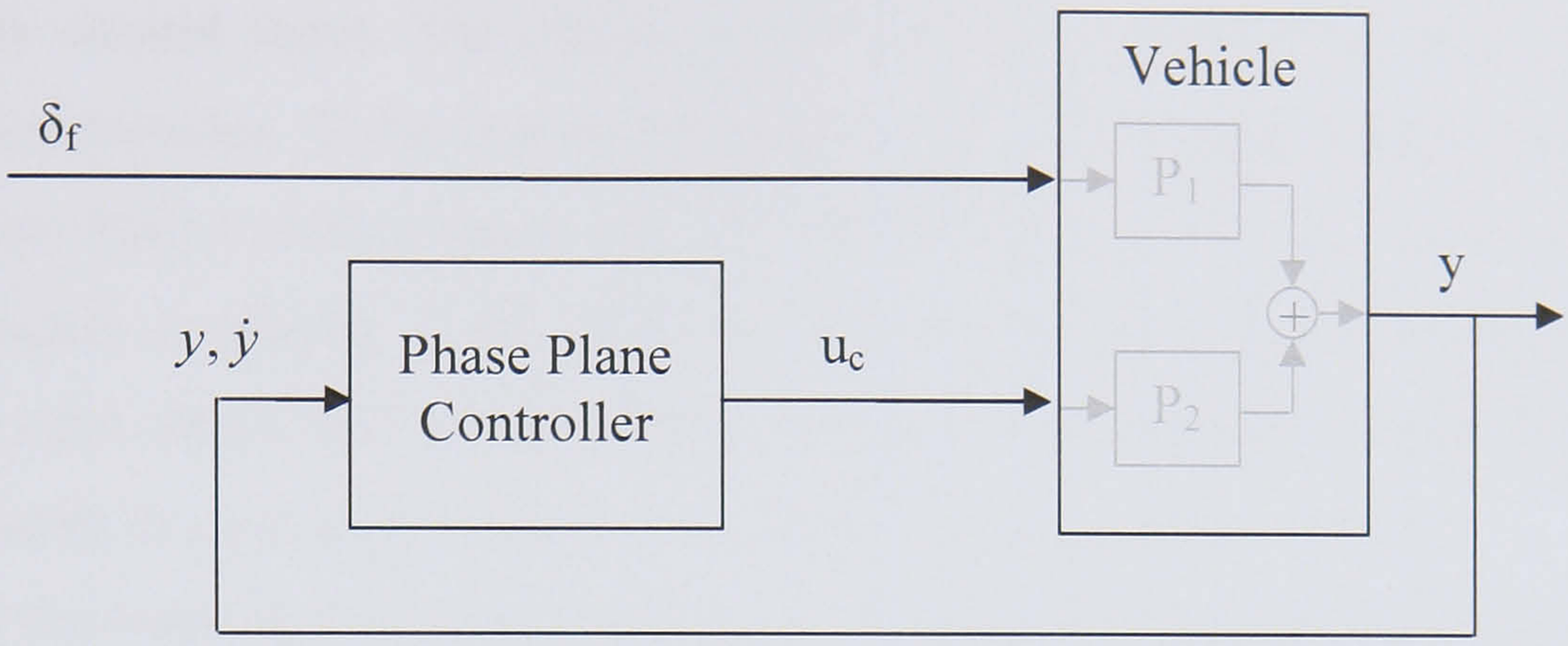

Figure 4.5 Phase plane control block diagram

A typical phase plane of the vehicle sideslip angle is shown in Figure 4.6 [He, 2004]. The phase curves were generated by setting the steering angle to zero while varying the initial conditions of the sideslip motion. From these phase curves, it can be seen that there is an equilibrium point at the origin corresponding to straight ahead driving where sideslip angle and its rate of change both equal to zero. It can also be seen that vehicle states in the second and fourth quadrant tend toward this equilibrium point while states in the first and third quadrants tend towards instability if they are not initially close to the origin. A stable region can be defined from the phase plane by observing where the system will return to the equilibrium point without intervention.

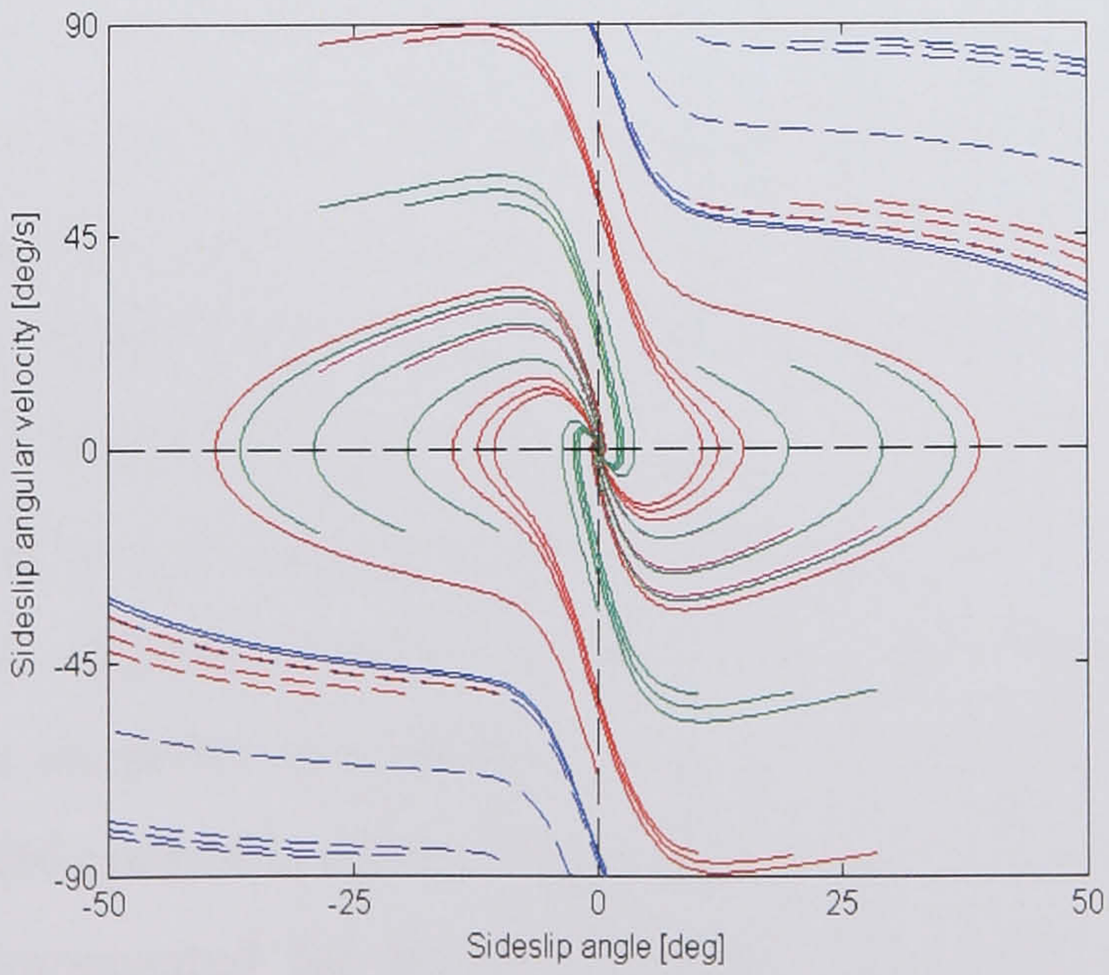

Figure 4.6 Typical phase plane plot of vehicle sideslip angle [He, 2004]

A phase plane stability control can be developed to prevent the system from approaching unstable states in the phase plane. A control boundary can be defined.

Inside this boundary the controller will not operate. If the vehicle state leaves the control boundary then an error signal defined by the distance to the boundary can be used as the control input. The choice of the control boundary will determine the control characteristics. If the control boundary is set as the stable region, the result will be a very hard control as there will be a very abrupt, high control demand as soon as the boundary is crossed. If the control boundary is chosen inside the stable region then the control action will be able to start correcting the potential instability earlier. This will result in a smoother control action but a more intrusive controller.

One of the benefits of a phase plane control is that the controller has a dead zone where it does not operate. Unless the vehicle is approaching an unstable state the controller does not interfere. This results in power savings for the controller and gives the driver less control interference. It also means that there will not be any interference with any other controllers that may be operating on the vehicle during stable driving conditions. The controller is also very tuneable. By changing the region of the control boundary the characteristics of the controller can be varied from an unobtrusive yet abrupt control to a smoother but maybe more intrusive control. One drawback to the control strategy is that it is only suited to stability controllers. Since there is no path tracking or reference model following capabilities it is not suited to improving the driveability of vehicles.

4.2.3. Internal Model Control

PID control is a purely feedback control. A logical progression is to include a feedforward element to the control strategy. The feedforward control can improve the responsiveness by introducing a phase advance and limiting the gain drop off at high frequencies. Internal model (IM) control is a robust feedback control that includes a feedforward element. The objective of the controller is to match the system state to a set point. Once the desired set point has been generated, it is input into a feedforward controller while the difference between the system state and internal model is subtracted from the set point in a feedback loop. It is due to this inclusion of the internal model that IM control is robust. The disturbances in the system and modelling inaccuracies are compensated for by the feedback from the internal model in the controller.

Consider the simple feedforward control shown in Figure 4.7. The transfer function is given by:

$$\frac{y}{x} = C_{ff} P \tag{4.6.}$$

Now, if C_{ff} is an exact inverse of the plant, $C_{ff} = P^{-1}$ then the transfer function becomes:

$$\frac{y}{x} = C_{ff} P = P^{-1} P = 1 \tag{4.7.}$$

So if the input, x, is the desired plant output, y, the controller will output u_c that will cause the plant to give the desired output, y. So $y = x$.

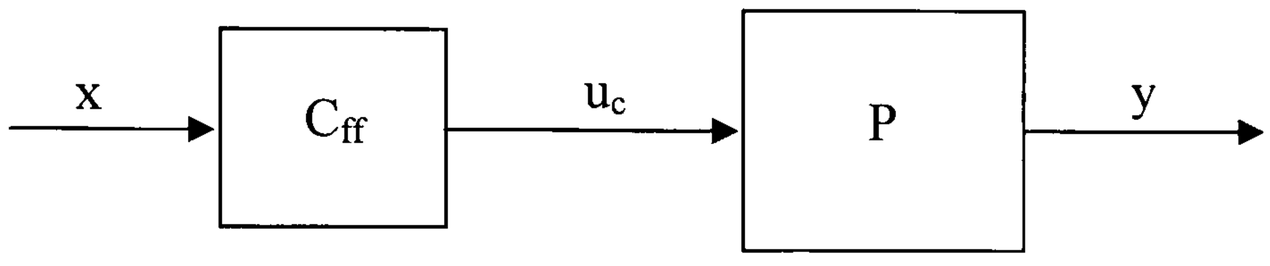

Figure 4.7 Basic feedforward control block diagram

To add feedback to the controller consider the basic feedback loop with the block diagram shown in Figure 4.8. This feedback loop can be modified into the control with the block diagram given by Figure 4.10, with the intermediate step shown in Figure 4.9. Here two feedback loops have been added with the transfer function $\hat{P}$. The output of these new blocks, $\hat{y}$, has been subtracted from the feedback loop and again from before the controller. This does not change the system dynamics, as shown in the following equation:

$$e = x - e_p - \hat{y} = x - \left(y - \hat{y}\right) - \hat{y} = x - y \tag{4.8.}$$

which is the same as e in Figure 4.8. The feedback controller, C_{fb}, can be converted by defining C_{inv} in the following way:

$$C_{inv} = \frac{C_{fb}}{1 + C_{fb}\hat{P}} \text{ or conversely } C_{fb} = \frac{C_{inv}}{1 - C_{inv}\hat{P}} \tag{4.9.}$$

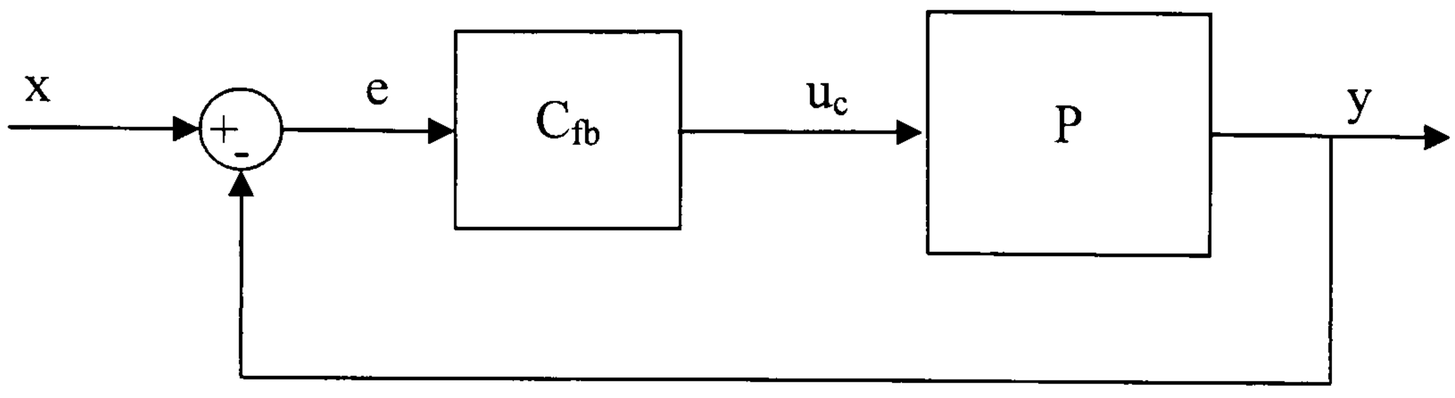

Figure 4.8 Basic feedback controller block diagram

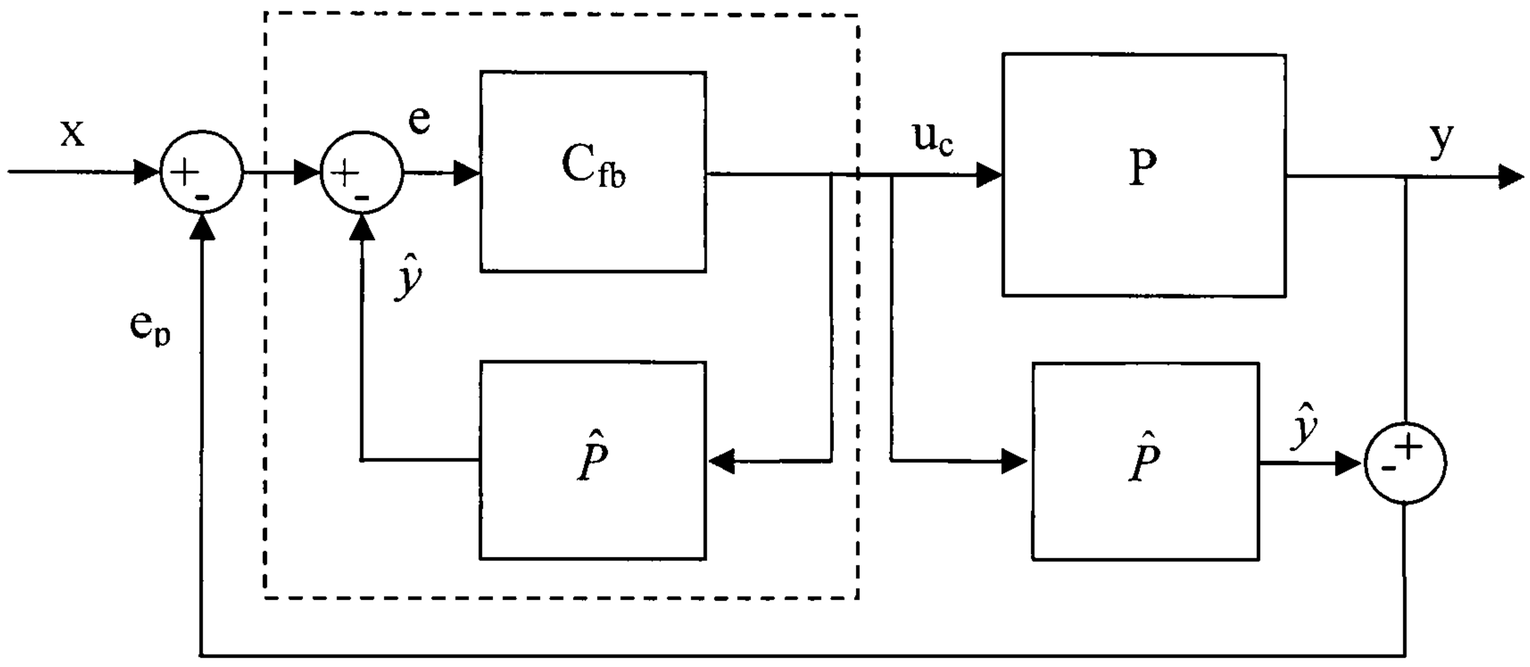

Figure 4.9 Internal model control from a feedback loop

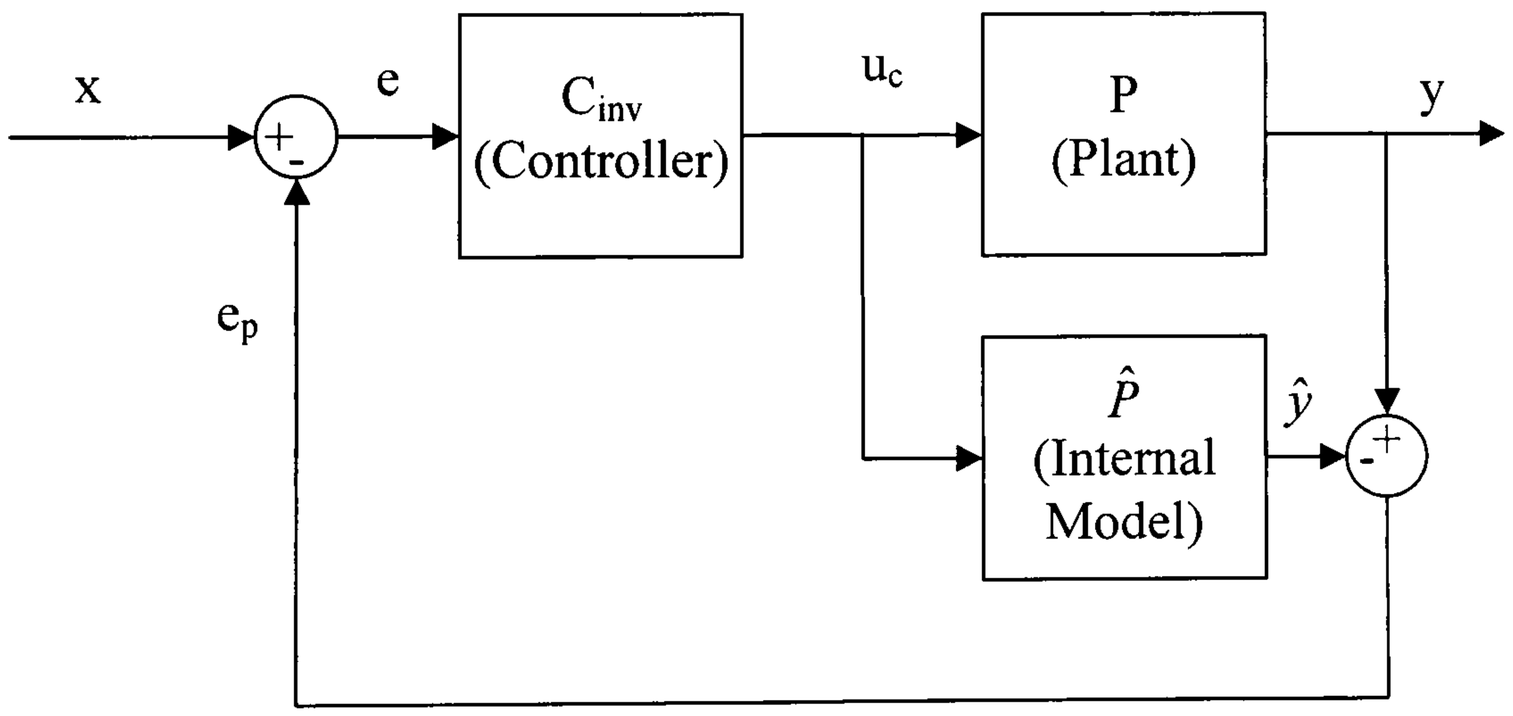

Figure 4.10 Internal model control block diagram

The block diagram in Figure 4.10 represents internal model control. In an ideal environment, the feedforward element can be realised by setting controller to be the inverse of the plant, $C_{inv} = P^{-1}$, and the internal model to be the same as the plant, $\hat{P} = P$. This way the difference between the plant and internal model would be zero,

$\hat{y} = y$, so there would be no feedback signal, $e_p = y - \hat{y} = 0$ and $e = x - e_p = x$ so the controller would represent the basic feedforward control shown previously in Equation (4.6) if $C_{ff} = C_{inv}$.

In IM control, the plant, P, is the system that is being controlled and the internal model, $\hat{P}$, is a model of the plant. In an ideal system the internal model would be an exact representation of the plant model and the controller, C_{inv}, would be an exact inverse model of the internal model and therefore also the plant, as described in the previous paragraph. The difference between the plant and internal model, e_p, would only be a result of the disturbances to the system. This difference is then used to modify the controller set point, x, and accounts for the disturbances in the system. The set point is then processed by the controller to create the plant input, u_c. Since the controller is an exact inverse of the plant, the plant output will match the set point exactly, compensating for the disturbances to the system.

Unfortunately, in the real world it is usually very difficult to model the plant exactly. There can be unmodelled dynamics which can not be included in the model due to their complexity or parameter variances due to wear that will have small effects on the system performance. In these cases when the internal model is not a precise model of the plant, any inaccuracies between the plant and internal model are just treated as disturbances. As long as the controller and internal model are stable and the controller is the inverse of the internal model then offset free control is gained [Rivals, 1996]. This leads to a robust control algorithm that can compensate for small disturbances and modelling inaccuracies.

The true benefit of IM control is this robustness due to the internal model. Consider the feedforward feedback control shown in Figure 4.11. The transfer function is given by:

$$\frac{y}{x} = \frac{P\left(C_{ff} + C_{fb}\right)}{1 + PC_{fb}} \tag{4.10.}$$

whereas the transfer function of the IM control is given by:

$$\frac{y}{x} = \frac{PC_{inv}}{1 + C_{inv}\left(P - \hat{P}\right)} \tag{4.11.}$$

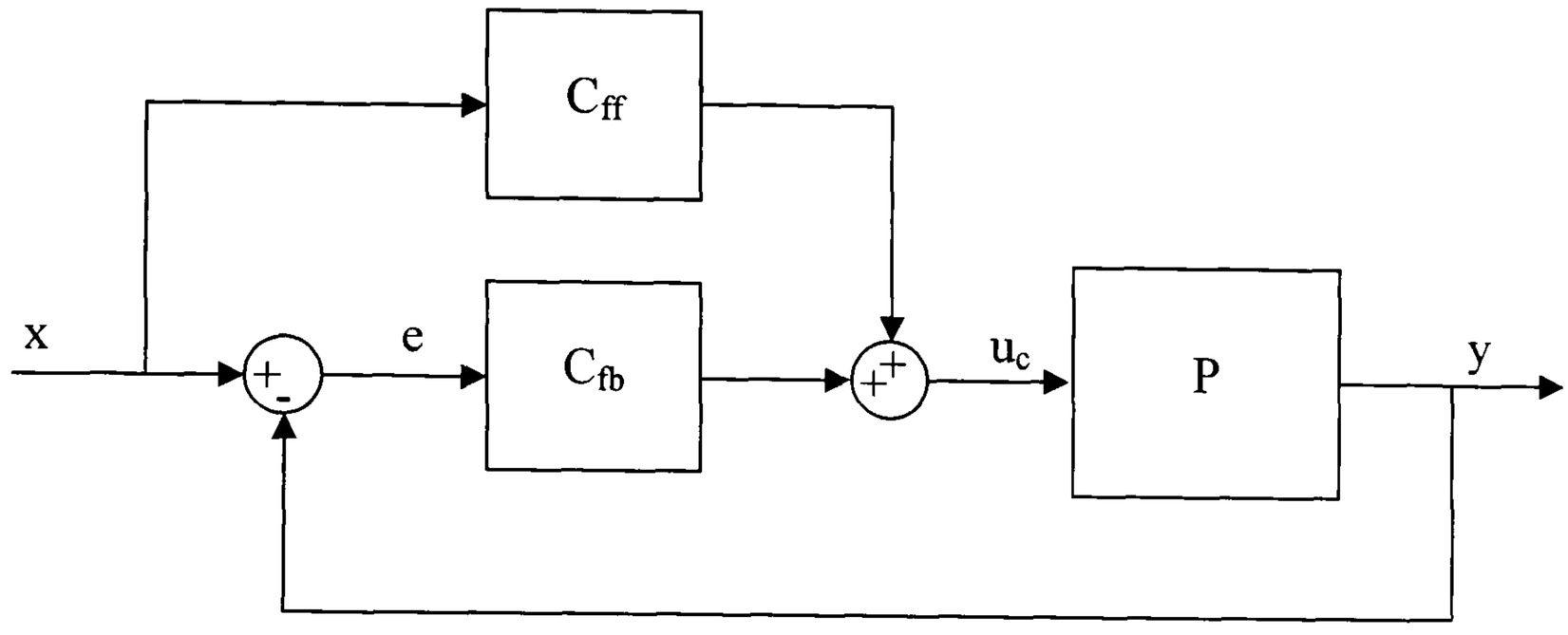

Figure 4.11 Feedforward feedback control block diagram

The two transfer functions have the same form and are very similar. In the feedforward feedback control if the models are perfect there is no feedback control required and the transfer function is simply PC_{ff}. However, in a real application the models will not be perfect and some feedback is required to compensate for this. The feedback gain is tuned manually to optimise the controller. With IM control if the models are perfect the control also becomes PC_{inv}. However, in real applications with imprecise models some feedback is incorporated. The advantage is that the amount of feedback does not have to be tuned, the internal model automatically tunes the feedback gain to compensate for modelling inaccuracies.

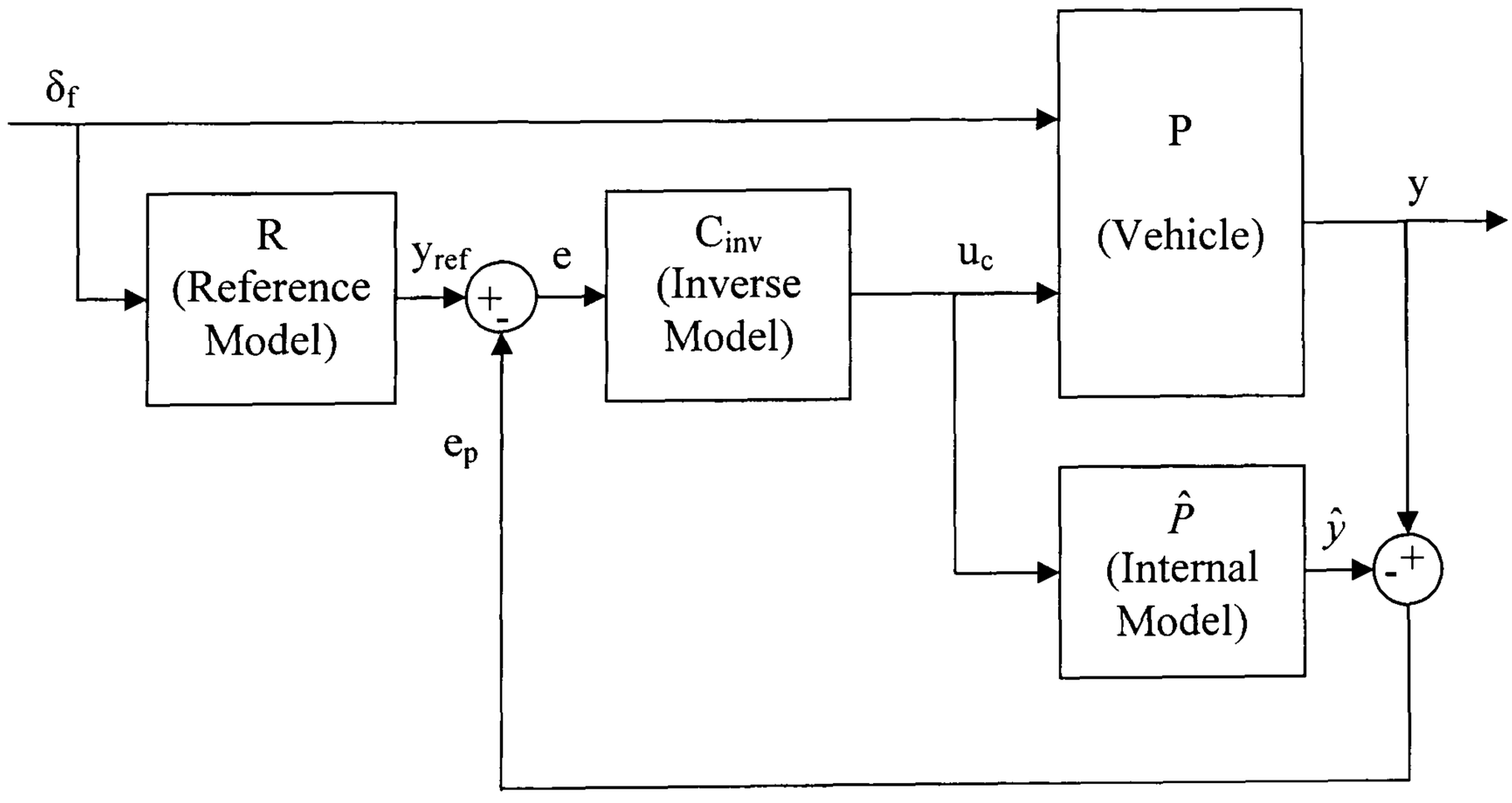

Figure 4.12 Modified IM control block diagram

The control presented in this work is slightly modified from the basic IM control as shown in Figure 4.12. There are two differences to the standard IM control. The first is that a reference model is used to create the set point and the second is that the vehicle model is a multiple input, multiple output model. Adding the reference model does not change the control architecture very much. It is just used to create the desired set point to get the ideal plant output. This is required because the driver inputs throttle and steer angle but the feedback loop uses the vehicle state as the control parameter. This requires the inputs to the inverse model to be the desired vehicle state, which is gained from the ideal reference model.

The other difference is that the vehicle model is a multiple input, multiple output model. The driver inputs of throttle and steer angle are directly input into the vehicle while the control action is implemented on a different vehicle system, either VTD or RMD. The adaptation of IM control to work in this situation is shown by [Smakman, 2000 a]. The details of the control can be seen in Figure 4.13 with the transfer function given by:

$$\frac{y}{\delta_f} = \frac{P_1 + \hat{P}_2^{-1}\left(P_2 R - P_1 \hat{P}\right)}{1 + \hat{P}_2^{-1}\left(P_2 - \hat{P}\right)} \tag{4.12.}$$

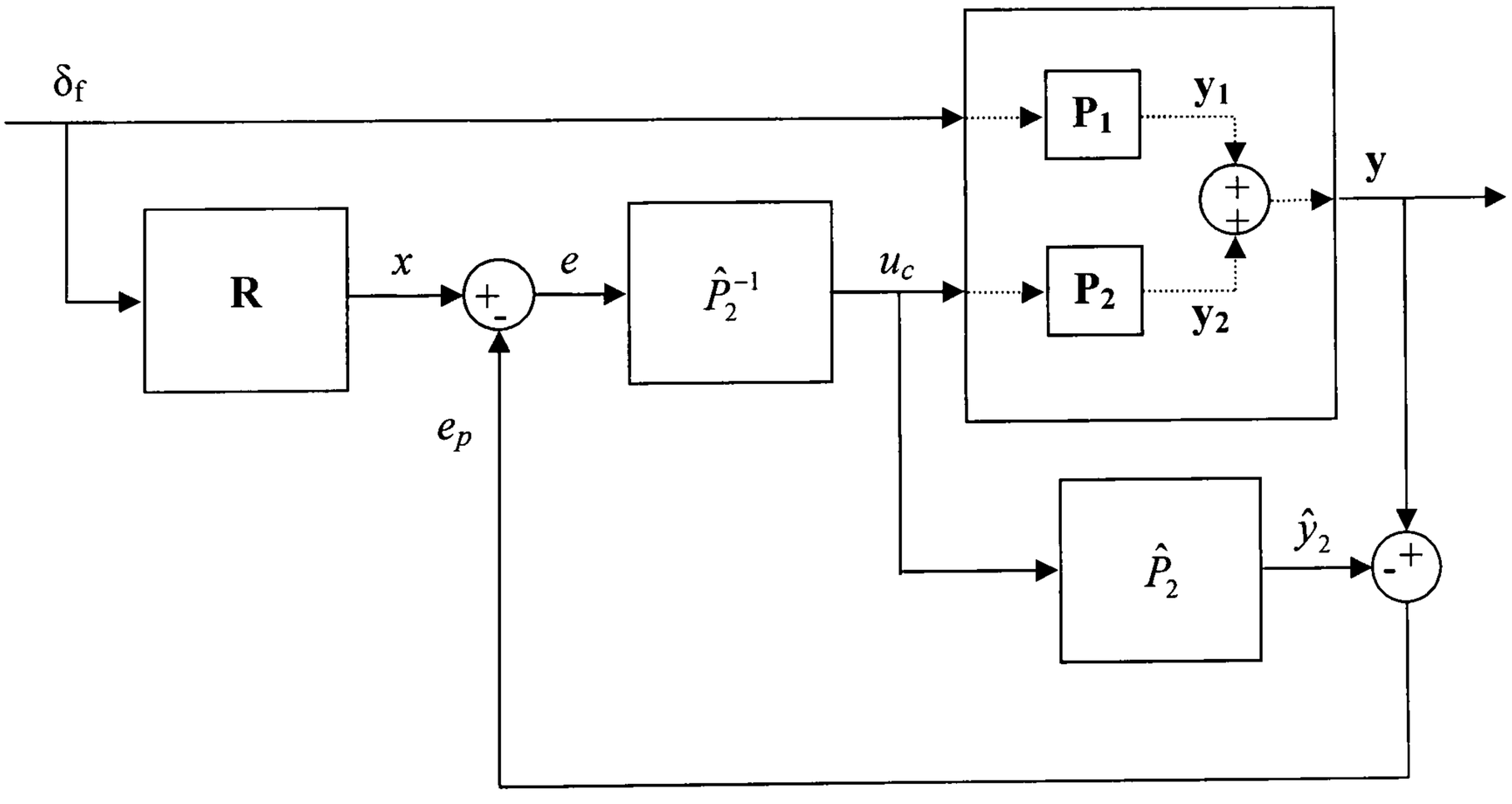

Figure 4.13 Multiple input IM control

The first part in adapting IM control to multiple inputs is to separate the vehicle into two models, one with the control action as the input, RMD or VTD, and another with all the other inputs, steering and throttle. In a linear system the vehicle model could be split in this manner and superposition would ensure that the sum of the outputs of the two models would create the same output as the original model. The model can also be split in such a way that the non-minimum phase part of the plant is separated into P_1. This allows P_2 to be minimum phase without any zeros in the positive s-plane that would become unstable poles in the inverse model. In a more complex non-linear model, splitting the model into separate components and using superposition may not be exactly possible but the technique can still be used as an approximation. Here the feedback signal is given by:

$$e_p = y - \hat{y}_2 \tag{4.13.}$$

where $\hat{y}_2$ is the output of the plant model $\hat{P}_2$ which approximates the part of the vehicle that models the control input, u_c, to the vehicle state, y. The input to the inverse model becomes:

$$e = x - e_p = x - \left(y - \hat{y}_2\right) \tag{4.14.}$$

Since $y = y_1 + y_2$ and $y_2 = \hat{y}_2 + d$, then:

$$y = y_1 + \hat{y}_2 + d \tag{4.15.}$$

where d represents any disturbances and modelling errors. Now substituting Equation (4.15) into Equation (4.14) gives:

$$e = x - \left(\left(y_1 + \hat{y}_2 + d\right) - \hat{y}_2\right) = x - y_1 + d \tag{4.16.}$$

Now considering that x is the ideal output created by the reference model, R, which is the desired output, y. You can set $x = y = y_1 + y_2$. Now substituting into Equation (4.16) and rearranging gives:

$$e = y_2 + d \tag{4.17.}$$

Therefore, the input, e, into the inverse model, $\hat{P}_2^{-1}$, is the ideal output, y2, compensated for any disturbances and modelling errors. The inverse model will then create the ideal control input, u_c, to match the vehicle output to the reference yaw rate. This shows the strength of IM control since the internal model and inverse model can

model the vehicle system that the controller acts on without needing to model the full system with the driver inputs. The IM controller just works to match the vehicle state to the ideal reference model behaviour through its own vehicle system treating everything else as a disturbance.

The final consideration is inverting the internal model and ensuring it is causal, that it has no dependence on input values from the future to be solved. If the numerator is of lower order than the denominator of the internal model transfer function, the inverse model will be non-causal. To remedy this problem, a filter must be added to the inverse model with the same order as the difference of order between the numerator and denominator. This introduces a time constant of the filter as a tuning parameter for the control.

IM control is more complex than the previously described PID control. It uses a reference model, plant model and inverse model. If these models are not understood and correctly used then errors can enter the system. However, the result is potentially a better controller. There is feedforward control as well as feedback in the system, which allows the IM controller to better predict plant changes and react earlier. Also, there are no control gains to be chosen or tuned, only the filter on the inverse model. This means that the controller is less tuneable to different conditions but at the same time it creates a more robust controller in conditions that have not been specifically tuned into the system.

4.2.4. Sliding Mode Control

Sliding mode control is a robust control strategy that is effective with non-linear systems. The block diagram is shown in Figure 4.14 with the following transfer function:

$$\frac{y}{\delta_f} = \frac{P_1 + P_2 C_{smc} R}{1 + P_2 C_{smc}} \tag{4.18.}$$

The controller is based on maintaining the state trajectory on a sliding surface in the state space. Once the desired sliding surface has been determined, the controller consists of two parts, the reaching phase and the sliding phase, as shown in Figure 4.15. The reaching phase is the part of the controller that pushes the state towards the sliding surface while the sliding phase aims to slide the state along the surface towards the desired state.

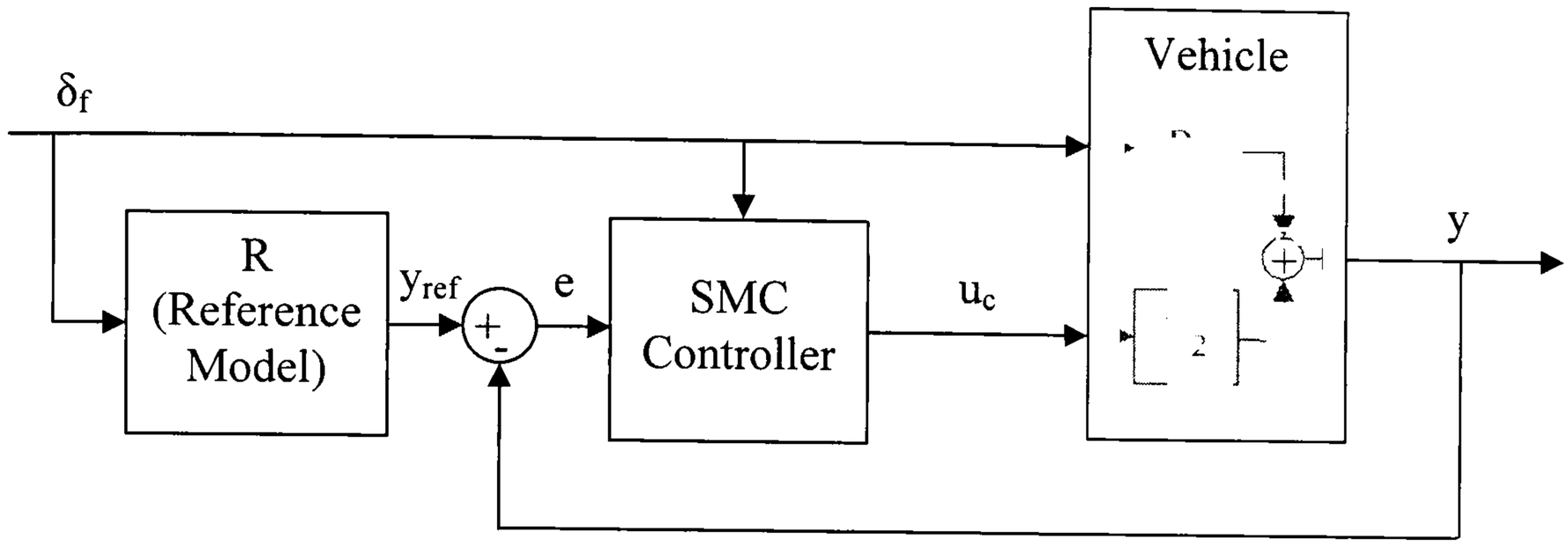

Figure 4.14 Sliding mode control block diagram

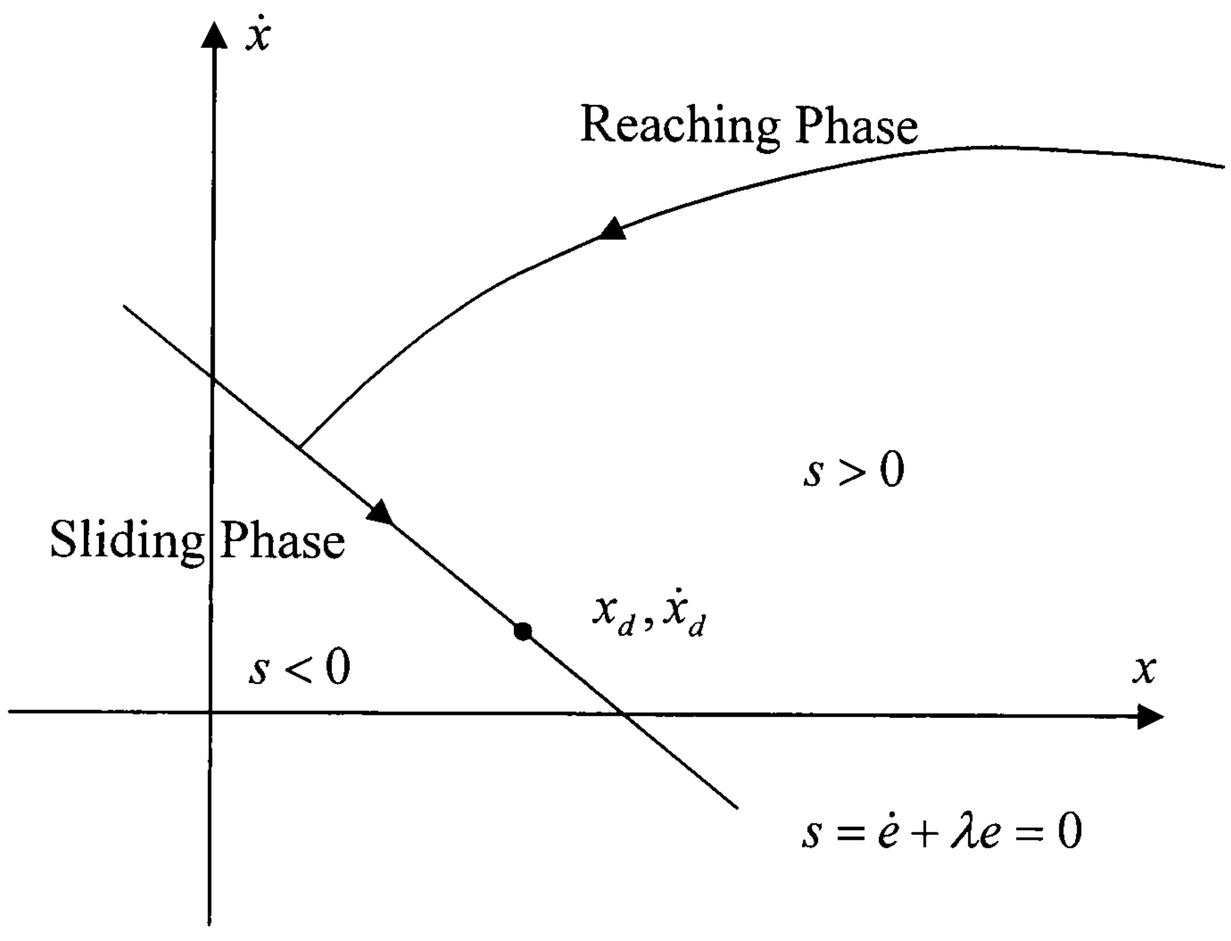

Figure 4.15 Sliding mode control diagram

The first part of creating a sliding mode controller is determining the sliding surface. The sliding surface is defined where a linear function of the tracking error is equal to zero. More specifically in a system given by Equation (4.19) it takes the form of a line given by Equation (4.20) where λ is the first order time constant to reach the desired state.

$$\dot{x} = f(x) + b(x)u \tag{4.19.}$$

$$\dot{e} + \lambda e = 0 \text{ where } e = x - x_d \tag{4.20.}$$

The sliding part of the controller will be satisfied if Equation (4.20) is satisfied. Substituting Equation (4.19) into Equation (4.20) gives the 'equivalent' control input

u_{eq} that will keep the state trajectory on the sliding surface. This is basically a non-linear inverse model control.

$$u_{eq} = b(x)^{-1}(-f(x)+\dot{x}_d - \lambda e) \tag{4.21.}$$

Before the sliding phase, the reaching phase of the controller needs to be addressed. To bring the state trajectory to the sliding surface, *s(x,t)* is defined as the distance of the states from the sliding surface and takes the form of Equation (4.22).

$$s(x,t) = e \tag{4.22.}$$

When $s = 0$ the state will reach the sliding surface. However, the controller has to work in the correct direction to draw the state towards the sliding surface. To ensure that the reaching phase on the controller always works to reduce *s*, a switching term is added to the controller. This gives the full control law as shown in Equation (4.23).

$$u = u_{eq} - k\,\mathrm{sgn}(s) \tag{4.23.}$$

where *k* determines the speed the system approaches the sliding surface. Substituting in Equation (4.21) gives

$$u = b(x)^{-1}(-f(x)+\dot{x}_d - \lambda e) - k\,\mathrm{sgn}(s) \tag{4.24.}$$

The value of *k* is determined by the inequality given in Equation (4.25).

$$\dot{s} \le -\eta\,\mathrm{sgn}(s) \tag{4.25.}$$

If this inequality, based on the Lyapunov stability criterion, is maintained it ensures that s and $\dot{s}$ will always be of opposite sign and the control action will always draw the state trajectory to the sliding surface. It also ensures the input output stability even if the states may not be stable. Substituting in for $\dot{s} = \dot{e} = \dot{x} - \dot{x}_d$ gives:

$$f(x)+b(x)u - \dot{x}_d \le -\eta\,\mathrm{sgn}(s) \tag{4.26.}$$

Now rearranging Equation (4.24) gives:

$$f(x)+b(x)u - \dot{x}_d + \lambda e = -k\,\mathrm{sgn}(s) \tag{4.27.}$$

Since λ does not affect the controller in the reaching phase because it is the time constant of the system reaching the desired state once it is on the sliding surface, it can be ignored when tuning *k*, which determines the rate at which the system

approaches the sliding surface. So from Equations (4.26) and (4.27) if $k \geq \eta$ the controller will always draw the state towards the sliding surface.

The final component of sliding mode control is a saturation function to replace the sign function in the reaching phase. In current automotive applications, sliding mode control would be applied using digital computers with discrete states. The nonlinearity of the sign function will result in chattering, as shown in Figure 4.16. This chattering is undesirable due to the high control effort required and the potential to excite high frequency dynamics.

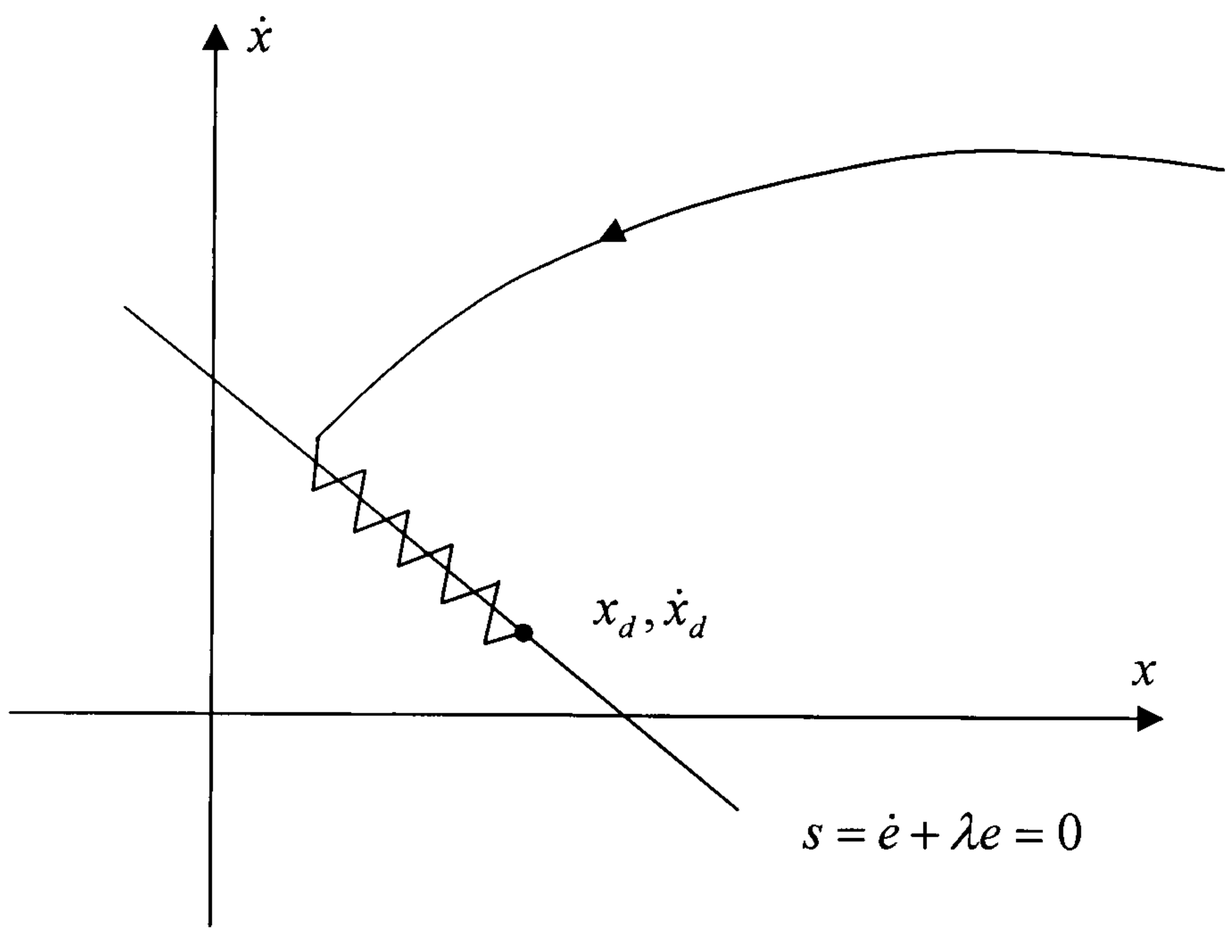

Figure 4.16 Chatter in sliding mode control

The solution to this problem is to replace the sign function with a saturation function giving the final control algorithm shown in Equation (4.28).

$$u = b(x)^{-1}\left(-f(x) + \dot{x}_d - \lambda e\right) - k \cdot sat\left(\frac{s}{\phi}\right) \qquad (4.28.)$$

The saturation function is shown in the following equation.

$$sat(x) = \begin{cases} x & if \quad |x| \leq 1 \\ \text{sgn}(x) & if \quad |x| > 1 \end{cases} \qquad (4.29.)$$

Once again sliding mode control is more complex than simple PID control. It requires a state space representation of the plant model that can be manipulated into the control equation and a desired reference behaviour. Although it is possible to represent the complete complex vehicle model in a state space form, solving these

complex equations for the control parameter can be very complex and involve a lot of computing power. A more reasonable solution is to use a simplified model that captures the essential dynamics in the control system. Using a simplified model results in a more efficient control algorithm but must always be done with care to ensure the system is adequately described. Another advantage of sliding mode control is that it is a robust control strategy. The control parameters, λ, k and ϕ, can be chosen to compensate for any uncertainties in the system modelling and disturbances in the environment. Also, the Lyapunov stability criterion guarantees the input output stability of the system, even if the stability of the states is not guaranteed.

4.3. Integrated Control Algorithms

The goal of this research is to increase the performance envelope of the vehicle while maintaining stability. This requires the integration of a driveability controller with a stability controller to create a multi-objective controller. The first step in integrating the individual controllers is to simply combine them. The most successful VTD controllers and RMD controllers are implemented at the same time to observe any interactions between them. These interactions can be positive or negative interactions and will show where an integrated control strategy needs to step in. Once the combined controllers have been observed the integrated control strategies can be developed.

The integrated control strategies will be switching strategies. Initially the driveability controller will be dominant and trying to push the performance envelope of the vehicle. As the vehicle begins to lose stability the integrated controller will have to switch the control precedence over to the stability controller. As the vehicle is stabilised the driveability controller can take over again. Obviously, the driveability control can not always be active and the performance of the vehicle will have to be restrained as it loses stability in order to allow the vehicle and driver to regain control.

4.3.1. PID Integration Control

The first integrated control is a simple PID controller used to integrate the two control actions. The PID integration control has the same components and works in the same way as the PID control described in Section 4.2.1. and has the same benefits and limitations that are outlined there. It is a very simple control strategy to

implement and it is very flexible. All it requires is an error signal and three gains, which can be tuned to give the best performance. It is also these gains that provide the limitation of the control strategy. In a non-linear system it can be very difficult to determine the best gains. Without the tools available in linear control the gain selection process can become a very long trial and error process.

The PID integration control takes a system state variable to create the error signal much like the independent controllers. However, instead of using the control output as an input into VTD or RMD, the integrated control output is used as a switching gain. This gain is saturated to values between 0 and 1 and multiplies the control outputs from the individual controllers to switch from one controller to another as shown in Equation (4.30).

$$\begin{aligned} K_1 &= K_{1ind} K_i \\ K_2 &= K_{2ind}(1 - K_i) \end{aligned} \tag{4.30.}$$

Here K_{1ind} and K_{2ind} are the outputs of the independent controllers, K_i is the saturated switching gain from the PID integration control and K_1 and K_2 are the final outputs to the actual control systems. In this manner as K_i goes from 1 to 0 the control precedence goes from the first independent controller to the second.

4.3.2. Adaptive Offset Gain PID Integration Control

The adaptive offset gain PID integration controller is a development of the simple PID integration control detailed in Section 4.3.1. It works in the same manner however, instead of merely saturating the PID integration control signal the PID controller uses adaptive gains and offsets these gains to delay the switching from the first independent controller to the second. The benefit of the adaptive gains is that the controller can be tuned much more precisely. The wide spectrum of vehicle states possible in the non-linear vehicle model require different control actions for different vehicle states. Using adaptive control with gain scheduling allows the integrated controller to better switch between the different independent controllers.

Offsetting the gains adds another parameter that can be tuned in the controller. The offset enables the integrated controller to delay the switching and with the adaptive offsets the length of the delay can be tuned for different vehicle states. This enables the switching point of the independent controllers to be delayed during slower dynamic vehicle states but allows quicker switches in faster dynamic situations.

Again, although the adaptive offset gains allow this greater degree of tuneability the drawback is that a much more detailed process must be used to determine the gains and their offsets for the entire range of possible vehicle states.

4.3.3. Phase Plane Integration Control

Phase plane control can also be used as a switching integration strategy. The switching integrated controller aims to switch from driveability control to stability control as the vehicle stability limits are approached. This is very similar to the basic phase plane stability control presented in Section 4.2.2. The phase plane control stabilises the vehicle as the stable limits are reached. In much the same way, the integrated phase plane control can allow the driveability control to work up to the stability limit without interference. At the stability limit the driveability control can be phased out by the same control boundary used by the phase plane stability control. This allows the phase plane stability control to be implemented without interference.

The phase plane integration control can also be extended to integrate other control systems. Each control system can have its own zone of operation defined on the phase plane shown, for example, by the different numbered and coloured regions in Figure 4.17.

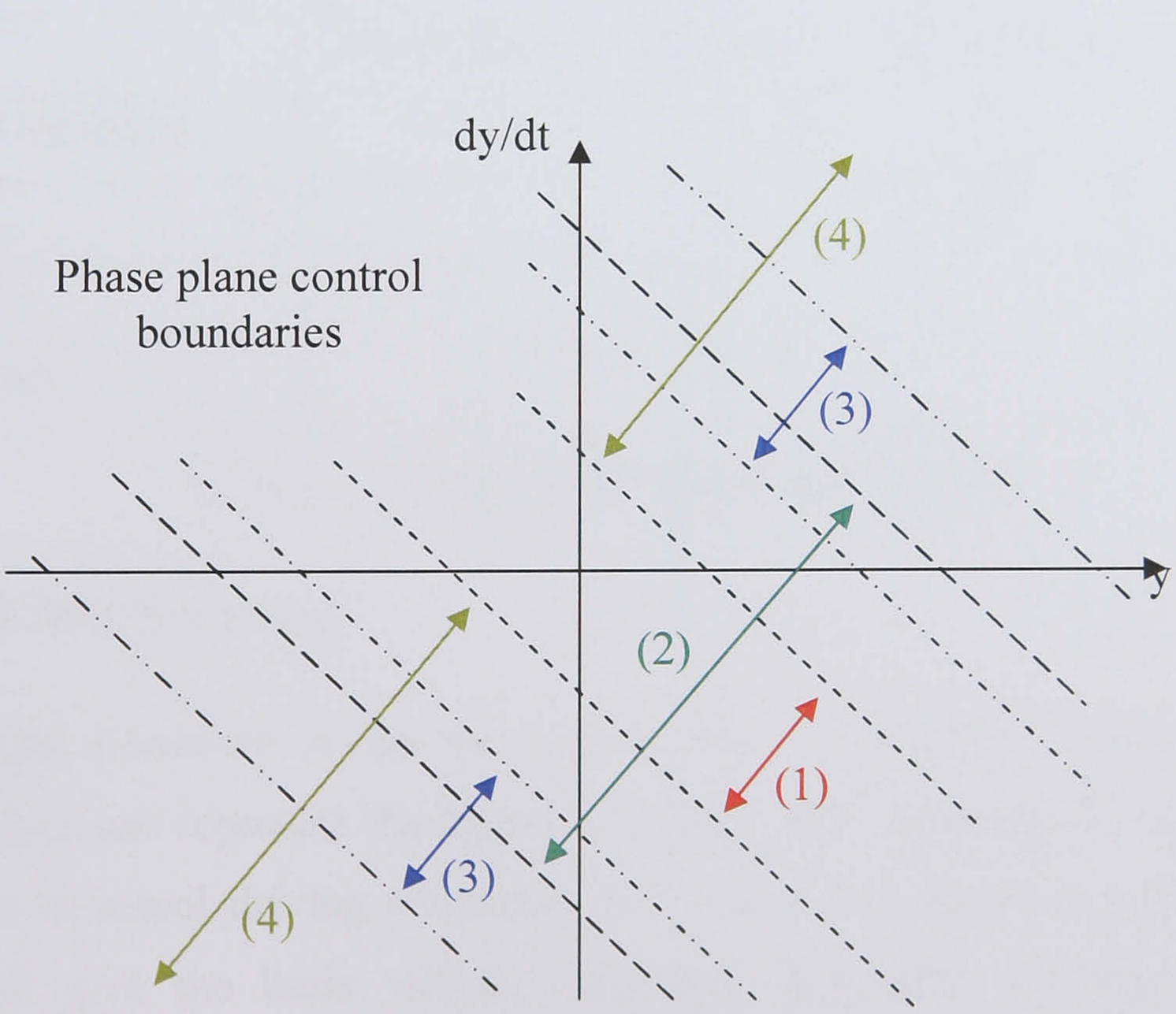

Figure 4.17 Example of multiple integrated phase plane controls

Multiple control boundaries can be defined and each control, represented by the different numbers and colours, has its own region of operation. In this way multiple

driveability and stability controls can all be integrated together and all operate where they are most effective.

4.4. Controller Evaluation

Choosing the method and tests used to evaluate the control strategies is extremely important. If the tests are not representative of the actual vehicle operating conditions the results obtained will be meaningless. In addition, if the tests do not cover the entire range of possible vehicle operation then the behaviour of the controllers will not be fully understood and erratic performance may result when the controllers are implemented on the vehicle. With this in mind, the objective of the tests is to simulate the entire range of vehicle performance. This will generate results that can be used to tune and develop the controllers as well as evaluate and compare the different control strategies. A list of tests is presented and compared in Table 4.1.

There are two sides to vehicle behaviour, the steady state handling and the transient handling of the vehicle. The steady state behaviour is given by steady state cornering while the transient handling can be evaluated with many different manoeuvres to test different aspects of vehicle behaviour.

	Steady state	Dynamic	Driveability	Stability
Steady State Cornering	X		X	
Step Steer		X	X	
Lane Change		X		X
Sinusoidal Steer		X	X	X

Table 4.1 Comparison of test manoeuvres

4.4.1. Steady State Cornering

Steady state cornering is the most basic way to evaluate vehicle handling. Although it does not represent the dynamic vehicle behaviour directly and it is not very common in actual driving situations, it is still a very useful test. Steady state cornering will give the basic vehicle behaviour. The basic understeer/oversteer balance can be observed and the ultimate cornering performance can be determined. Even though the manoeuvre is a steady state manoeuvre, the speed, steer angle and other vehicle parameters can be increased or decreased for different simulations to see how this baseline vehicle behaviour changes. Observing the changes in vehicle

behaviour with the changing vehicle parameters can then give insight into the dynamic behaviour of the vehicle.

4.4.2. Transient Manoeuvres

Although insight into the dynamic behaviour of a vehicle can be made with steady state cornering tests, transient manoeuvres are required to properly observe the dynamic vehicle characteristics. There are many different manoeuvres that can be performed depending on what aspect of vehicle handling is being explored. Basic transient manoeuvres are constant velocity test where the steering input follows a given profile. The next distinction in transient manoeuvres is the forward speed. If only purely lateral dynamics are being observed then the manoeuvres can be carried out at constant forward velocity. This will enable a simpler vehicle model and therefore faster simulation times. It will also simplify the results as there will be no influence from any longitudinal dynamics. Even if the longitudinal dynamics are within the scope of the work, it is useful to begin with constant velocity tests to simplify the evaluation process before moving on to accelerating or decelerating tests, in much the same way that steady state cornering tests are useful to begin with before moving on to transient manoeuvres. Once the vehicle has been evaluated with constant velocity tests, the same tests can be performed while accelerating or decelerating to evaluate the effects of the longitudinal dynamics on the vehicle handling.

Another distinction in the test is the coefficient of friction between the road surface and tyres. Again, initially it is useful to evaluate the vehicle behaviour on a high grip, uniform surface. This will give a good representation of the vehicle handling but vehicles also operate in low grip conditions, either on loose road surfaces or more commonly in the rain or snow. The vehicle behaviour can change dramatically as the road surface characteristics vary since most of the forces operating on the vehicle are generated from the tyres and their interaction with the road. In addition to testing vehicles on uniform surfaces with different coefficients of friction, tests can be carried out on split-μ surfaces. These tests are usually designed to simulate patches of ice on the road in active yaw controls that use the brakes or an active drivetrain to stabilise the vehicle. The tests are usually straight line braking or standing start tests where one side of the vehicle is on a high grip surface while the

other side is on a low grip surface. Since this work is mainly concerned with the lateral handling dynamics of a racing car on a track with a uniform surface, split-μ tests will not be carried out although tests on low-μ surfaces will be evaluated.

All the following tests can be evaluated both at constant velocity or while accelerating or decelerating as well as on high grip and low grip surfaces.

Step steer test

The most basic dynamic vehicle manoeuvre is a step steer test. The test is a basic test where there is a step input in the steering angle. This test shows the rise time and settling characteristics of the vehicle dynamics. Another benefit of the step steer test is that if it is run at constant velocity, it can be run to a steady state, which enables the steady state cornering to be evaluated at the same time. The test is also an open loop test so there is no feedback through a driver model that could affect the clarity of the results. One shortfall of the step steer test is that it does not show the effects of changing the direction of steering. The vehicle only goes from running in a straight line to cornering in one direction. This means that the vehicle is always in a stable state before the steering input.

Lane change test

Another transient manoeuvre is the lane change test. The lane change test again shows rise time and settling characteristics but with the change from steering in one direction to the other when the vehicle could be in an unstable state, the benefit of this test is that it can be used to evaluate the vehicle stability better than the step steer test. It is commonly used when designing vehicle stability controllers for passenger cars since it simulates an emergency avoidance manoeuvre. A similar manoeuvre is the double lane change test. In the double lane change test the vehicle first moves from its current lane to an adjacent lane and then quickly back into the first lane again. Once more this test simulates a realistic emergency avoidance manoeuvre and so it is a commonly used test. The lane change and double lane change tests can be run as open loop tests with a predetermined steering profile to give the basic manoeuvre or more commonly as closed loop tests. In a more complex simulation with a driver model, the driver model can make the vehicle follow a lane change path to include the driver dynamics in the closed loop.

Sinusoidal steer test

The sinusoidal steer test is generally used to test the path tracking and ultimate stability limits of vehicle handling. To achieve this it is usually run with an open loop, increasing amplitude, sinusoidal steering input and the test is run until the vehicle loses stability. The test starts with a small steer angle amplitude which results in stable vehicle behaviour but as the amplitude of the steering angle is increased the vehicle reaches higher and higher g-forces before ultimately losing stability. The progression from stable handling to the final loss of stability shows how the vehicle behaviour follows a reference behaviour before it develops into an uncontrollable state. This can help with the development of driveability and stability controllers which can be designed to control the development of the instabilities in the vehicle state. Sinusoidal steer tests can also be run with increasing or varying frequency.

4.5. Control Algorithms and Evaluation Conclusions

Many different control algorithms have been used in vehicle control. One of the most simple to implement is PID control. PID control works to minimise an error signal and can be tuned with proportional, integral and derivative gains. An adaptive control strategy can be created by using gain scheduling to finely tune the controller to different vehicle states. Phase plane control can be used as a stability controller by defining a stable region of vehicle handling on the phase plane. An error signal is created when the vehicle leaves the control boundary and is defined by the distance the vehicle state is from this boundary. A more complex control strategy is internal model control, which incorporates feedforward into a feedback controller. It also uses an internal model to compensate for any unmodelled disturbances. Sliding mode control is also more complex than the PID control but does not require a linearised model like internal model control. The sliding mode control aims to push the vehicle state towards a stable state trajectory and then moves the state along this trajectory towards the desired state.

The integrated control strategies are developed from observing the interactions between the controllers when they are simply combined. By recognising the positive and negative interactions of the individual controllers a multi-objective integrated strategy can be developed. The integrated strategies are generally switching strategies that designate controller dominance based on the vehicle state. Initially the

driveability control will have precedence but as the vehicle reaches the limits of handling the stability controller will take over. PID control can be used to implement an integrated strategy by using the control output to switch between the different individual controllers. Again, an adaptive strategy can be developed to further tune the controller to be more effective across the range of vehicle behaviour. Another control that can be used as a switching controller is the phase plane control. The stability boundary can be defined on the phase plane and let the driveability control operate within the stable limits while the stability control gets precedence beyond the stable limits.

The tests and methods used to evaluate the controllers can determine the relevance of the results. Steady state cornering tests can be used to assess the stable handling characteristics of the vehicle including the oversteer/understeer balance. Although insight can be gained into the dynamic behaviour of the vehicle with steady state cornering, transient handling tests are required to get a more accurate evaluation. Transient handling tests include the step steer, lane change, fishhook and sinusoidal steering tests. All these tests can show different aspects of the transient behaviour of the vehicle. In addition to the different manoeuvres available, these tests can be run while accelerating or decelerating and on surfaces with low or high grip.

5. *Independent Control Strategy Tuning*

Chapter 5 presents the independent controller tuning. Each control algorithm presented in Chapter 4 is developed into an independent controller for roll moment distribution driveability and stability control and variable torque distribution driveability and stability control. The gain selection and tuning process is described and presented for each independent controller.

5.1. Introduction to Control Tuning

This chapter presents the independent controller tuning. The control strategies presented in Chapter 4 will be developed into independent controllers with specific control objectives. Each control strategy will be evaluated for its effectiveness in controlling both roll moment distribution and variable torque distribution to improve driveability as well as stability. First roll moment distribution controllers are tuned followed by the variable torque distribution controllers. The full vehicle model will be used to tune the controllers in order to get an accurate representation of the vehicle dynamics.

The controllers will be tuned with step steer test manoeuvres. The step steer test is chosen since the transient vehicle behaviour is excited but it also settles and reaches a steady state. The driveability controllers are tuned with an increasing velocity step steer test. This test is run with an initial velocity of 22 m/s accelerating at 1.5 m/s^2. The step steer angle is 1.5 degrees at the wheels. This test is chosen because it begins in the middle of the handling range then pushes to the vehicle limit. It has a medium velocity and steer angle and results in a 0.7g manoeuvre. This is within the handling limits of the vehicle so there is scope for the control action. The increasing velocity of the test allows the control response to be observed as the vehicle approaches instability.

The stability controllers are also tuned with a step steer test but at constant velocity. The test is run at 25 m/s with a steer angle of 2.5 degrees. This steer angle and velocity are chosen since individually they are in the middle of the range for this vehicle but they produce a manoeuvre that is right on the stability limit. Since the

vehicle is already at the handling limit increasing the velocity is not necessary and only adds complexity.

5.2. Roll Moment Distribution Control

Roll moment distribution (RMD) control changes the understeer/oversteer balance of the vehicle by altering the vertical tyre forces as described in Section 2.1. The modelled vehicle's passive roll moment distribution is 0.54, which gives a slightly greater roll stiffness at the front axle of the vehicle. If the roll moment is moved towards the front the load transfer across the front axle increases. Since the lateral tyre force is non-linear with respect to normal force, the increase in lateral force at the loaded tyre is less than the reduction in lateral force at the unloaded tyre. The result is that the combined lateral force from the front axle decreases and understeer is promoted. The opposite is true if the roll moment distribution is moved to the rear of the vehicle.

The roll moment distribution is described by:

$$c_{K_d} = c_{K_{d_s}} + \Delta c_{K_d} \tag{5.1.}$$

Here $c_{K_{d_s}}$ is the passive roll moment distribution and Δc_{K_d} is the control action. c_{K_d} can vary from 0 to 1 with 0 representing all the roll moment distributed to the rear axle and 1 representing all the roll moment distributed to the front axle. However it is limited to values between 0.15 and 0.85 since it would be impractical to reduce the roll moment distribution of an axle to zero. Since no hardware has been specified, these values are generic and would need to be determined for an actual application.

5.2.1. PID Control

PID control is a basic control that only requires an error signal and some simple mathematical manipulation. As presented in Section 4.2.1, it can be fine tuned through the gain selection. This makes it a good basic control strategy. Although the gains can be fine tuned to give the desired system response, selecting the best gains can prove to be difficult if the system behaviour changes over the range of operation.

Yaw rate tracking PID control

A driveability control can be created from the vehicle yaw rate. The objective of the controller is to use the roll moment distribution to control the understeer/oversteer balance of the vehicle to track a desired reference yaw rate. The difference between the actual vehicle yaw rate and the reference yaw rate is used as the error signal for the PID controller. A block diagram of the controller is shown in Figure 5.1.

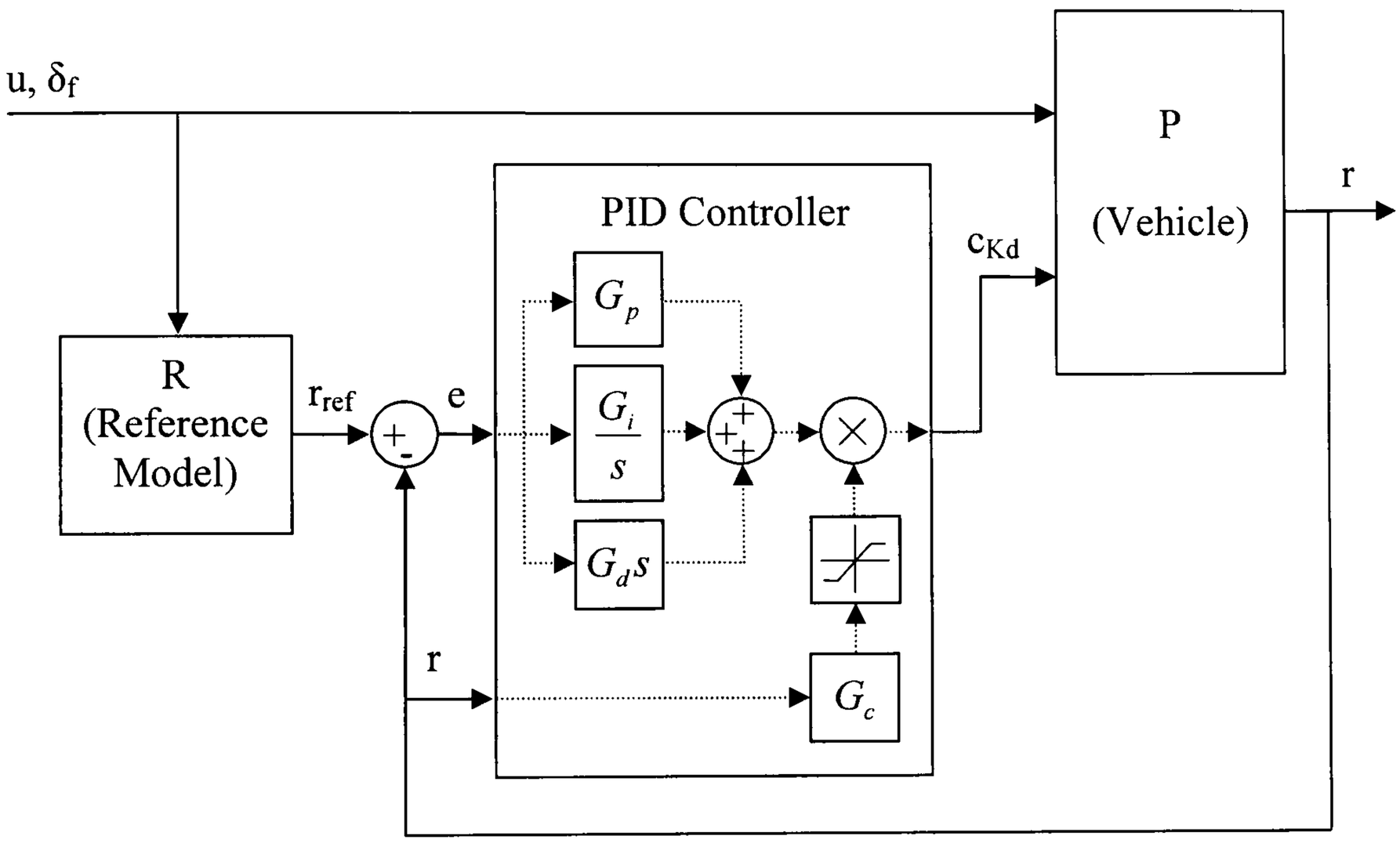

Figure 5.1 RMD yaw rate tracking PID control block diagram

This block diagram differs from the control presented in Figure 4.1 due to the inclusion of the reference model and the saturation function. The reference model is used to create the desired reference yaw rate. The error signal is then created by subtracting the actual yaw rate from the reference yaw rate. The reference yaw rate is obtained from a steady state model given by the following equation:

$$r_{ref} = \frac{u\delta_f}{(a+b)+Ku^2} \tag{5.2.}$$

where K is the stability margin given by:

$$K = \frac{m(bC_r - aC_f)}{(a+b)C_fC_r} \tag{5.3.}$$

A linear model is chosen since linear behaviour is predictable. When a vehicle nears limit handling the behaviour becomes increasingly non-linear, which is less predictable. By using a linear reference model the range of the linear vehicle behaviour can be extended further into the limit handling area of vehicle behaviour and ease the demand on the driver. However, it is also possible to push the vehicle to instability by demanding a response it can not achieve.

The control output is determined from the following equation that is slightly modified from the basic PID control given in Section 4.2.1.

$$\Delta c_{K_d} = rG_c\left(G_p\left(r - r_{ref}\right) + G_i\int\left(r - r_{ref}\right)\cdot dt + G_d\frac{d}{dt}\left(r - r_{ref}\right)\right) \qquad (5.4.)$$

where $-1 \le rG_c \le 1$

Here G_p, G_i, and G_d are the proportional, integral and derivative gains. The saturated rG_c term is added to the control law to account for the fact that the roll moment distribution is non-directional. If the error signal, r-r_{ref}, is positive and r is positive then the controller will distribute the roll moment forward to promote understeer. In this case the basic control would result in the correct control action. However, if r is negative and the error signal is negative, the basic PID controller will not promote understeer as required. An extra term is needed to ensure the control action works in the correct direction. By multiplying the error signal by r the correct control action is ensured. However, r, has a small value and would decrease the overall gain of the controller if it was used by itself. Ideally the function $\mathrm{sgn}(r)$ would be used.

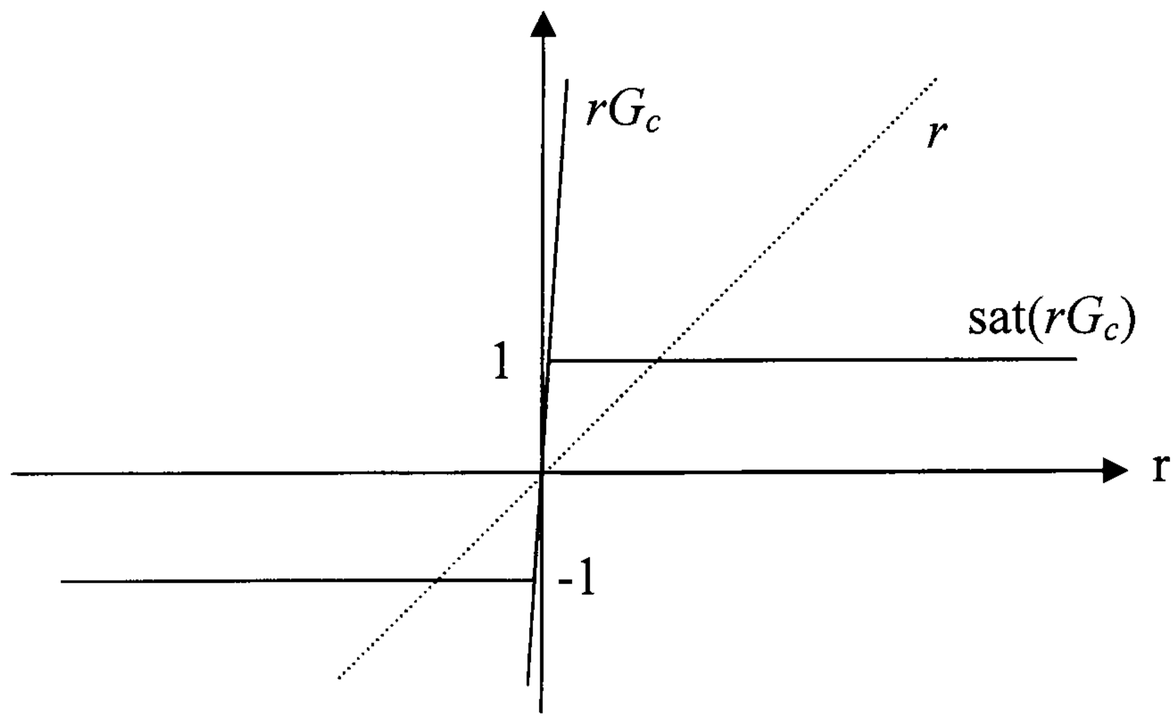

Figure 5.2 Diagram of the saturation function sat(rG_c)

This would not affect the overall control gain. The disadvantage of using the $\text{sgn}(r)$ function is that it adds a discontinuity to the controller. Discontinuities in the control equations can be difficult to solve and can slow down or potentially crash the control program. An alternative to the sign function is a saturation function, shown in Figure 5.2.

Although the saturation function also introduces a discontinuity into the system, it is more forgiving for values of r close to zero. The derivative still has a finite value around zero, unlike the derivative of the sign function which is undefined at zero.The saturation function will limit the values between -1 and 1 but a large gain is required. A large gain ensures the switching from -1 to 1 operates over a small range of input resulting in a function very similar to the sign function without the discontinuity. Multiplying r by a large gain, G_c, will ensure that the output of the saturation function will not affect the overall controller gain. G_c is set to 50, which is large enough to ensure the saturated function does not influence the overall control gain.

The difficulty in implementing a successful PID control strategy is selecting and optimising the gains to work in all conditions the system operates under. As mentioned at the beginning of the chapter, the gains are tuned using an increasing velocity step steer test run at 22 m/s with a steer angle of 1.5 degrees. The controller tuning is shown in Figure 5.3.

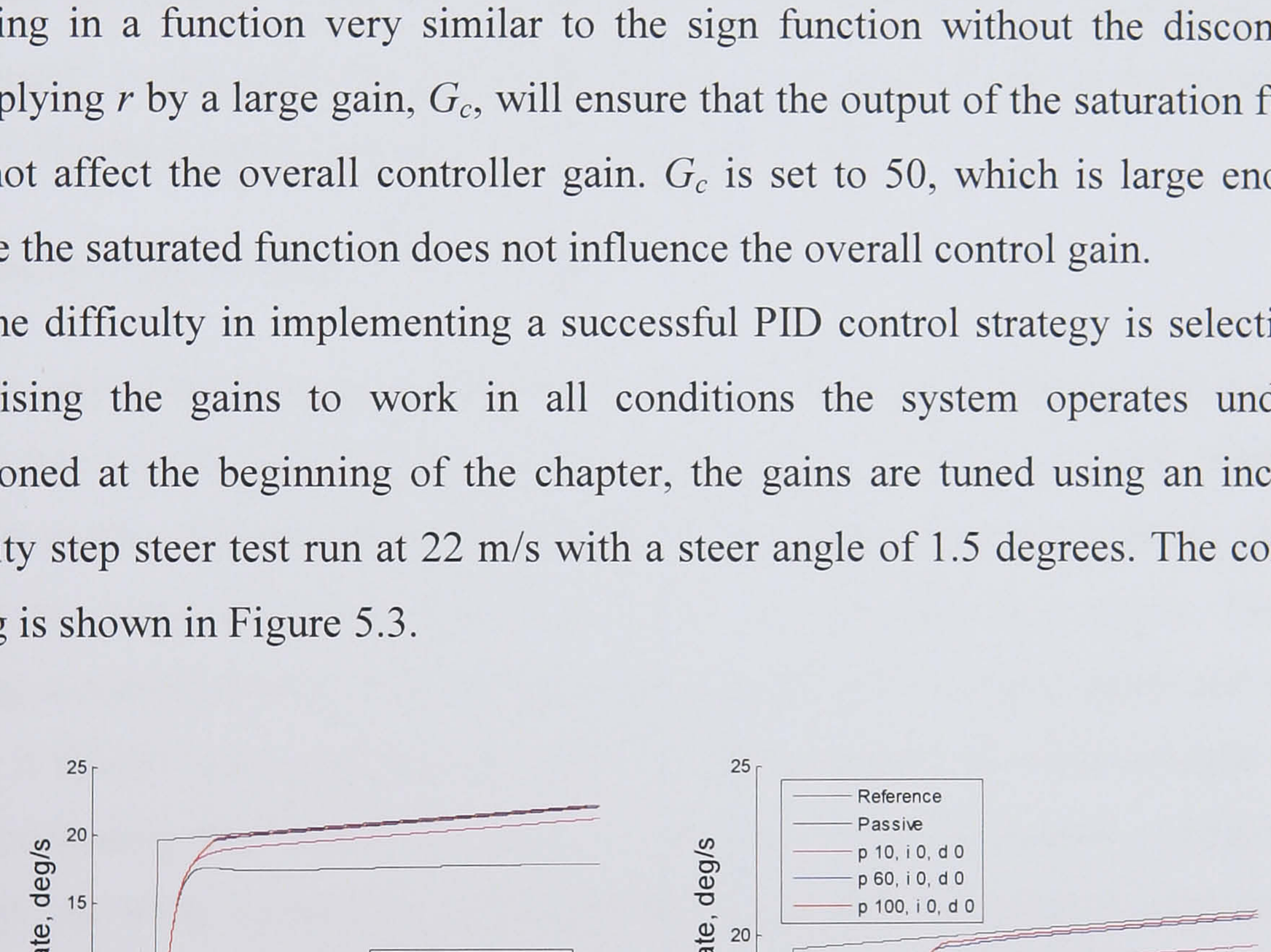

Figure 5.3 PID gain selection of the RMD yaw control

The proportional gain is the first gain to tune. Figure 5.3.a shows the effect of the proportional gain. A gain of 10 gives improved response but as the gain is increased to 60 the vehicle response starts to match the reference signal. If the proportional gain is increased much more than this the improvement in performance is negligible, as shown in Figure 5.3.b, which is a detail of Figure 5.3.a from 0.2 to 1.0 second. With the proportional gain set at 60 there is still some steady-state error that can be removed with the integral gain. Figure 5.3.c and Figure 5.3.d show the response to the same test with increasing integral gain and a detail view of the same results. An integral gain of 1 takes some time to remove the steady-state error while a gain of 20 overshoots the reference signal. An integral gain of 10 allows the controller to maintain the desired yaw rate. Since there is no oscillation, a derivative gain is unnecessary so the gains for this controller can now be set at 60 for the proportional gain, 10 for the integral gain and 0 for the derivative gain.

Sideslip angle tracking PID control

One way of increasing the stability of a vehicle is to reduce the sideslip angle. If a vehicle has a small sideslip angle, the tyre slip angles will also be small. With small tyre slip angles, the tyre forces will not be close to saturating which leaves plenty of margin to create additional forces to direct and stabilise the vehicle. However, creating a control strategy that uses the sideslip angle as the error signal and aims to reduce it to zero is not practical. It is not possible to reduce the sideslip angle to zero since producing the lateral forces to enable the vehicle to corner requires some sideslip. As such, tuning the controller and choosing the control gains becomes difficult because increasing the control gains will never reduce the error (sideslip angle) to zero. To create a more reasonable control strategy a sideslip error signal needs to be defined. Once again, the linear reference model is used to create a reference sideslip angle that the controller aims to track.

The objective of this PID control is to minimise the sideslip angle by matching it to a linear reference model. A block diagram of the control is given by Figure 5.4. The feedback signal is the difference between the reference and the actual sideslip angle. The reference sideslip angle is given by the two degree of freedom linear state space model in Equation (5.5).

$$\begin{bmatrix}\dot{\beta}\\ \dot{r}\end{bmatrix}=\begin{bmatrix}-\dfrac{C_f+C_r}{mu} & -\dfrac{mu^2+\left(aC_f-bC_r\right)}{mu^2}\\ -\dfrac{aC_f-bC_r}{I_{zz}} & -\dfrac{a^2C_f+b^2C_r}{I_{zz}u}\end{bmatrix}\begin{bmatrix}\beta\\ r\end{bmatrix}+\begin{bmatrix}\dfrac{C_f}{mu}\\ \dfrac{aC_f}{I_{zz}}\end{bmatrix}\left[\delta_f\right] \qquad (5.5.)$$

$$y=\begin{bmatrix}\beta\\ r\end{bmatrix}$$

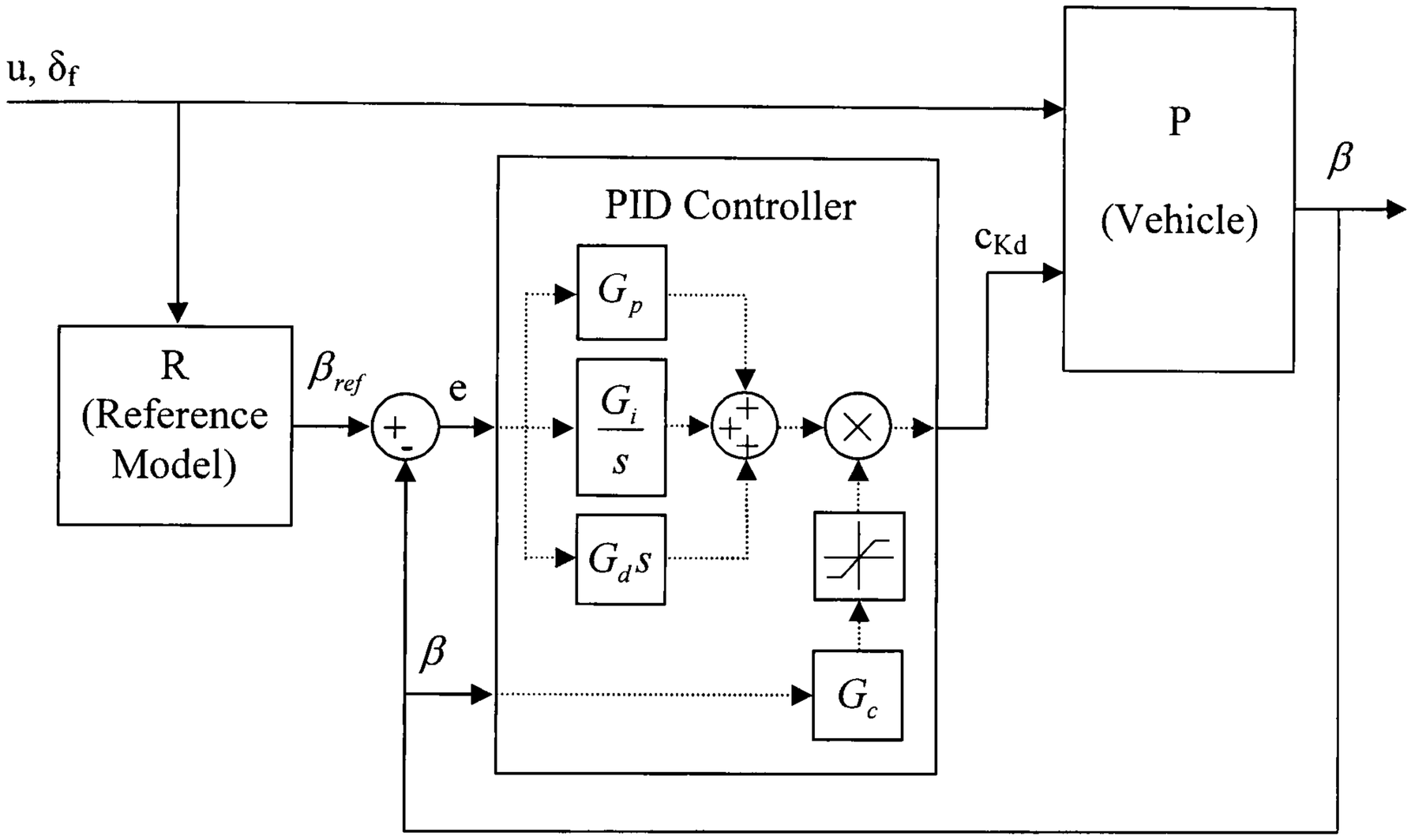

Figure 5.4 RMD sideslip angle tracking PID control block diagram

The control signal has a very similar structure to the PID yaw rate tracking control and is given by the following equation:

$$\Delta c_{K_d}=\beta G_c\left(G_p\left(\beta_{ref}-\beta\right)+G_i\int\left(\beta_{ref}-\beta\right)dt+G_d\left(\dot{\beta}_{ref}-\dot{\beta}\right)\right) \qquad (5.6.)$$

where $-1\le\beta G_c\le 1$

Here the saturation function is used in the same way it was used in the yaw rate tracking control of the previous section. βG_c is again described by the same function given in Figure 5.2. The purpose is to ensure that the control action is not affected by the direction the vehicle is turning. As the sideslip angle increases beyond the reference signal the roll moment is distributed further to the front of the vehicle. The effect of this control action is to create a larger lateral load transfer across the front axle. With a large lateral load transfer at the front of the vehicle, the ability to create

lateral force at the rear increases and decreases at the front promoting understeer and a reduction in the sideslip angle.

Again, the gain selection is the critical part of creating an effective control. The test run is a step steer test run at 25 m/s with a steer angle of 2.5 degrees. This test manoeuvre is chosen because it is right on the limit of vehicle stability. The proportional control is adjusted first. As shown in Figure 5.5.a increasing the proportional gain reduces the sideslip angle, which is the desired effect. However, increasing the proportional gain beyond 15 does not result in a further decrease in sideslip angle. The derivative gain is used to damp out the system response. Unfortunately, as shown in Figure 5.5.b, introducing a derivative gain does not have the desired effect, it actually creates oscillations. For this reason the derivative gain is set to zero. The final gain to tune is the integral gain. Increasing the integral gain removes the steady state error, as shown in Figure 5.5.c. Using an integral gain of 50 removes the steady state error and shows the best settling characteristics.

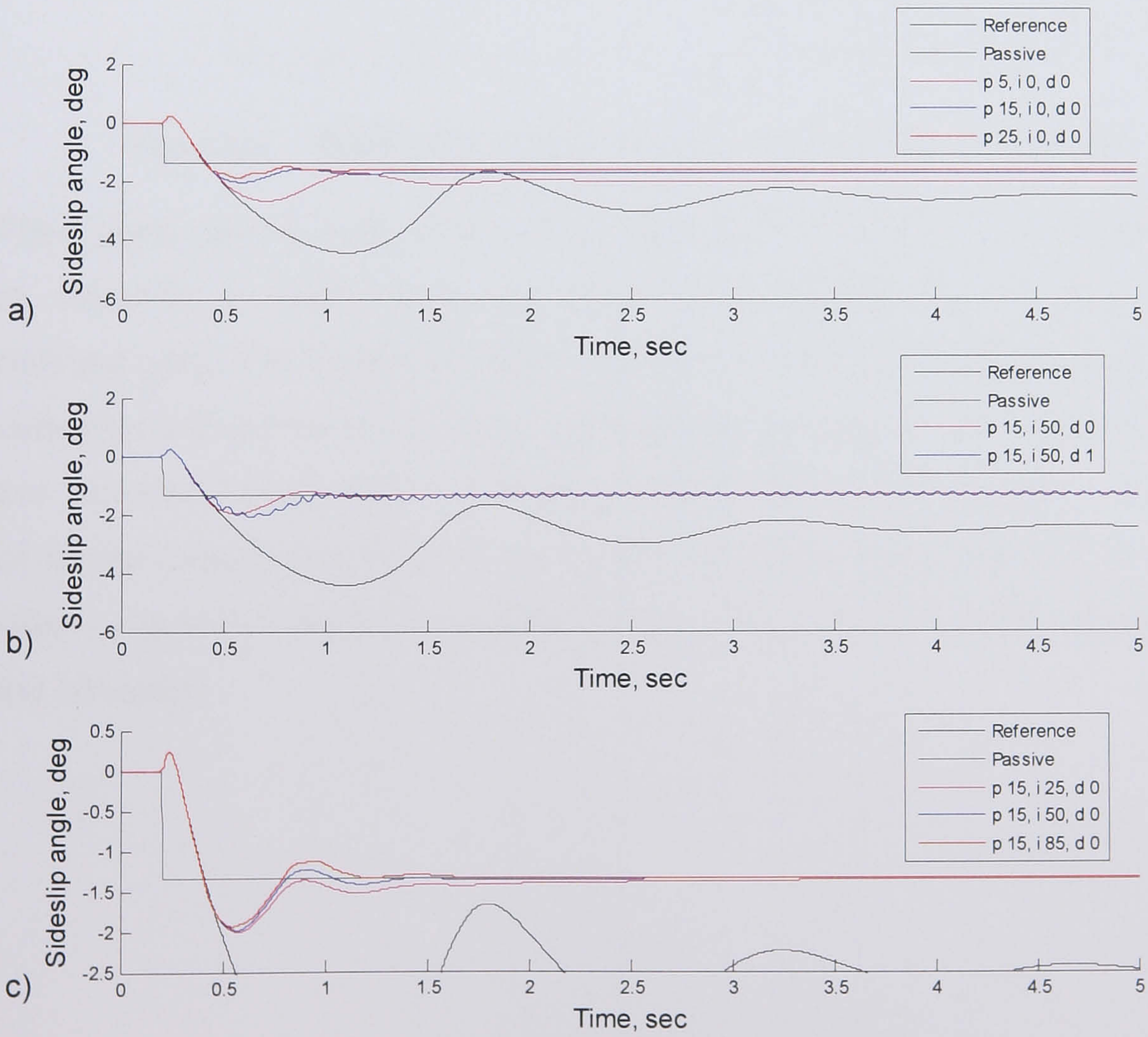

Figure 5.5 PID gain selection of the RMD sideslip angle control

5.2.2. Sideslip angle phase plane stability control

Phase plane control is a control strategy used to stabilise system dynamics. Section 4.2.2 showed that the phase plane plot of a system state shows the dynamic behaviour of that state. Using the phase plane, the control can stabilise the system by limiting the trajectory of the phase curve. Used with sideslip angle, phase plane control can confine the sideslip behaviour to stable bounds with less gain tuning than required by PID control. The controller takes the form shown in Figure 5.6.

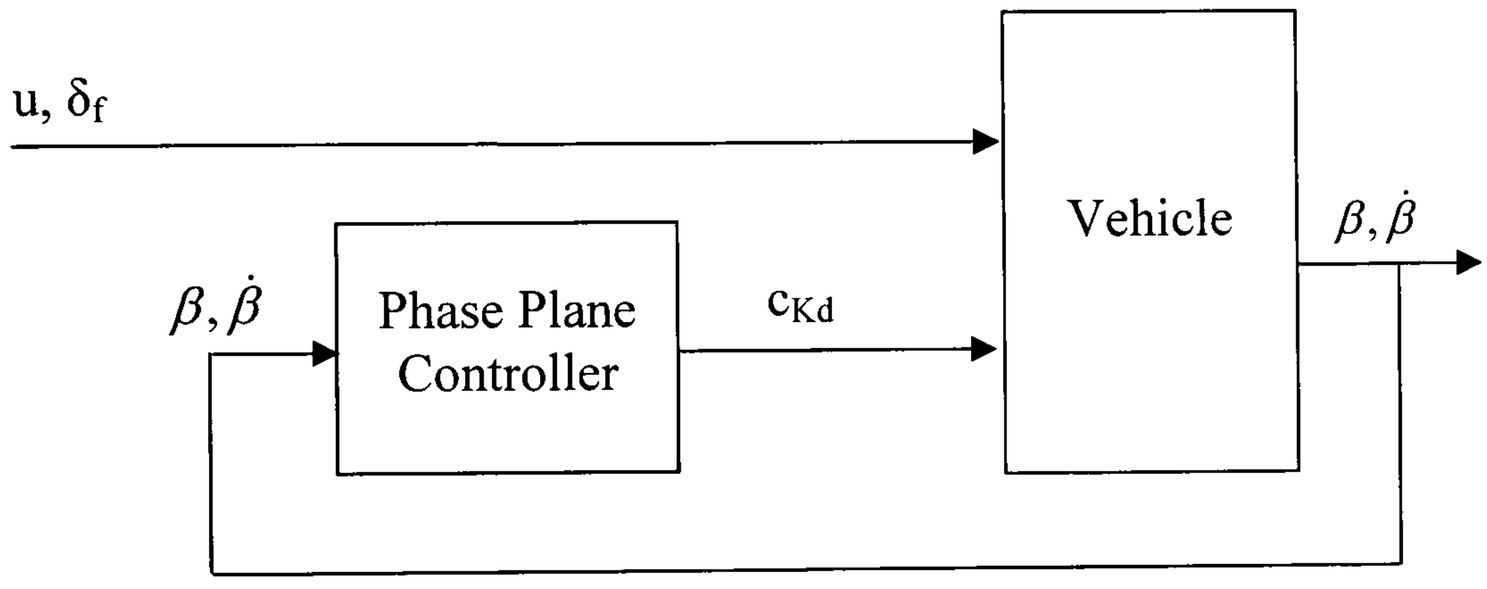

Figure 5.6 RMD phase plane stability control block diagram

Phase plane control does not have the integral and derivative gains that need to be tuned, however, a control boundary needs to be defined and it does have a proportional gain. The control boundary defines the region in the phase plane where the controller will not be active. This conserves energy and also limits the amount of control intrusion during stable operating. Outside the control boundary, the error signal for the control is defined by the distance from the vehicle state to the control boundary. Figure 5.7 shows an example phase curve with two different choices of control boundary.

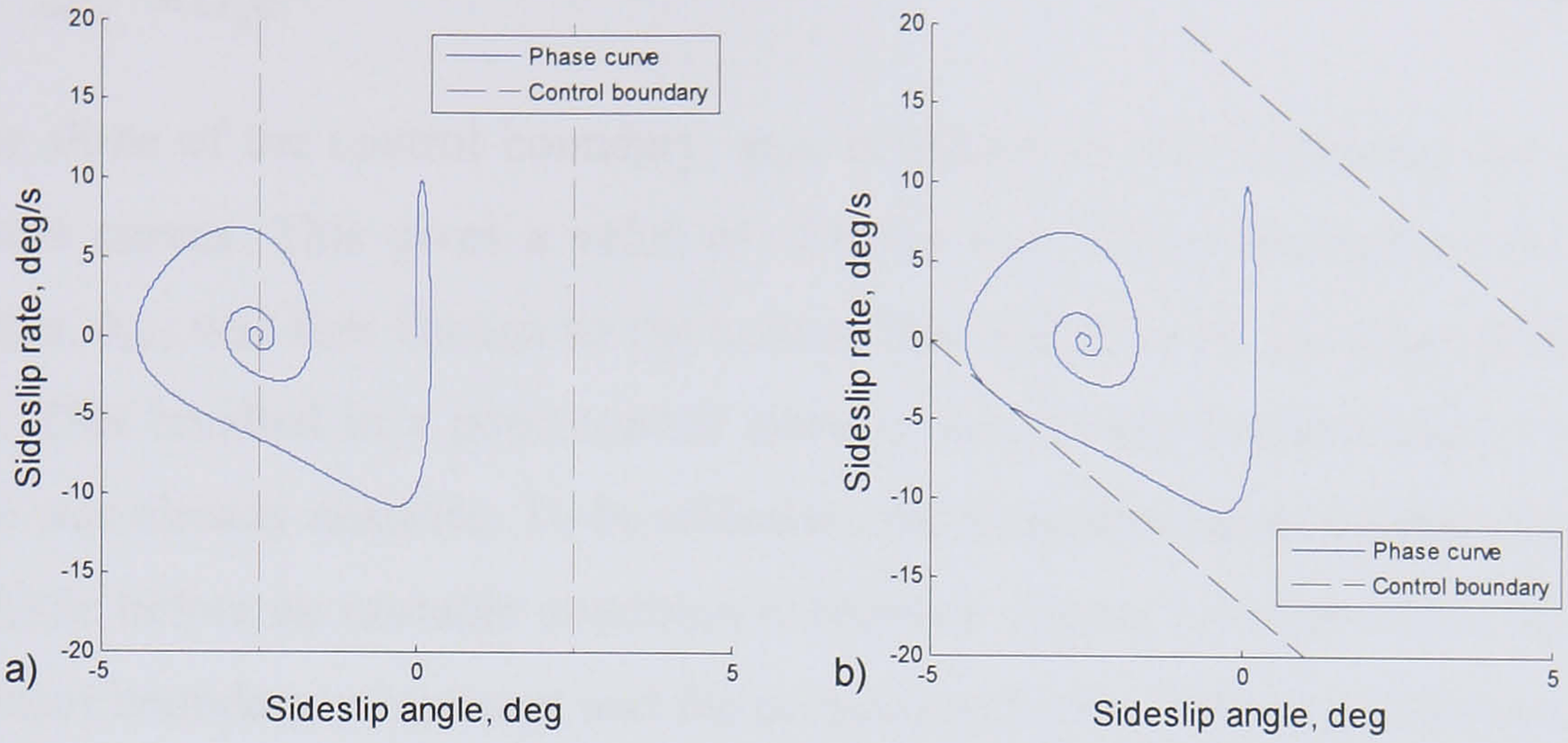

Figure 5.7 Control boundaries on the phase plane

A simple control boundary can be defined by limiting the absolute value of the sideslip angle, as shown in Figure 5.7.a. Although limiting the sideslip is the aim of stability controllers, this choice of control boundary has the disadvantage that the sideslip rate is not considered. Also, with this choice of boundary the phase curves can intersect this control boundary at high angles. This results in abrupt control actions due to the large rate of change in the control error signal.

A better choice of control boundary considers the sideslip rate as well as the sideslip angle. A vehicle state with a high sideslip angle can still be tolerated if the sideslip rate is the opposite sign and reducing the sideslip angle. The other benefit of the control boundary presented in Figure 5.7.b is that it minimises the angle that the phase curves intersect the control boundary, resulting in a more progressive controller. The control boundary is given by the following equation:

$$C_b = m_{cb}\beta \pm b_{cb} \tag{5.7.}$$

Where "$+b_{cb}$" is for the upper boundary and "$-b_{cb}$" is for the lower boundary.

With the control boundary determined, the error signal is defined as the distance from the vehicle state to the control boundary, given by:

$$e = \frac{\left|\dot{\beta} - m_{cb}\beta \mp b_{cb}\right|}{\sqrt{m_{cb}^2 + 1}} \tag{5.8.}$$

Where "$-b_{cb}$" is used if the state is above the control boundary and "$+b_{cb}$" is used when it is below the control boundary. The error signal is then put through a proportional amplifier to create the control signal given by:

$$\Delta c_{K_d} = G_p e \tag{5.9.}$$

The slope of the control boundary, m_{cb}, is chosen so that it matches the angle of the phase curves. This gives a value of -5.0 for m_{cb}. The y-intercept of the control boundary, b_{cb}, was first chosen so the control boundary lies on the edge of the stable region. This resulted in a poor control since it would only become active when the vehicle was already unstable. To be effective, the controller needs to begin stabilising the vehicle before an unstable condition is reached. Figure 5.8 shows the selection of the control boundary y-intercept and the proportional gain. The dashed lines represent the control boundary in these figures. In the legend, p is the proportional gain and b is the y-intercept. The test was once again a step steer test at 25 m/s and 2.5 degrees steer angle.

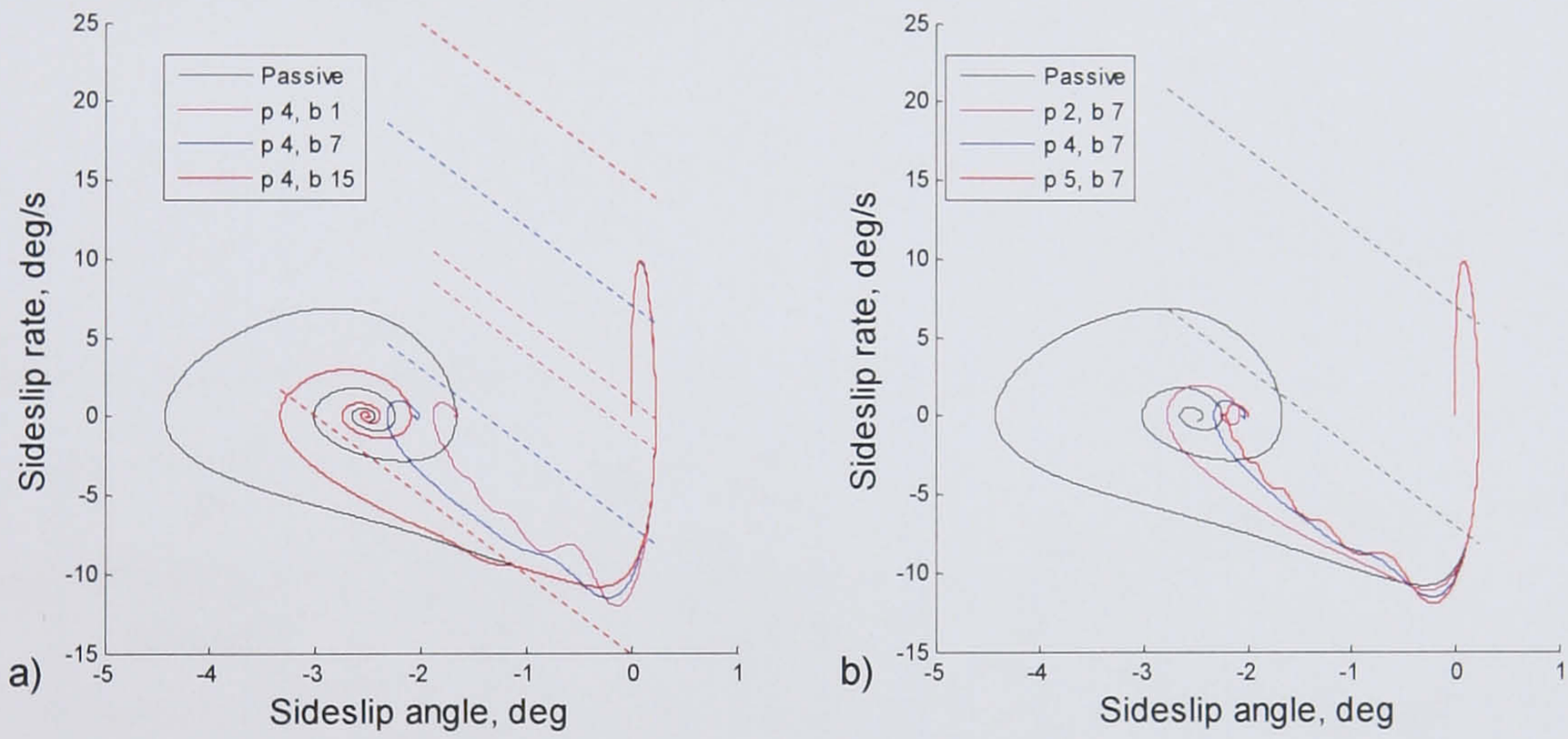

Figure 5.8 Control boundary and gain selection of the RMD phase plane sideslip angle control

Figure 5.8.a shows that although the vehicle is eventually stabilised, there is some oscillation around the steady state when the control boundary is chosen to be wider, with a large value for b_{cb}. This is due to the vehicle being closer to the stability limits. Oscillations in the phase curve can also be noticed if the control boundary is very narrow. In this case the controller is aiming to overly constrain the sideslip behaviour. Oscillations in the phase curve can also be noticed as the proportional gain is increased in Figure 5.8.b. These oscillations are caused by increasing the gain and forcing the system too much. If the gain is too small, oscillations around the steady state occur. As a result, the proportional gain is set to 4 while m_{cb} is set to -5 and b_{cb} is set to 7.

5.2.3. Internal Model Control

Internal model (IM) control includes a feedforward element in the control to improve the system performance. The PID and phase plane control strategies already mentioned only have feedback. The feedforward in IM control allows a quicker response and reduces the load on the feedback control. The other advantage of IM control is the inclusion of the internal model that compensates for noise and external disturbances to the system. This enables the feedback loop to automatically compensate for these disturbances rather than relying on gain tuning.

Yaw rate tracking internal model control

The yaw rate tracking internal model control has the structure described in Section 4.2.3 with the block diagram shown in Figure 5.9.

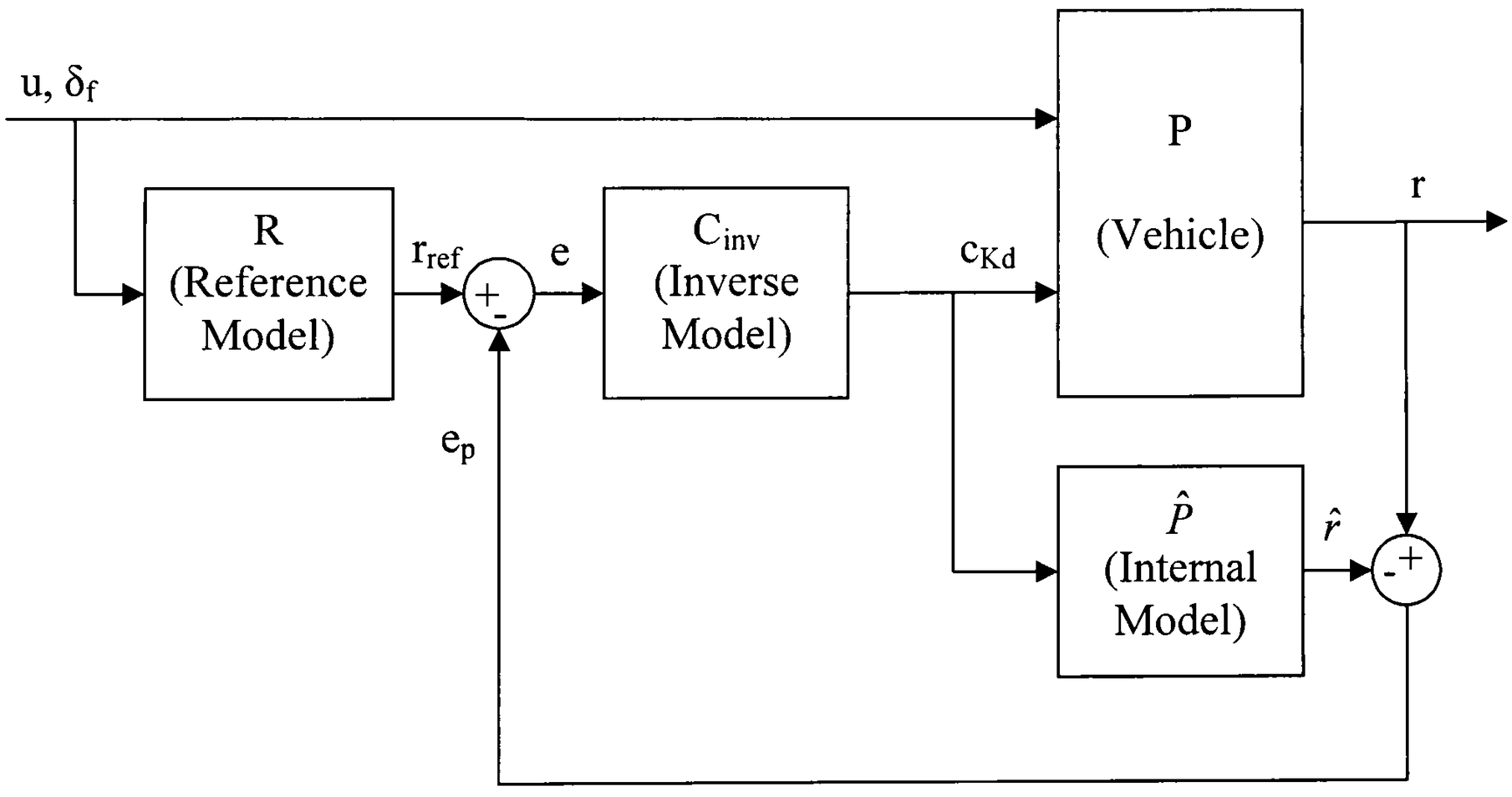

Figure 5.9 RMD yaw rate tracking IM control block diagram

For the yaw rate tracking control the yaw rate reference model is the same steady state model used in the PID yaw rate tracking controller, given in Equation (5.2). The reference yaw rate is modified by subtracting the difference of the actual vehicle yaw rate and the internal model yaw rate. The internal model, $\hat{P}$, is given by the following equations:

$$M_{tot}u\left(\dot{\beta}+r\right)=F_{y_f}+\Delta F_{y_f}+F_{y_r}+\Delta F_{y_r}$$
$$I_{zz}\dot{r}=a\left(F_{y_f}+\Delta F_{y_f}\right)-b\left(F_{y_r}+\Delta F_{y_r}\right) \quad (5.10.)$$

where ΔF_{y_f} and ΔF_{y_r} are the changes in lateral force due to the roll moment distribution given by:

$$\begin{aligned}\Delta F_{y_f}&=\Delta c_{K_d}G_{roll}a_{y_f}\\ \Delta F_{y_r}&=-\Delta c_{K_d}G_{roll}a_{y_r}\end{aligned}\text{, where } \Delta c_{Kd}=c_{Kd_s}-c_{Kd} \quad (5.11.)$$

Here G_{roll} is a gain that sets the maximum lateral force available from the controller, a_{yf} and a_{yr} are the lateral accelerations at the front and rear axles and Δc_{Kd} is the change in roll moment distribution given by the actual roll moment distribution subtracted from the static roll moment distribution. Equation (5.10) can be represented as a state space model for easier implementation:

$$\begin{bmatrix}\dot{\beta}\\ \dot{r}\end{bmatrix}=\begin{bmatrix}-\frac{C_f+C_r}{mu} & -\frac{mu^2+aC_f-bC_r}{mu^2}\\ -\frac{aC_f-bC_r}{I_{zz}} & -\frac{a^2C_f+b^2C_r}{I_{zz}u}\end{bmatrix}\begin{bmatrix}\beta\\ r\end{bmatrix}+\begin{bmatrix}\frac{C_f}{mu} & \frac{G_{roll}\left(a_{y_f}-a_{y_r}\right)}{mu}\\ \frac{aC_f}{I_{zz}} & \frac{G_{roll}\left(aa_{y_f}+ba_{y_r}\right)}{I_{zz}}\end{bmatrix}\begin{bmatrix}\delta_f\\ \Delta c_{K_d}\end{bmatrix} \quad (5.12.)$$

$$y=\begin{bmatrix}\beta\\ r\end{bmatrix}$$

The plant model needs to give yaw rate solely as a function of Δc_{Kd} without influence from the steering angle, as required by the control algorithm in Section 4.2.3. Setting the steer angle to zero in Equation (5.12) and observing the yaw rate given by changing the roll moment distribution would not work. If the steering angle is zero, the model would remain on a straight path regardless of the roll moment distribution. There would be no lateral load transfer and therefore changing Δc_{Kd} would have no effect on the yaw rate. To solve this problem there are two models running in parallel. Both are given by Equation (5.12) and both have the same steering angle input given by the driver. However, one model runs with the passive roll moment distribution while the other has the active roll moment distribution. The difference between these two models represents the transfer function of roll moment distribution to the yaw rate, without the influence of the steering angle.

The linear internal model needs to be inverted to create C_{inv}, the inverse model. The first step is representing the state space model as a transfer function using the following equation:

$$\frac{y(s)}{u(s)} = C(sI - A)^{-1}B + D \tag{5.13.}$$

where the state space is given by:

$$\dot{x} = Ax + Bu$$
$$y = Cx + Du \tag{5.14.}$$

Since C is the identity matrix and D is zero, given by Equation (5.12), the transfer function representation is simplified giving the following matrix of transfer functions:

$$C(sI - A)^{-1}B + D = \begin{bmatrix} \frac{B_{11}s + (A_{12}B_{21} - A_{22}B_{11})}{s^2 - (A_{11} + A_{22})s + (A_{11}A_{22} - A_{12}A_{21})} & \frac{B_{12}s + (A_{12}B_{22} - A_{22}B_{12})}{s^2 - (A_{11} + A_{22})s + (A_{11}A_{22} - A_{12}A_{21})} \\ \frac{B_{21}s + (A_{21}B_{11} - A_{11}B_{21})}{s^2 - (A_{11} + A_{22})s + (A_{11}A_{22} - A_{12}A_{21})} & \frac{B_{22}s + (A_{21}B_{12} - A_{11}B_{22})}{s^2 - (A_{11} + A_{22})s + (A_{11}A_{22} - A_{12}A_{21})} \end{bmatrix} \tag{5.15.}$$

Here A_{ij} represents the element in the ith row and jth column of the A matrix of the state space model given in Equation (5.12). The transfer function of u_m to y_n is given by the element in the nth row and mth column of the transfer function matrix in Equation (5.15). In the case of a yaw rate tracking, roll moment distribution control, the transfer function of interest is from c_{Kd} to r. This results in the following transfer function:

$$\frac{r}{\Delta c_{K_d}} = \frac{B_{22}s + (A_{21}B_{12} - A_{11}B_{22})}{s^2 - (A_{11} + A_{22})s + (A_{11}A_{22} - A_{12}A_{21})} \tag{5.16.}$$

The transfer function can be inverted by swapping the numerator and denominator. However, since the numerator is only a first order equation in s while the denominator is a second order equation in s, when the function is inverted the resulting inverse transfer function is non-causal. It needs to be multiplied by a first order lag to ensure it is solvable. So the inverse function is given by:

$$\frac{\Delta c_{K_d}}{r} = \frac{G\left(s^2 - (A_{11} + A_{22})s + (A_{11}A_{22} - A_{12}A_{21})\right)}{(\tau s + 1)(B_{22}s + (A_{21}B_{12} - A_{11}B_{22}))} \tag{5.17.}$$

where G is the controller gain and τ is the time constant. The inverse function has all of its poles and zeros in the negative s-plane which results in a stable minimum phase function.

The gain and time constant need to be tuned. Figure 5.10 shows the time constant and gain tuning results. The manoeuvre used is the same increasing velocity step steer test used in the previous yaw rate tracking controller gain selection. Figure 5.10 shows the selection of the time constant and gain.

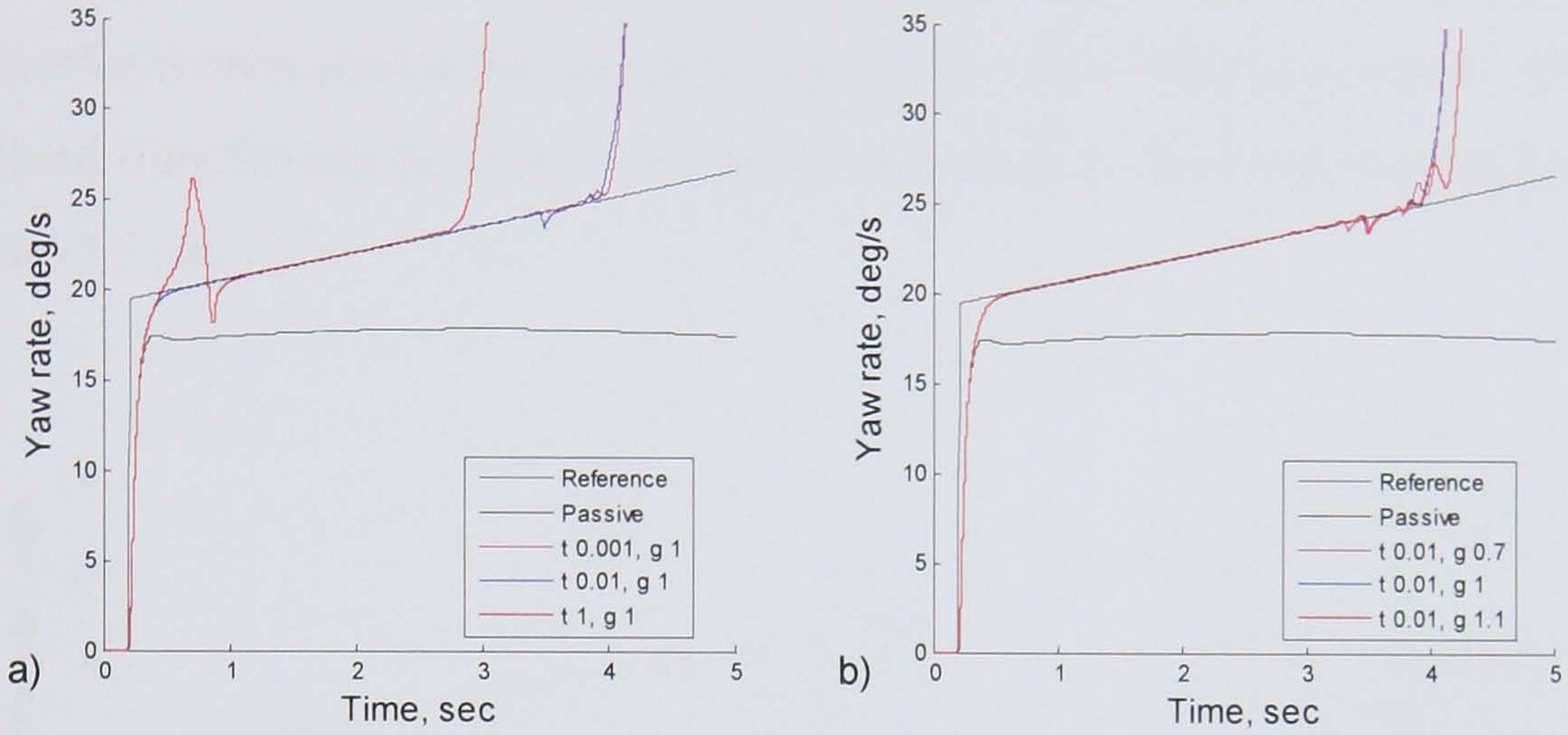

Figure 5.10 Time constant and gain selection of the RMD IM yaw rate control

As shown in Figure 5.10.a, reducing the time constant below 0.01 does not noticeably improve the controller performance. The system dynamics cannot take advantage of a faster control action. It just takes more computing power and gives no benefit. Increasing the time constant causes significant deterioration in the vehicle behaviour. The control action is too slow and it does not manage to keep up with the system dynamics. Therefore a time constant of 0.01 is used. The gain selection shows that a gain of 1.0 gives the best performance. This is expected since the inverse model should match the internal and plant models without an additional gain or tuning.

Figure 5.10 also shows that the controller pushes the vehicle beyond its stable limits. The reference yaw rate is created with a steady state model based on a linear vehicle. As the controller pushes the actual vehicle towards this reference behaviour, the vehicle can not match the linear behaviour and loses stability. The process of losing stability is shown in Figure 5.11. The final few seconds of the increasing step steer manoeuvre are shown where the vehicle loses stability. Figure 5.11.a shows the yaw rate tracking the reference yaw rate. As the manoeuvre progresses the yaw rate begins to oscillate around the reference signal. The controller tries to maintain the reference yaw rate by pushing the roll moment to the front axle as the yaw rate rises above the reference and back to the rear axle as it drops below the reference yaw rate.

This is seen in Figure 5.11.b while Figure 5.11.c shows the resulting vertical forces on the tyres.

As the roll moment is moved to the front axle the front right (inside) tyre loses contact with the ground. Conversely, when the vehicle yaw rate drops below the reference yaw rate, the roll moment is moved to the rear of the vehicle and the same load transfer is seen across the rear axle, but not in such a dramatic manner. The result of the load transfer can be seen in the lateral forces of the front and rear axles, shown in Figure 5.11.d.

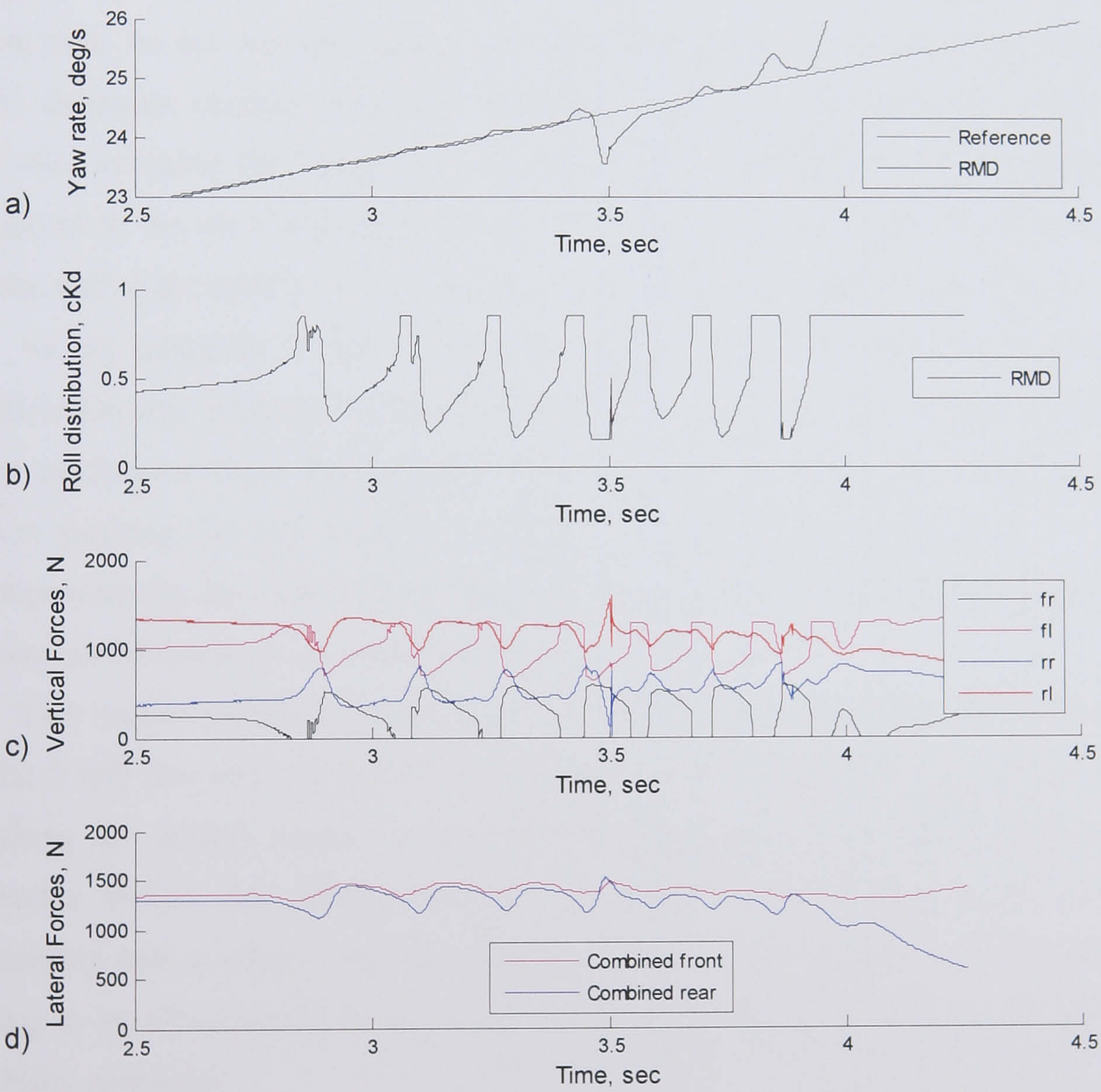

Figure 5.11 RMD IM yaw rate control loss of stability

As the roll moment is moved to the front of the vehicle, the combined lateral force of the front axle will decrease due to the saturation of the non-linear tyres. During stable, steady state handling, the front and rear lateral forces will be equal resulting in

a balanced vehicle with a constant yaw rate. If the forces are not equal, yaw accelerations are created. Since the manoeuvre has an increasing velocity, the reference yaw rate also slowly increases, meaning that the front axle lateral force should always be slightly larger than the rear.

At 2.5 seconds into the manoeuvre, the roll moment is moved slightly to the rear relative to the passive vehicle, causing a larger lateral load transfer across the rear axle, reducing the ability to produce lateral force and promoting the larger yaw rate. The yaw rate begins to increase and as it becomes greater than the reference yaw rate the roll moment is moved to the front of the vehicle. The lateral load transfer at the front of the vehicle increases causing a reduction in the lateral force created at the front axle. As the rear axle lateral load transfer decreases the lateral force at the rear axle increases quickly, matching the lateral forces of the two axles. This rapid increase in lateral force almost pushes the vehicle to instability 3.5 seconds into the manoeuvre, but the vehicle recovers. Now the controller moves the roll moment back to the rear of the vehicle to keep following the increasing reference yaw rate.

As the demands of the manoeuvre and the lateral accelerations increase, the vehicle has less potential to react and can not keep up with the controllers demands. The oscillations begin and instability is introduced. The final loss of stability comes when pushing the roll moment towards the front of the vehicle can no longer compensate for the overshoot in the yaw rate and the rear axle loses the ability to create lateral forces as the vehicle spins out.

This loss of stability is expected. The vehicle is not a linear system and at some point it will lose stability as it tries to emulate a linear system. If the active control is pushing the vehicle further towards the linear behaviour, the vehicle will become unstable before the passive vehicle. Although no controller should introduce instability into a vehicle, it is not of great concern since the IM yaw rate control is going to be incorporated in an overall vehicle control system, which will include a stability controller.

Sideslip angle tracking internal model control

The sideslip angle tracking internal model control has a very similar structure to the yaw rate tracking IM control. The difference is only that the reference model, internal model and inverse model output sideslip angle. The block diagram used is the

same as shown in Figure 5.9, but feeding back sideslip angle. Again the reference model is given by Equation (5.5). The same internal model is also used as presented in the previous section in Equations (5.10) and (5.12). The inverse model is determined using the same process to get Equation (5.15). But the inverse is taken from c_{Kd} to β, which gives:

$$\frac{\Delta c_{K_d}}{\beta} = \frac{s^2 - (A_{11} + A_{22})s + (A_{11}A_{22} - A_{12}A_{21})}{(\tau s + 1)(B_{12}s + (A_{12}B_{22} - A_{22}B_{12}))} \tag{5.18.}$$

Where the A and B matrix are given by Equation (5.12). Once again a first order time lag has to be added to the non-causal system in order to solve it.

Since the models are very similar, it is expected that the time constant and gain should be very similar to those found in the IM yaw rate control. Setting $G = 1$ and $\tau = 0.01$ gives the following inverse transfer function shown in the pole-zero-gain format:

$$\frac{\Delta c_{K_d}}{\beta} = \frac{6.415 \times 10^6 (s + 20.84)(s + 12.16)}{(s - 1.351 \times 10^6)(s + 100.0)} \tag{5.19.}$$

The resulting pole-zero plot is shown in Figure 5.12 while Figure 5.12.b shows a detailed view of the pole and zeros closer to the origin.

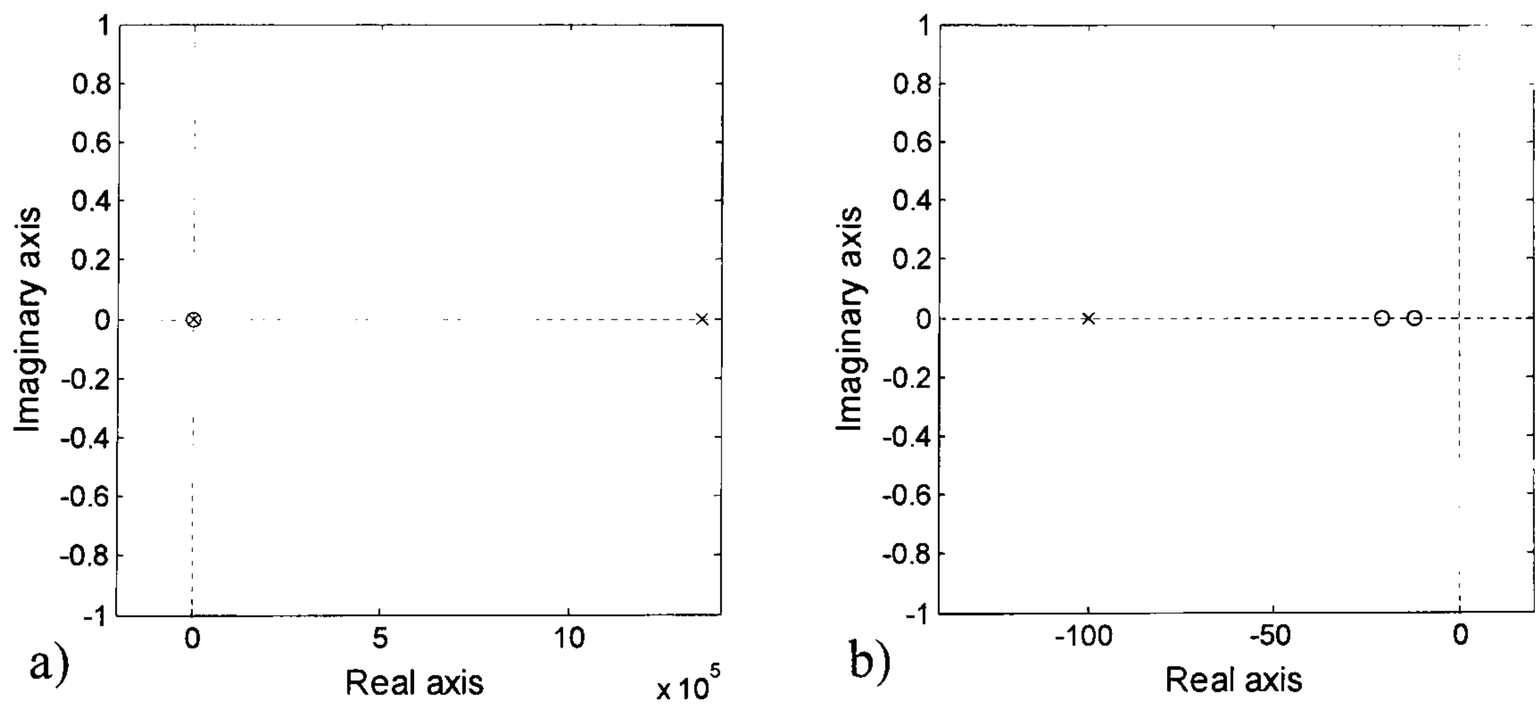

Figure 5.12 Zero-pole plot of the inverse model

As shown, there is a pole far out on the positive real axis. This results in an unstable system and a very poor controller. Figure 5.13 shows the results of a step steer manoeuvre. The inverse model can not give a meaningful value for Δc_{K_d} and the resulting controller does not track the sideslip angle at all, almost immediately sending the vehicle into an unstable state.

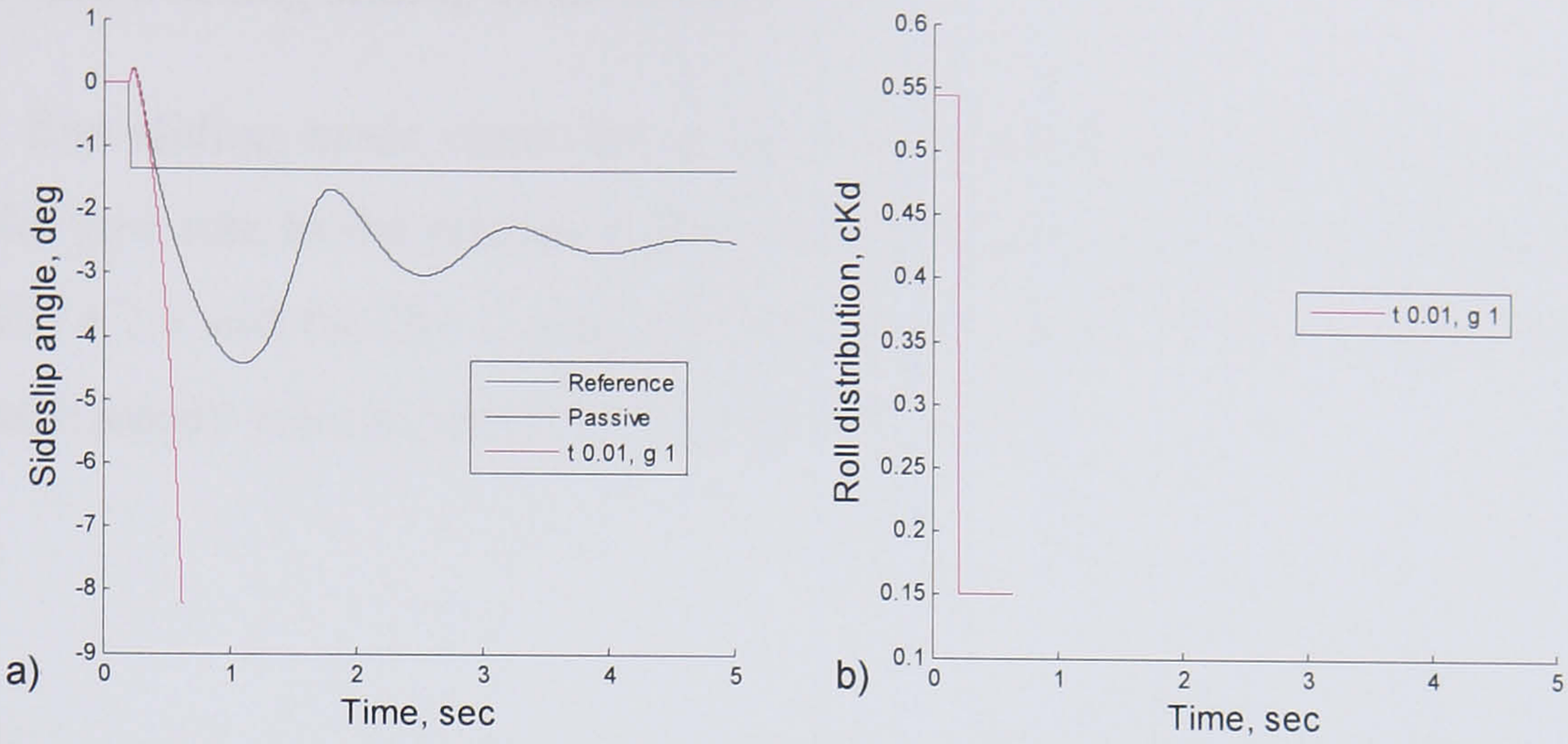

Figure 5.13 RMD IM sideslip angle control

This poor correlation of the roll moment distribution to the sideslip angle is not unexpected and it cannot be solved by using different time constants or gains. Altering the roll moment distribution has an indirect effect on the lateral tyre forces, specifically due to the nonlinearity of the tyre. Trying to model this correctly in a linear model is always going to be difficult. It is possible to do, as shown by the IM yaw rate control, but the sideslip angle is less directly linked to the tyre lateral forces. By observing Equation (5.10), the sideslip angle is also a function of the yaw rate. This means that any modelling errors in the yaw rate are compounded when the sideslip angle is calculated. On top of this, when the model is inverted it is non-causal and needs a first order time lag to be added which adds yet another source for inaccuracies to enter the control. So although RMD IM control works for yaw rate tracking, sideslip angle tracking involves too many modelling inadequacies and the introduction of too many inaccuracies to be effective.

5.2.4. Sliding Mode Control

Sliding mode (SM) control is a robust control that can compensate for inaccuracies in the system models. Due to this robustness it is also an effective control strategy for non-linear systems. As presented in Section 4.2.4, SM control incorporates feedforward like IM control but the parameters of the SM control can be tuned to be robust within the limits of the modelling inaccuracies.

Yaw rate tracking sliding mode control

The first sliding mode controller is the yaw rate tracking control, which aims to match the yaw rate to the reference yaw rate. The structure of the controller is given in Section 4.2.4 and the block diagram is shown in Figure 5.14. The reference model is the same steady state model given by Equation (5.2).

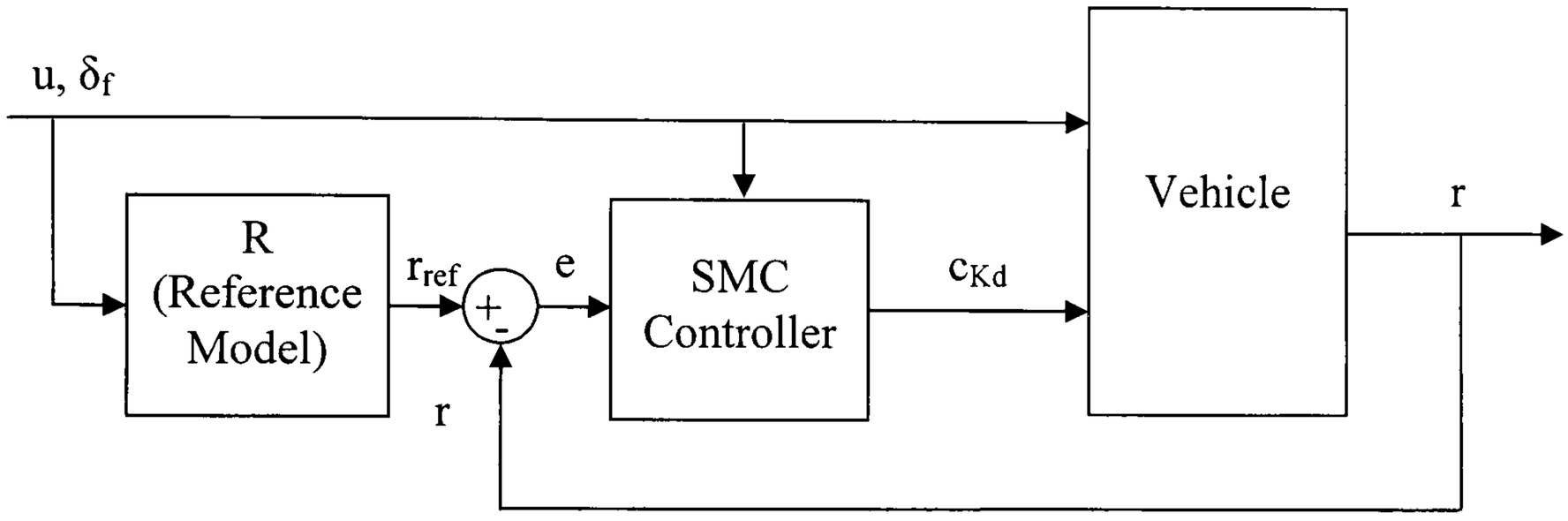

Figure 5.14 RMD yaw rate tracking SM control block diagram

The model in the sliding mode controller takes the form given by:

$$\dot{x} = f(x) + b(x)u \tag{5.20.}$$

In the case of roll moment distribution yaw rate tracking control, this is given by:

$$\dot{r} = \begin{bmatrix} -\dfrac{aC_f - bC_r}{I_{zz}} & -\dfrac{a^2C_f + b^2C_r}{I_{zz}u} \end{bmatrix} \begin{bmatrix} \beta \\ r \end{bmatrix} + \begin{bmatrix} \dfrac{aC_f}{I_{zz}} & \dfrac{G_{roll}\left(aa_{y_f} + ba_{y_r}\right)}{I_{zz}} \end{bmatrix} \begin{bmatrix} \delta_f \\ \Delta c_{K_d} \end{bmatrix} \tag{5.21.}$$

Which is taken from Equation (5.12). The tracking error the control aims to reduce is defined by:

$$e = r - r_{ref} \text{ and its derivative is given by } \dot{e} = \dot{r} - \frac{d}{dt} r_{ref} \tag{5.22.}$$

The first part of the SM control is bringing the vehicle state to the sliding surface. The distance from the vehicle state to the sliding surface is simply defined as the tracking error:

$$s(x,t) = e \tag{5.23.}$$

Once the vehicle state reaches the sliding surface the surface is defined by the following linear function of the tracking error:

$$\dot{e}+\lambda e=0 \text{ or } \left(\dot{r}-\frac{d}{dt}r_{ref}\right)+\lambda\left(r-r_{ref}\right)=0 \tag{5.24.}$$

Substituting $\dot{r}$ from Equation (5.21) into Equation (5.24) gives the initial control equation:

$$\left(-\frac{aC_f-bC_r}{I_{zz}}\beta-\frac{a^2C_f+b^2C_r}{I_{zz}u}r+\frac{aC_f}{I_{zz}}\delta_f+\frac{G_{roll}\left(aa_{y_f}+ba_{y_r}\right)}{I_{zz}}\Delta c_{K_d}-\frac{d}{dt}r_{ref}\right)+\lambda\left(r-r_{ref}\right)=0 \tag{5.25.}$$

The final control law is determined by solving Equation (5.25) for Δc_{K_d} and including the saturated switching term to ensure the control always works to bring the state to the sliding surface without chatter, as presented in Section 4.1.4:

$$\Delta c_{K_d}=-\frac{I_{zz}}{G_{roll}\left(aa_{y_f}+ba_{y_r}\right)}\cdots$$
$$\left(-\frac{aC_f-bC_r}{I_{zz}}\beta-\frac{a^2C_f+b^2C_r}{I_{zz}u}r+\frac{aC_f}{I_{zz}}\delta_f-\frac{d}{dt}r_{ref}+\lambda\left(r-r_{ref}\right)+k\cdot sat\left(\frac{r-r_{ref}}{\varepsilon}\right)\right) \tag{5.26.}$$

The control variables must be tuned to take advantage of the robustness that sliding mode control allows. The three gains that must be tuned are λ, the time constant for the system to reach the desired state once it is on the sliding surface, k, the control gain that determines the rate the system approaches the sliding surface and ε, the width of the saturation function around the sliding surface that prevents chatter. Figure 5.15 shows the selection of the control parameters. The time constant, λ, does not have much effect in this control strategy, as shown in Figure 5.15.a. This is due to the fact that $s(x,t)=e$, and e is the tracking error. As the vehicle state reaches the sliding surface, the tracking error has already been reduced and the vehicle state is already near the desired state. The result is a controller that is insensitive to changes in λ, as shown in Figure 5.15.a.

The robust characteristics of sliding mode control come from the ability to compensate for model parameter variations in k. With the uncertainties in the vehicle model, setting $k=15$ ensures a robust control. The control response can be seen in Figure 5.15.a, which also shows the insensitivity of the controller to tuning λ. Due to this insensitivity, λ has been set to 0.01, the same as the time constant for the IM control, which shares the same models. The final control gain that requires tuning is ε. The width of the saturation band around the sliding surface prevents control chatter, but if it is set too wide the effectiveness of the controller will be

compromised. The results of tuning ε are shown in Figure 5.15.b. Setting $\varepsilon = 0.01$ radians removes the chatter while ensuring the accuracy of the controller. Smaller values of ε do not noticeably improve the system response. The greater accuracy associated with a smaller saturation band ends at $\varepsilon = 0.01$. At larger values of ε, the wider saturation band results in a loss of yaw rate tracking performance. This is because the control action is diluted by the saturation function as it approaches the reference yaw rate.

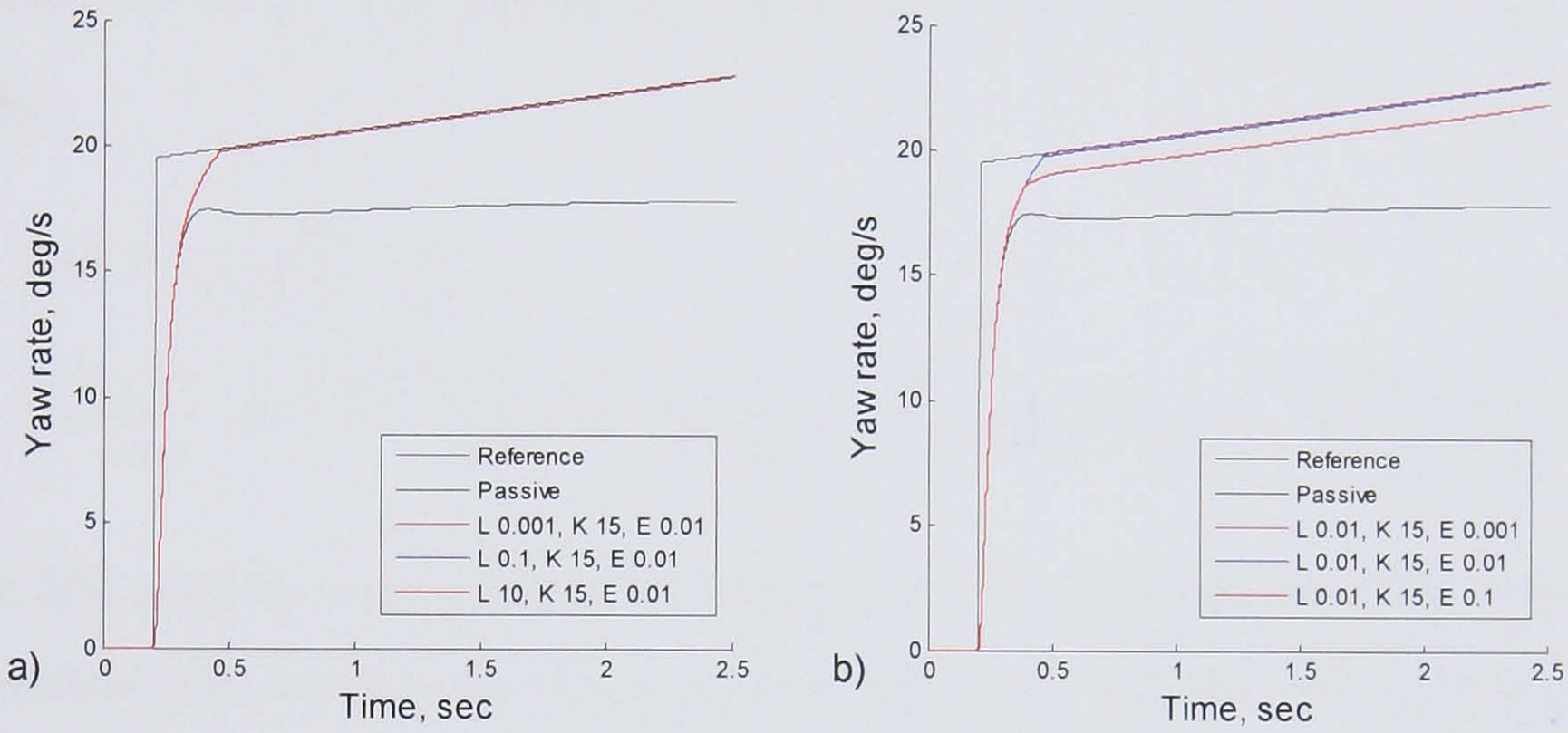

Figure 5.15 Gain selection of the RMD SM yaw rate control

Sideslip angle tracking sliding mode control

The sideslip angle tracking, sliding mode control aims to reduce the sideslip angle by reducing the tracking error with a linear reference model, given by Equation (5.5). It uses the same block diagram as the SM yaw rate tracking control given in Figure 5.14, with the exception that the sideslip angle is fed back to the controller. The tracking error is given by:

$$e = \beta - \beta_{ref} \text{ and its derivative is given by } \dot{e} = \dot{\beta} - \dot{\beta}_{ref} \qquad (5.27.)$$

Where the reference model is given by the state space model in Equation (5.5). The distance from the vehicle state to the sliding surface is once again simply defined by the tracking error giving:

$$s(x,t) = e \qquad (5.28.)$$

Once the vehicle state reaches the sliding surface the surface is defined by the same linear function of the tracking error as in the SM yaw rate tracking control, given by:

$$\dot{e} + \lambda e = 0 \text{ or } \left(\dot{\beta} - \dot{\beta}_{ref}\right) + \lambda\left(\beta - \beta_{ref}\right) = 0 \tag{5.29.}$$

The equation for the control is also similar to the yaw rate tracking SM control. The control model, from Equation (5.20), is given by:

$$\dot{\beta} = \begin{bmatrix} -\dfrac{C_f + C_r}{mu} & -\dfrac{mu^2 + aC_f - bC_r}{mu^2} \end{bmatrix} \begin{bmatrix} \beta \\ r \end{bmatrix} + \begin{bmatrix} \dfrac{C_f}{mu} & \dfrac{G_{roll}\left(a_{y_f} - a_{y_r}\right)}{mu} \end{bmatrix} \begin{bmatrix} \delta_f \\ \Delta c_{K_d} \end{bmatrix} \tag{5.30.}$$

This is taken from Equation (5.12). Equation (5.30) is substituted into Equation (5.29) and solved for Δc_{K_d}. The saturation function is added to create the control equation given by:

$$\Delta c_{K_d} = -\frac{mu}{G_{roll}\left(a_{y_f} - a_{y_r}\right)} \cdots \left(-\frac{C_f + C_r}{mu}\beta - \left(\frac{mu^2 + aC_f - bC_r}{mu^2} \right) r + \frac{C_f}{mu}\delta_f - \dot{\beta}_{ref} + \lambda\left(\beta - \beta_{ref}\right) + k \cdot sat\left(\frac{\beta - \beta_{ref}}{\varepsilon} \right) \right) \tag{5.31.}$$

The SM sideslip angle control is created using the same models as the IM sideslip angle control. The result is that the same problems arise with the sliding mode control. When the model is solved for Δc_{K_d}, it is essentially inverted to create the control equation. This results in a similar model to the unstable inverse model used in the sideslip angle tracking IM control and results in the same unstable behaviour in the sliding mode control. Figure 5.16 shows the results of the controller. Like the IM control, it is unable to track the sideslip angle and destabilises the vehicle. Once again, the modelling inadequacies are too great for the sliding mode control to be effective, regardless of the gains selected.

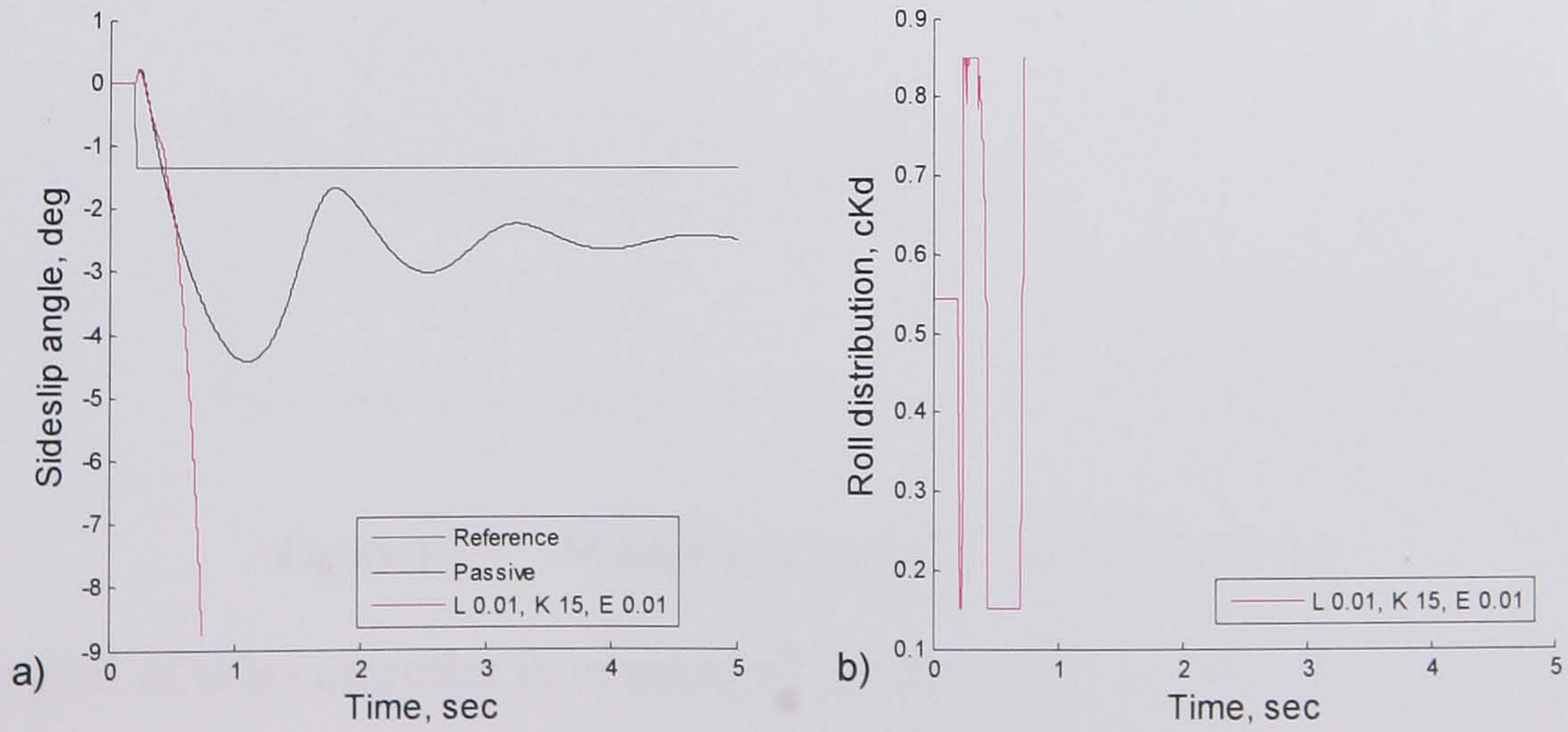

Figure 5.16 RMD SM sideslip angle control

5.3. Torque Distribution Control

Torque distribution control allows the driving force to be split unevenly between the rear tyres. By directing the driving force to the wheels individually, direct yaw moments can be induced on the vehicle, as shown in Section 2.2. The torque distribution of the vehicle is given by $c_{D_r} = 0.5 + \Delta c_{D_r}$ where Δc_{D_r} is the change in torque distribution given by the controller. c_{D_r} varies from 0 to 1 where 0 represents all the torque distributed to the left wheel and 1 represents all the torque distributed to the right wheel. Since the vehicle is rear wheel drive, torque is only split between the rear wheels. The hardware is not specified but examples of torque vectoring systems can be found in the literature review in Chapter 2.

5.3.1. Wheel load control

Wheel load control is a simple proportional control strategy. The torque split across the differential is proportional to the ratio of the normal force split across the axle. This is shown in the following equation:

$$c_{D_r} = \frac{F_{z_{rr}}}{F_{z_{rr}} + F_{z_{rl}}} \tag{5.32.}$$

The block diagram for this controller is shown in Figure 5.17.

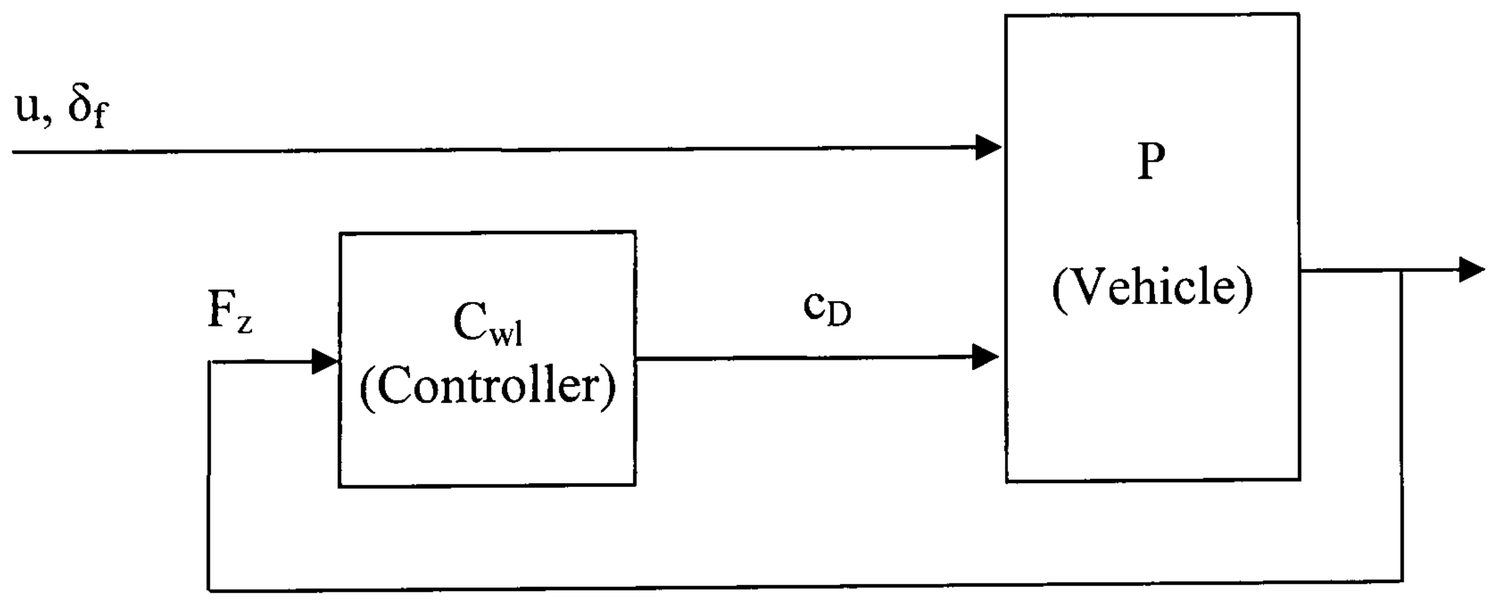

Figure 5.17 Wheel load control block diagram

The goal of this controller is to maximise the potential of the tyres to create lateral and longitudinal forces. Since the tyres are capable of producing more longitudinal and lateral force with greater normal force the torque is split across the axle to give

more torque to the tyre with the greater vertical load. The result is the torque being directed to the tyres most capable of translating it into longitudinal and lateral forces. A secondary effect is to increase the yaw rate of the vehicle. During cornering the load is transferred to the outside wheels, the torque will then be biased toward the outside tyres as well. Driving the outside tyres with more torque will increase the yaw rate and reduce understeer. One benefit of this control strategy is that there are no gains to tune.

The vehicle response to a constant velocity step steer is shown in Figure 5.18. The manoeuvre is run at 20 m/s with a 2.0 degree step steer. Figure 5.18.a shows the normalised longitudinal force at the rear tyres. In the passive vehicle the torque distribution to each wheel through the open differential is almost equal. However, the inside tyre has less vertical force acting on it due to load transfer. This means that the tyre has to operate at a higher normalised longitudinal force and closer to its saturation limits. By comparison, the wheel load control distributes more torque to the outside wheel, which has more vertical force. This equalises the normalised longitudinal forces and brings the inside tyre away from its saturation limits.

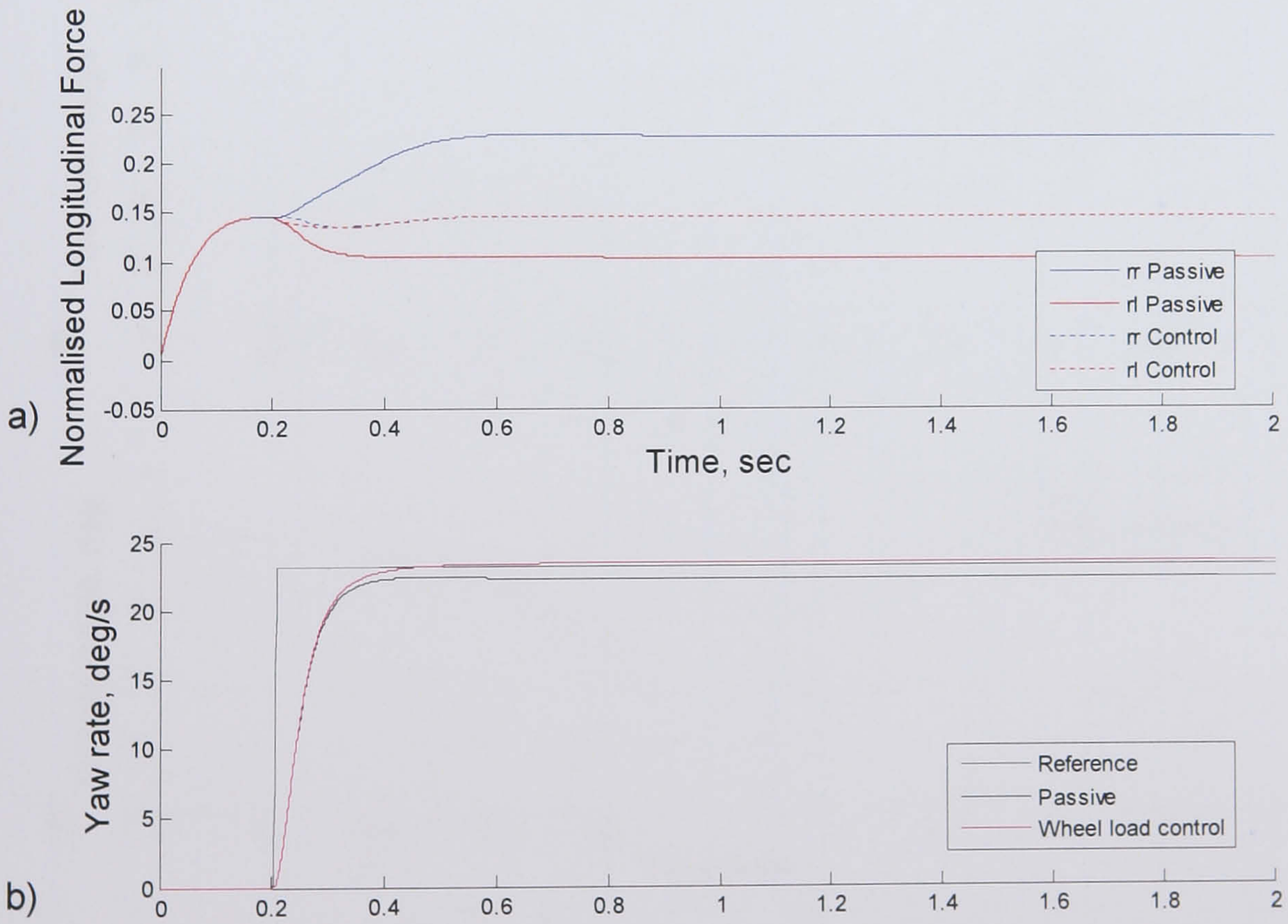

Figure 5.18 Normalised longitudinal force and yaw rate response of the VTD wheel load control

Figure 5.18.b shows the yaw rate response. Although the controller is not a yaw rate tracking control, the linear reference yaw rate has been included as a reference. As expected, distributing more torque to the outside tyre has the effect of increasing the yaw rate. Despite equalising the normalised longitudinal forces on the tyres, wheel load control is not a very good stand alone stability controller. This is shown by the yaw rate and sideslip response to the constant velocity step steer test in Figure 5.19. The test is the same used to tune all the stability controllers and run at 25 m/s with a 2.5 degree step steer angle. The problem with the wheel load control as a stability control is that it increases the yaw rate. This promotes instability in the vehicle and for this reason the wheel load control will not be compared to the other controllers as an independent controller in Chapter 6. Despite this major drawback, wheel load control can be a useful component in an integrated control strategy and it will form part of the final integration strategy presented in Chapter 7. In the integrated strategy it is used to delay the saturation of the inside rear tyre as the vehicle tracks the longitudinal vehicle velocity demanded by the test manoeuvres.

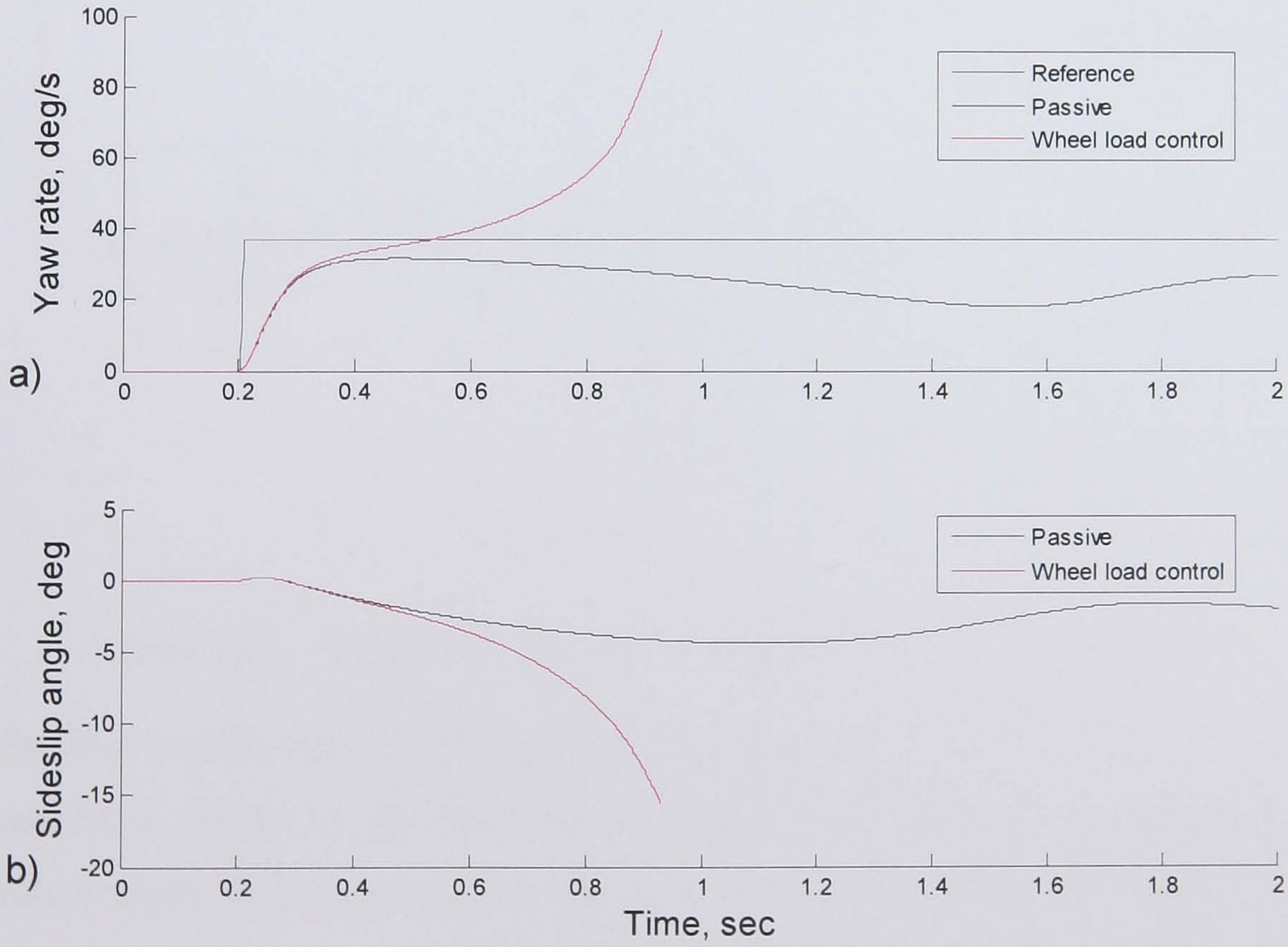

Figure 5.19 Yaw rate and sideslip angle response of the VTD wheel load control

5.3.2. PID Control

Once again as described in Section 4.2.1 and 5.2.1, PID control is a basic control that can be fine tuned to match the system requirements. However, it can be difficult to tune the control to work under all system operating conditions if the system response changes considerably over the range of operation.

Yaw rate tracking PID control

Yaw rate tracking controls can be used to promote driveability. The torque distribution PID, yaw rate tracking control is much like the RMD PID yaw rate tracking control. The aim is to follow a reference yaw rate and provide a linear vehicle response. The block diagram of this control is shown in Figure 5.20.

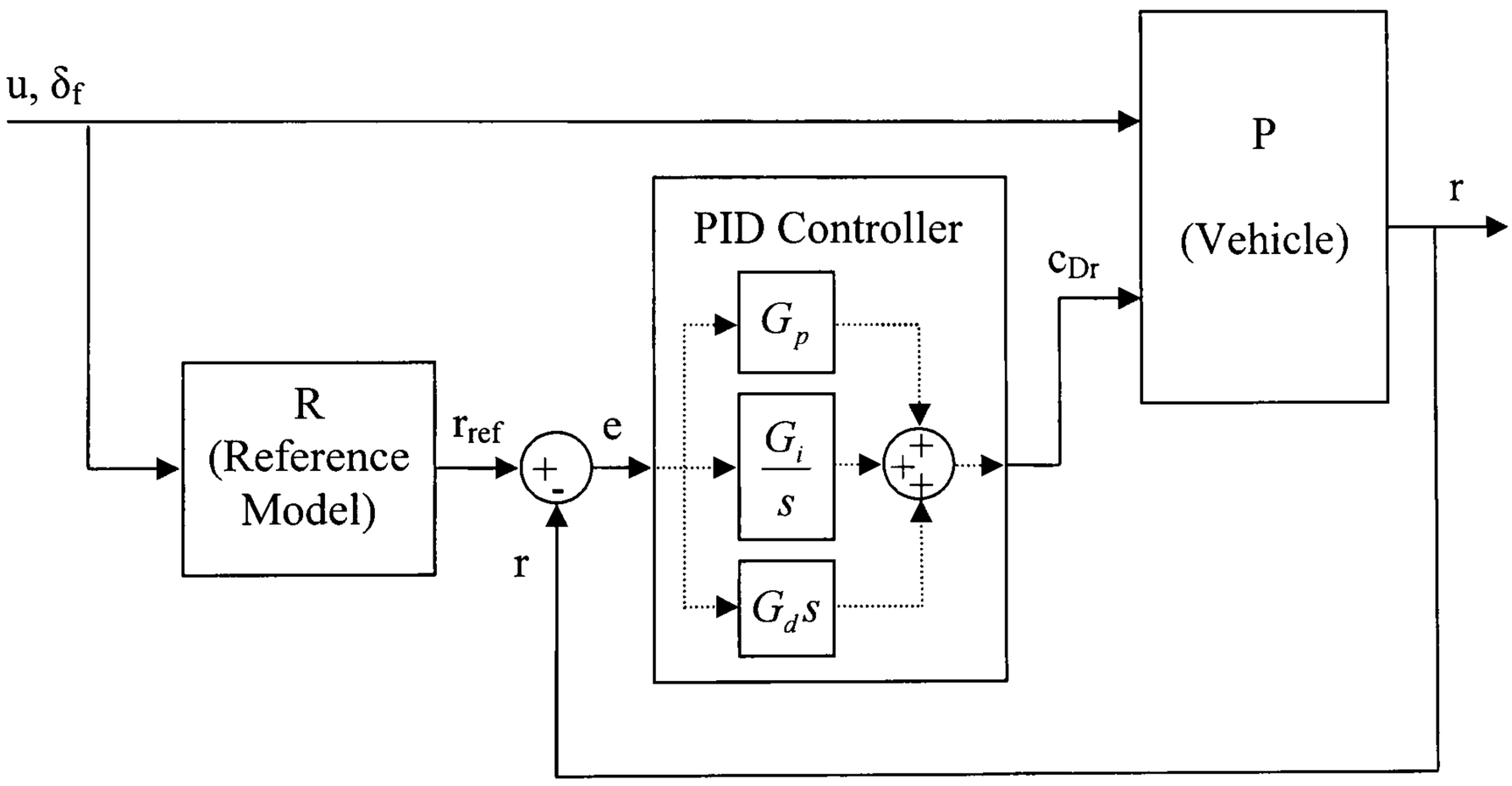

Figure 5.20 VTD PID yaw rate tracking control block diagram

The first requirement of such a control is to create a desired reference yaw rate. The reference model is the same steady state model used in the RMD yaw rate controllers given by Equation (5.2). This creates a reference yaw rate that the vehicle should track. Once again, the error signal is the difference in the actual yaw rate and the reference yaw rate. The output is the torque distribution required to match the reference yaw rate given by:

$$\Delta c_{D_r} = G_p\left(r - r_{ref}\right) + G_i \int\left(r - r_{ref}\right)\cdot dt + G_d\left(\dot{r} - \frac{d}{dt} r_{ref}\right) \qquad (5.33.)$$

Unlike roll moment distribution, torque distribution can create direct yaw moments, not just encourage understeer or oversteer. This means that additional terms to ensure the controller works in both left and right hand corners are not needed since the sign of the error signal already directs the torque distribution correctly. If the vehicle has a smaller yaw rate than the reference yaw rate, which is usually the case, the controller redirects the torque towards the outside wheel. This allows the vehicle to achieve a higher yaw rate. The converse is also true. If the vehicle yaw rate is higher than the reference yaw rate then the torque is distributed toward the inside wheel which decreases the yaw rate of the vehicle. The gain selection is shown in Figure 5.21.

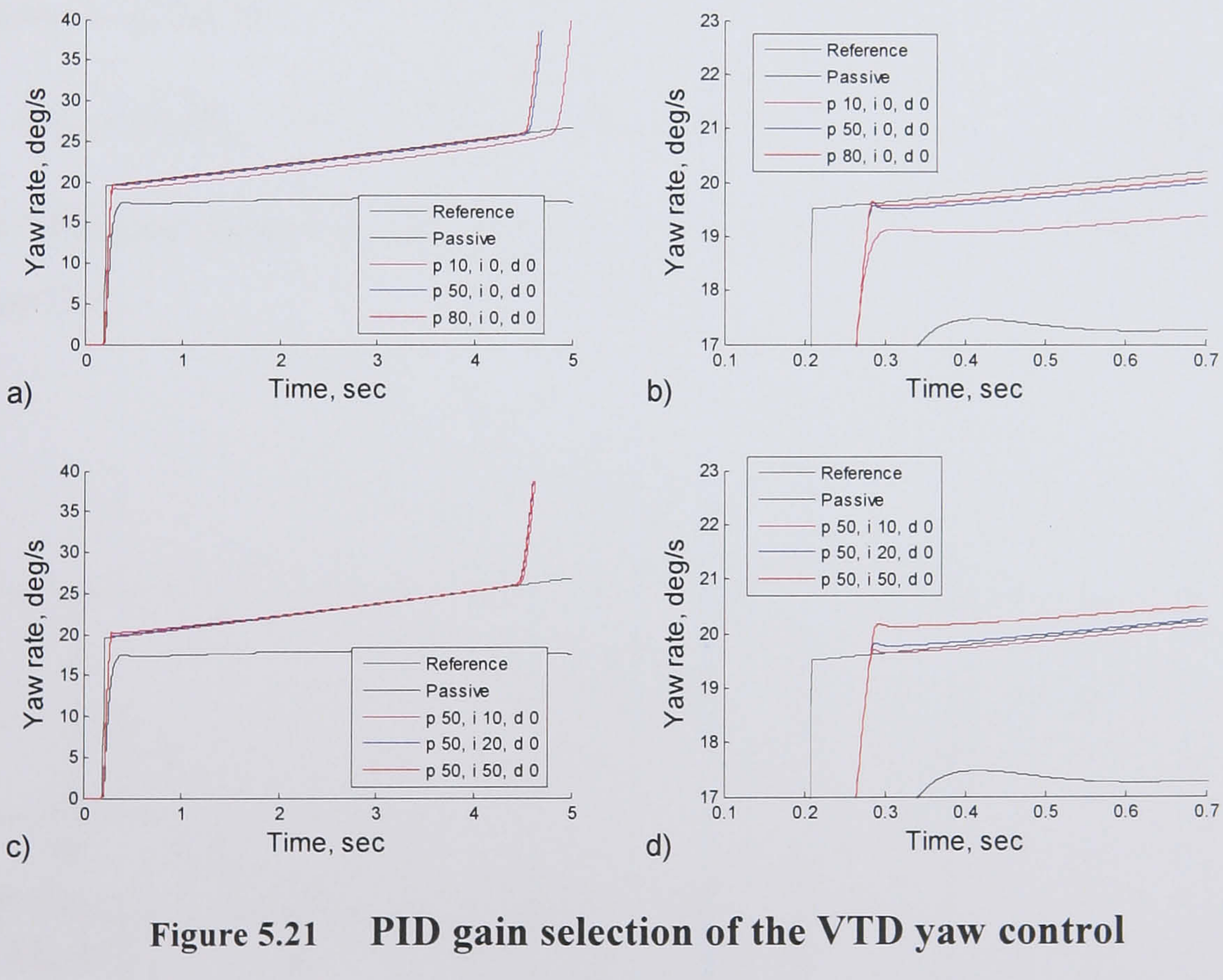

Figure 5.21 PID gain selection of the VTD yaw control

Figure 5.21.a shows that a proportional gain larger than 50 does not improve the system response while below 50, the gain does not track the yaw rate well. With the gain set at 50 there is some steady-state error, as shown in the detail view in Figure 5.21.b. Figure 5.21.c shows that an integral gain can remove this error. A gain of 20 manages to compensate for the steady-state error with minimal overshoot. Although the overshoot is slightly less with a smaller gain of 10, the steady state error is still

present. This can be seen in the detail view in Figure 5.21.d. Finally, the derivative gain is not needed since the system response is well damped. The gains are set at 50 for the proportional gain, 20 for the integral gain and 0 for the derivative gain.

As with the RMD yaw rate controllers, the VTD PID yaw rate control pushes the vehicle beyond the stable limits as it tries to match the reference model. Again, this is expected and does not present a concern due to the inclusion of the controller in an overall vehicle control strategy with a stability controller.

Sideslip angle tracking PID control

The variable torque distribution, sideslip angle tracking PID control has the same structure as the roll moment distribution, sideslip angle tracking PID controller. The control objectives are the same, to reduce the sideslip angle by matching a linear reference model. The block diagram is given by Figure 5.22 and the equation for the PID control is given by:

$$\Delta c_{D_r} = G_p\left(\beta_{ref} - \beta\right) + G_i \int\left(\beta_{ref} - \beta\right)dt + G_d\left(\dot{\beta}_{ref} - \dot{\beta}\right) \qquad (5.34.)$$

The reference model is also given by the linear state space model given in Equation (5.5).

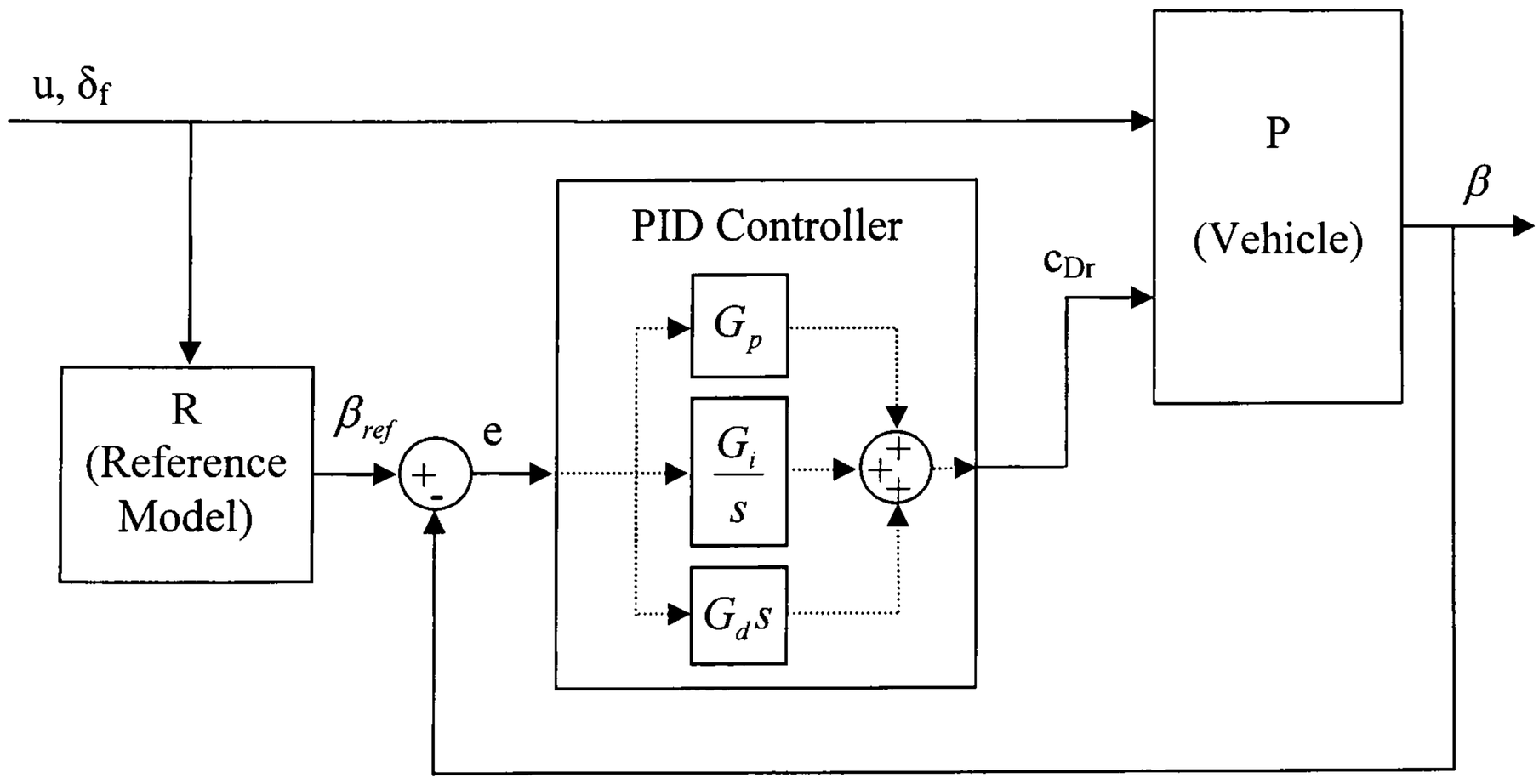

Figure 5.22 Sideslip angle reduction PID control block diagram

As the sideslip angle error increases beyond the reference signal, more torque is distributed to the inside wheel. Driving the inside wheel creates a contra-cornering yaw moment and promotes understeer. However, as the lateral load transfer increases the vertical force on the inside tyre decreases, potentially reducing the effectiveness of the controller.

The gain selection for this stability control is shown in Figure 5.23. Figure 5.23.a shows the selection of the proportional gain. As the gain is increased, the sideslip angle response becomes more restricted but there is some oscillation and steady state error. An initial proportional gain of 100 is chosen since gains greater than this do not give much improvement. The next objective is to remove the oscillation with the derivative gain, shown in Figure 5.23.b. The derivative gain of 7 manages to reduce the oscillations without increasing the gain too much.

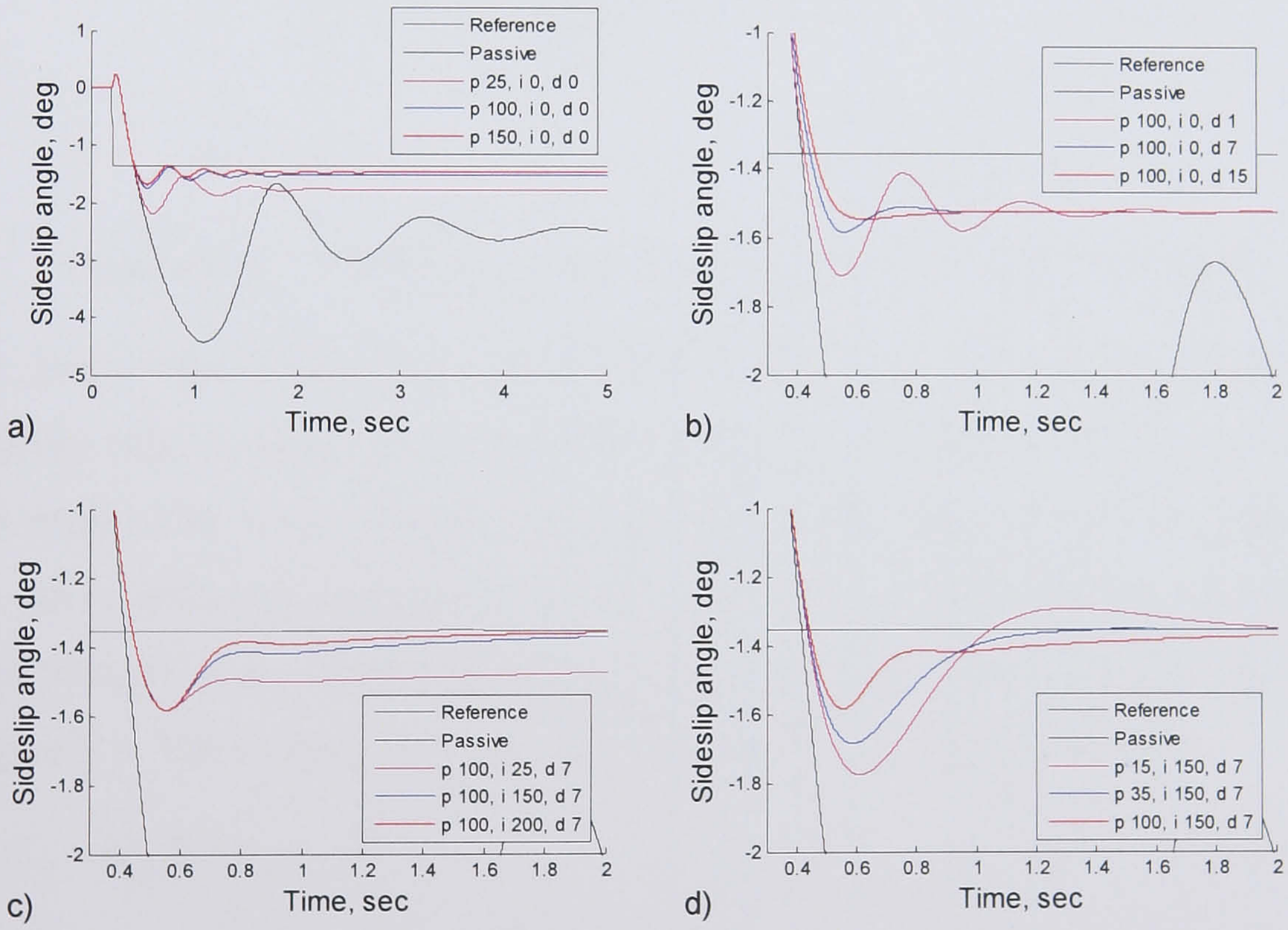

Figure 5.23 PID gain selection of the VTD sideslip angle control

Now the steady state error can be reduced with the integral gain, shown in Figure 5.23.c. A gain of 150 removes the steady state error while larger gains do not considerably improve the control response. As shown in the final tuning step, once integral action is added to the controller, the proportional and derivative gains do not need to be pushed as high. Therefore, the proportional gain can be reduced. Figure 5.23.d shows that reducing the proportional gain does lead to a slight increase in

overshoot but results in a quicker settling time. The final gains are set at 35 for the proportional gain, 150 for the integral gain and 7 for the derivative gain.

5.3.3. Sideslip angle phase plane stability control

Phase plane control can also be used with variable torque distribution. The control structure is the same as the RMD phase plane control presented in Section 5.2.2 and Section 4.2.2, with a block diagram given by Figure 5.24.

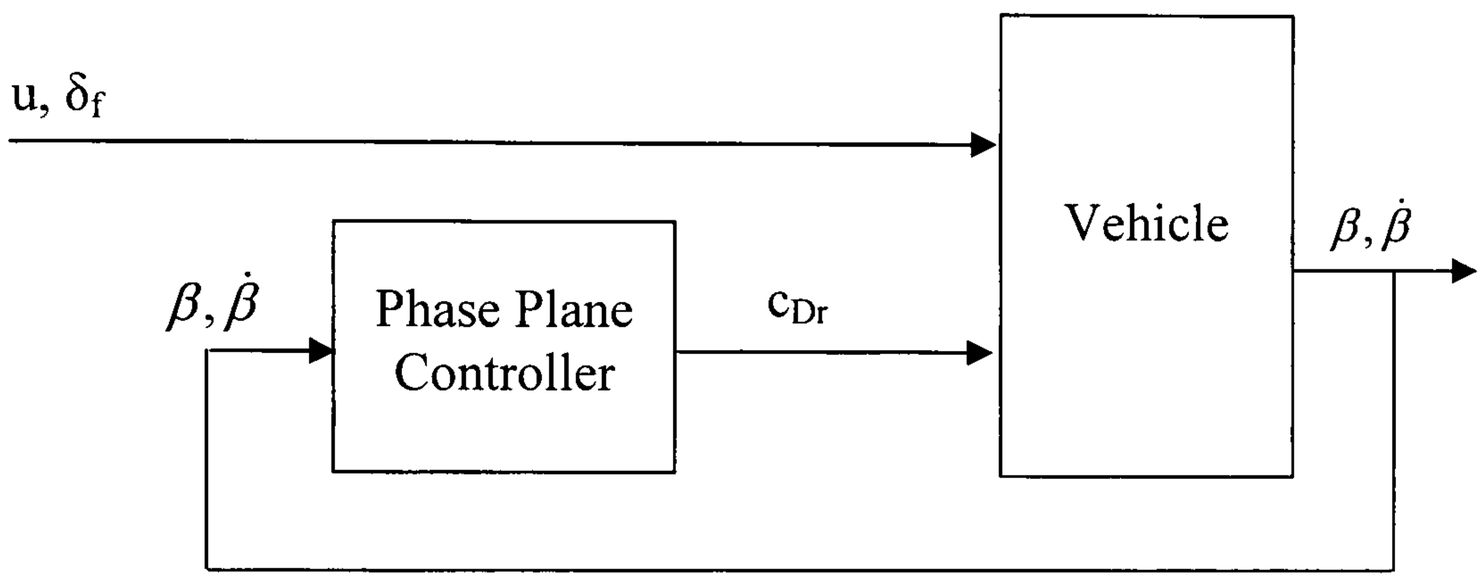

Figure 5.24 VTD phase plane stability control block diagram

The goal of the control is to stabilise the vehicle by bounding the sideslip angle and sideslip rate. A phase plane is created with the sideslip rate plotted against the sideslip angle. The control boundary is created on the phase plane and defines the vehicle states where the control becomes active. The control boundary is created in the same manner as the RMD phase plane control boundary presented in Section 5.2.2 and Figure 5.7. The control boundary and error signal are again defined by:

$$C_b = m_{cb}\beta \pm b_{cb} \tag{5.35.}$$

$$e = \frac{\left|\dot{\beta} - m_{cb}\beta \mp b_{cb}\right|}{\sqrt{m_{cb}^2 + 1}} \tag{5.36.}$$

The error signal is then put through a proportional amplifier to create the control signal given by:

$$\Delta c_{D_r} = G_p e \tag{5.37.}$$

The slope of the control boundary, m_{cb}, is once again chosen so that it matches the angle of the phase curves. This gives the same value of -5.0 since it is the same

vehicle that is being controlled. The control boundary and gain selection are shown in Figure 5.25. The test manoeuvre used to set the control boundary and gain is once again a step steer test run at 25 m/s with a steer angle of 2.5 degrees.

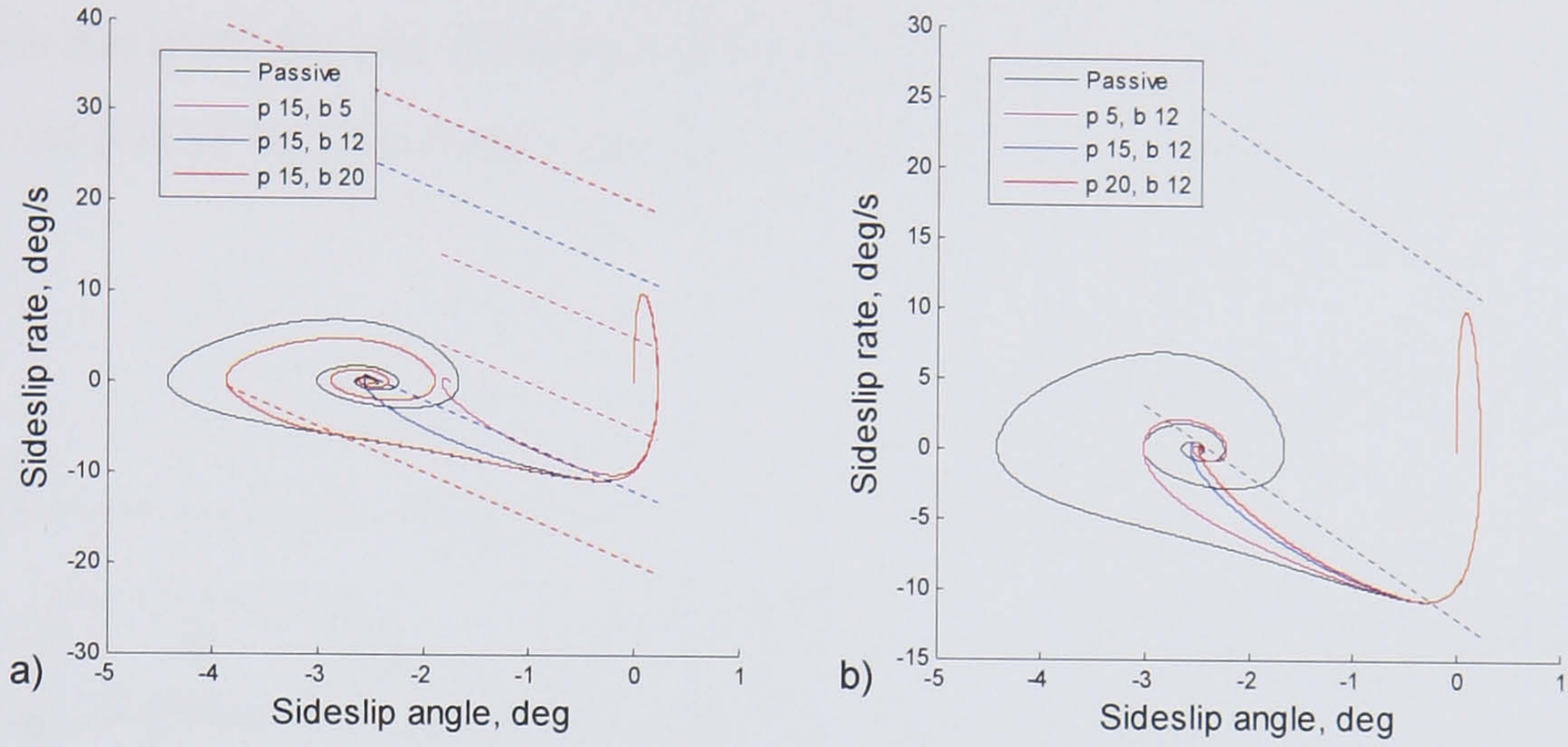

Figure 5.25 Control boundary and gain selection of the VTD phase plane sideslip angle control

The y-intercept for the control boundary is chosen to be $b_{cb} = 12$. Figure 5.25.a shows that larger values result in large oscillations of the sideslip since the vehicle is very close to the stability limit before the control becomes active. A narrower control boundary requires more control action from the torque distribution to stabilise the vehicle. Figure 5.25.b shows that the control gain is set at 15 for the same reasons. A value smaller than 15 results in oscillation since the vehicle state grows to be more unstable before the controller manages to stabilise the vehicle while larger values do not result in better performance.

5.3.4. Internal Model Control

Internal model control is well suited to the task of yaw rate tracking due to the inclusion of a feedforward element in the control. As described in Section 4.2.3 and presented for RMD control in Section 5.2.3, IM control consists of an internal model that automatically tunes the feedback loop of the control to compensate for modelling inadequacies and external disturbances.

Yaw rate tracking internal model control

The torque distribution internal model control has the same structure as the roll moment distribution IM control outlined in Section 5.2.3. The block diagram can be

seen in Figure 5.26. For the yaw rate tracking, torque distribution control the reference model is the same steady state model used previously to create the desired yaw rate, again given by Equation (5.2). The reference yaw rate is modified by subtracting the difference of the actual vehicle yaw rate and the internal model yaw rate. This accounts for any differences between the actual vehicle and the internal and inverse models as well as compensating for external disturbances to the system.

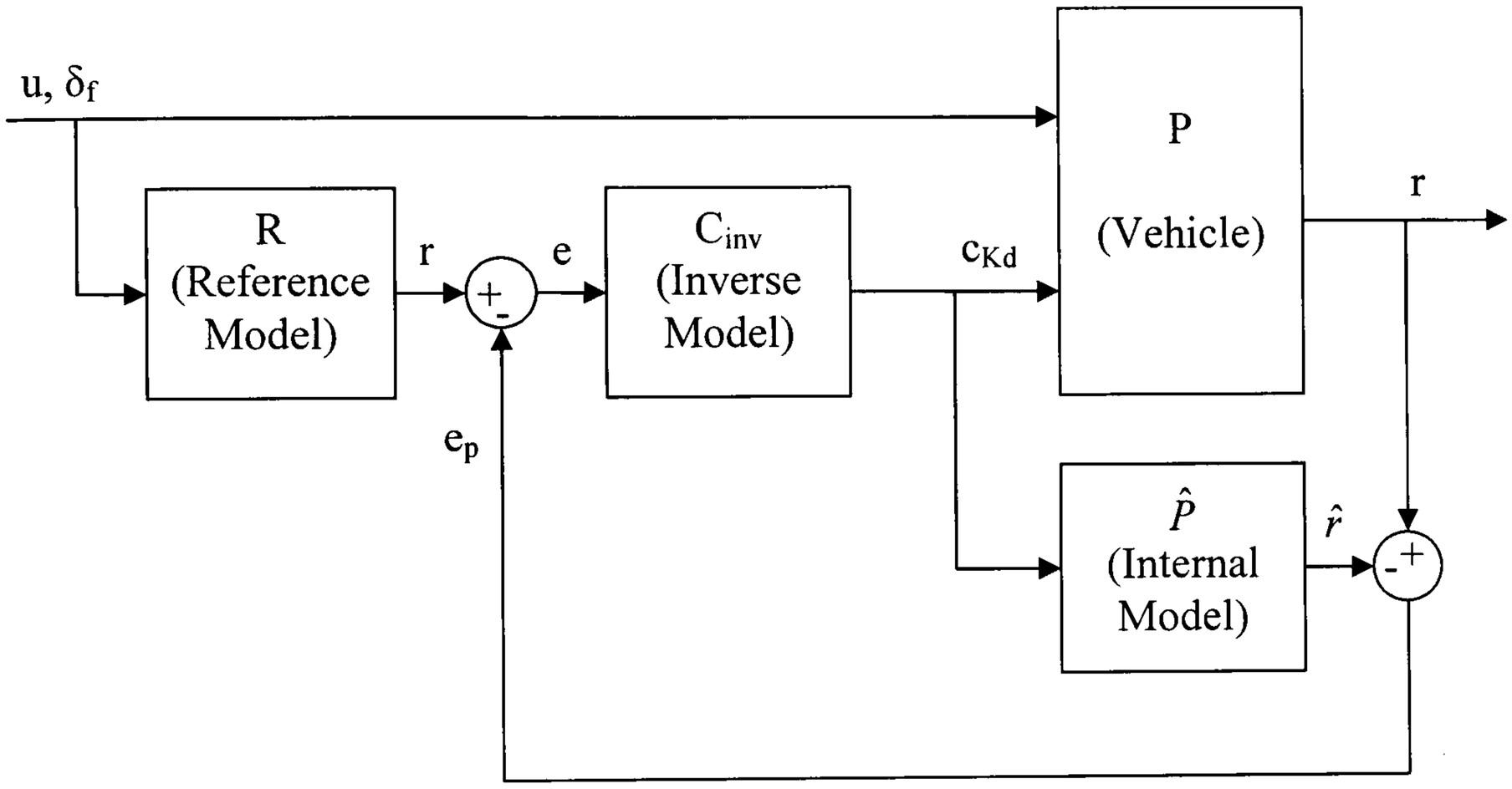

Figure 5.26 VTD reference model yaw rate tracking IM control block diagram

The internal model is given by the following equations:

$$M(\dot{v}+ur)=F_{y_f}+F_{y_r}$$
$$I\dot{r}=aF_{y_f}+bF_{y_r}-t\Delta F_{x_r} \tag{5.38.}$$

where ΔF_{x_r} is the difference in longitudinal forces of the rear wheels given by:

$$\Delta F_{x_r}=G_{diff}c_{D_r} \tag{5.39.}$$

Here G_{diff} is a gain that sets the maximum torque difference across the axle. The equations are rearranged into the state space form given by:

$$\begin{bmatrix}\dot{\beta}\\ \dot{r}\end{bmatrix}=\begin{bmatrix}-\frac{C_f+C_r}{mu} & -\frac{mu^2+aC_f-bC_r}{mu^2}\\ -\frac{aC_f-bC_r}{I_{zz}} & -\frac{a^2C_f+b^2C_r}{I_{zz}u}\end{bmatrix}\begin{bmatrix}\beta\\ r\end{bmatrix}+\begin{bmatrix}\frac{C_f}{mu} & 0\\ \frac{aC_f}{I_{zz}} & -\frac{tG_{diff}}{I_{zz}}\end{bmatrix}\begin{bmatrix}\delta_f\\ \Delta c_{D_r}\end{bmatrix} \quad (5.40.)$$

$$y=\begin{bmatrix}\beta\\ r\end{bmatrix}$$

To obtain the yaw rate given by the torque distribution without the influence of the steering angle, δ_f is set to zero. The isolation of the torque distribution in the internal model is required by the control structure as outlined in Section 4.2.3. Unlike RMD IM control, setting δ_f to zero has no effect on the transfer function from torque distribution to yaw rate since yaw moments can be produced without requiring lateral acceleration to be present in the vehicle.

Once again, when the model is in state space form it can be easily inverted with respect to yaw rate to create the inverse model, as described in Section 5.2.3. The following transfer function gives the required torque distribution for a desired yaw rate.

$$\frac{\Delta c_{D_r}}{r}=\frac{G\left(s^2-\left(A_{11}+A_{22}\right)s+\left(A_{11}A_{22}-A_{12}A_{21}\right)\right)}{\left(\tau s+1\right)\left(B_{22}s+\left(A_{21}B_{12}-A_{11}B_{22}\right)\right)} \quad (5.41.)$$

This can be further simplified since $B_{12}=0$ giving the stable, minimum phase transfer function:

$$\frac{\Delta c_{D_r}}{r}=\frac{G\left(s^2-\left(A_{11}+A_{22}\right)s+\left(A_{11}A_{22}-A_{12}A_{21}\right)\right)}{\left(\tau s+1\right)\left(B_{22}s-A_{11}B_{22}\right)} \quad (5.42.)$$

The time constant selection is illustrated in Figure 5.27.a. A time constant of 0.01 matches the system response to the reference yaw rate. Using a larger time constant results in some overshoot which is undesirable and a smaller time constant shows no improvement. This is the same time constant used in the RMD IM control. The use of the same time constants is expected since the controllers are both working on the same vehicle system. The gain selection is shown in Figure 5.27.b. As expected, a gain of 1 provides the best match with larger or smaller gains resulting in steady state error. Once again, the controller pushes the vehicle beyond its stability limits like the other yaw rate tracking controllers already presented.

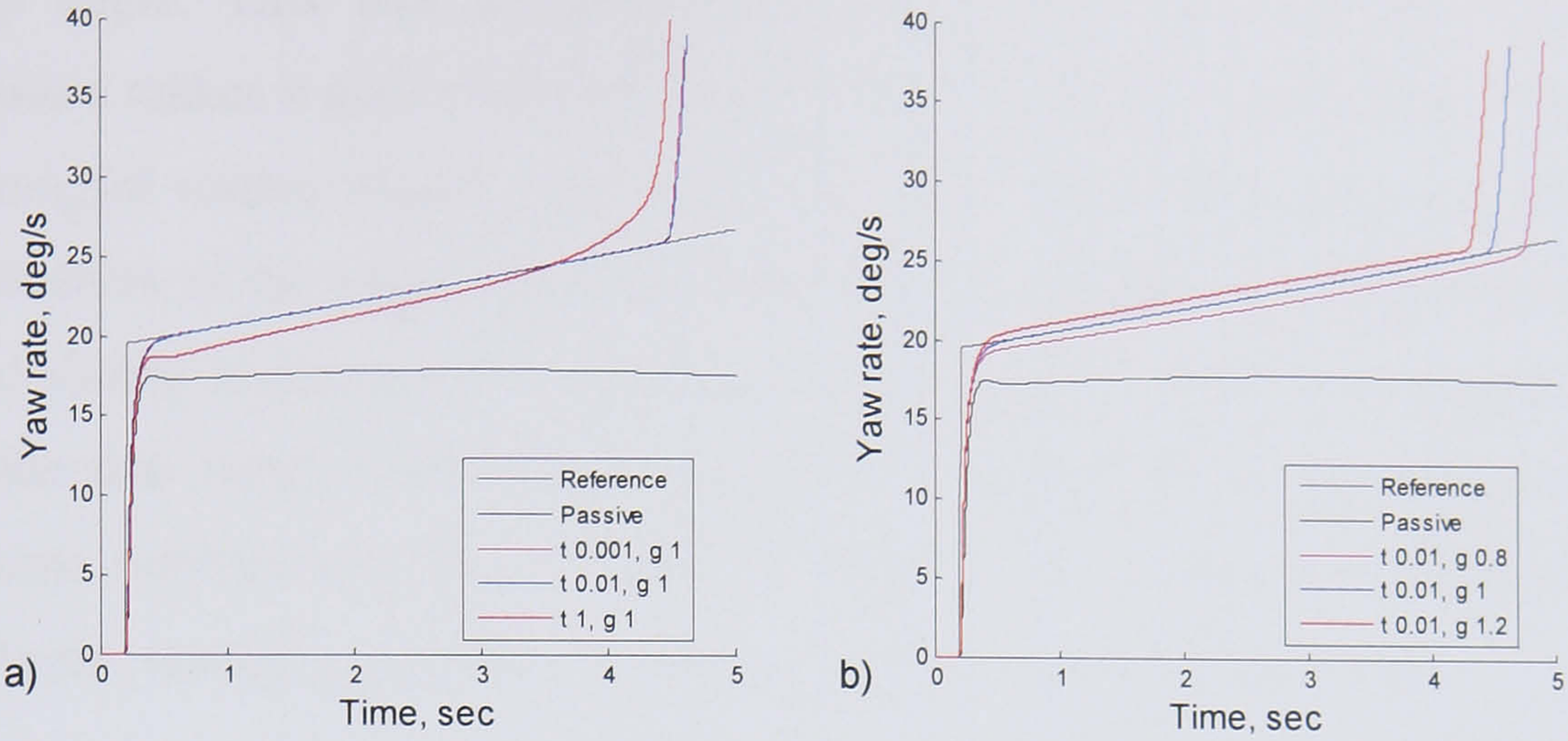

Figure 5.27 IMC time constant and gain selection of the VTD yaw control

Sideslip angle tracking internal model control

The sideslip angle tracking IM control is very similar to the yaw rate tracking IM control and can be described by the same block diagram given in Figure 5.26. The difference is that a desired sideslip angle is fed back instead of the yaw rate. The reference model for the sideslip angle is the same model used in the VTD PID sideslip angle control, given by Equation (5.5). The internal model is the same model used in the VTD IM control given by Equation (5.40). Along with the vehicle, they feedback the sideslip angle so the inverse model acts on sideslip to create the required control action. The inverse model is also derived from Equation (5.40). The state space model is inverted using the same process outlined in Section 5.2.3, but it is inverted with respect to the sideslip angle to give the following inverse transfer function.

$$\frac{\Delta c_{D_r}}{\beta} = \frac{G\left(s^2 - \left(A_{11} + A_{22}\right)s + \left(A_{11}A_{22} - A_{12}A_{21}\right)\right)}{\left(\tau s + 1\right)\left(B_{12}s + \left(A_{12}B_{22} - A_{22}B_{12}\right)\right)} \tag{5.43.}$$

This equation can be simplified by realising that $B_{12} = 0$ from Equation (5.40). This requires a second first order lag to be added to enable the inverse model to be solved. The resulting inverse model is given by:

$$\frac{\Delta c_{D_r}}{\beta} = \frac{G\left(s^2 - \left(A_{11} + A_{22}\right)s + \left(A_{11}A_{22} - A_{12}A_{21}\right)\right)}{\left(\tau s + 1\right)\left(\tau s + 1\right)A_{12}B_{22}} \tag{5.44.}$$

Since $B_{12} = 0$ in the internal model and therefore also in the inverse model from Equation (5.40), changing the torque distribution only has a secondary effect on the sideslip angle. The torque distribution modifies the yaw rate which then affects the

sideslip angle. This lack of connection between the sideslip angle and torque distribution makes it particularly difficult to create an inverse model that will produce a meaningful control signal, especially when the estimations in tyre modelling and simplification of the model itself are considered. Much like the RMD sideslip angle IM and sliding mode controls, these model inadequacies result in an extremely poor controller that cannot track the sideslip angle. Results from the controller using the same time constant and gain as the VTD IM yaw rate control are shown in Figure 5.28. Again, changing the gains shows no improvement on the controller.

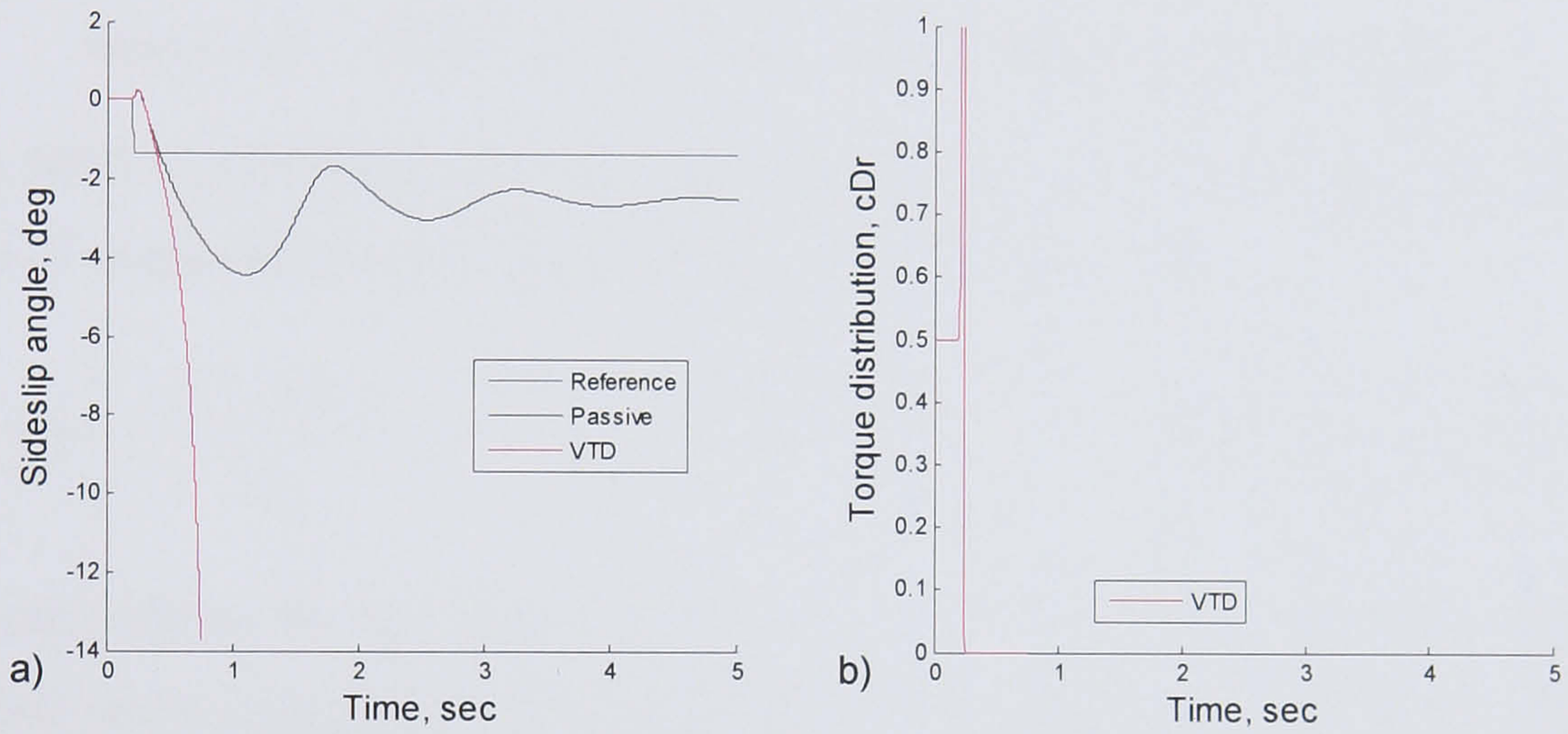

Figure 5.28 VTD IM sideslip angle control

5.3.5. Sliding Mode Control

Sliding mode control is a control that gains robustness by compensating for inaccuracies in the gain tuning. As presented in Section 4.2.4, the gains are defined to take into account the variations in model parameters and signal uncertainties. This provides a robust control.

Yaw rate tracking sliding mode control

The variable torque distribution sliding mode control has the same strategy as the RMD sliding mode control presented in Section 5.2.4 with the block diagram shown in Figure 5.29. The goal is to match the vehicle yaw rate to the reference yaw rate by keeping the vehicle state on the sliding surface of the controller. The reference model is once again the steady state model provided by Equation (5.2).

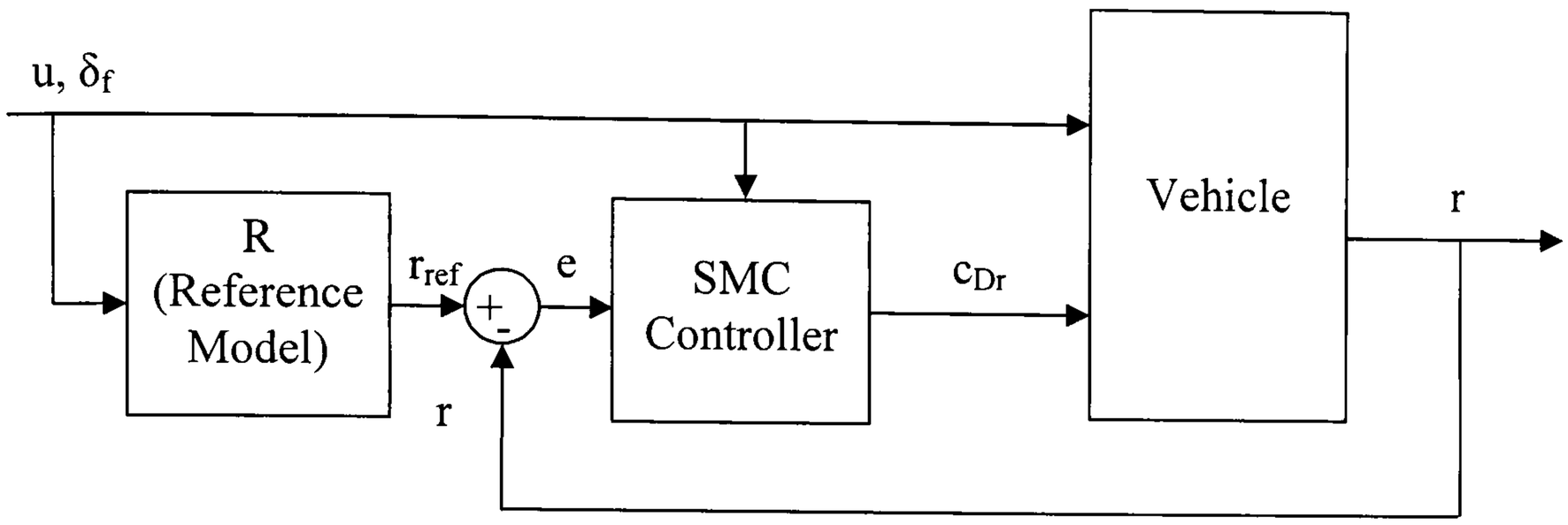

Figure 5.29 VTD yaw rate tracking SM control block diagram

The form of the sliding mode control equation is taken from Equation (5.20). In the case of torque distribution sliding mode control this is given by:

$$\dot{r} = \begin{bmatrix} -\dfrac{aC_f - bC_r}{I_{zz}} & -\dfrac{a^2C_f + b^2C_r}{I_{zz}u} \end{bmatrix} \begin{bmatrix} \beta \\ r \end{bmatrix} + \begin{bmatrix} \dfrac{aC_f}{I_{zz}} & -\dfrac{tG_{diff}}{I_{zz}} \end{bmatrix} \begin{bmatrix} \delta_f \\ \Delta c_{D_r} \end{bmatrix} \quad (5.45.)$$

This is taken from the state space model in Equation (5.40). The tracking error is the same yaw rate tracking error used in the previous controllers given by the difference between the actual yaw rate and the reference yaw rate shown in Equation (5.22). Again the error signal representing the distance of the vehicle state from the sliding surface is the tracking error given by Equation (5.23). The sliding surface is defined by the same linear function of the tracking error given in Equation (5.24). Substituting Equation (5.45) in to (5.24) and rearranging gives:

$$\left(-\frac{aC_f - bC_r}{I_{zz}}\beta - \frac{a^2C_f + b^2C_r}{I_{zz}u}r + \frac{aC_f}{I_{zz}}\delta_f - \frac{tG_{diff}}{I_{zz}}\Delta c_{D_r} - \frac{d}{dt}r_{ref} \right) + \lambda\left(r - r_{ref}\right) = 0 \quad (5.46.)$$

To get the final control, Equation (5.46) is solved for Δc_{D_r} and the saturation function is added to prevent chatter, as outlined in Section 4.2.4. The resulting control law is given by:

$$\Delta c_{D_r} = \frac{I_{zz}}{tG_{diff}}\left(-\frac{aC_f - bC_r}{I_{zz}}\beta - \frac{a^2C_f + b^2C_r}{I_{zz}u}r + \frac{aC_f}{I_{zz}}\delta_f - \frac{d}{dt}r_{ref} + \lambda\left(r - r_{ref}\right) + k \cdot sat\left(\frac{r - r_{ref}}{\varepsilon}\right)\right) \quad (5.47.)$$

There are three parameters to tune in the controller, λ, k and ε. λ is a time constant that determines the rate at which the vehicle state moves towards the desired state once it is on the sliding surface. k determines the rate at which the state

approaches the sliding surface and ε sets the width of the saturation function around the sliding surface to prevent chatter. Like the RMD SM control, the distance from the sliding surface is defined by the tracking error. As the control brings the vehicle state to the sliding surface it is already minimising the state error, which means that once again the control is insensitive to λ. Figure 5.30.a shows the insensitivity of the control to λ. Like the previous controllers, the time constant is set to $\lambda = 0.01$.

The robust nature of controller comes from compensating for the modelling uncertainties in setting the value of *k*. This means that the value of *k* for VTD sliding mode control is set to $k = 10$.

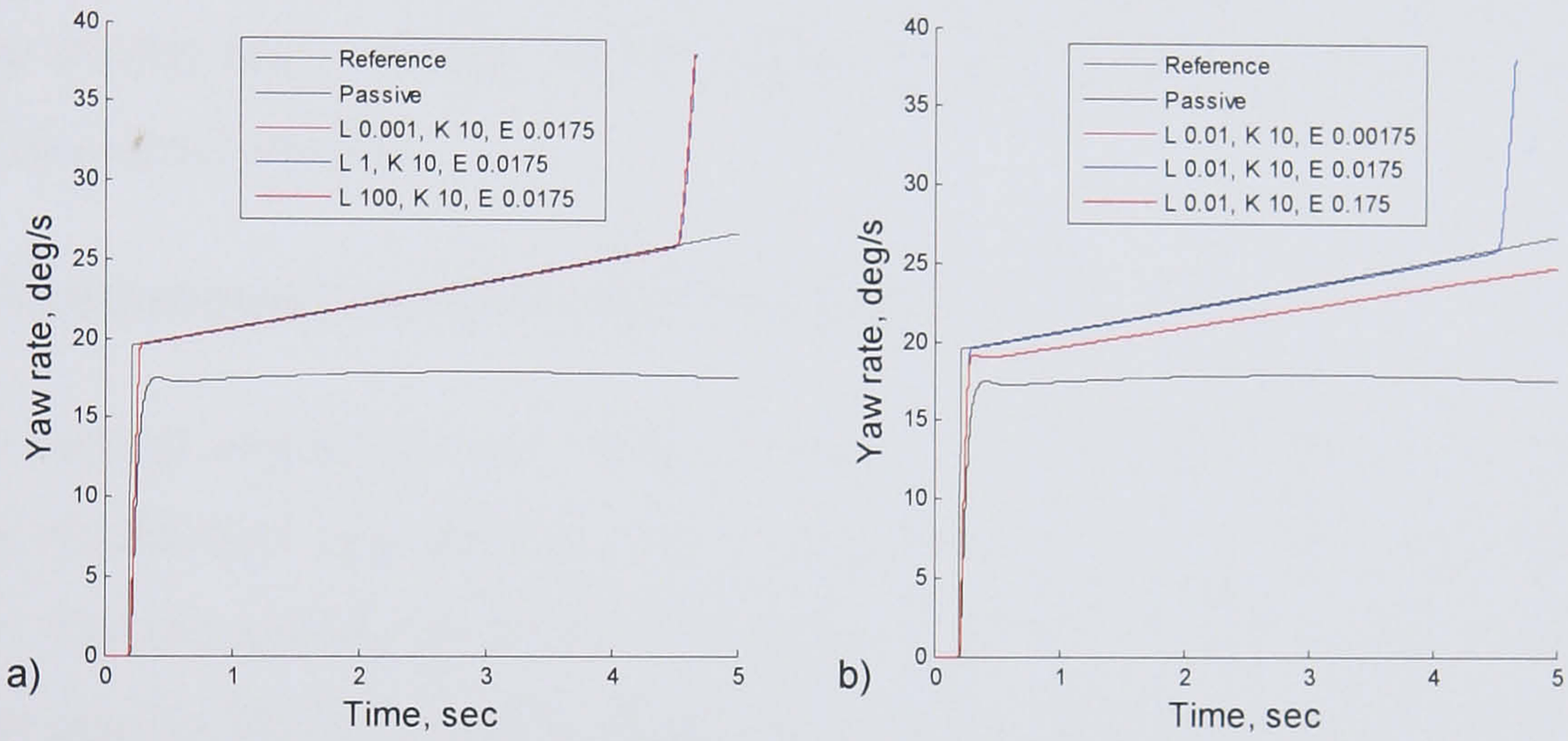

Figure 5.30 Gain selection of the VTD SM yaw rate control

The final gain is ε, which determines the width of the saturation function around the sliding surface and prevents any control chatter. Figure 5.30.b shows the gain selection. A value of $\varepsilon = 0.0175$ radians, 1.0 degrees, tracks the reference yaw rate well. Reducing the width of the saturation function provides no addition benefit and larger values of ε reduce the controller tracking performance.

Sideslip angle tracking sliding mode control

The sideslip angle tracking, sliding mode control aims to reduce the sideslip angle by tracking a reference sideslip angle created with a linear model. Once again the structure of the sideslip angle sliding mode control is the same as the SM controllers presented previously in this chapter. The block diagram is the same as that shown in Figure 5.29 and the reference sideslip angle is given by the linear state space model in Equation (5.5). Again the control comes from an equation of the form given by

Equation (5.20). This comes from the state space model in Equation (5.40) and for VTD sideslip angle control is given by:

$$\dot{\beta} = \begin{bmatrix} -\frac{C_f + C_r}{mu} & -\frac{mu^2 + aC_f - bC_r}{mu^2} \end{bmatrix} \begin{bmatrix} \beta \\ r \end{bmatrix} + \begin{bmatrix} \frac{C_f}{mu} & 0 \end{bmatrix} \begin{bmatrix} \delta_f \\ \Delta c_{D_r} \end{bmatrix} \qquad (5.48.)$$

It is obvious from Equation (5.48) that when it is multiplied out, Δc_{D_r} is multiplied by zero and drops out of the equation. This is due to the indirect relationship between the torque distribution and the sideslip angle. Section 5.3.4 already shows that the relationship was not close enough to create an inverse model to be used in an internal model control, and this indirect relationship again prevents an effective sliding mode control. For this reason, sideslip angle sliding mode control is not developed any further.

5.4. Independent Control Tuning Conclusions

The control strategies were developed into individual controllers for both roll moment distribution and variable torque distribution to control both driveability and stability. The driveability controllers were developed as yaw rate tracking controllers and were tuned with an increasing velocity step steer test run at the higher end of the vehicle handling range. The stability controllers aimed to constrain the sideslip angle and were tuned with a constant velocity step steer test at the limits of vehicle handling.

PID control provided controllers for both RMD and VTD to control both stability and driveability. This is due to the simple control algorithm and its ability to be tuned. Phase plane control is effective at constraining the sideslip behaviour of the vehicle for both RMD and VTD. Internal model control worked well with both RMD and VTD for the yaw rate tracking driveability controllers. However, the inverse model describing the relationship of sideslip angle to either roll moment distribution or variable torque distribution contained too many modelling inaccuracies to develop effective controllers. Sliding mode control was similar to IM control for the reason that it provided good driveability controllers but failed to make effective stability controllers. Once again, the model relating sideslip angel to either RMD or VTD was too inaccurate.

6. *Independent Control Comparison*

Chapter 6 presents a comparison of the independent controllers. The driveability controllers and stability controllers will be compared as separate groups to determine which strategies perform the best. Each strategy will be analysed to find their different merits and weaknesses. The best controllers will then be used to create the combined controllers. These will be simple combinations of the controllers run together to determine any interactions between them. The interactions of these combined controllers will form the basis of the multi-objective integration strategies. Throughout the figures in this chapter, the reference model will be shown as a grey signal and the passive vehicle will be in black.

6.1. Driveability Control

The driveability controllers are all yaw rate tracking controllers. They aim to follow a steady state reference yaw rate to linearise the vehicle behaviour. The benefit of a linear vehicle response is that the dynamics are predictable for the driver. Predictable, linear dynamics make driving less complex and reduces driver workload. There are six driveability controllers developed in Chapter 5, PID control, internal model (IM) control and sliding mode (SM) control for both roll moment distribution and variable torque distribution.

The controllers are first compared using the accelerating step steer test used to tune them. They are then compared in two more step steer tests. These are run at similar lateral accelerations with varying longitudinal velocities. The step steer test is used once again due to the simplicity of interpreting the results while varying the velocity and steer angle provide different vehicle states to ensure control robustness. Next, an increasing velocity, increasing sinusoidal steer test is evaluated. Although the results are not as simple to analyse, this test shows the behaviour of the controllers in a manoeuvre that increases in severity. The controller performance can be evaluated throughout the vehicle handling range.

Another way to evaluate the controllers across the vehicle handling range is through the lateral acceleration gain and yaw rate rise time. This shows the dynamic

response of the controllers as the lateral acceleration of the vehicle increases. Finally, the controllers are evaluated on a low friction surface using the initial accelerating step steer test. Once again, this ensures the controllers are robust to parameter changes.

6.1.1. Driveability Control Results

The first comparison for the controllers is an increasing velocity step steer test run with an initial velocity of 22 m/s, increasing at 1.5 m/s^2 and a steer angle of 1.5 degrees. This is the same manoeuvre used to tune the driveability controllers. The yaw rate results are shown in Figure 6.1.

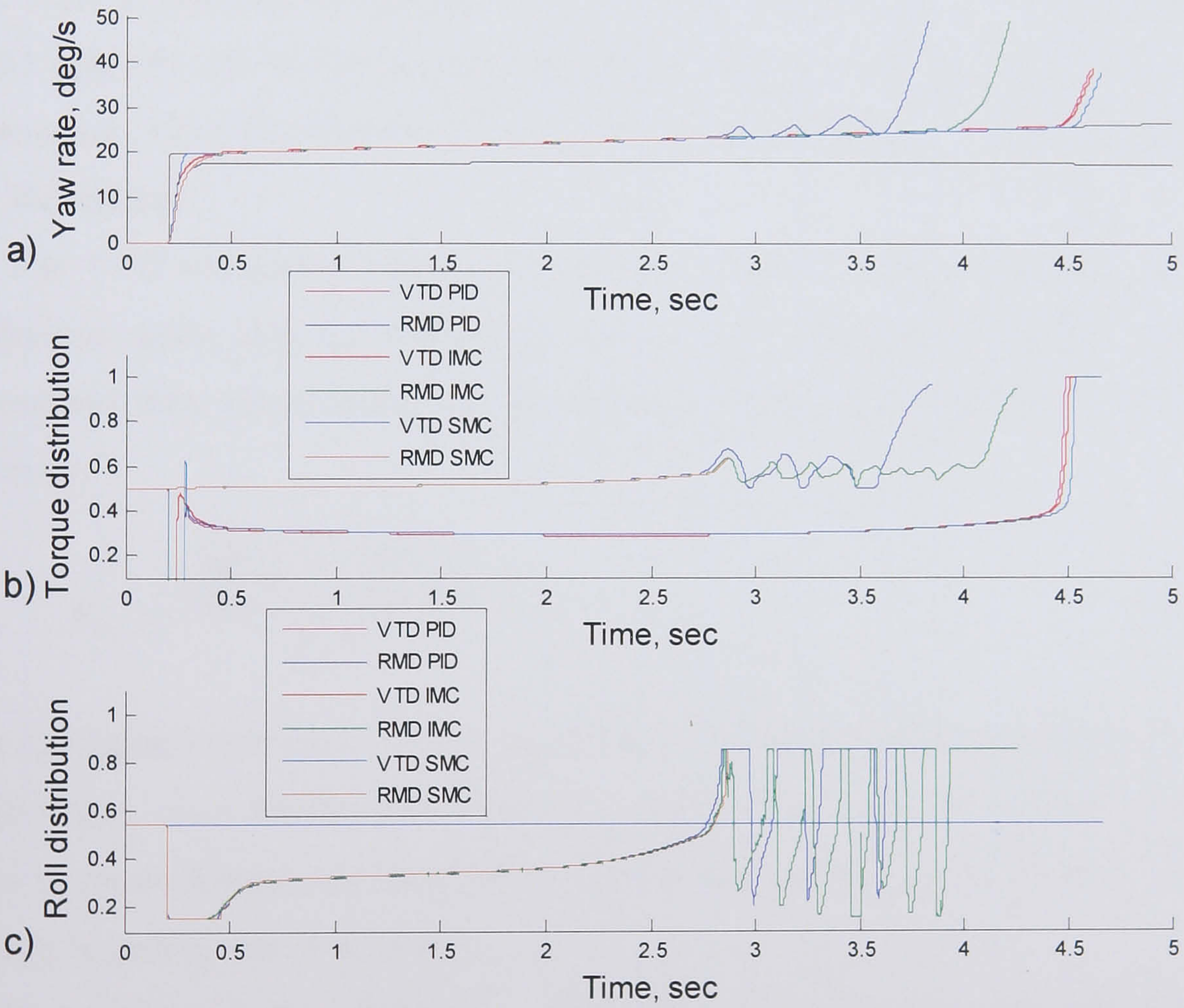

Figure 6.1 Step steer yaw rate results of the driveability controls, 22 m/s initial velocity, 1.5 m/s^2 acceleration, 1.5 deg steer angle

The controllers all manage to track the reference yaw rate well. The control actions of the three VTD controllers are very similar and the same is true of the RMD controllers. This can be theoretically expected since the goal of the controllers is the same, they are all trying to match the reference yaw rate. However, it was not obvious

that the control strategies would all be able to match the yaw rate equally in practice. There is one control output that will track the yaw rate successfully, and in both VTD and RMD the controllers find the required control action, they just calculate it using different algorithms.

There are some differences that occur at the start and end of the manoeuvre. At the end of the manoeuvre, the VTD controllers perform better than the RMD controllers by maintaining the vehicle stability longer while tracking the yaw rate. The RMD sliding mode control drops out first, around 2.8 seconds. While the PID and IM RMD controllers continue on, with the PID controller losing stability shortly after 3.8 seconds, and the IM control lasting till just after 4.2 seconds. There is some variation in the torque distribution for the RMD controllers. This is due to the open differential. The VTD controllers all manage to follow the reference yaw rate longer than the RMD controls, all losing stability very close together around 4.6 seconds into the manoeuvre. The PID control drops out first shortly followed by the IM control then the SM control.

The VTD controllers manage to keep the vehicle stable longer than the RMD controllers since they do not saturate the tyres as quickly. Figure 6.2 shows the normalised root mean square of the combined lateral and longitudinal tyre forces given by:

$$F_{rms} = \frac{\sqrt{\left(\sum F_x\right)^2 + \left(\sum F_y\right)^2}}{\sum F_z} \tag{6.1.}$$

The normalised root mean square tyre force corresponds to the magnitude of the tyre force vector on a friction circle plot. F_{rms} shows how well the vehicle is using the tyres to create lateral and longitudinal forces. The larger F_{rms} is, the more force the vehicle is getting out of the tyres.

In variable torque distribution, when the controllers are trying to match the reference yaw rate, they distribute more torque to the outside tyre. This is also the tyre that is more heavily loaded. The result is that the controllers distribute the torque to the tyre that is more capable of producing longitudinal and lateral forces. On the other hand, roll moment distribution transfers the roll moment to the rear of the vehicle, causing more lateral load transfer at the rear axle. This produces more even tyre loads

at the front of the vehicle giving more grip to allow the front axle to turn in better and match the reference yaw rate.

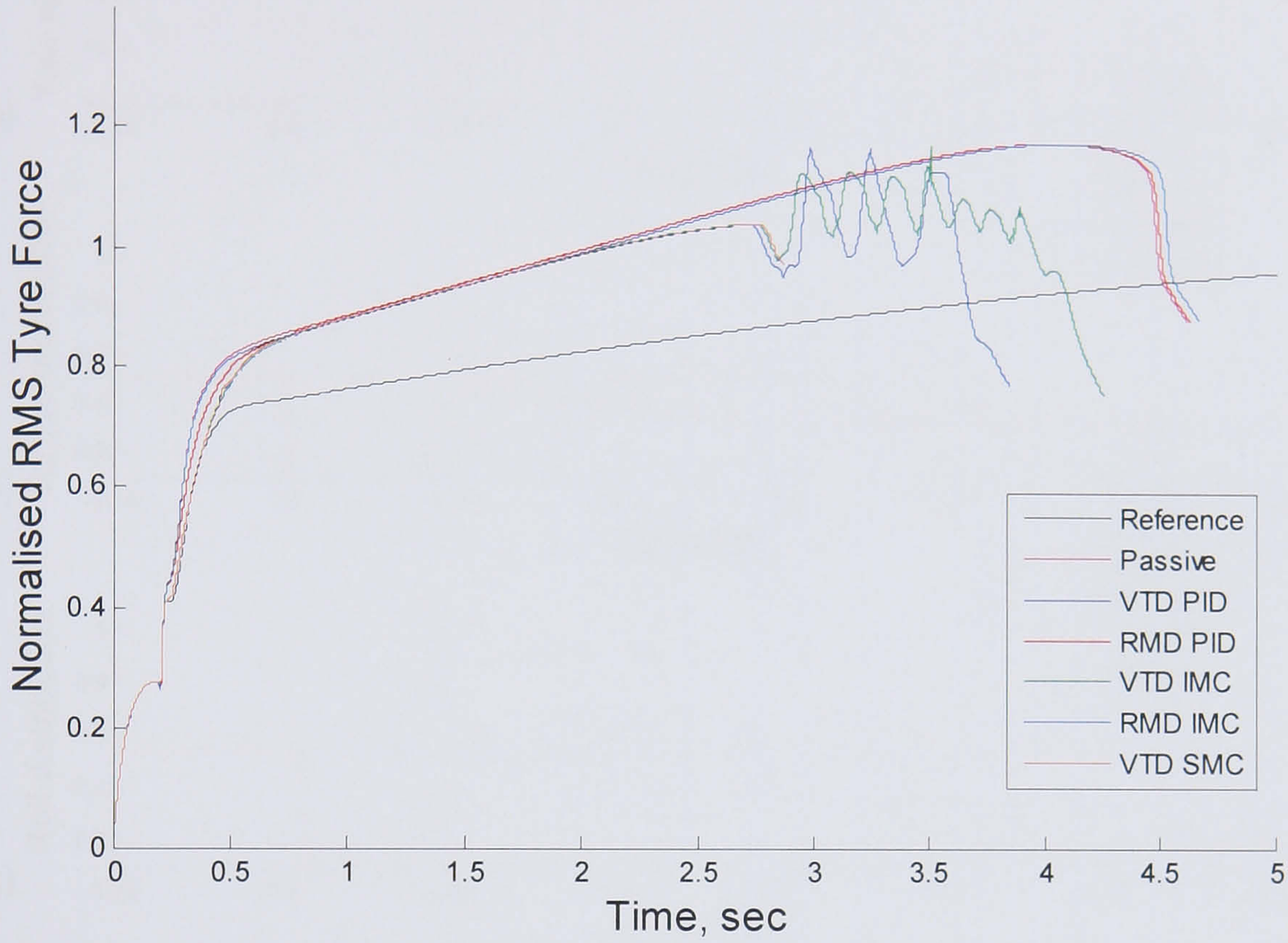

Figure 6.2 Normalised RMS tyre force results of the driveability controls, 22 m/s initial velocity, 1.5 m/s^2 acceleration, 1.5 deg steer angle

However, by increasing the roll stiffness at the rear axle, the control is also reducing the combined grip of the rear tyres. Although the handling balance is improved, it results in less efficient use of the overall tyre forces and the RMD controllers lose stability before the VTD controllers for the same manoeuvre. As shown in Figure 6.2, the result is that the VTD controllers manage to get more lateral and longitudinal forces from the tyres and extract more of their potential to create forces than the RMD controllers.

The differences at the start of the manoeuvre can be seen in the detail view of Figure 6.1 shown in Figure 6.3. Two controllers match the reference yaw rate together before the rest. These are the VTD PID and sliding mode controllers. These two controllers manage to get more force out of the tyres earlier than the other controllers, as shown in Figure 6.2. The other four controllers all match the reference yaw rate later. The VTD IM control manages to match the reference yaw rate next after initially following the fast controllers. The RMD PID control is the fastest RMD controller and follows the VTD IM control but is obscured by it in Figure 6.3.a.

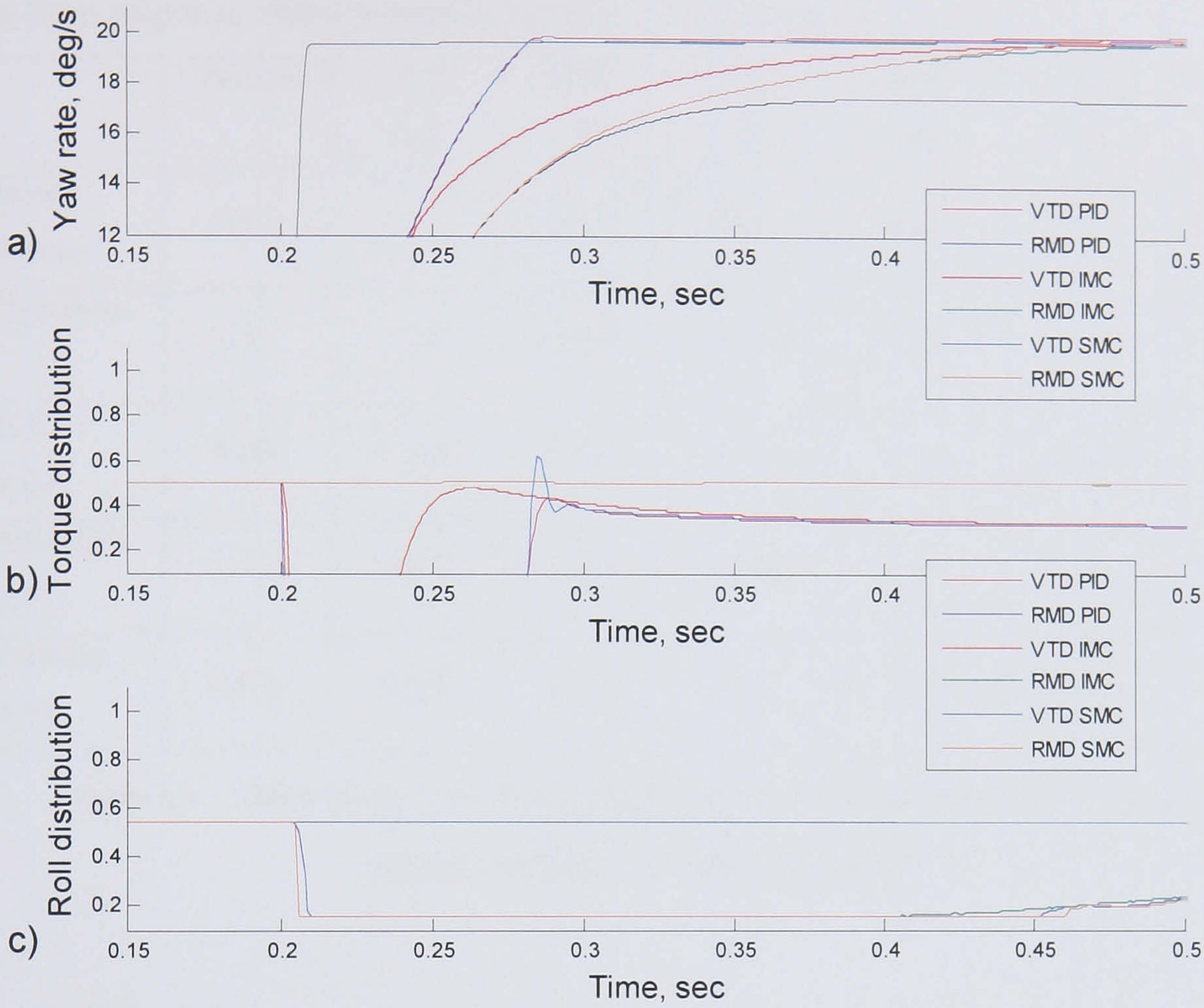

Figure 6.3 Detail of Figure 6.1 from 0.15 to 0.5 seconds

The RMD IM and SM controllers both rise up to match the reference yaw rate later. The reason the RMD controllers are slower than the VTD controllers is that roll moment distribution requires lateral load transfer to be effective. During the initial phases of the manoeuvre there is too little lateral load transfer to affect the handling of the vehicle. This is why the control signals become saturated early in the manoeuvres. The RMD controllers need to saturate the control signal to even get the smallest amount of control action. On the other hand, the VTD controllers can induce yaw moments at any time as long as the tyres still have potential to create longitudinal forces. This ability to create lateral forces at low lateral accelerations improves the yaw rate response time.

The controllers all perform well in the previous step steer manoeuvre, but that is expected since it is the same manoeuvre that was used to tune the control gains. The controllers are tested in two other manoeuvres. Both manoeuvres are carried out at constant velocity to let the vehicle reach a steady state. This allows analysis of the rise time, overshoot and settling time. The first test, shown in Figure 6.4, is a high speed,

constant velocity step steer manoeuvre run at 40 m/s with a 0.5 degree steering input. The time response characteristics are shown in Table 6.1.

	Passive	VTD PID	RMD PID	VTD IMC	RMD IMC	VTD SMC	RMD SMC
% Steady state error	-20.2	0.137	0.217	-8.48e-5	-0.255	-0.374	-0.299
% Overshoot	4.21	1.35	0.100	0.00	5.17e-3	1.78	3.03e-4
63% Rise time (s)	0.084	0.043	0.121	0.056	0.120	0.042	0.120
10-90% Rise time (s)	0.141	0.053	0.232	0.188	0.261	0.053	0.231
1% Settling time (s)	0.671	0.080	0.332	0.538	0.633	0.077	0.299

Table 6.1 Step steer yaw rate results of the driveability controls, 40 m/s initial velocity, 0.5 deg steer angle

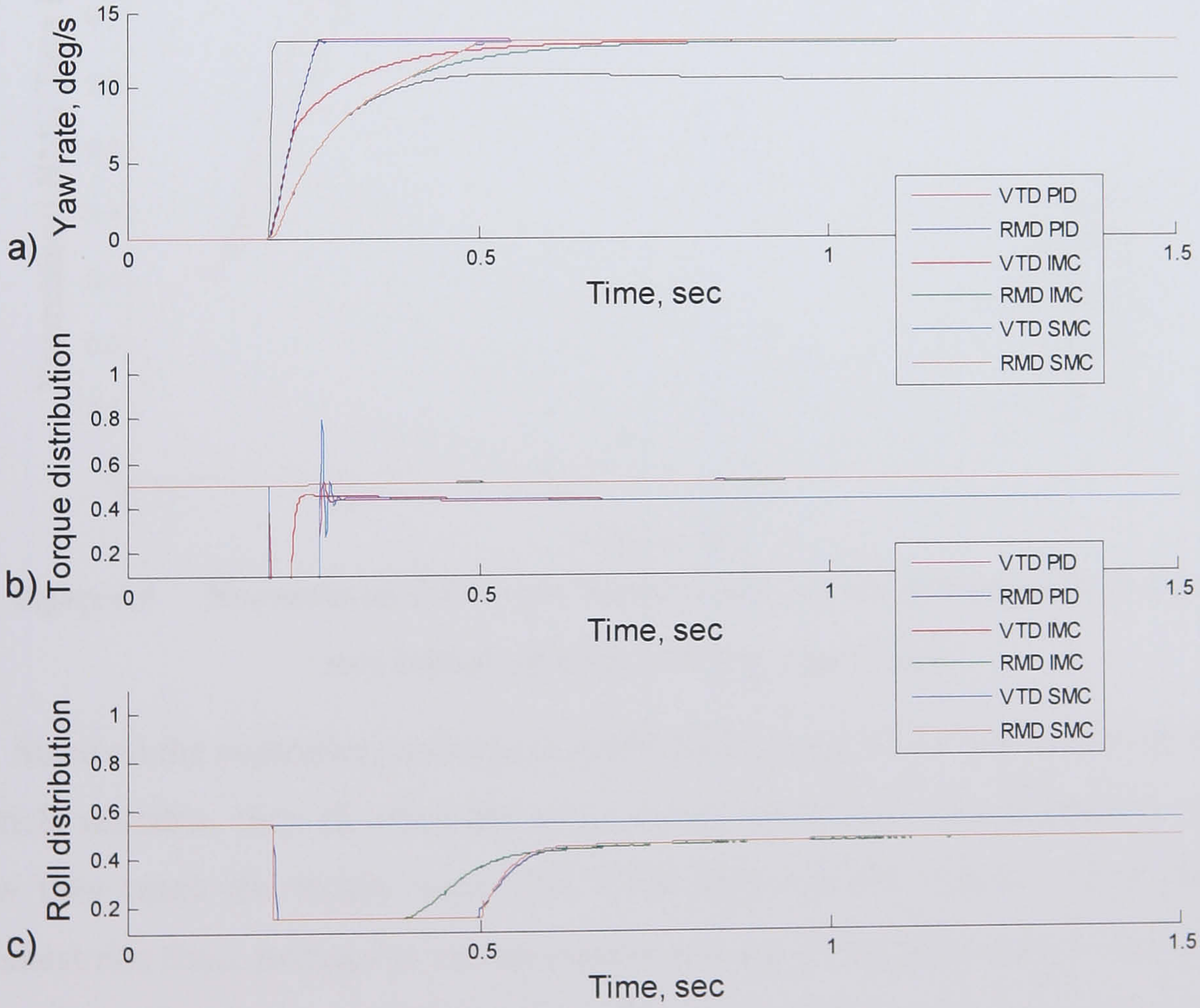

Figure 6.4 Step steer yaw rate results of the driveability controls, 40 m/s initial velocity, 0.5 deg steer angle

This manoeuvre is slightly less demanding and as a result none of the controllers lose stability once they match the reference yaw rate. The results are very similar to the previous manoeuvre. The quickest response time comes from the VTD PID and SM controllers while the VTD IM controller matches the reference yaw rate next. Once again the slowest rise time comes from the RMD controllers. The VTD PID and SM control show very similar characteristics with the only difference being a slightly greater overshoot percentage for the SM control. The RMD controllers are all very similar but the main difference being a slower 10-90% rise time for the IM control. This is mirrored in the VTD IM control. The 63% rise time is similar but the IM controllers end with a larger 10-90% rise time.

The amount the controllers exploit the available tyre force is shown once again in the normalised root mean square tyre force, shown in Figure 6.5.

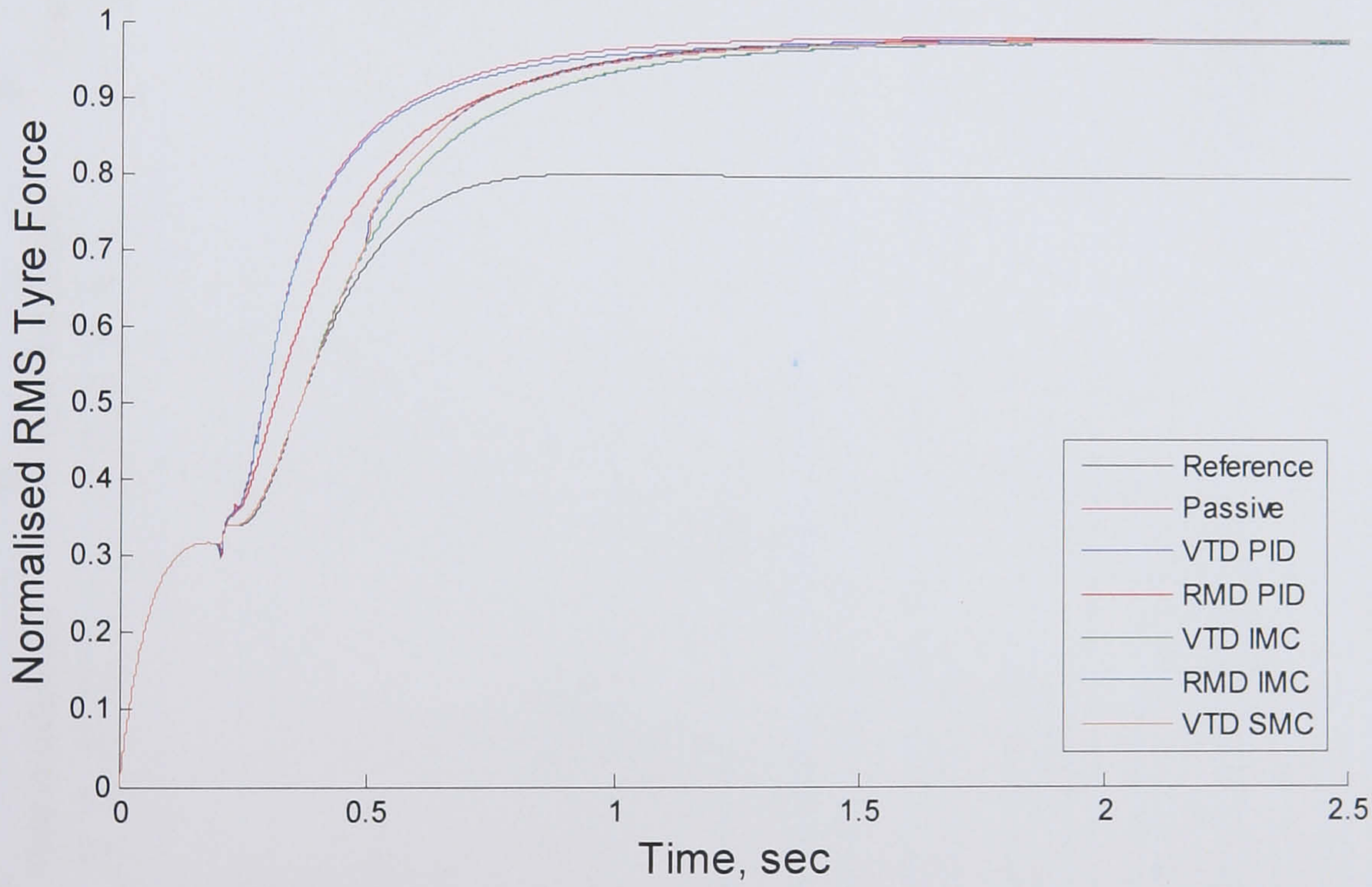

Figure 6.5 Normalised RMS tyre force results of the driveability controls, 40 m/s initial velocity, 0.5 deg steer angle

Since all the controllers manage to match the reference yaw rate and none send the vehicle unstable, they all reach the same steady state force. The difference comes in how they reach the steady state. The VTD PID and SM control, which have the quickest rise time, manage to extract more force out of the tyres earlier than the other controllers. The RMD controllers are not able to exploit the tyre forces as early as the VTD controllers and the result is that they lag behind with slower rise times.

A low speed manoeuvre is presented in Figure 6.6. This is also a constant velocity step steer manoeuvre. It is run at 15 m/s with a 3.5 degree step steer angle. The time response characteristics are given in Table 6.2. The results of all the controllers are very similar. The RMD PID and SM control reach the reference yaw rate first but only by a slim margin. This is easier to see in Figure 6.7 which shows a detailed view of Figure 6.6 from 0.15 to 0.55 seconds. However, the differences are very small and they do not have significantly faster rise times than the other controllers. They do have the largest percentage overshoot compared to the other controllers, although this is still only 1% overshoot.

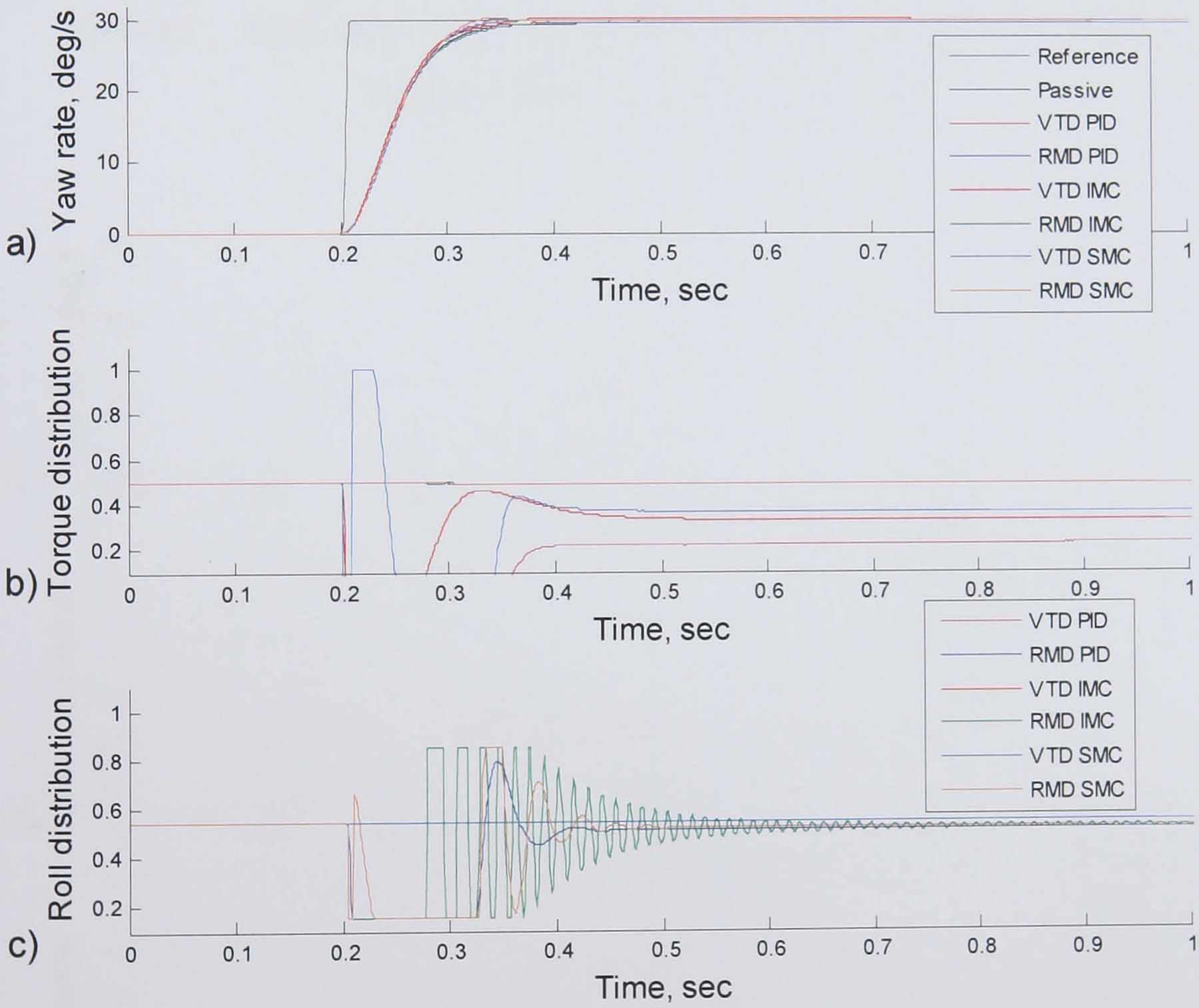

Figure 6.6 Step steer yaw rate results of the driveability controls, 15 m/s initial velocity, 3.5 deg steer angle

	Passive	VTD PID	RMD PID	VTD IMC	RMD IMC	VTD SMC	RMD SMC
Steady state error	-1.10	0.344	0.219	-2.50e-3	-0.0123	-0.250	-0.0461
% Overshoot	0.0693	0.492	1.08	4.76e-3	1.07e-3	0.129	0.915
63% Rise time (s)	0.061	0.059	0.062	0.059	0.062	0.061	0.062
10-90% Rise time (s)	0.081	0.078	0.078	0.078	0.086	0.078	0.078
1% Settling time (s)	0.162	0.141	0.147	0.189	0.187	0.136	0.122

Table 6.2 Step steer yaw rate results of the driveability controls, 15 m/s initial velocity, 3.5 deg steer angle

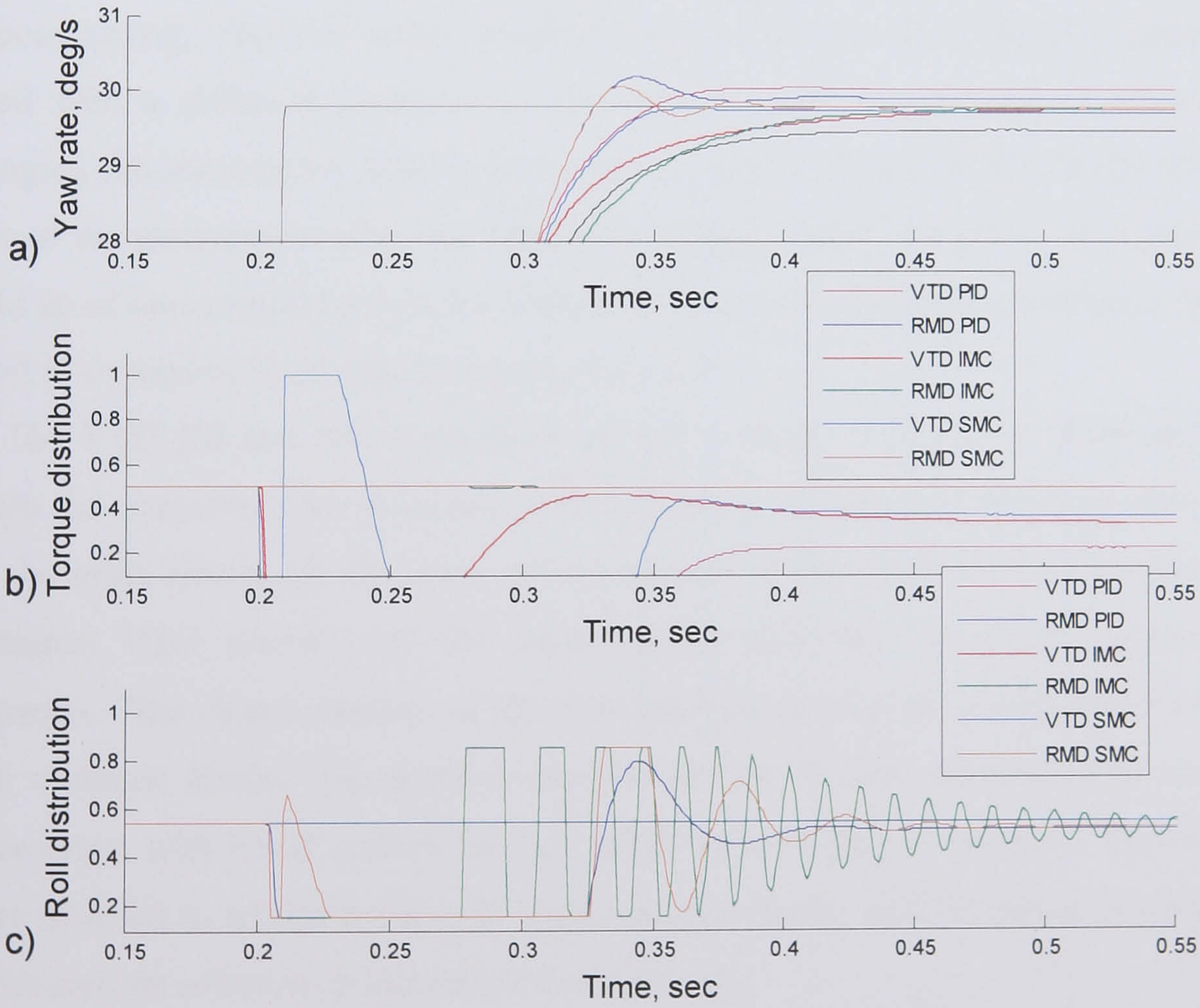

Figure 6.7 Detail of Figure 6.6 from 0.15 to 0.55 seconds

The main point of interest from this manoeuvre is the oscillation in the RMD control signal. The IM control has a particularly large oscillation in the control action. The oscillations come from poor controller tuning. The controllers were tuned using a

step steer manoeuvre but in a different range of the vehicle handling. Although the internal model control algorithm is designed to be robust with model compensating internal and inverse models, the difference in operating conditions is too great. The problem stems from the indirect nature of roll moment distribution. Since roll moment distribution does not create yaw moments directly, the simplified models are not very good at accurately describing the control dynamics. The models and controllers can be tuned to work at a specific set point but are not flexible enough to operate over the entire range of the vehicle handling.

The RMD SM control and RMD PID control also show some oscillation but not to the same degree as the IM control. The SM controller is also inherently designed to be robust and work around modelling uncertainties, but it still requires properly tuned gains. In this manoeuvre the controller is not well damped. It overshoots and oscillates around the reference yaw rate. The control gains and inverse model are not optimised for this manoeuvre. The RMD PID control is also affected by the problem of poor tuning. There is some overshoot and oscillation since the PID gains were tuned with a different manoeuvre. The integral gain in particular is affected by changing the manoeuvre. This is due to the integral error signal that builds up at the start of the manoeuvre when the vehicle is lagging behind the reference signal. This build up of the integral term in the control changes with different manoeuvres and can result in overshoot if the gain is not properly tuned.

The VTD IM and SM controllers are not as badly affected by these problems. Again the controllers are designed to be robust in the face of modelling uncertainty but the main reason for the more precise control is the mechanism of creating yaw moments. VTD actively induces forces at the rear tyres to directly induce yaw moments. This direct creation of the yaw moment is easy to model precisely, even with a simple model. The result is that the inverse models are also more accurate. Conversely, with RMD control the yaw moments are created indirectly. This is much more difficult to model accurately with a simple model and the result is controllers which are less robust to different test manoeuvres.

The normalised root mean square tyre forces are shown in Figure 6.8. The controllers show very similar use of the vehicle tyre forces. Although this is not guaranteed by the similarity of the yaw response, it is certainly not surprising that similar tyre forces would be required to track the same yaw rate. Figure 6.8.b shows a

more detailed view that again shows the VTD PID and SM controllers exploiting the tyre forces just a little more than the other controllers. The oscillations of the RMD controllers can also be seen coming through into the tyre forces.

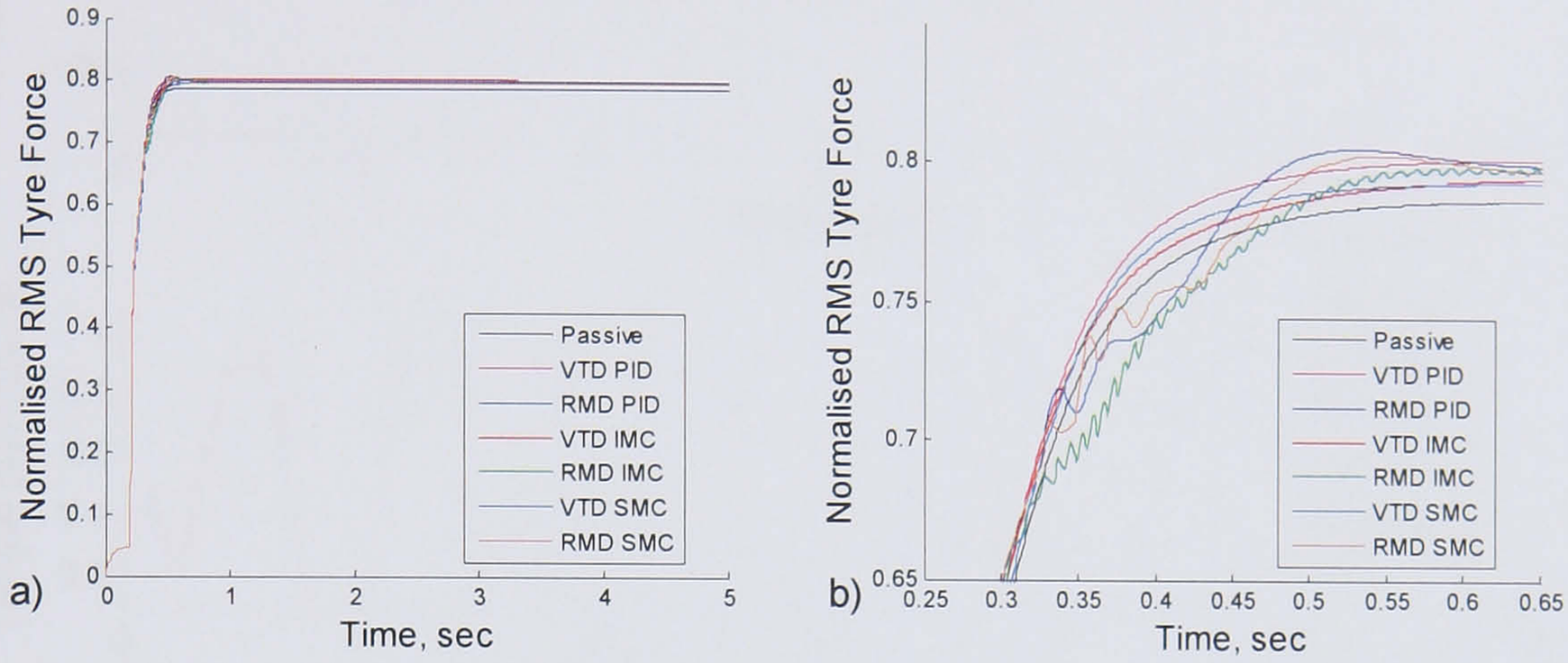

Figure 6.8 Normalised RMS tyre force results of the driveability controls, 15 m/s initial velocity, 3.5 deg steer angle

The sinusoidal steer test shows the vehicle behaviour as the test manoeuvre becomes progressively more severe. The test starts at 15 m/s and accelerates at 0.5 m/s^2 while the sinusoidal steer angle begins at 1.0 degree and increases at 0.5 deg/s. Figure 6.9 shows the time response for the yaw rate tracking controllers. As expected, the controllers manage to follow the reference yaw rate well. This is shown by the yaw rate error in Figure 6.9.d defined by:

$$E_{yaw} = \int \left| r - r_{ref} \right| dt \qquad (6.2.)$$

This represents the area under a graph of the absolute value of the yaw rate error. Any error between the vehicle yaw rate and reference yaw rate will be summed. The graph shows that the controllers have less yaw error than the passive vehicle throughout the manoeuvre with the VTD controllers showing the least error. The three VTD controllers all show a very similar response, as do the three RMD controllers. This is once more due to the fact they are following the same control objective. They all find the control action to reduce the yaw rate error but with different algorithms. In fact the RMD controllers show the same yaw rate error as the VTD controllers, but with an offset that corresponds to the yaw rate error they accumulated at the beginning of the manoeuvre when there was insufficient lateral load transfer to affect the vehicle dynamics.

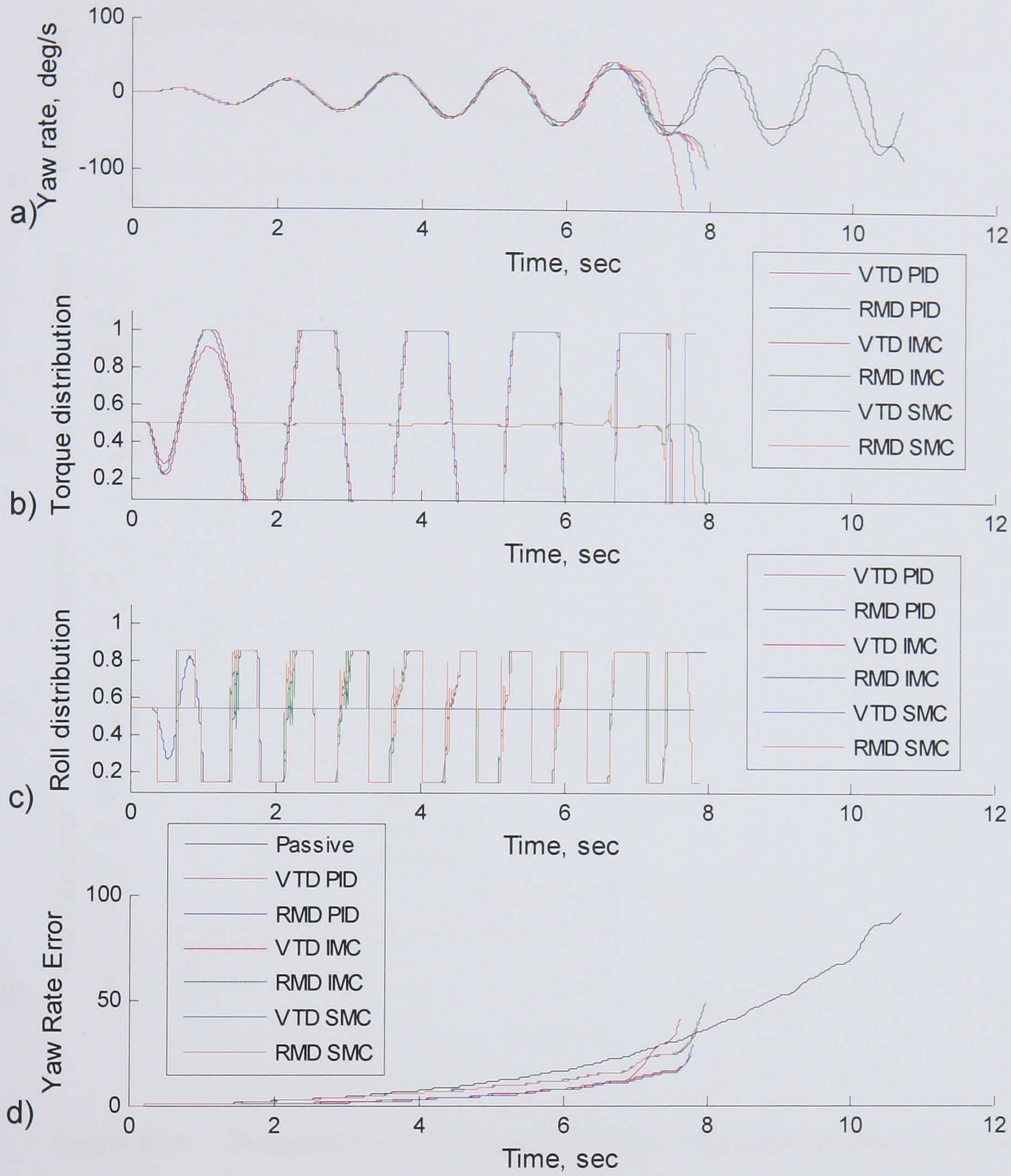

Figure 6.9 Time response of the driveability controllers in the increasing sinusoidal steer test

As seen before, they also lose stability before the passive vehicle. This is because the controllers are pushing the vehicle to follow a reference yaw rate created by a linear model. At some point this reference yaw rate will go beyond the limits of the vehicle and the controllers will push the vehicle to instability.

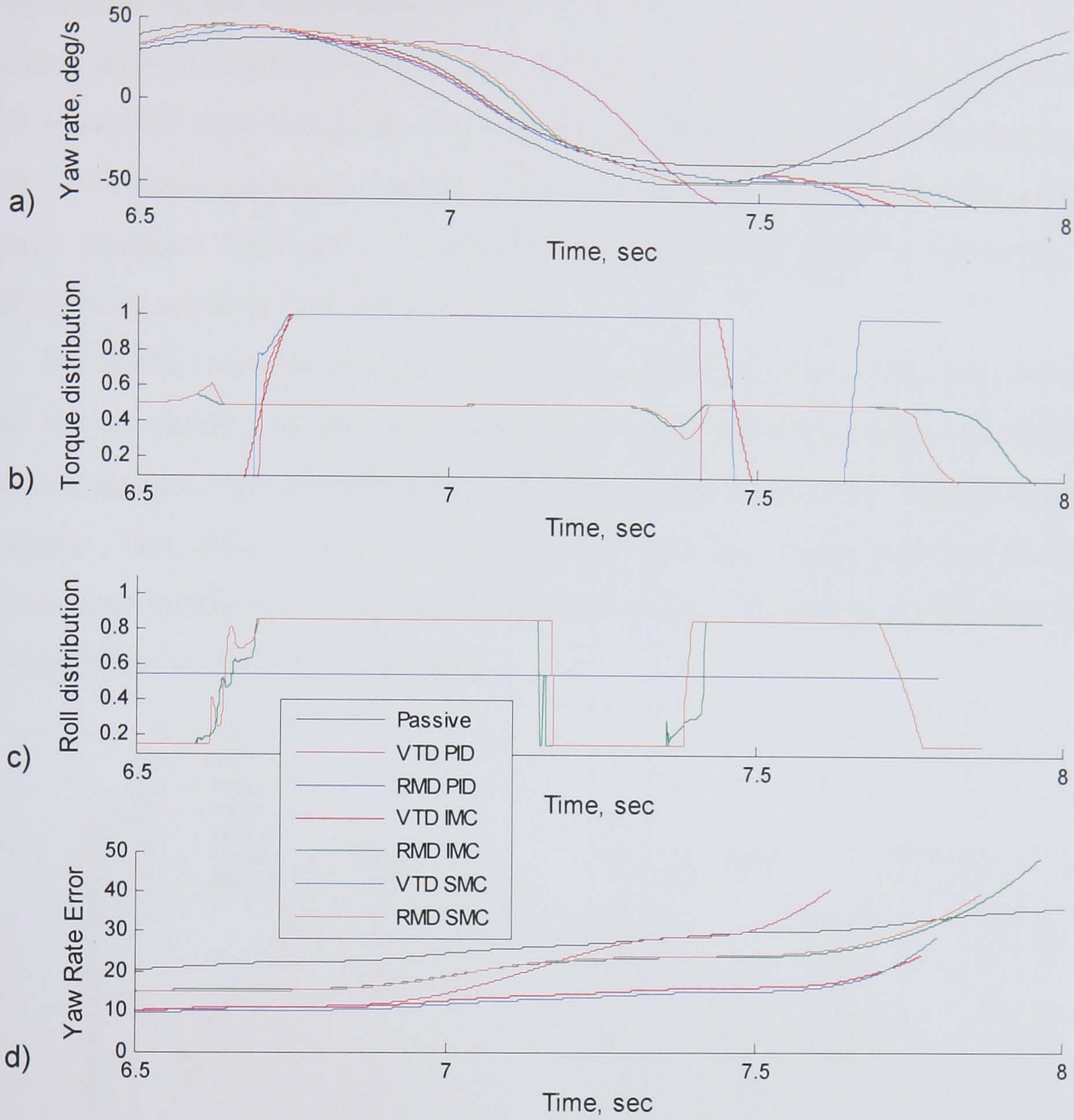

Figure 6.10 Detailed view of sinusoidal time response of the driveability controllers

Figure 6.10 shows the final seconds of the manoeuvre in more detail. Figure 6.10.c shows the oscillatory behaviour of the RMD IM control is present once again, and to a lesser degree in the SM control, even though it does not show in the yaw rate. Figure 6.10.a shows the VTD PID control is not performing as well as it did in the step steer manoeuvres. It drives the vehicle very hard and pushes the yaw rate, making it diverge from the reference yaw rate. This is a result of the gains being tuned for the more aggressive step steer manoeuvre, which requires more abrupt control action and higher gains. The sinusoidal steer test does not have the same rate of change of steer angle and the PID control could be more efficient with adaptive gains.

The VTD IM control performs better in this test, matching the VTD SM control. The reason for the improvement in the IM controller is the same reason why the PID control does not perform as well. The rate of change of the steer angle is a lot less in the sinusoidal steer test so the IM control is not affected by its slower response time. The SM control manages to perform the best of the all the controllers once again. The quick response time and robust nature of the control mean it can adapt well to different manoeuvres and test conditions.

The RMD controllers are all very similar and do track the reference yaw rate well but not as closely as the VTD controllers. They lack the ability to influence the vehicle dynamics in the early stages of the test when there is not sufficient lateral load transfer. This error carries forward through the rest of the manoeuvre. Once the manoeuvre builds in severity, the controllers do perform well and their error builds at a similar rate to the VTD controllers.

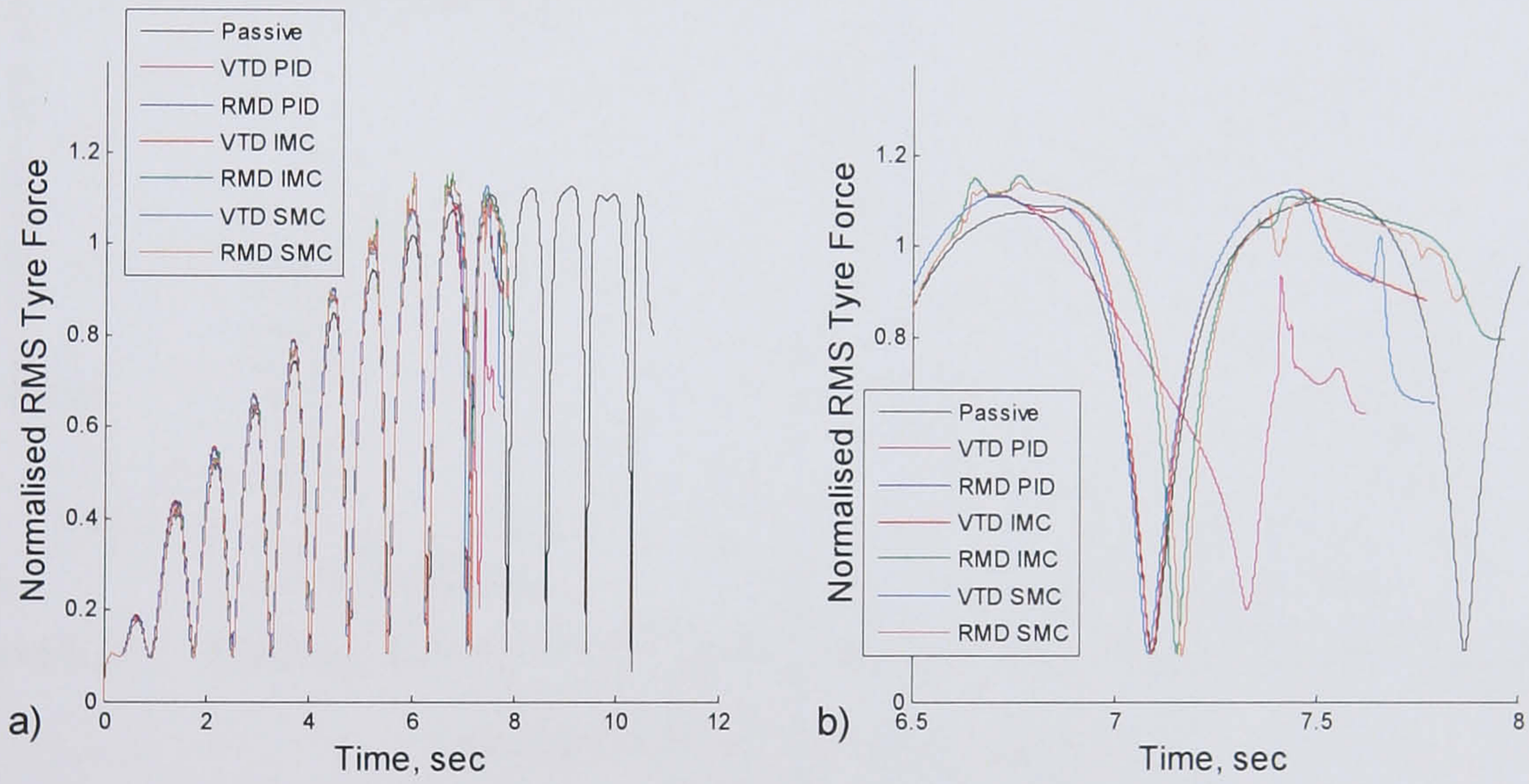

Figure 6.11 Normalised RMS tyre force from the sinusoidal steer test of the driveability controllers

The normalised root mean square tyre force is shown in Figure 6.11. Again the VTD SM control extracts the greatest forces from the tyres although it is joined by the VTD IM control. This is once more due to the VTD IM control matching the behaviour of the VTD SM control in the sinusoidal steer test. The VTD PID control matches the other VTD controllers until it loses stability due to being too aggressive. The RMD controllers are not far behind the VTD SM and IM controllers. They are able to perform better in this less aggressive manoeuvre with the RMD SM and IM controllers able to last the longest.

The final comparison is given in Figure 6.12 which shows the lateral acceleration gain and the 63% yaw rate rise time across a range of lateral accelerations created by running constant velocity step steer tests at 20 m/s while incrementing the steering angle in subsequent tests to increase the lateral acceleration. These results show how linear the vehicle response is as the lateral acceleration increases. The reason the driveability controllers aim to match a linear reference model is to linearise the system response. A linear system is much more predictable for the driver and makes the driver task easier. If the linear response can be pushed further towards the limit handling threshold the driver workload will be decreased and the result is a vehicle that is easier for the driver to control. A constant lateral acceleration gain shows that the lateral acceleration of the vehicle increases linearly with increasing steer angle.

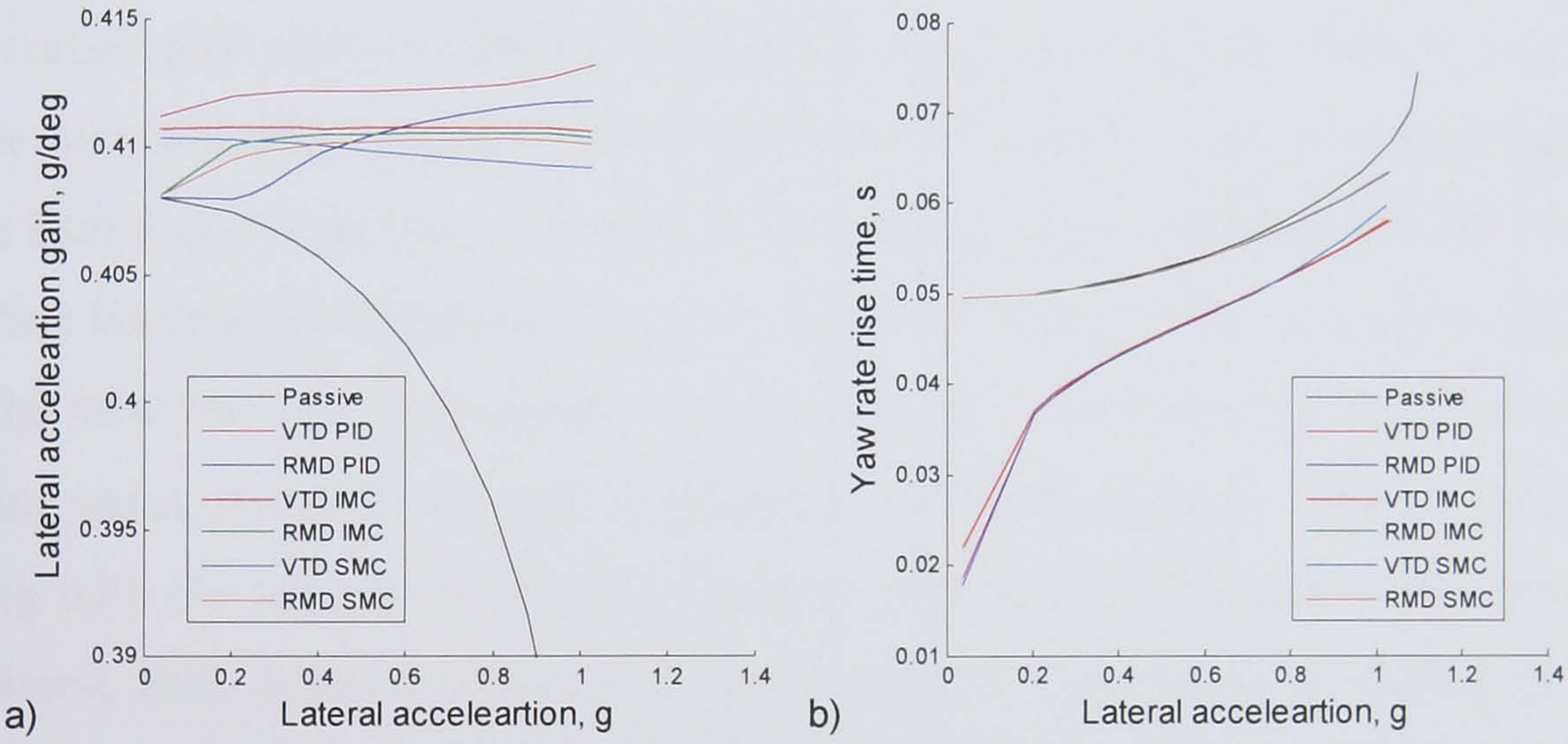

Figure 6.12 Lateral acceleration gain and rise time of the driveability controls during step steer manoeuvres

All the controllers are effective at improving the system response and maintaining a more constant lateral acceleration gain. The most effective is VTD IM control. It manages to keep the lateral acceleration gain almost constant across the whole range of lateral accelerations. This corresponds to a linear response of the lateral acceleration from the steer angle. VTD SM control is almost as good. Although the lateral acceleration gain slowly decreases as the lateral acceleration increases, it still varies very little. The VTD PID control is the opposite, the lateral acceleration gain slowly increases, and at a slightly greater rate. This corresponds to the controller overshooting the reference yaw rate and reaching steady states with a higher lateral acceleration. As explained before, this is due to the gain tuning. The gains are tuned to track the reference yaw rate and remove any steady state error. However, as the actual

manoeuvre diverges from the test manoeuvre used to tune the gains, they may no longer be the best gains that produce the best vehicle behaviour. As can be seen, as the lateral acceleration increases the controller gives a vehicle response with a progressively higher lateral acceleration gain due to overshooting the reference yaw rate.

The RMD controllers all begin with lower lateral acceleration gains since RMD is not effective until the vehicle has built up some lateral acceleration. The RMD PID control shows a similar behaviour to the VTD PID control, with the lateral acceleration gain slowly rising. Again this corresponds to the controller overshooting the reference model and is due to the gain tuning. The IM and SM controllers have built in models that allow the controller to adapt to different manoeuvres. This results in the RMD IM and SM controllers managing to maintain a more constant lateral acceleration gain once the lateral acceleration is sufficient for the controllers to work. Of the two controllers, the IM control manages to maintain a more constant gain into lower lateral accelerations, although the SM control is very similar. The IM control is effective because the feedback control is constantly tuned by the internal model.

The yaw rate rise time shows how quickly the vehicle dynamics respond to the steering input. A quick rise time is desirable for drivers since it creates a more direct feeling with the vehicle. Figure 6.12.b shows the lag in RMD due to the delay from the lateral load transfer. Although it does improve the rise time slightly at higher lateral accelerations, this improvement is not very significant compared to the improvement given by the VTD controllers. The VTD controllers do manage to improve the rise time, especially at low lateral accelerations. VTD can induce yaw moments immediately as the manoeuvre begins and improves the response time throughout the range of lateral accelerations. The behaviour of the three VTD controllers is very similar. Once again, this is due to the fact that the controllers all follow the same objective but just use different algorithms to calculate the control action.

These test manoeuvres show that the controllers are effective at matching the reference yaw rate over a range of vehicle manoeuvres, but they have all been run on a high grip road surface. To test the robustness of the controllers the following results were obtained by simulating the manoeuvres on a wet road surface with a coefficient of friction, $\mu = 0.7$. Figure 6.13 shows the results of the same accelerating step steer

manoeuvre used to tune the controllers but on a low friction road surface. These results can be compared to those given for the high friction surface in Figure 6.1. Again the reference yaw rate is in grey while the passive vehicle is shown by the black signal.

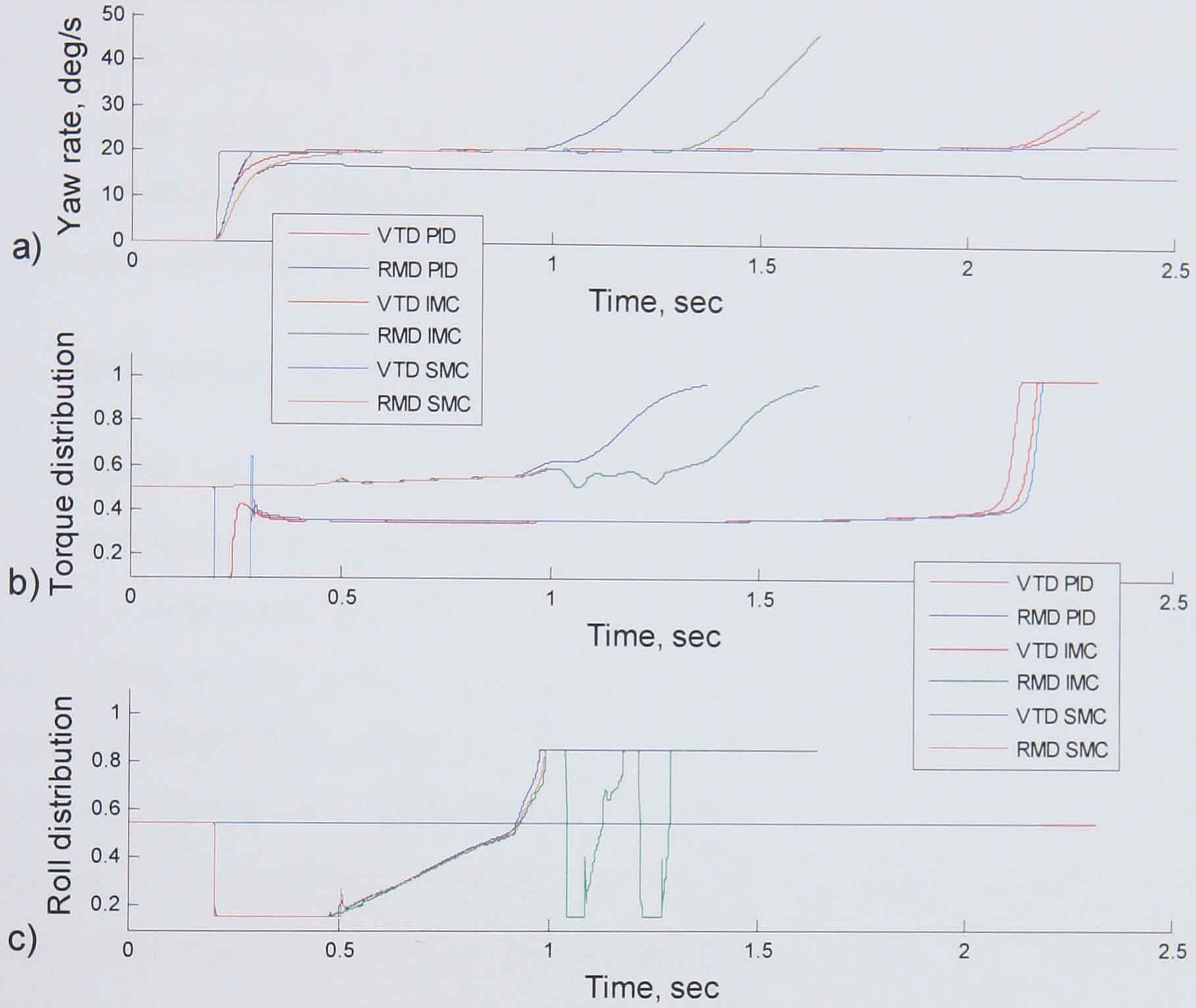

Figure 6.13 Step steer yaw rate results of the driveability controls, 22 m/s initial velocity, 1.5 m/s^2 acceleration, 1.5 deg steer angle, μ=0.7

The controllers still manage to push the vehicle to match the reference yaw rate. The main difference is that the vehicle becomes unstable much sooner. This is simply because the reference yaw rate is still calculated using the same steady state equation, Equation (5.2), with the same tyre cornering stiffness resulting in the same reference yaw rate despite the lower grip surface. Even if a road surface estimator was used to predict the coefficient of friction and modify the tyre cornering stiffness, the reference yaw rate would not change much in the linear model. Yaw rate is primarily a function of the balance of the lateral forces from the front and rear axles, seen in Equation (5.3). Reducing the cornering stiffness of all the tyres together will not have a large effect on the vehicle balance in the simple steady state model and the reference yaw

rate will remain around the same value. In fact, the steady state yaw rate of the linear model changes by less than 3% when the friction coefficient is reduced to 0.7 in a 2.0 degree step steer test run at 25 m/s.

The controllers are still effective in meeting their goal of matching the reference yaw rate but they are pushing the vehicle towards an unrealistic target. Due to the non-linear tyres, changes in the road surface friction do not give proportional changes to the vehicle yaw rate. If a road surface friction estimator could be used to modify the reference model by some other means than just proportionally decreasing cornering stiffness of the tyres, the controllers would work just as well in matching the reference yaw rate but would be trying to follow a more reasonable target.

6.1.2. Driveability Control Conclusions

The RMD controllers are effective at matching the reference yaw rate however, they do not manage to exploit the tyre forces as effectively as the VTD controllers. The other concern with their behaviour is the oscillations in the control signal at low speed. Despite this, the most promising RMD controller is, by a small margin, the PID control. The RMD PID control manages to follow the yaw response of the RMD SM control but shows less oscillation at low speed. RMD IM control is the least promising. It does manage to match the reference yaw rate but with a much slower rise time. The controller also oscillates at low speeds, although not as much at the SM control.

The VTD controllers show a better response. One reason for this is that the torque distribution can affect the vehicle handling and induce yaw moments immediately without waiting for the lateral load transfer to build up. The most effective VTD controller is the SM control, although there is not much difference when compared to the PID control. The PID control is almost as good and is very effective at matching the reference yaw rate. However, the SM control is better at adapting to different manoeuvres. The PID control shows more overshoot as the manoeuvres diverge from its tuning set point while the built in robustness of the SM control manages to cope with these changes better. The IM control also manages to cope with different manoeuvres well but it has a slower rise time compared to the other controllers in the step steer tests.

As a result the best driveability controller is given by the variable torque distribution, yaw rate tracking, sliding mode control. The best roll moment distribution controller is given by the RMD PID control.

6.2. Stability Control

Stability controllers were developed for both VTD and RMD but unlike the driveability controllers that were all yaw rate tracking controllers, there are two different strategies for the stability controllers. Both strategies aim to reduce and constrain the sideslip angle but they use different methods. The first strategy is the reference sideslip angle tracking control and the second is the sideslip phase plane stability control. As presented in Chapter 5, the reference sideslip angle tracking control works in much the same way as the driveability controllers using a PID control but it aims to match the sideslip angle. The phase plane controllers use a proportional control based on an error signal defined by the distance from the vehicle state to the control boundary on a sideslip phase plane plot. The wheel load control is not presented here with the stability controllers since it was already determined to be ineffective as a stand alone stability control. It is used in the final integration strategy, which is presented in Chapter 7.

Like the driveability controllers, the first test used to evaluate the different control strategies is the same test used to tune them. This is the constant velocity step steer test. It is run at the limits of vehicle handling to determine how effectively the controllers stabilise the vehicle. Then the controllers are tested in two more step steer tests, also run at the limits of vehicle handling but at faster and slower velocities. These test manoeuvres show that the controllers are robust to different test manoeuvres. After the step steer tests, the controllers are evaluated with the same increasing velocity, increasing sinusoidal steer test used to evaluate the driveability controllers. This test evaluates how well the controllers can maintain the stability of the vehicle as the manoeuvre keeps increasing in severity.

Next the sideslip angle gain and understeer gradient are evaluated across the range of lateral accelerations. These results show the dynamic response of the controllers throughout the performance range of the vehicle. Finally, like the driveability controllers, the stability controllers are evaluated on a low friction surface. This test evaluates how robust the controllers are in adverse conditions.

6.2.1. Stability Control Results

The differences in the two stability control strategies can be seen in the sideslip angle results presented in Figure 6.14. This is the same step steer test used to tune the controllers run at 25 m/s with a 2.5 degree step steer. The time response characteristics corresponding to Figure 6.14 are presented in Table 6.3.

	Passive	VTD PID	RMD PID	VTD PP	RMD PP
% Steady state error	96.1	-9.96e-5	0.0147	80.5	52.5
% Overshoot	66.9	24.6	46.7	4.97	12.6
63% Rise time (s)	0.253	0.165	0.162	0.244	0.218
10-90% Rise time (s)	0.241	0.121	0.102	0.258	0.212
1% Settling time (s)	3.627	0.993	1.149	0.842	1.27

Table 6.3 Step steer sideslip results of the stability controls, 25 m/s initial velocity, 2.5 deg steer angle

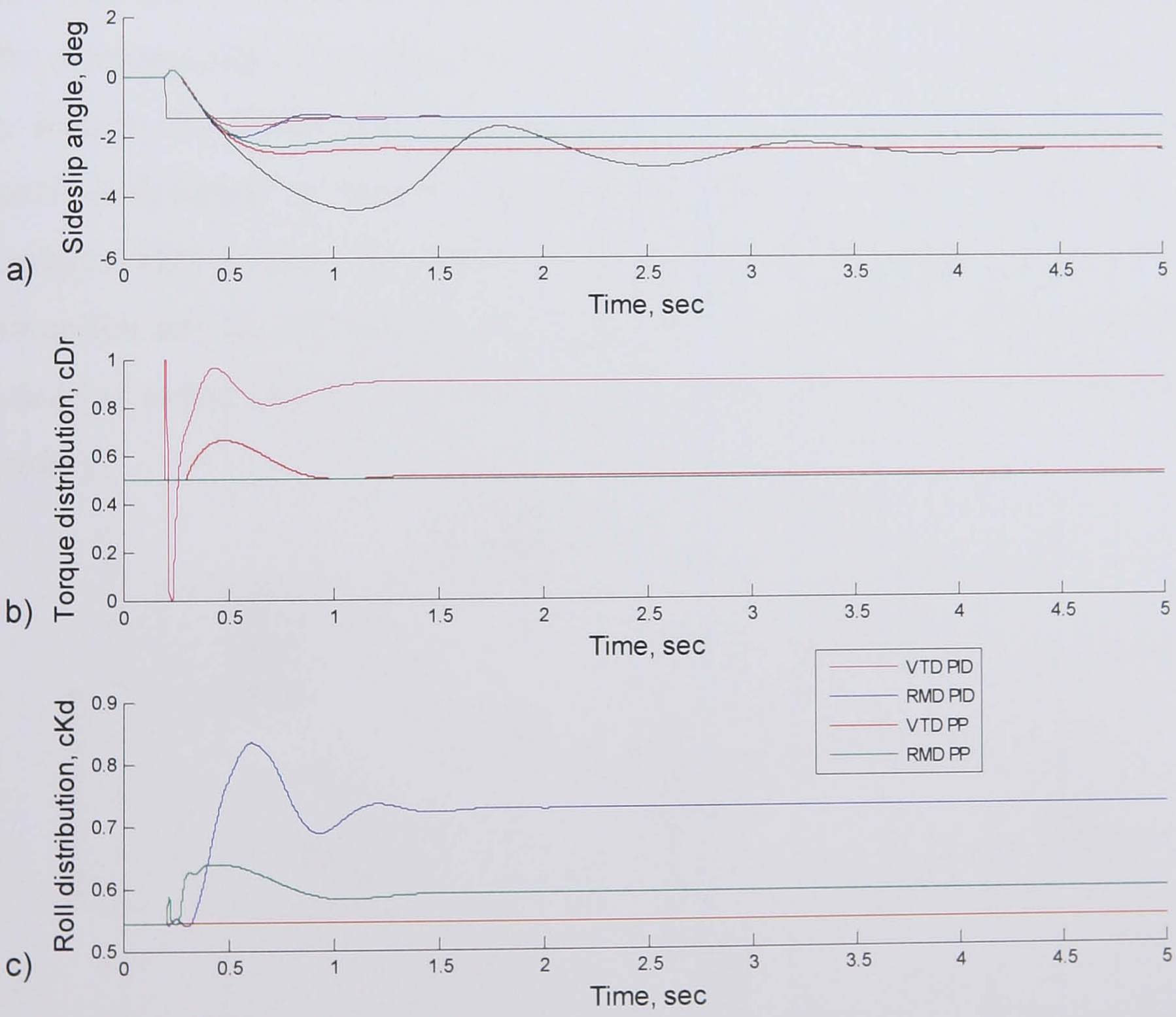

Figure 6.14 Step steer sideslip results of the stability controls, 25 m/s initial velocity, 2.5 deg steer angle

The obvious difference is that the PID controllers aim to match the reference sideslip angle while the phase plane controllers just try and limit the sideslip behaviour. The result is that the PID controllers use a lot more control action to reduce the sideslip angle and match the reference signal. The phase plane controllers let the vehicle run with more sideslip angle and only introduce the control action as the sideslip behaviour reaches the control boundary. This limits the amount of control intervention and the energy used by the controller.

The sideslip angle phase plane and normalised root mean square tyre force are shown in Figure 6.15. The phase plane results, and Table 6.3, show that although the PID controls reduce the sideslip angle more than the phase plane controls, they have more overshoot and oscillation, especially the RMD PID control. The reason the RMD PID control has more oscillation and overshoot than the VTD PID control is that it cannot alter the vehicle balance before there is lateral load transfer. By the time enough load transfer is present the sideslip angle is already overshooting the reference signal. The RMD PID control then has to work harder to bring the sideslip angle back to the reference signal, resulting in the overshoot and oscillations. This same effect is also seen in the RMD phase plane control but to a much lesser degree since the control is designed to become active only once the vehicle reaches the control boundary. This means the gains are tuned to accommodate a delayed control intervention and do not result in the overshoot or oscillations. Also the control does not need to reduce the sideslip angle as much as the PID control to reach the control boundary.

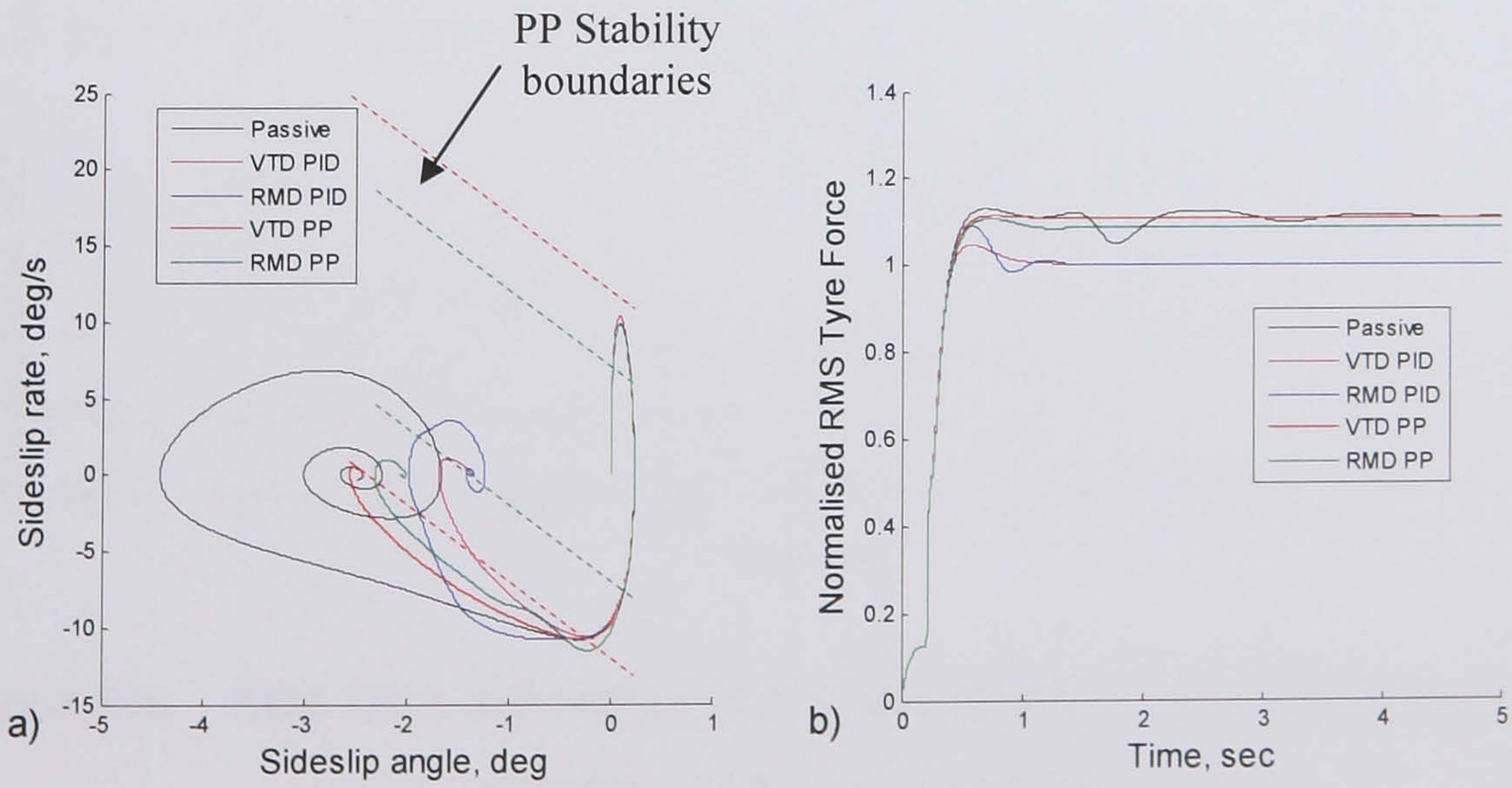

Figure 6.15 Step steer phase plane response and normalised RMS tyre force of the stability controls, 25 m/s initial velocity, 2.5 deg steer angle

Figure 6.15.b shows the normalised root mean square tyre force. The PID controllers have lower steady state normalised forces. This is because they reduce the sideslip angle more. If the vehicle has a smaller sideslip angle, the tyre slip angles will also be smaller and the tyres will not be creating as much force. This leaves more available potential to create lateral forces in the tyres and allows the driver to give additional steering input without saturating the tyres. The cost of this is larger control intervention into the vehicle dynamics and more energy consumption. Although the phase plane controllers stabilise the vehicle with higher normalised root mean square tyre forces they still achieve the goal of stabilising the vehicle.

The controllers are expected to produce good results for this manoeuvre since this is the same test used to tune the gains. Figure 6.16 shows the sideslip angle results from a higher speed manoeuvre run at 40 m/s with a 1.0 degree steer angle.

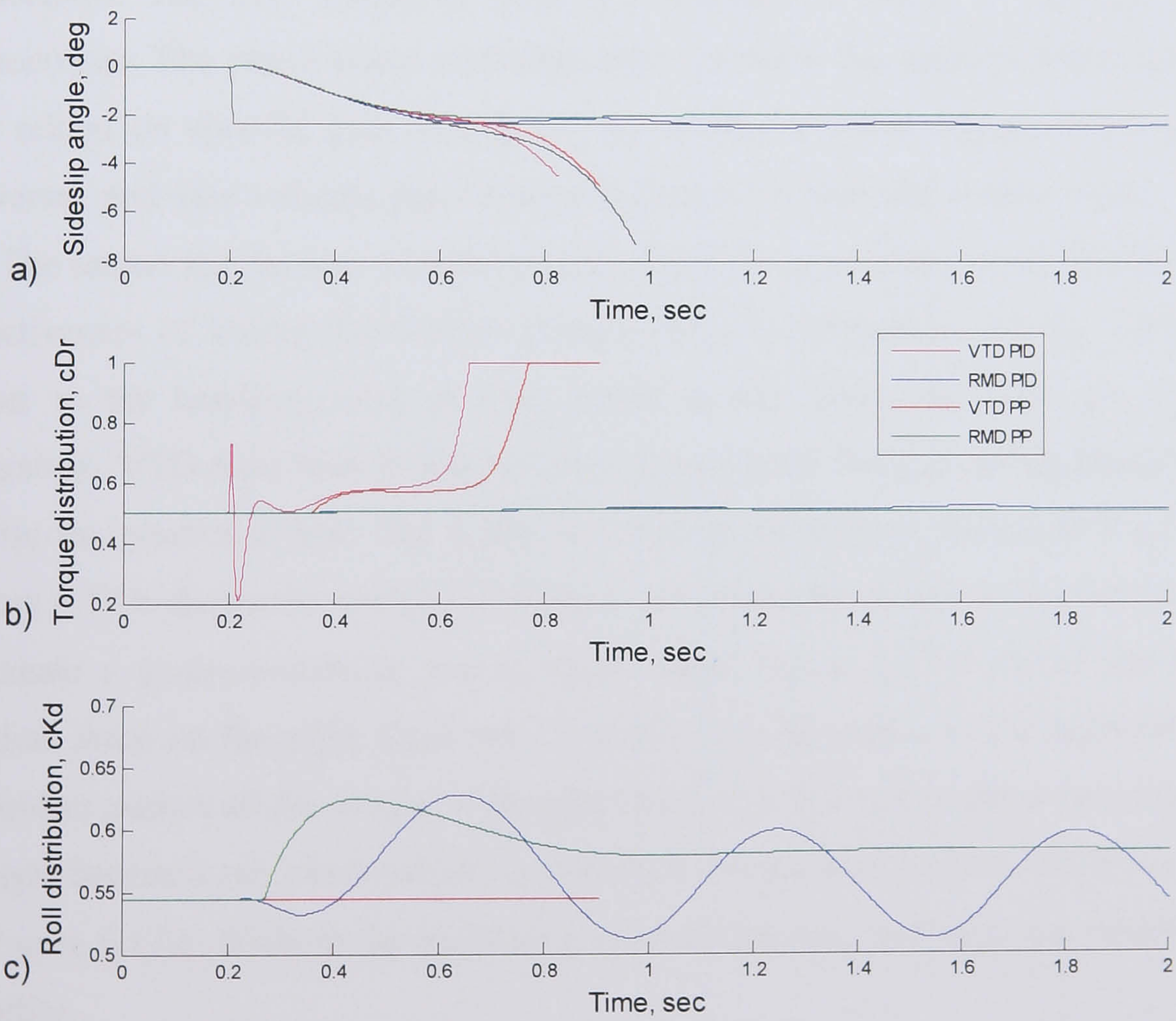

Figure 6.16 Step steer sideslip results of the stability controls, 40 m/s initial velocity, 1.0 deg steer angle

The most obvious results from this test are that not only does the passive vehicle become unstable but both of the VTD controllers also lose stability. The RMD phase

plane controller still works effectively at reducing the sideslip angle and controlling the vehicle but the PID control shows some oscillations. As a result there is no steady state error or settling time given for the RMD PID control in Table 6.4 since it does not reach a steady state by the end of the simulation.

	Passive	VTD PID	RMD PID	VTD PP	RMD PP
% Steady state error	-	-	-	-	-17.4
% Overshoot	-	-	6.68	-	7.77
63% Rise time (s)	-	-	0.252	-	0.219
10-90% Rise time (s)	-	-	0.286	-	0.237
1% Settling time (s)	-	-	-	-	0.850

Table 6.4 Step steer sideslip results of the stability controls, 40 m/s initial velocity, 1.0 deg steer angle

The oscillations occur because the controller was tuned with a different test manoeuvre. The PID controller does not manage to adapt to different vehicle manoeuvres. The phase plane controller does not have the same problem since it is less reliant on specific gain tuning. It only defines a stable region, which is more universal, and uses a simple proportional amplifier to create the control signal.

The reason for the loss of stability with the VTD controllers is due to the reduced effectiveness of torque distribution at high lateral accelerations. As the vehicle gets closer to the handling limit at high lateral accelerations, the tyres get closer to saturating. VTD then tries to extract more forces from the already saturated tyres to realise the control action. The result is a loss of stability as shown in Figure 6.17. Figure 6.17.b shows the controller trying to distribute the torque to the rear right tyre to create a contra-cornering yaw moment while Figure 6.17.d shows the reduced vertical force on the right hand tyre. Just after 0.6 seconds into the manoeuvre, the controller pushes all the torque to the right hand tyre but due to the reduced tyre load the tyre becomes saturated and can not produce the required longitudinal force, shown in Figure 6.17.c. Without the stabilising contra-cornering yaw rate, the vehicle losses stability.

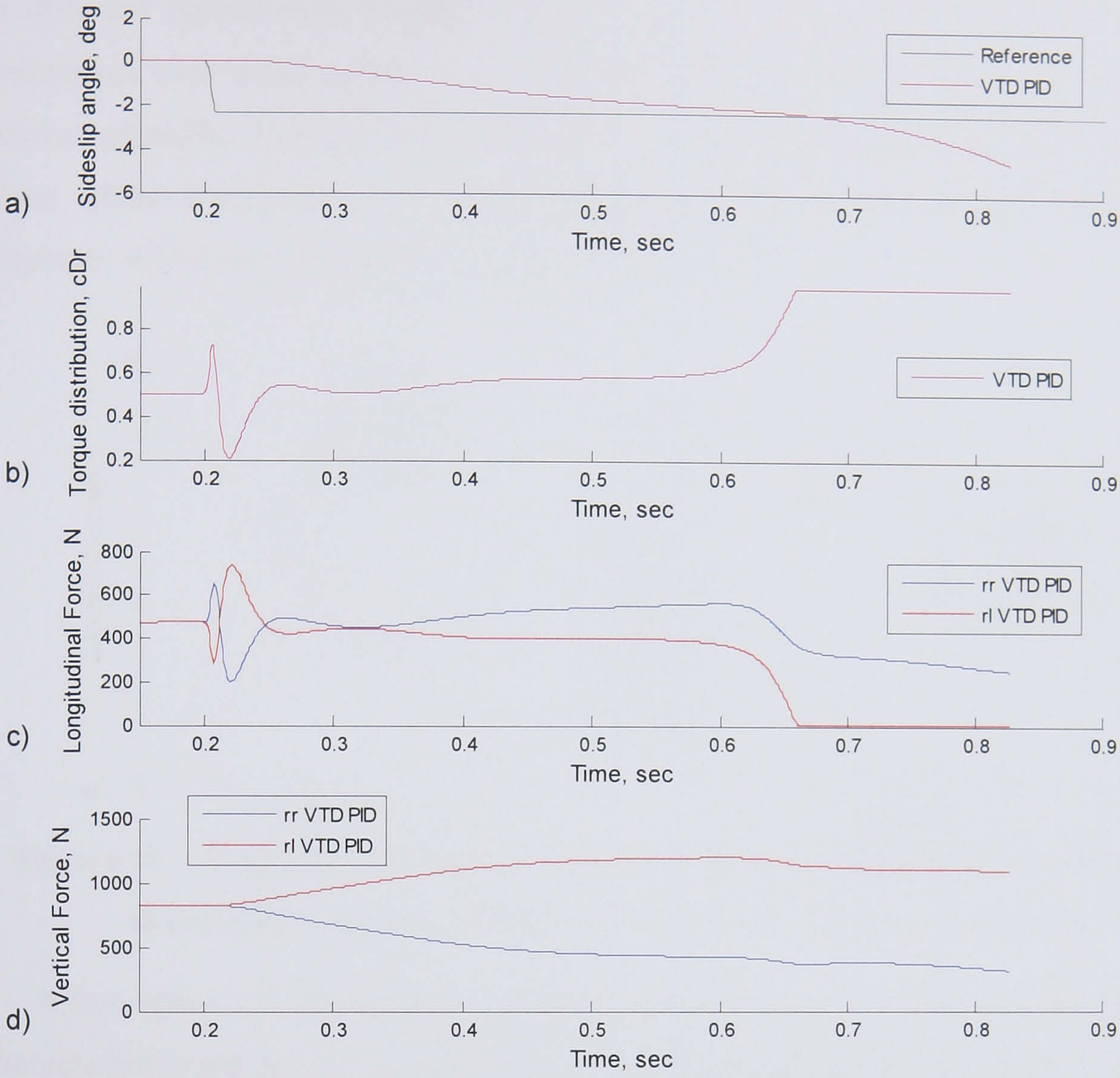

Figure 6.17 Loss of stability of the VTD PID stability control in a step steer, 40 m/s initial velocity, 1.0 deg steer angle

The conflict in the VTD controllers could be solved if the vehicle was front wheel drive or a brake based system was used. In a front wheel drive vehicle even if the front tyre did saturate due to too much demand from the VTD stability control, the result would be a decrease in the amount of lateral force available form the front axle. This would still promote understeer and stability. In a brake based system, the problem of saturating the tyre is not as great since the stability control would aim to brake the outside tyre which has more vertical force.

The phase plane and normalised root mean square tyre force are shown in Figure 6.18. The passive vehicle and VTD controllers diverge quickly from the stable region in the phase plane while the RMD PID control shows the oscillatory behaviour. Once again, the reason for this is that the control gains were tuned and optimised with a

different manoeuvre. The result is that the control behaviour does not adapt very well to different manoeuvres. Figure 6.18.b shows that the PID controllers reduce the normalised root mean square force more than the phase plane controls before they become unstable. This is because they aim to lower the sideslip angle more than the phase plane controllers. The RMD phase plane control shows the most stable response, which corresponds to the phase plane results.

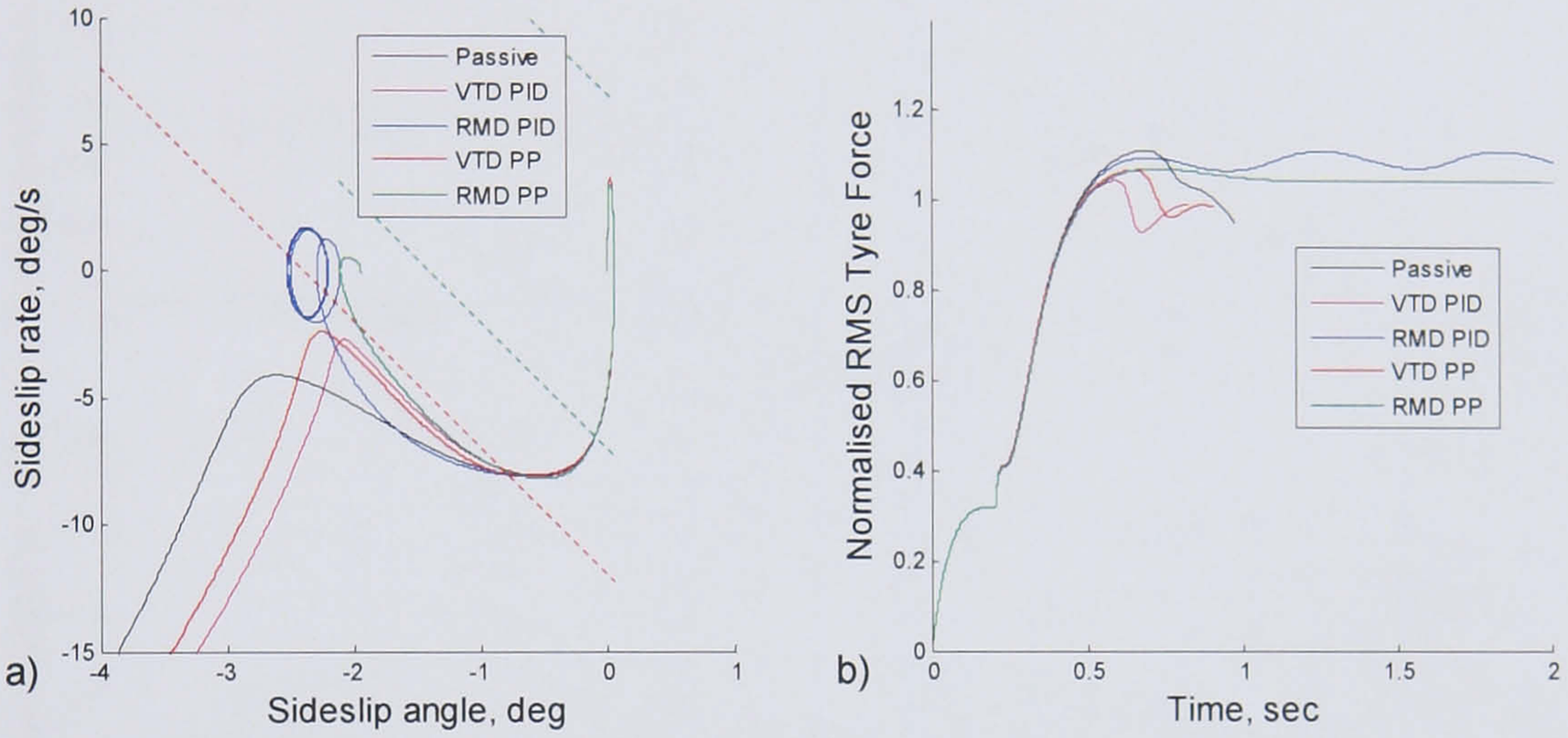

Figure 6.18 Step steer phase plane response and normalised RMS tyre force of the stability controls, 40 m/s initial velocity, 1.0 deg steer angle

A low speed test manoeuvre is presented in Figure 6.19 while the time response characteristics are shown in Table 6.5. The manoeuvre is another constant velocity step steer run at 20 m/s with a steer angle of 4.0 degrees. In this manoeuvre, the VTD controllers manage to stabilise the vehicle without saturating the tyres.

	Passive	VTD PID	RMD PID	VTD PP	RMD PP
% Steady state error	217	79.8	51.8	218	185
% Overshoot	158	44.8	73.7	26.2	28.4
63% Rise time (s)	0.243	0.187	0.168	0.246	0.239
10-90% Rise time (s)	0.175	0.108	0.069	0.189	0.191
1% Settling time (s)	11.4	1.69	1.43	6.20	1.84

Table 6.5 Step steer sideslip results of the stability controls, 20 m/s initial velocity, 4.0 deg steer angle

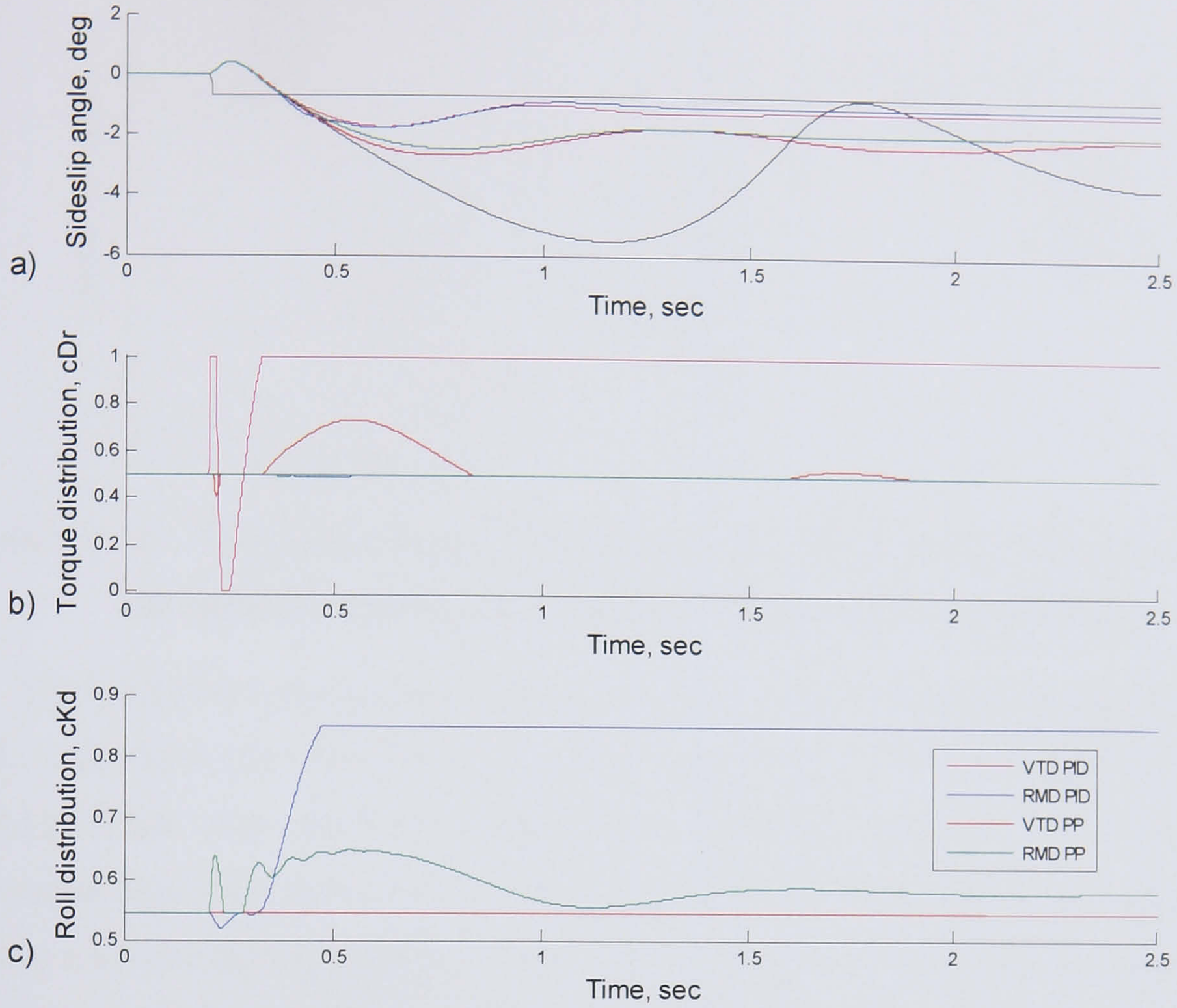

Figure 6.19 Step steer sideslip results of the stability controls, 20 m/s initial velocity, 4.0 deg steer angle

Again, the VTD and RMD PID controllers both push the vehicle towards the reference sideslip angle but do not reach it despite saturating the controllers. However, they do reduce the sideslip angle more than the phase plane controllers, with the RMD PID control getting closest to the reference signal. Saturating the controllers and reducing the sideslip angle more than the phase plane controllers uses more energy.

The phase plane controllers also manage to stabilise the vehicle and use less control power but do not reduce the sideslip angle as much. The VTD phase plane controller has a long settling time which can be seen by the oscillations in the time response and the phase plane shown in Figure 6.20.a. This shows that the phase plane controllers are also susceptible to degraded control performance as the test manoeuvres diverge further from the test used to tune the controller.

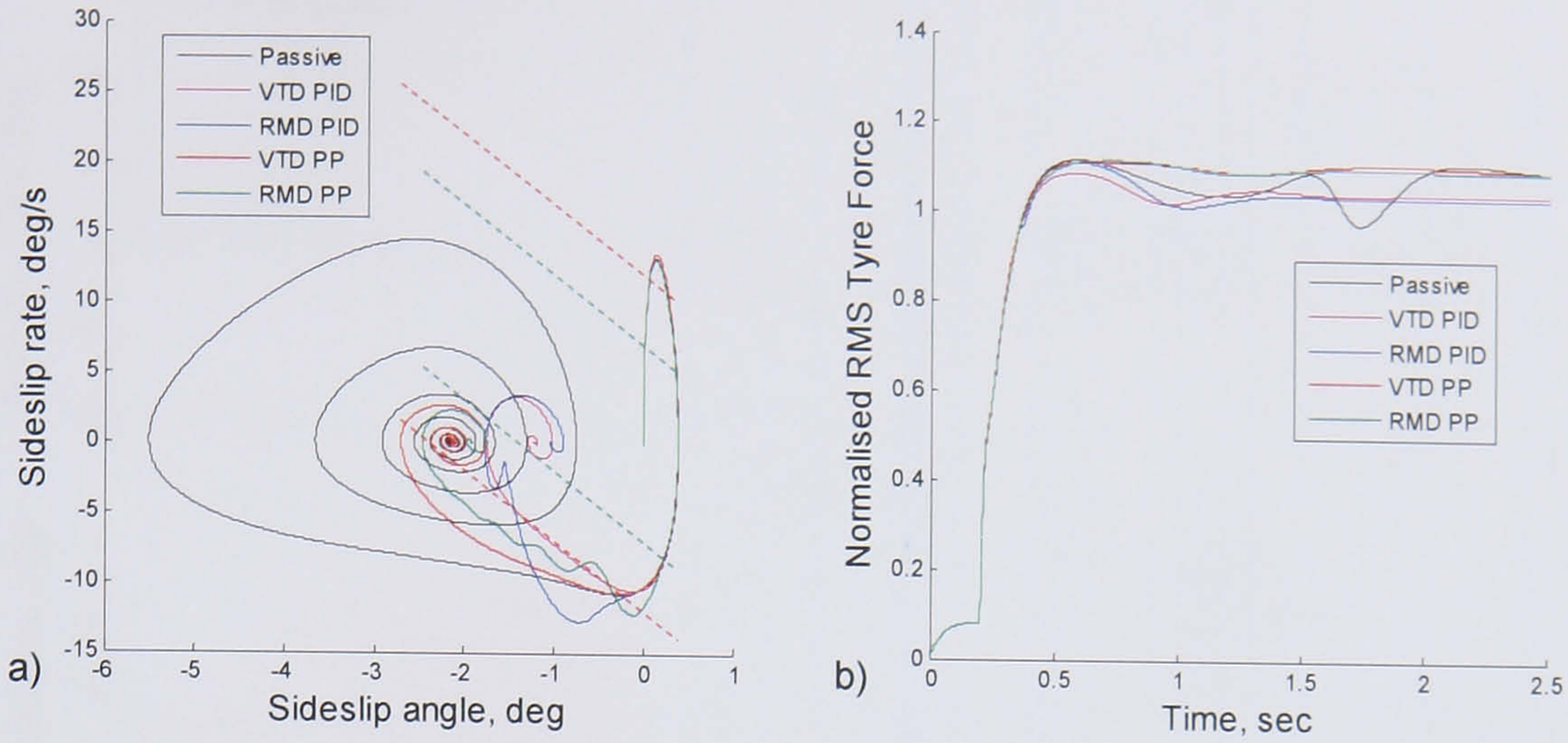

Figure 6.20 Step steer phase plane response and normalised RMS tyre force of the stability controls, 20 m/s initial velocity, 4.0 deg steer angle

The normalised root mean square tyre force, given in Figure 6.20.b, shows that the PID controllers use less force from the tyres. Since the PID controllers reduce the sideslip angle more than the phase plane controllers, the tyres are further from saturating and they have more potential to produce forces to direct the vehicle. This leaves a greater stability margin for the vehicle to respond to the driver's inputs.

The true test of stability controllers comes from trying to maintain vehicle stability in an increasingly demanding manoeuvre. This is given by the increasing velocity, increasing sinusoidal steer angle test shown in Figure 6.21. This is the same test that is presented in Section 6.1.1 with an initial velocity of 15 m/s accelerating at 0.5 m/s^2 and an initial steer angle of 1.0 degree increasing at 0.5 degrees/s. In this test the passive vehicle is the first to lose stability, 10.5 seconds into the manoeuvre. The first controller to lose stability is the RMD PID control after 16.4 seconds. The controller is trying to match the reference sideslip angle. Since the reference model is linear, the reference sideslip angle will gradually increase with the increasing velocity and steer angle. As the manoeuvre progresses this reference sideslip angle will actually increase beyond the stable bounds of the vehicle. At this point the reference tracking controller will actually be encouraging the instability. This can be seen by the RMD PID controller pushing the roll moment distribution to the rear of the vehicle trying to increase the sideslip angle just before losing stability.

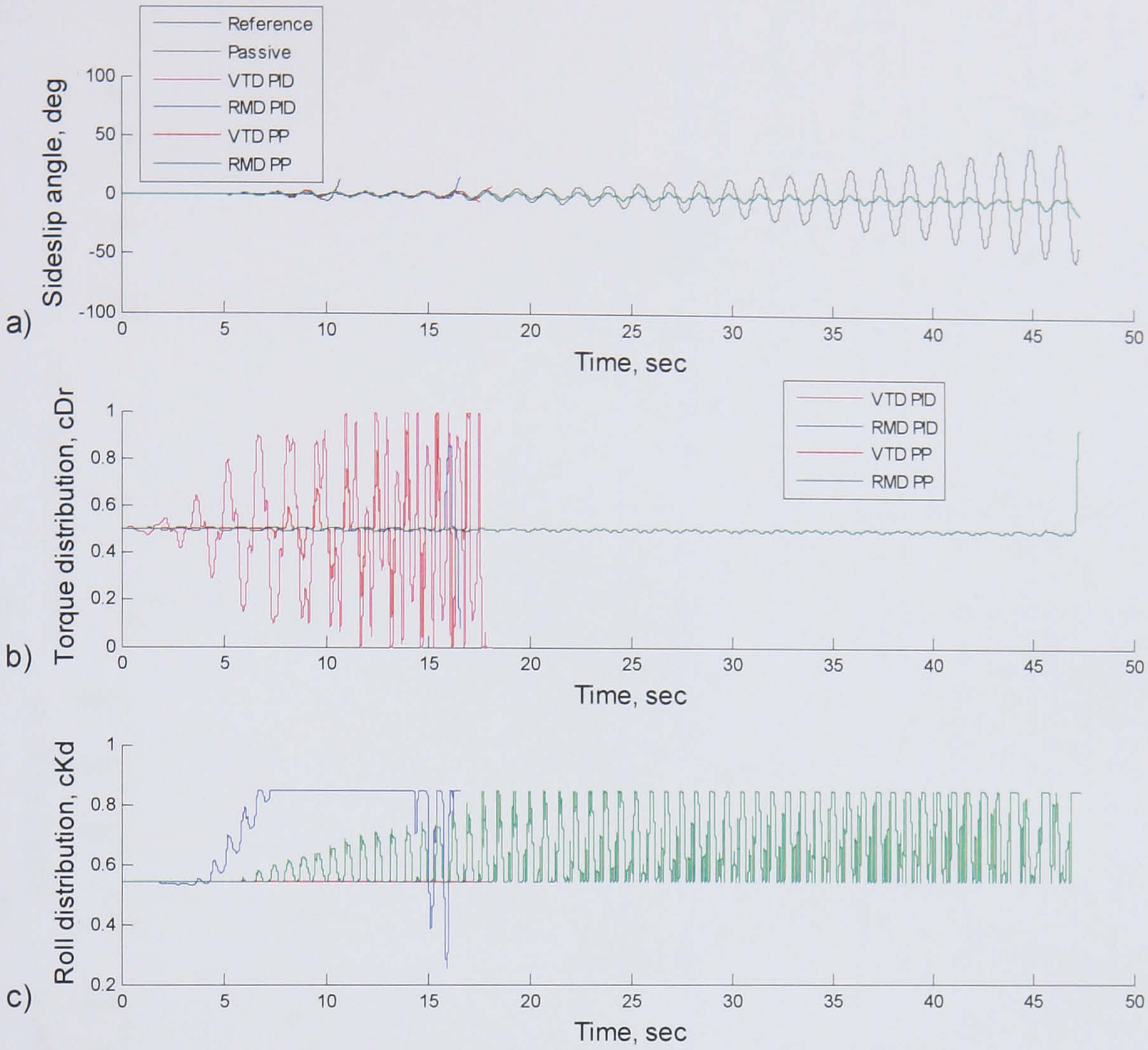

Figure 6.21 Sinusoidal time response of the stability controllers

The VTD phase plane controller is the next control to lose stability after 17.4 seconds. Again, the VTD controller cannot maintain the vehicle stability due to the lateral load transfer reducing the effectiveness of the controller. As the lateral load transfer increases in magnitude with each sinusoidal steer input, the inside tyre eventually saturates and the longitudinal force it can produce is reduced. After the inside tyre saturates the control can no longer produce any contra-cornering yaw moment and the vehicle loses stability. This is shown in Figure 6.22 just after 17 seconds when the longitudinal force of the rear right tyre suddenly decreases. The VTD PID control is the next to lose stability. It fails after 18.0 seconds for the same reasons as the VTD phase plane control. Once more it fails because the tyres saturate due to the lateral load transfer and the linear reference sideslip angle increases beyond the stable limits of the vehicle.

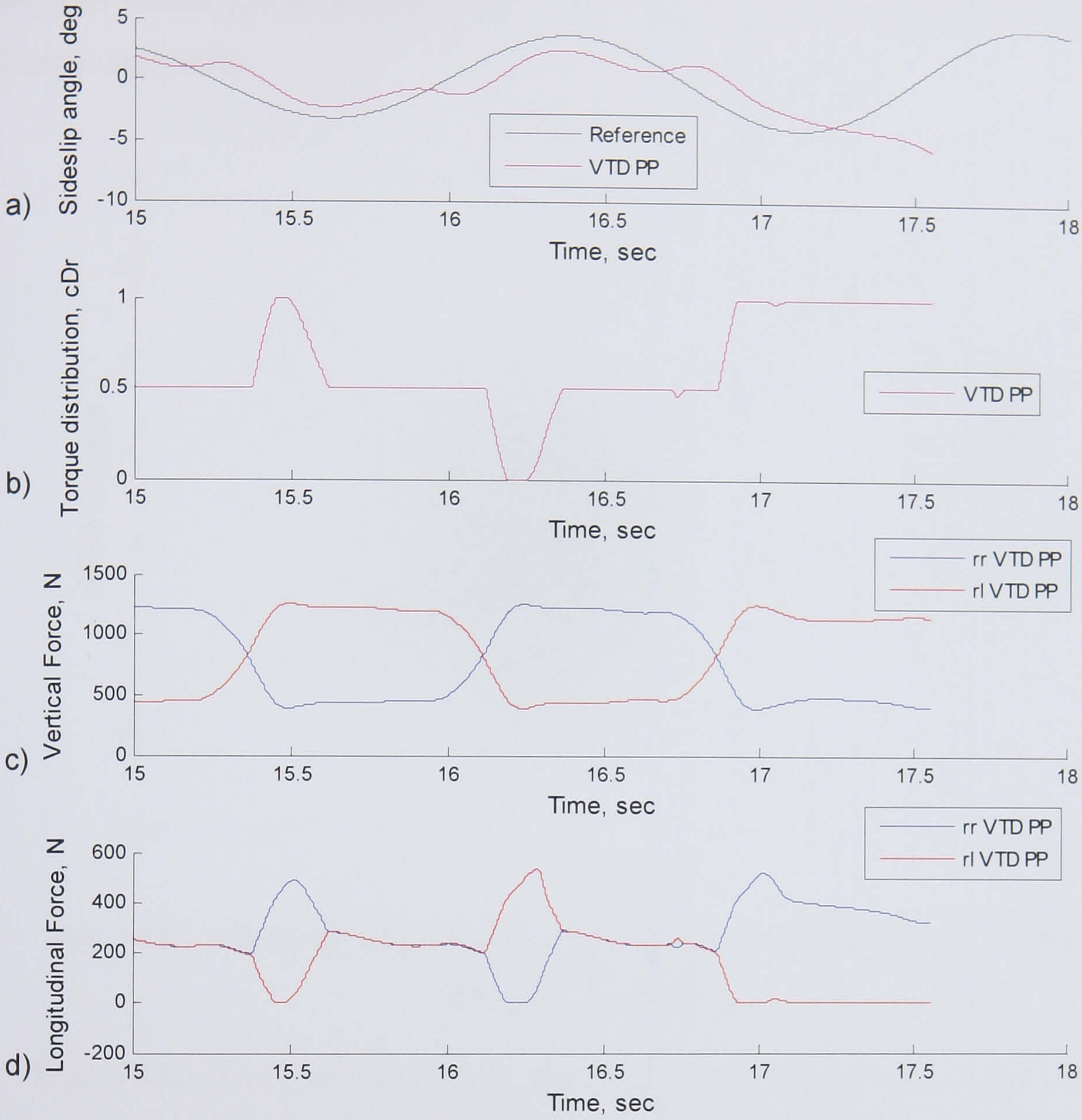

Figure 6.22 Loss of stability of the VTD phase plane control

The controller that lasts the longest and is the best at stabilising the vehicle is the RMD phase plane control. It outlasts all the other controllers by a significant margin, ending at 47.2 seconds. This is more than double the time of the other controllers. There are two reasons for the success of the RMD phase plane control. The first reason is the control objective it uses. It is only concerned in limiting the vehicle sideslip behaviour not following the increasing linear model. The second reason is the method of realising the control. Roll moment distribution actively controls the vertical forces on the tyres to achieve its objective. Although lateral load transfer is required to control the vertical tyre forces, this is not an issue since a stability controller is only required to work during severe manoeuvres when there is lateral load transfer. The result is that RMD becomes more effective as the manoeuvre becomes more extreme

and the lateral load transfer increases. This is the opposite of VTD, which loses its ability to induce yaw moments as the lateral load transfer increases and the tyres get closer to saturating.

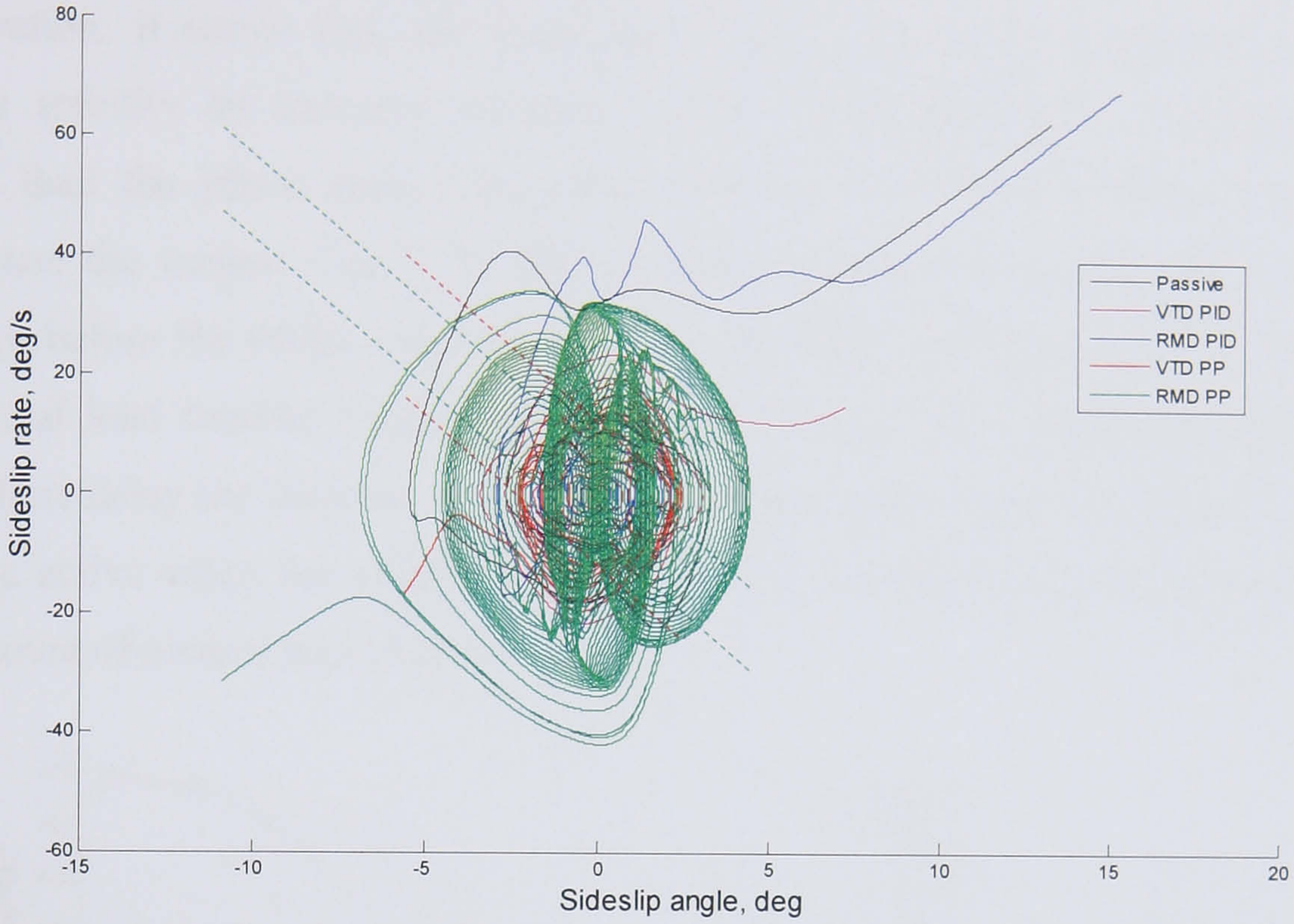

Figure 6.23 Sideslip angle phase plane from the sinusoidal steer test of the stability controllers

Figure 6.23 shows the phase plane plot of the increasing sinusoidal steer test. It is interesting to note that although the vehicle state during RMD phase plane control increases beyond the control boundary and even to some large sideslip angles, the vehicle stability is still maintained. The control boundary was specifically chosen to allow a progressive control action. This allows the controller to start introducing a stabilising action smoothly before the vehicle state becomes too unstable.

The controller response over a range of lateral accelerations is shown in Figure 6.24. The VTD controllers try to linearise the sideslip angle gain by tracking a linear reference model. They are effective and manage to create a more linear system response. The phase plane controllers do not linearise the sideslip angle gain at all. This is expected since the control strategy is not to linearise the vehicle response, just to stabilise the vehicle. A linear vehicle response is desirable, but only if the response that is linearised corresponds to a feeling the driver can sense. A driver can certainly sense the sideslip angle when the vehicle loses control but it is not a motion that is directly controlled. During normal vehicle operation the driver expects zero sideslip

but actively controls the yaw behaviour with the steering wheel. Therefore, it is desirable to have a linear response from the steering wheel to the yaw rate but creating a linear response to the sideslip angle is not necessary.

The understeer gradient is the amount of steer angle required to give 1g of lateral acceleration. It shows that the controllers reduce the sideslip angle and maintain vehicle stability by inducing understeer. PID controllers induce understeer much earlier than the phase plane controllers with the VTD PID controller promoting understeer the earliest. The VTD PID controller manages to increase the understeer gradient before the RMD controller because the RMD controller needs to wait until the lateral load transfer builds up to become effective. The reason the phase plane controllers delay the increase in understeer is due to their control strategy. They only become active when the vehicle state crosses the control boundary. This minimises the amount of control intervention.

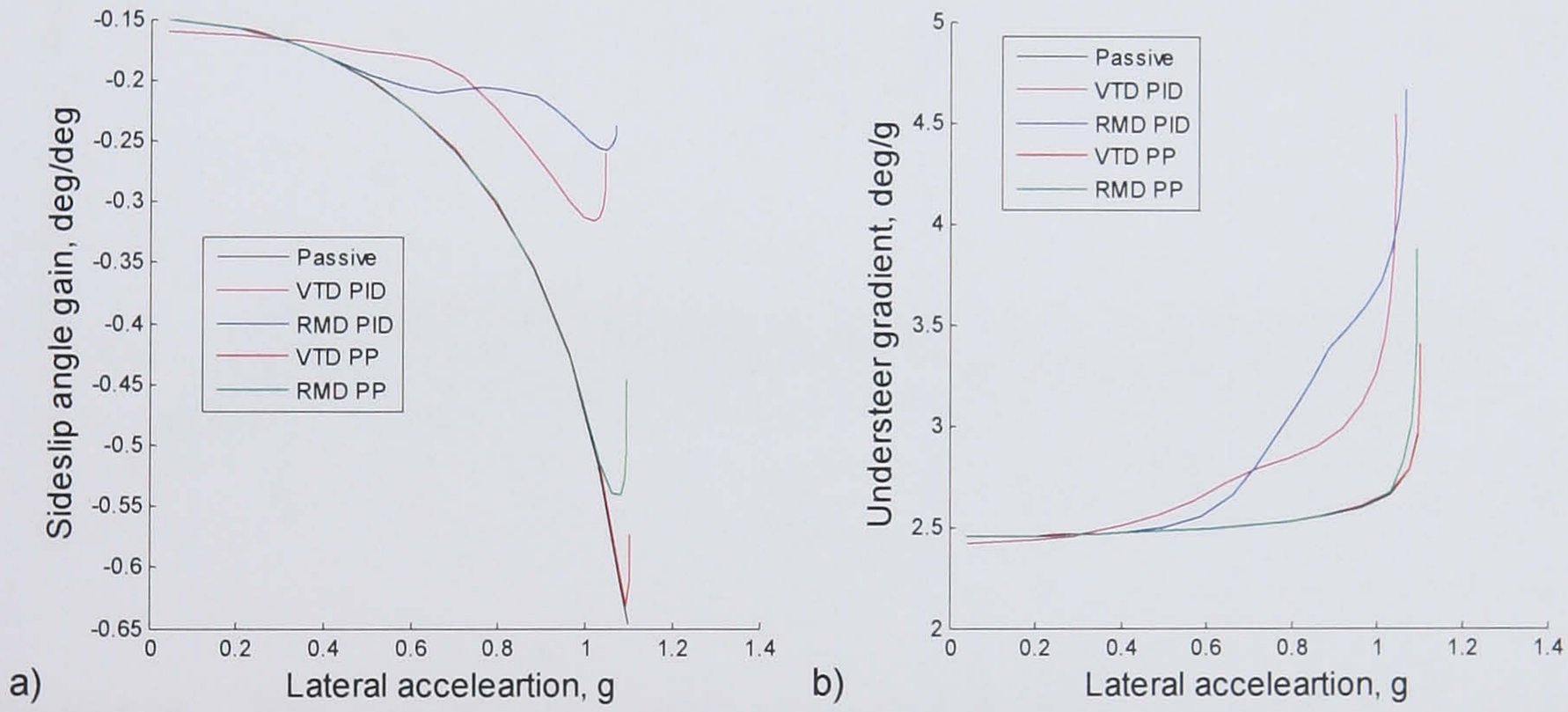

Figure 6.24 Sideslip angle gain and understeer gradient of the stability controllers

The final test of the stability controllers is to evaluate them on a low friction surface. Once again a coefficient of friction of $\mu = 0.7$ is used to simulate a wet road surface. The test manoeuvre is the same increasing velocity, increasing sinusoidal steer test shown previously but with the modified road surface friction coefficient. The sideslip results are shown in Figure 6.25. All the simulations run longer on the low friction surface. The reason for this is that the frequency of the steering input is relatively fast and the tyre forces are not able to build up as much on the low friction surface. The result is that the vehicle state does not build up instability as quickly as it did on the high friction road surface.

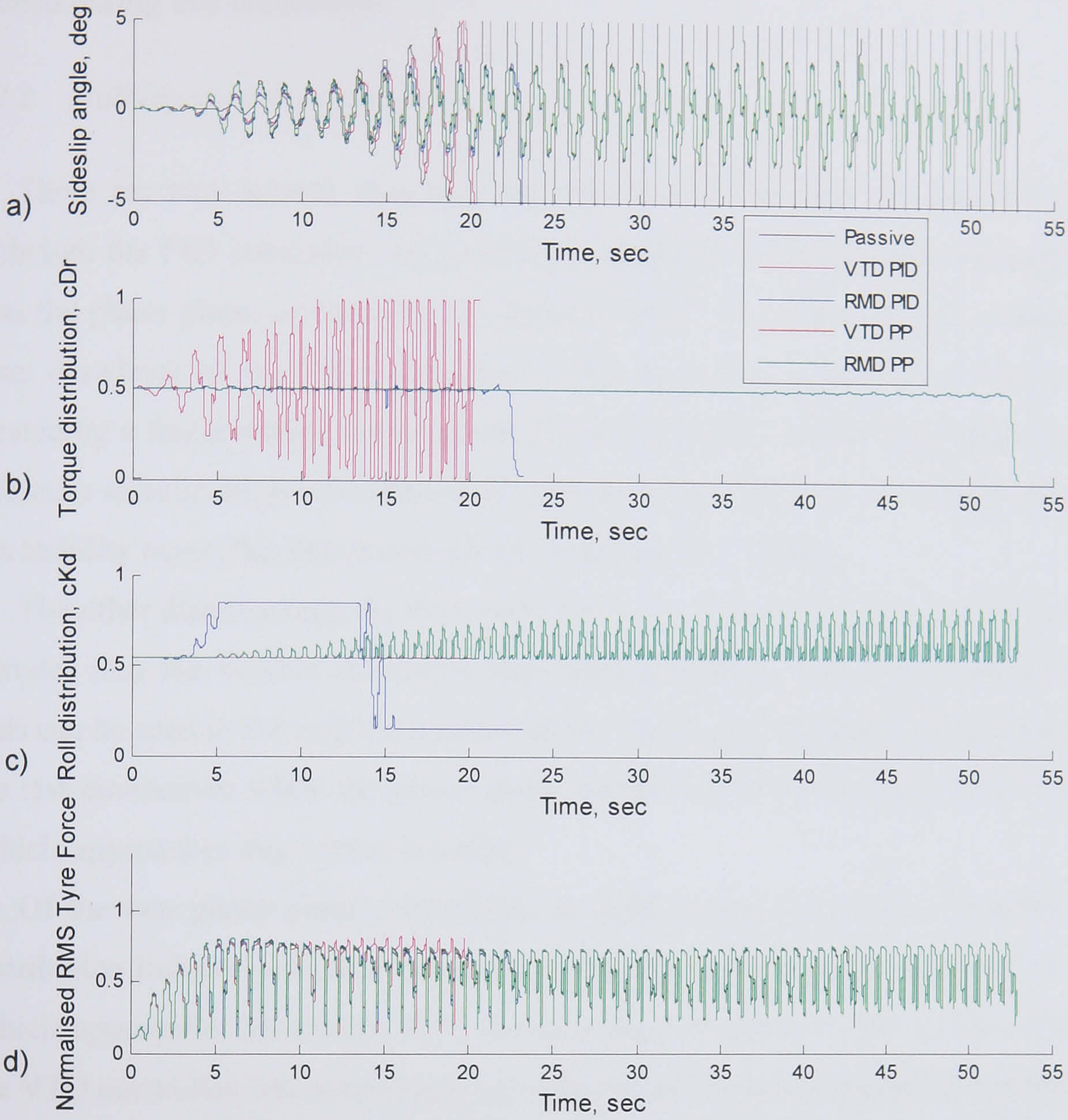

Figure 6.25 Sinusoidal time response of the stability controllers on a wet road

Once again the RMD phase plane control manages to maintain vehicle stability the longest, running for 52.9 seconds. It is interesting to note that the PID controllers actually destabilise the vehicle before the passive vehicle loses stability. The passive vehicle loses stability at 43.2 seconds while the VTD PID lasts 20.5 seconds and the RMD PID ends at 23.1 seconds. The reason the PID controllers promote this instability is because they are trying to track the same increasing sideslip angle goal. The reference model is not modified with regard to the lower friction and creates the same sideslip angle calculated with a friction coefficient of $\mu = 1.0$. The controllers keep pushing the vehicle towards the linear sideslip angle goal that becomes out of reach earlier due to the reduced friction. The VTD phase plane controller runs into a

simulation problem and stops 2.1 seconds into the manoeuvre so the data is extremely limited during this manoeuvre.

6.2.2. Stability control conclusions

There are two control strategies and two control methods for stability control. Although the PID controllers do generally manage to reduce the sideslip angle more than the phase plane controllers, this does not result in a better control strategy. The main drawback of the PID controllers is that they track a reference sideslip angle created by a linear model. As shown in the increasing sinusoidal steer angle test, this reference sideslip angle can increase beyond the stable limits of the vehicle. The result is a stability controller that is actively destabilising the vehicle.

The other disadvantage the PID control has over the phase plane strategy is that it intrudes into the vehicle dynamics more and potentially uses more control power. This can be seen in the step steer manoeuvres. The PID controllers operate throughout the test manoeuvre while the phase plane controllers do not become active until the vehicle approaches the control boundary.

Of the two phase plane controllers, the RMD control is better. Variable torque distribution induces yaw moments through the longitudinal forces in the tyres. As the vehicle approaches its stability limit the tyres begin to saturate. The result is that when the VTD controller wants to create a contra-cornering yaw moment, it distributes the torque to the inside tyre, which is unloaded, and saturates it destabilising the vehicle. On the other hand, RMD control manipulates the vertical tyre forces. This becomes more effective as the manoeuvres become more extreme. The result is a control strategy that can maintain vehicle stability during very severe manoeuvres, as shown in the increasing sinusoidal steer test.

Therefore the best stability control is the roll moment distribution phase plane controller while the best VTD control is also the phase plane controller.

6.3. Combined Control

Roll moment distribution and variable torque distribution will be combined to observe the interactions between them. The combined controllers will consist of one driveability control and one stability control implemented on the same vehicle at the same time without any modification. This means that the combined controllers cannot

contain two RMD controllers or two VTD controllers since this would require an integration strategy to determine which control output should be used. The most promising RMD and VTD, driveability and stability controllers, as determined from Section 6.1.2 and Section 6.2.2, will be combined. The positive and negative interactions will be observed and used to design the multi-objective integration strategy.

6.3.1. Combined Control Results

The best combination of controllers would be VTD SM driveability control and RMD phase plane stability control. This will be referred to as 'Tdrive Rstab'. The other option is to have RMD PID driveability control with VTD phase plane stability control. This will be referred to as 'Rdrive Tstab' and is expected not to perform as well due to the limitations of the VTD stability control. Figure 6.26 shows the yaw rate and sideslip angle results for the combined controllers from the same step steer test used to tune the driveability controllers. This test is run with an initial velocity of 22 m/s and accelerating at 1.5 m/s^2 with a steer angle of 1.5 degrees. The results show that there are some conflicts between the controllers. As expected, the first of the two combined controllers, with VTD yaw rate tracking and RMD stability, provides slightly better results by maintaining stability longer even though the control action is very oscillatory.

The second combined controller, 'Rdrive Tstab', destabilises the vehicle very early in the manoeuvre and only tracks the yaw rate for 0.1 seconds. The RMD yaw rate tracking controller is distributing the roll moment to the rear axle, creating more lateral load transfer to increase the yaw rate. At the same time the VTD stability control is driving the inside rear wheel, which is being unloaded, to try and induce a contra-cornering yaw moment. As expected the vehicle loses stability and as the yaw rate increases beyond the reference yaw rate, the RMD controller pushes the yaw moment to the front axle in an attempt to reduce the yaw rate but it is too late to stabilise the vehicle.

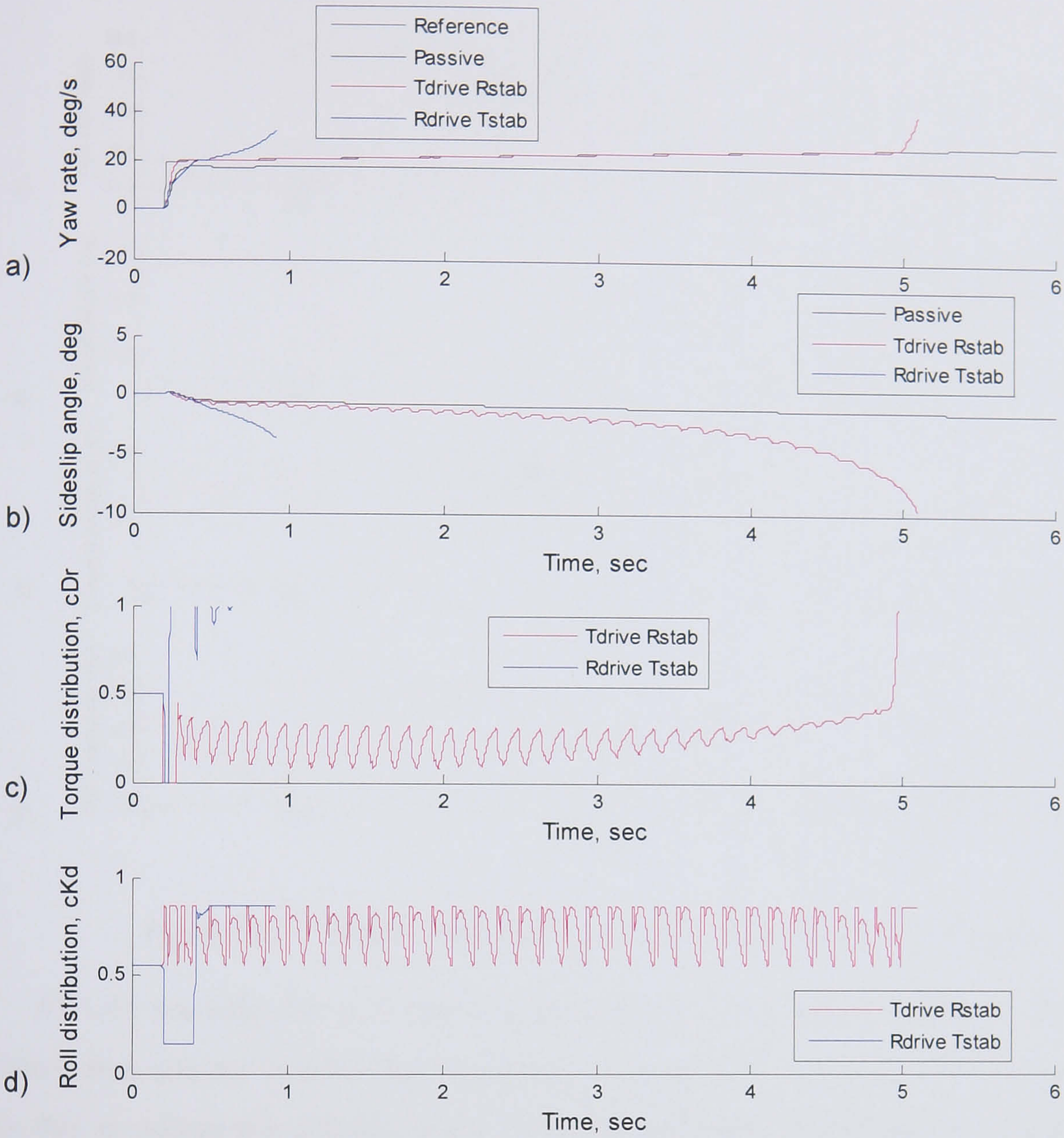

Figure 6.26 Step steer results of the combined controls, 22 m/s initial velocity, 1.5 m/s^2 acceleration, 1.5 deg steer angle

The 'Tdrive Rstab' controller does manage to track the yaw rate and keep the vehicle stable longer, although with oscillations in the control signals. The driveability control on its own lasts just over 4.6 seconds compared to 5.1 seconds for the combined control. This can be considered an improvement. However, the control action is very oscillatory which is undesirable. The reason for the oscillations can be seen in Figure 6.27.

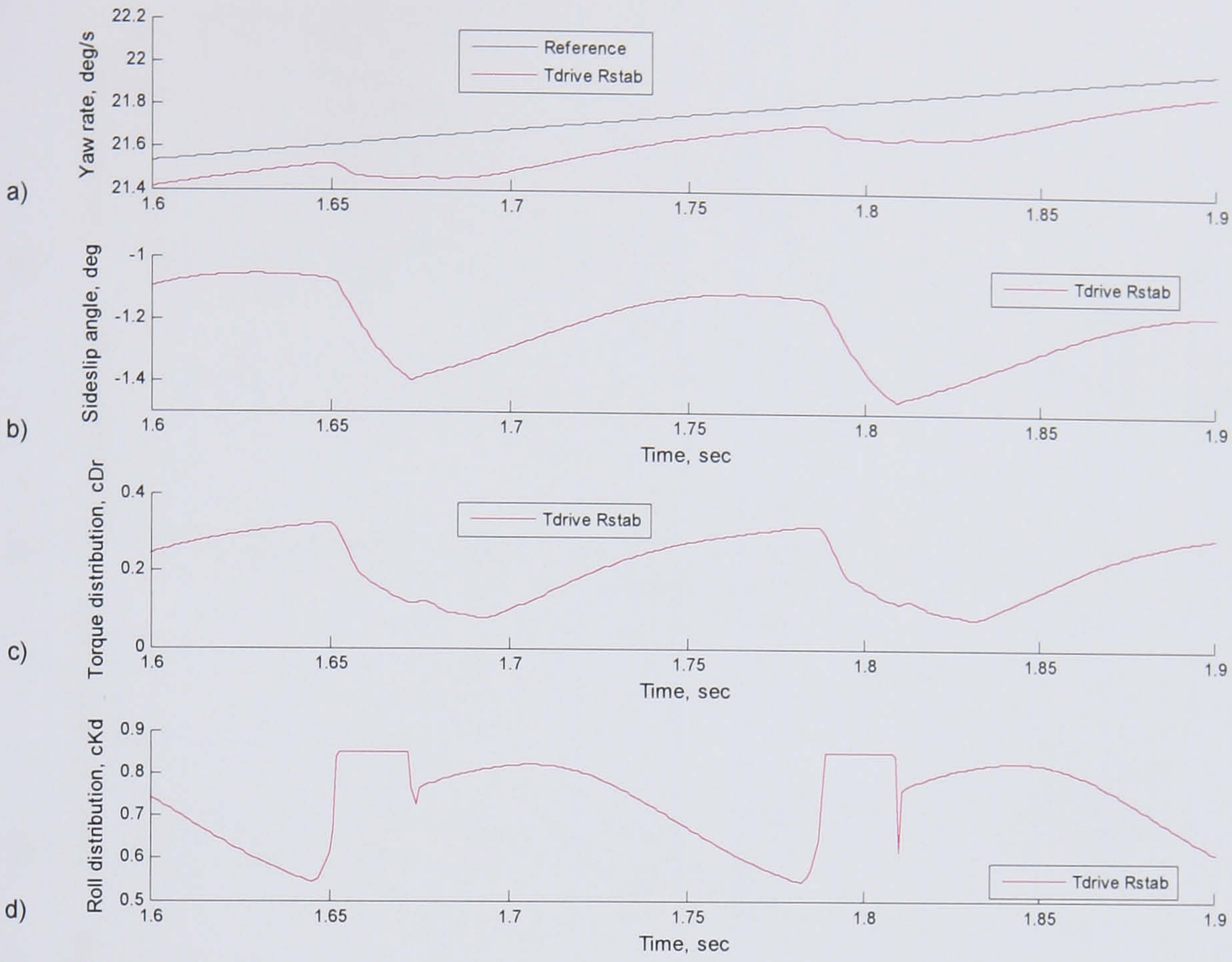

Figure 6.27 Detail view of Figure 6.26 from 1.6 to 1.9 seconds

At 1.65 seconds, the yaw rate is approaching the reference signal and the torque distribution control is reducing, becoming more equal between the left and right tyres. As this is occurs the sideslip angle increases and the roll moment is pushed to the front of the vehicle. By 1.655 seconds, the yaw rate has diverged from the reference yaw rate. In reaction to this the torque distribution control sends torque to the left tyre to increase the yaw rate. After 1.7 seconds, the sideslip angle decreases and the roll moment moves back toward the centre of the vehicle. The decrease in sideslip angle also corresponds to an increase in yaw rate and the system builds up to start the cycle again. The phase plane controller is tuned with the response of the vehicle to its own control actions. However, in the combined control the effect it has is increased by the VTD control. The result is this oscillatory behaviour, which could be improved by retuning the controller.

A high speed step steer test is presented in Figure 6.28. This test is run at a constant velocity of 40 m/s and a steer angle of 0.5 degrees.

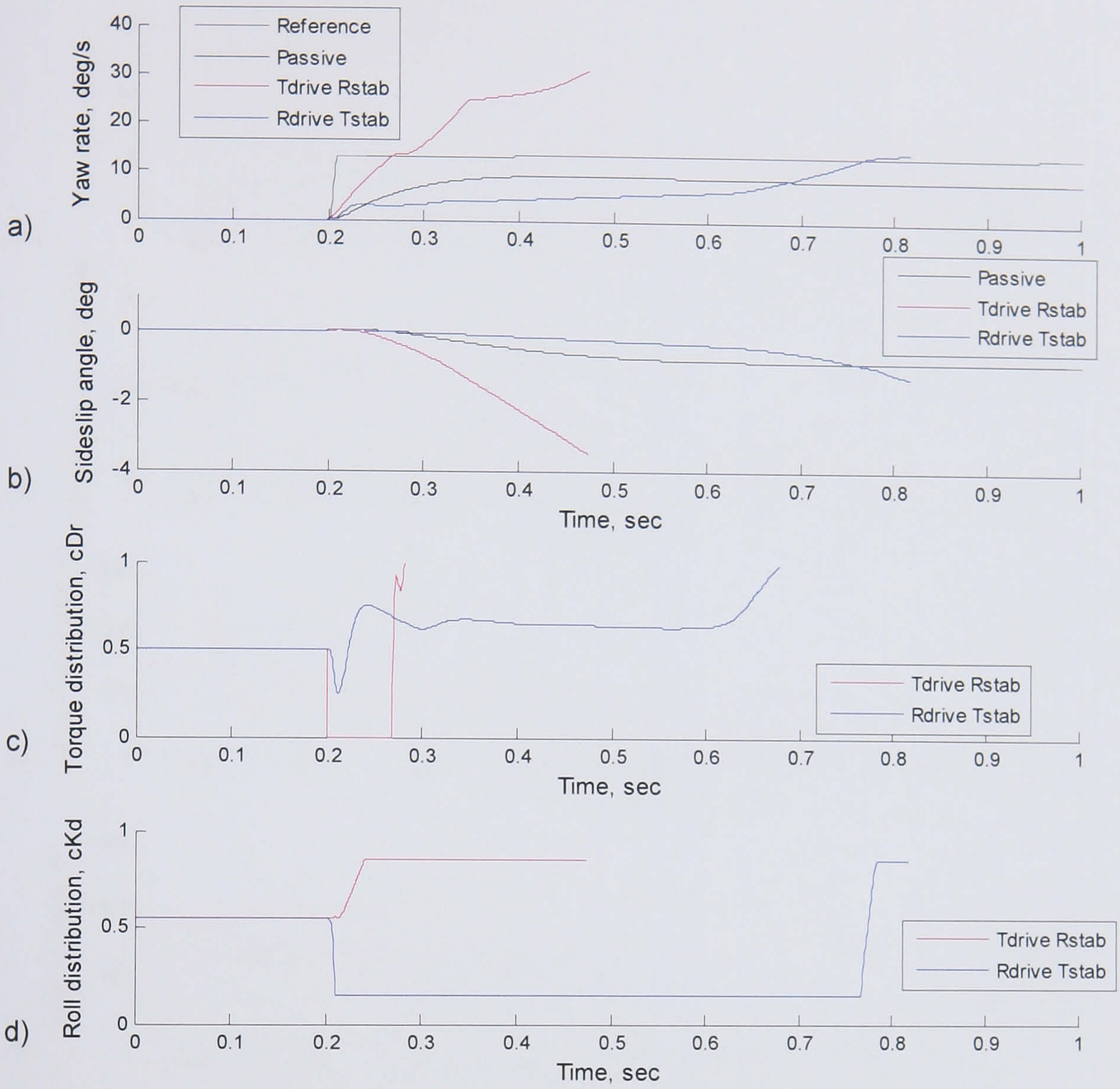

Figure 6.28 Step steer results of the combined controls, 40 m/s initial velocity, 0.5 deg steer angle

Once again, both combined controllers lose stability before the passive vehicle. During this test the preferred 'Tdrive Rstab' controller sends the vehicle unstable first. However, it does bring the vehicle yaw rate to the reference signal but can only manage to track it for 0.02 seconds before losing stability. The driveability control is too forceful in tracking the yaw rate and destabilises the vehicle. As the yaw rate diverges from the reference signal and the sideslip angle increases, the stability control is not powerful enough to bring the vehicle back to a stable state.

The 'Rdrive Tstab' control manages to maintain vehicle stability longer than the preferred 'Tdrive Rstab' control. However, it tracks the reference yaw rate worse than the passive vehicle. The yaw rate along with the control action and tyre forces are shown in Figure 6.29.

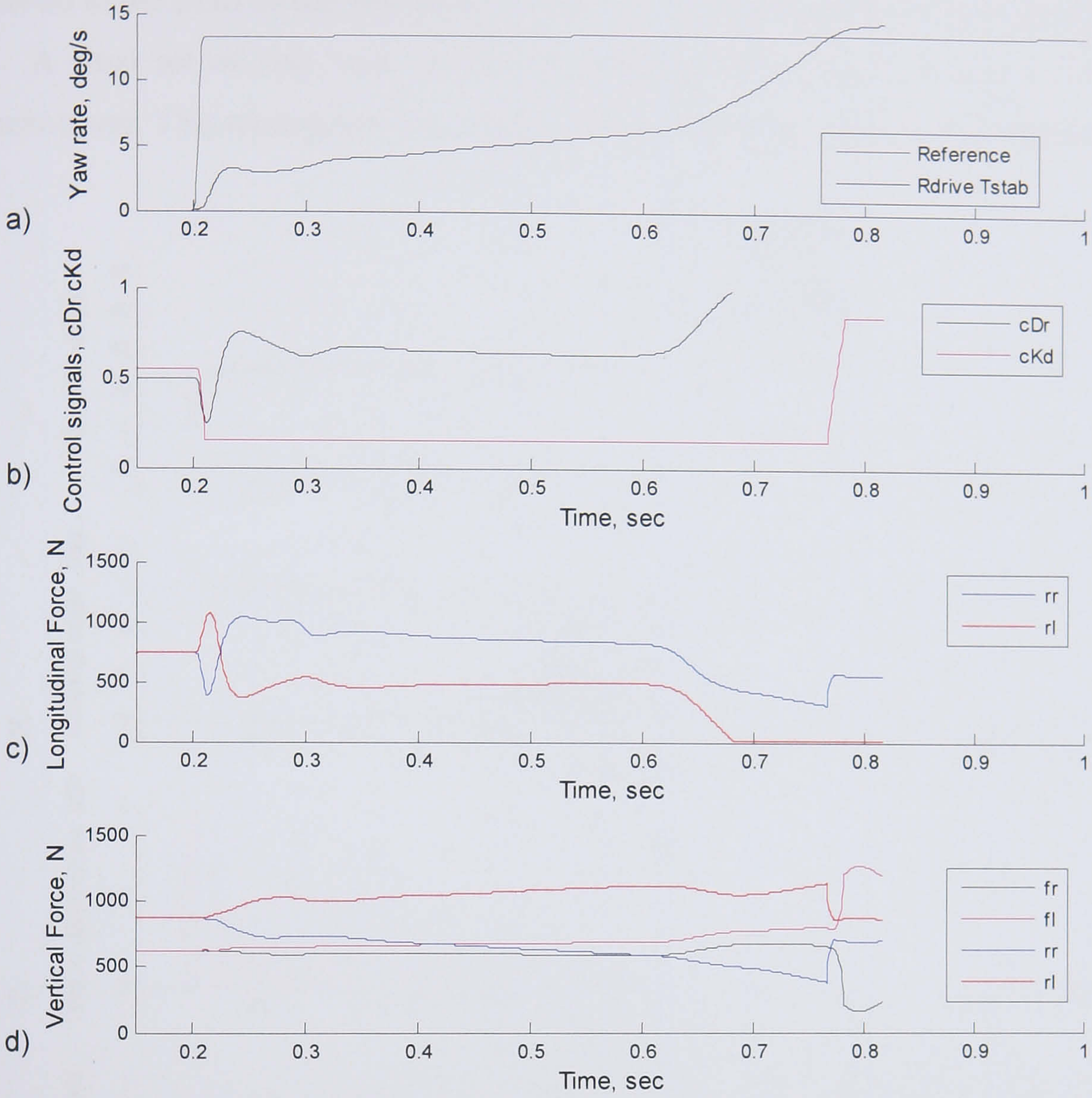

Figure 6.29 Step steer yaw rate results and control action of the 'Rdrive Tstab' control, 40 m/s initial velocity, 0.5 deg steer angle

The roll moment distribution is moved to the rear of the vehicle to promote oversteer and increase the yaw rate. This increases the lateral load transfer across the rear axle and increases the load on the outside rear tyre. At the same time the torque is distributed to the inside tyre to promote understeer and reduce the sideslip angle. Immediately these two control actions are counter productive however there is enough load on the inside rear tyre for the VTD to induce a stabilising yaw moment. As the manoeuvre progresses the RMD is holding the roll moment at the rear of the vehicle to increase the yaw rate. Just after 0.6 seconds, as the yaw rate keeps increasing and the sideslip angle also increases, the VTD starts distributing more torque to the inside tyre. The effect is counter productive. Sending more torque to the inside tyre actually reduces the longitudinal force it creates because the tyre saturates. This destabilises

the vehicle and as the yaw rate shoots past the reference signal, the roll moment is moved to the front of the vehicle but it is too late to maintain the vehicle stability.

A final set of step steer results are presented in Figure 6.30 for a low speed manoeuvre. This manoeuvre was run at 15 m/s with a steer angle of 3.5 degrees.

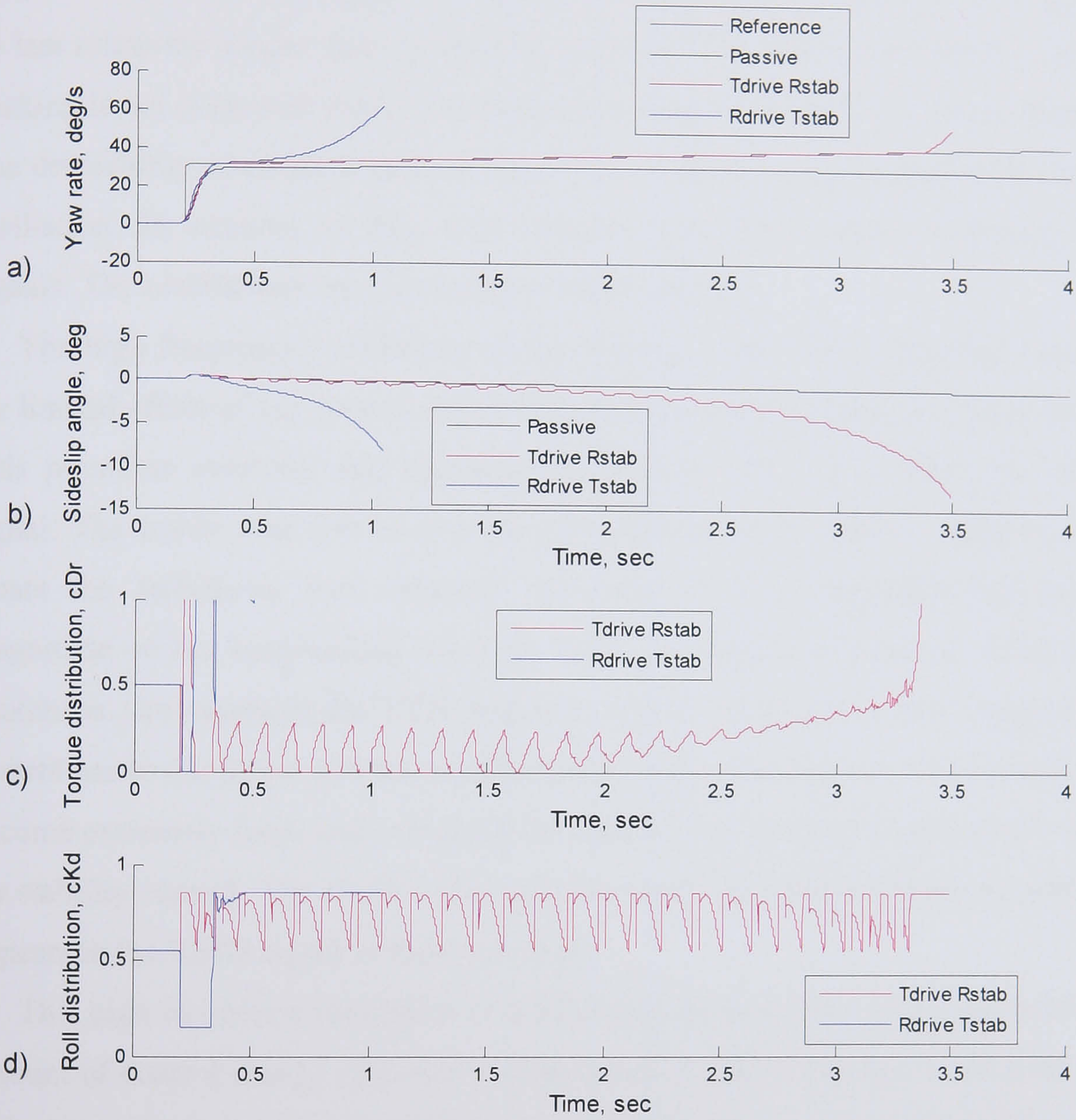

Figure 6.30 Step steer results of the combined controls, 15 m/s initial velocity, 3.5 deg steer angle

The results from this low speed test are very similar to those presented in Figure 6.26. The passive vehicle once again remains stable the longest while the 'Rdrive Tstab' controller has the familiar negative control interactions. The unloading of the inside tyre by the driveability control causes the stability control to saturate the tyre when it tries to induce a stabilising moment by transferring more torque to the unloaded tyre. The effort is counter productive and destabilises the vehicle even more. The 'Tdrive Rstab' controller again shows some potential by tracking the yaw rate

longer and more closely than either the passive vehicle or the 'Rdrive Tstab' controller. Unfortunately, it loses stability before the passive vehicle and once again shows the oscillatory behaviour seen in the medium speed test.

The combined controllers show better results in the increasing velocity, increasing sinusoidal steer test. Although they both lose stability before the passive vehicle, they do last relatively longer than in the step steer test. However, the reference yaw rate tracking is not improved much over the passive vehicle. Figure 6.31 shows the results. The driveability controllers in both cases show a good control signal with very little oscillation. In contrast to this, both stability controllers show oscillating control signals. The oscillations are seen better in Figure 6.32.

The high frequency oscillations in the 'Rdrive Tstab' VTD controller come from the limited effect of the control action. The RMD control unloads the inside rear tyre. This promotes oversteer and increases the vehicle yaw rate to track the reference signal. The inside rear tyre is also the tyre that the VTD control wants to drive to create the stabilising yaw moment. However, if it is unloaded the maximum magnitude of the longitudinal force the VTD can induce is reduced. Therefore the maximum yaw moment the VTD stability control can create is also reduced so the control has to use larger actions to influence the vehicle dynamics. The control actions become extremely large and overshoot the desired yaw rate and creates more work for the stability control. The result is the high frequency oscillatory behaviour, which also appears in the RMD signal in Figure 6.32.d.

This high frequency oscillation is undesirable. In an actual vehicle application, the amount of control energy required to realise such a high frequency oscillation is very high. Not only is the power consumption high but the actuators required to produce the oscillatory signal become large, heavy and usually very expensive. If these high power actuators were not available and this high frequency oscillating control was still implemented on a vehicle the resulting dynamics would not necessarily match the simulation. The simulation model would have to be modified to account for the actuator dynamics to get an accurate representation of the resulting vehicle dynamics. Fortunately, this combined control is not being designed for actual implementation on a vehicle. It is simply being used to expose the positive and negative interactions of the independent controllers.

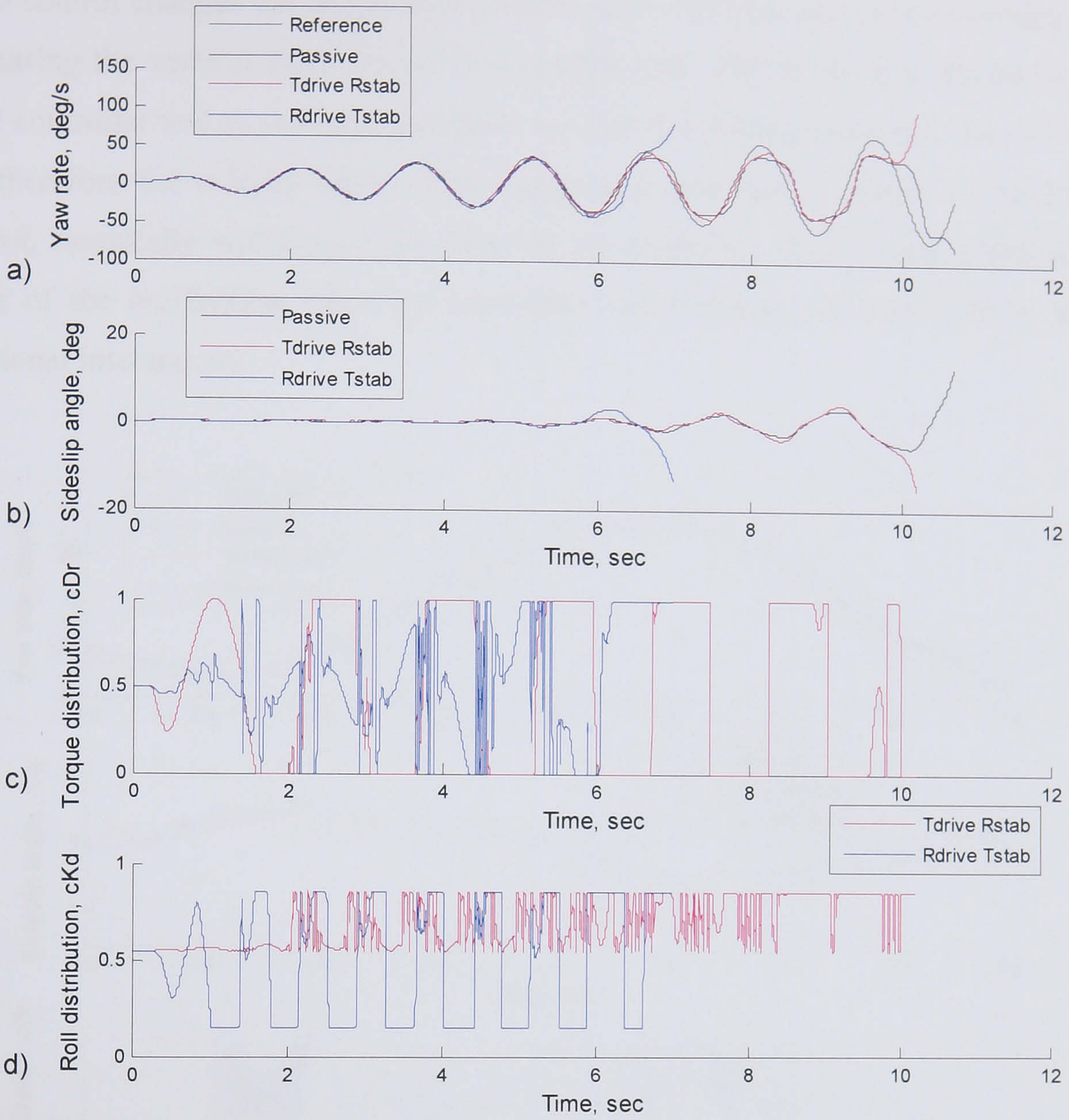

Figure 6.31 Increasing sinusoidal steer results of the combined controls

The oscillations in the 'Tdrive Rstab' appear for similar reasons that they did in the step steer tests. The VTD is driving the outside rear wheel to induce a pro-cornering yaw moment. As the yaw rate approaches the reference signal, the sideslip angle increases and the RMD moves the roll moment to the front axle to promote understeer. This also reduces the load on the outside rear tyre that the VTD is driving and reduces its effect as well. As the sideslip angle decreases, the RMD moves the roll moment back towards the rear of the vehicle, which decreases the understeer and also loads the outside rear tyre making the VTD more effective.

The RMD stability control was tuned to handle the effects it has on the vehicle alone, however when it is implemented in the combined control the effect it has on the vehicle dynamics is increased due to the interactions it has with the VTD. As the

RMD control changes the lateral load transfer across the rear axle it is increasing and decreasing the vertical force on the rear outside tyre. This is the tyre driven by the VTD controller and as the load fluctuates so does the driving force and the yaw rate and therefore the sideslip angle. This compounds any control action of the RMD control, essentially multiplying the effect of the controller. This double effect is the cause of the oscillations since the controller was tuned on its own without these additional interactions.

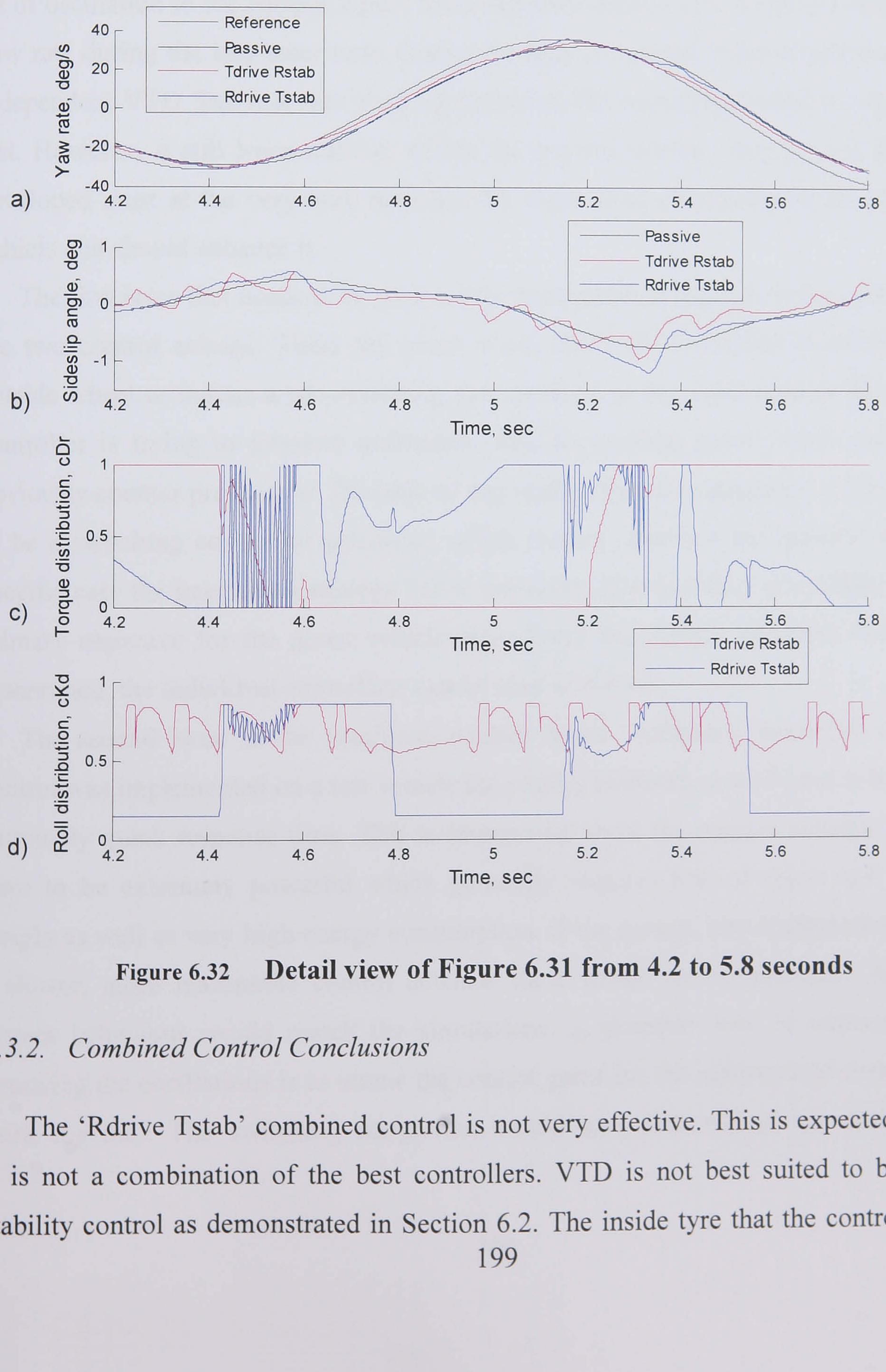

Figure 6.32 Detail view of Figure 6.31 from 4.2 to 5.8 seconds

6.3.2. Combined Control Conclusions

The 'Rdrive Tstab' combined control is not very effective. This is expected since it is not a combination of the best controllers. VTD is not best suited to being a stability control as demonstrated in Section 6.2. The inside tyre that the controller is

trying to drive to create the stabilising yaw moment is being unloaded. This problem is compounded when it is combined with an RMD yaw rate tracking control. The RMD control is causing even more lateral load transfer across the rear axle, which causes the rear inside tyre to saturate even earlier. Even with an integration strategy, this conflict of control actions is too great. Therefore an integration strategy will not be developed for RMD driveability controllers integrated with a VTD stability control.

The 'Tdrive Rstab' combined controller shows more potential. Although there is a lot of oscillation in the control signal, the combined control does match the reference yaw rate during the step steer tests. It also manages to remain stable longer than the independent VTD SM yaw rate tracking control in the increasing velocity step steer test. However, it still loses stability before the passive vehicle. Any control system developed must at the very least maintain the same level of stability as the passive vehicle and should enhance it.

The first issue that needs to be resolved by an integration strategy is the conflict in the two control actions. There are cases where the VTD controller is driving the outside wheel to induce a pro-cornering yaw moment at the same time as the RMD controller is trying to promote understeer. Besides wasting power, this conflict is obviously counter productive. The base of any multi-objective integration strategy has to be a switching control to determine which control objective has priority. In this specific case the integration strategy has to determine if driveability or stability is the primary objective for the given vehicle state. Once the control objective has been determined, the individual controllers can be used to meet it.

The second issue in the combined control is the oscillatory behaviour. If this control was implemented on a test vehicle the control hardware would have to have an extremely quick response time. This is impractical since the control actuator would have to be extremely powerful which generally requires lots of space and added weight as well as very high energy consumption. If the system was implemented with a slower, more reasonable control actuator there would be no guarantee that the system behaviour would match the simulations. A possible way of reducing and removing the oscillations is to retune the control gains for the independent controls to work together. The switching integration would also help reduce the oscillatory

behaviour because the controllers would work without interference and under the conditions that they were tuned.

7. Integrated Control

Chapter 7 presents the multi-objective integrated control strategy and results. First, an initial integrated control is presented in Section7.1. This integrated controller was presented in a paper at the SAE 2005 World Congress [Cooper, 2005]. Section 7.2 continues the development of the integration strategy, incorporating the new independent controllers and the lessons learned from Chapter 5 and Chapter 6. Then the results of the final integrated controller are presented in Section 7.3.

7.1. Initial Integration Strategy and Results

The goal of the multi-objective integrated strategy is to improve the vehicle driveability while maintaining its stability. The driveability is improved by linearising the vehicle yaw response to the drivers steering inputs. Specifically this is done by a linear reference model tracking yaw rate control, as presented in Section 6.1. The stability is maintained by limiting the sideslip behaviour, seen in Section 6.3. However, these two goals conflict with each other. Tracking the linear reference yaw rate increases the sideslip behaviour and promotes instability. Conversely, containing the sideslip behaviour limits the yaw rate response. Therefore, the main role of the multi-objective integration strategy is to determine which independent controller should have priority.

The integration strategy will take the form of a switch. This switch will let the yaw rate tracking driveability controller take precedence until vehicle instability is detected. At this point the integration strategy phases out the yaw rate tracking control and gives the stability control priority. This will prevent both controllers from trying to operate at the same time and creating conflicting control actions, as discussed in Section 6.3.2.

7.1.1. Initial Integrated Control Strategy

The following initial integration strategy was developed for a paper that was presented at the SAE 2005 World Congress [Cooper, 2005]. The control consists of a VTD IM yaw rate tracking control and a RMD PID sideslip reduction control. These

two independent controllers are integrated with a sideslip based adaptive PID switching control. The block diagram of the full integrated control is shown in Figure 7.1 while Figure 7.2 shows the diagram of the integrated controller block.

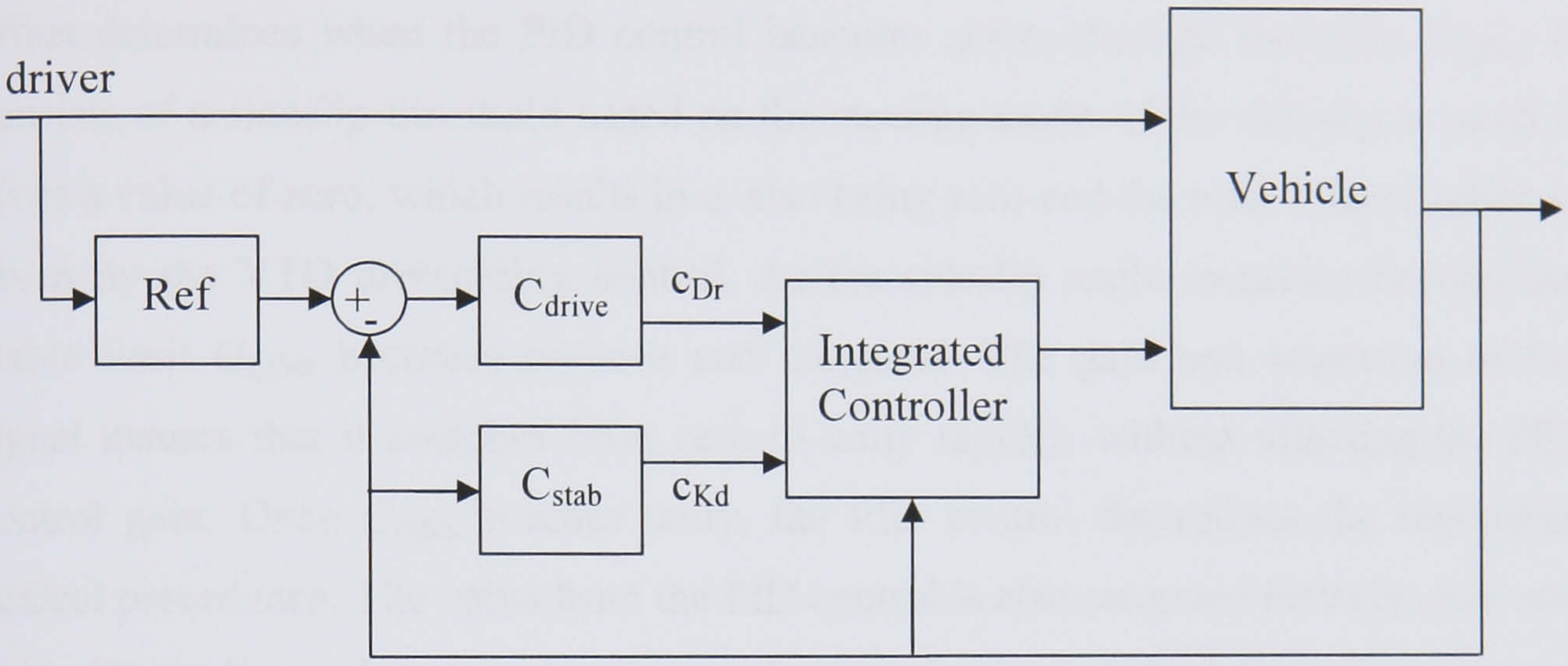

Figure 7.1 Integrated control full block diagram

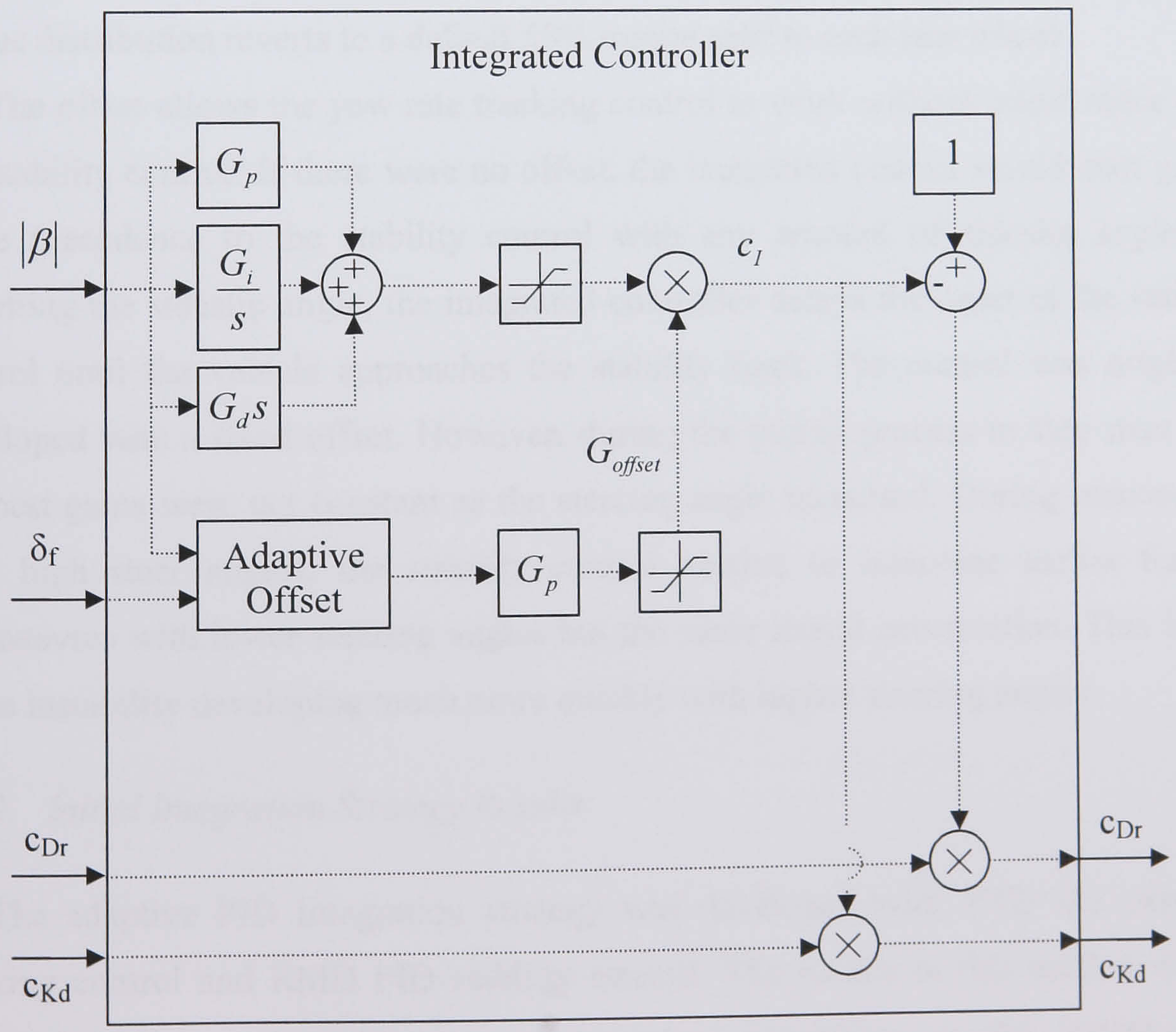

Figure 7.2 Block diagram of the integrated controller

The goal of this integration strategy is to switch from the yaw rate tracking control to the stability control when the sideslip angle increases beyond the stable limit. The control inputs of the integrated controller come from the independent controllers. The integrated controller determines c_I, which gives each independent control precedence based on the sideslip angle, which is adaptive based on the steer angle. The adaptive offset determines when the PID control becomes active through the gain, G_{offset}. It consists of a sideslip threshold based on the steering angle. If the sideslip is small it gives a value of zero, which results in c_I also being zero and the total control action is given by the VTD driveability control. As the sideslip angle increases beyond the stable limit G_{offset} becomes positive and increases. The gain and saturation of the signal insures that it switches from zero to unity rapidly, without affecting the PID control gain. Once G_{offset} reaches unity, the PID control determines the individual control precedence. The value from the PID control is also saturated between zero and unity. This allows the control action to be completely switched from the yaw rate tracking control to the stability control without altering their individual control actions. When the control precednce is switched to the stability control, the VTD torque distribution reverts to a default 50% torque split to each rear wheel.

The offset allows the yaw rate tracking control to work without interference from the stability control. If there were no offset, the integrated control would start giving some precedence to the stability control with any amount of sideslip angle. By offsetting the sideslip angle, the integrated controller delays the onset of the stability control until the vehicle approaches the stability limit. The control was originally developed with a fixed offset. However, during the tuning process in step steer tests the best gains were not constant as the steering angle increased. During manoeuvres with high steer angles, the stability control needed to intervene earlier than at manoeuvres with lower steering angles but the same lateral acceleration. This is due to the instability developing much more quickly with higher steering angles.

7.1.2. Initial Integration Strategy Results

The adaptive PID integration strategy was developed with VTD IM yaw rate tracking control and RMD PID stability control. The results in this section will be obtained by integrating these two independent controllers as the strategy was originally implemented, named the original initial integrated control. Since the

original design of this integration strategy, other independent controllers have been developed, namely the VTD SM yaw rate tracking control and the RMD phase plane stability control. Results will also be provided and compared for the integration of these two controllers, named the revised initial integrated control.

The first results come from a constant velocity step steer test run at 25 m/s with a 2.5 degree step steer angle. Figure 7.3 shows the yaw rate and sideslip results where "Original" designates the integration strategy with the VTD IM driveability control and RMD PID stability control. "Revised" designates the same initial integration strategy but using the VTS SM driveability control and the RMD phase plane stability control. The yaw rate results in Figure 7.3.a show that both integrated controllers get close to matching the reference yaw rate before the stability control quickly takes precedence. Since this manoeuvre is almost at the limits of the vehicle it is expected that the yaw rate controllers will be quickly phased out to stabilise the vehicle. Therefore the vehicle will not track the reference yaw rate. The yaw rate also settles quicker for both controllers compared to the passive vehicle. As expected the revised integration control outperforms the original integration control. The revised control settles the quickest with more damping and a higher steady state yaw rate.

The sideslip results, in Figure 7.3.b, show a similar behaviour. Both controllers show a quicker settling time than the passive vehicle while the revised control has a more damped response. The original control reduces the sideslip angle more. This is due to using the PID sideslip angle tracking stability control. It works to reduce the sideslip to the reference signal whereas the phase plane control only limits the sideslip behaviour to a stable region. The use of the PID sideslip angle tracking stability control also leads to the oscillation in the original integration control that occurs around one second into the manoeuvre. The stability control overshoots the reference sideslip angle. This allows the driveability control to temporarily take precedence again. This quick switching between the stability and driveability controls creates the oscillation. One more thing to note from Figure 7.3.c and Figure 7.3.d is that if c_I is between zero and unity, the integration strategy allows partial precedence to each independent control. So they can both be active together. Although it is not noticeable for the revised control in this test, the original control settles with both controllers active.

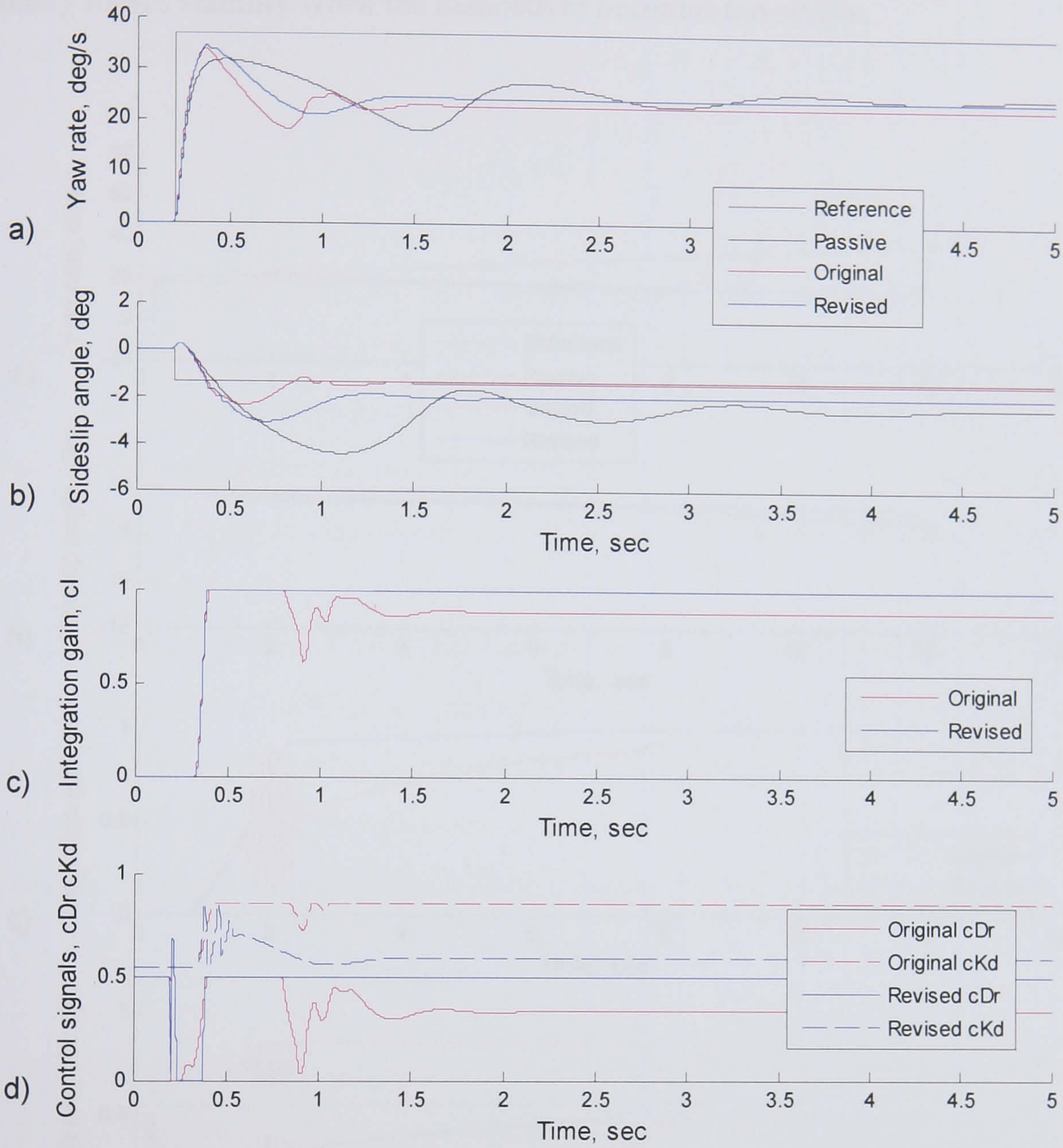

Figure 7.3 Step steer results for the initial integrated controls, 25 m/s velocity, 2.5 deg steer angle

Figure 7.4 shows the results for an accelerating step steer test. This is the same test used to tune the driveability controllers in Chapter 5. The yaw rate results in Figure 7.4.a show that the integrated controllers initially follow the yaw rate. As the vehicle approaches its stability limits the integration strategy gives precedence to the stability control, which stabilises the vehicle. The manoeuvre continues to become progressively more severe and eventually the controllers can no longer maintain stability. At this point the vehicle loses stability. Figure 7.4.b shows the sideslip response. Initially the vehicle sideslip increases until the stability controllers are given precedence around two seconds into the manoeuvre. At this point the controllers

stabilise the vehicle and maintain a fairly constant sideslip angle until the vehicle finally looses stability when the manoeuvre becomes too severe.

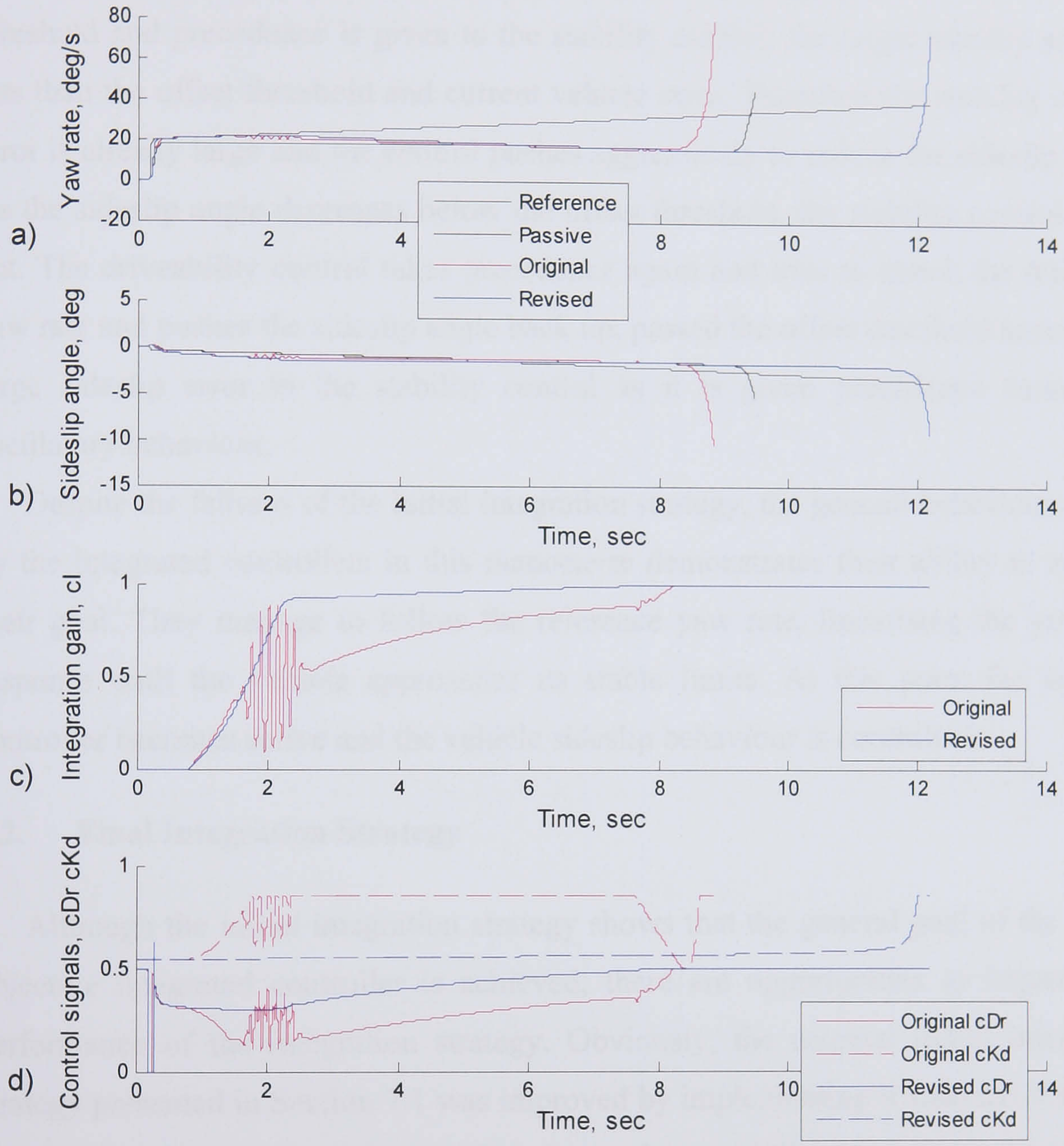

Figure 7.4 Step steer results for the initial integrated controls, 22 m/s initial velocity, 1.5 m/s^2 acceleration, 1.5 deg steer angle

Once again, the revised integration control performs better than the original control by maintaining stability longer and showing less oscillatory behaviour. The original control shows a very oscillatory behaviour during the switching process from the driveability control to the stability control. This is not desirable due to the power required in the control actuators. The reason for the oscillations and for the early loss of stability comes from the RMD PID stability control. As detailed in Section 6.2, the PID control aims to track the reference sideslip angle rather than limit the sideslip

behaviour. In trying to match the reference sideslip angle, the stability control forces the vehicle dynamics and tries to reduce the sideslip angle too much. The reference sideslip angle that the stability control is aiming to match is well within the vehicle's stability limits. So as the sideslip angle passes the integrated controller's offset threshold and precedence is given to the stability control, the target sideslip angle is less than the offset threshold and current vehicle state. Therefore the stability control error is already large and the control pushes aggressively to reduce the sideslip angle. As the sideslip angle decreases below the offset threshold, the stability control is cut out. The driveability control takes precedence again and tries to match the reference yaw rate and pushes the sideslip angle back up, passed the offset threshold again. This large sideslip error in the stability control as it is given precedence causes the oscillatory behaviour.

Despite the failures of the initial integration strategy, the general behaviour shown by the integrated controllers in this manoeuvre demonstrates their ability to achieve their goal. They manage to follow the reference yaw rate, linearising the yaw rate response until the vehicle approaches its stable limits. At this point the stability controller becomes active and the vehicle sideslip behaviour is controlled.

7.2. Final Integration Strategy

Although the initial integration strategy shows that the general goal of the multi-objective integrated controller is achieved, there are opportunities to improve the performance of the integration strategy. Obviously, the original initial integration strategy presented in Section 7.1 was improved by implementing it with the VTD SM yaw rate tracking control and RMD phase plane stability control in the revised controller. This removed the oscillations and resulted in a smoother vehicle response. However, the integration strategy can also be improved. The final integration strategy is shown in Figure 7.5 and presented in the following sections. It has the same overall block diagram shown in Figure 7.1.

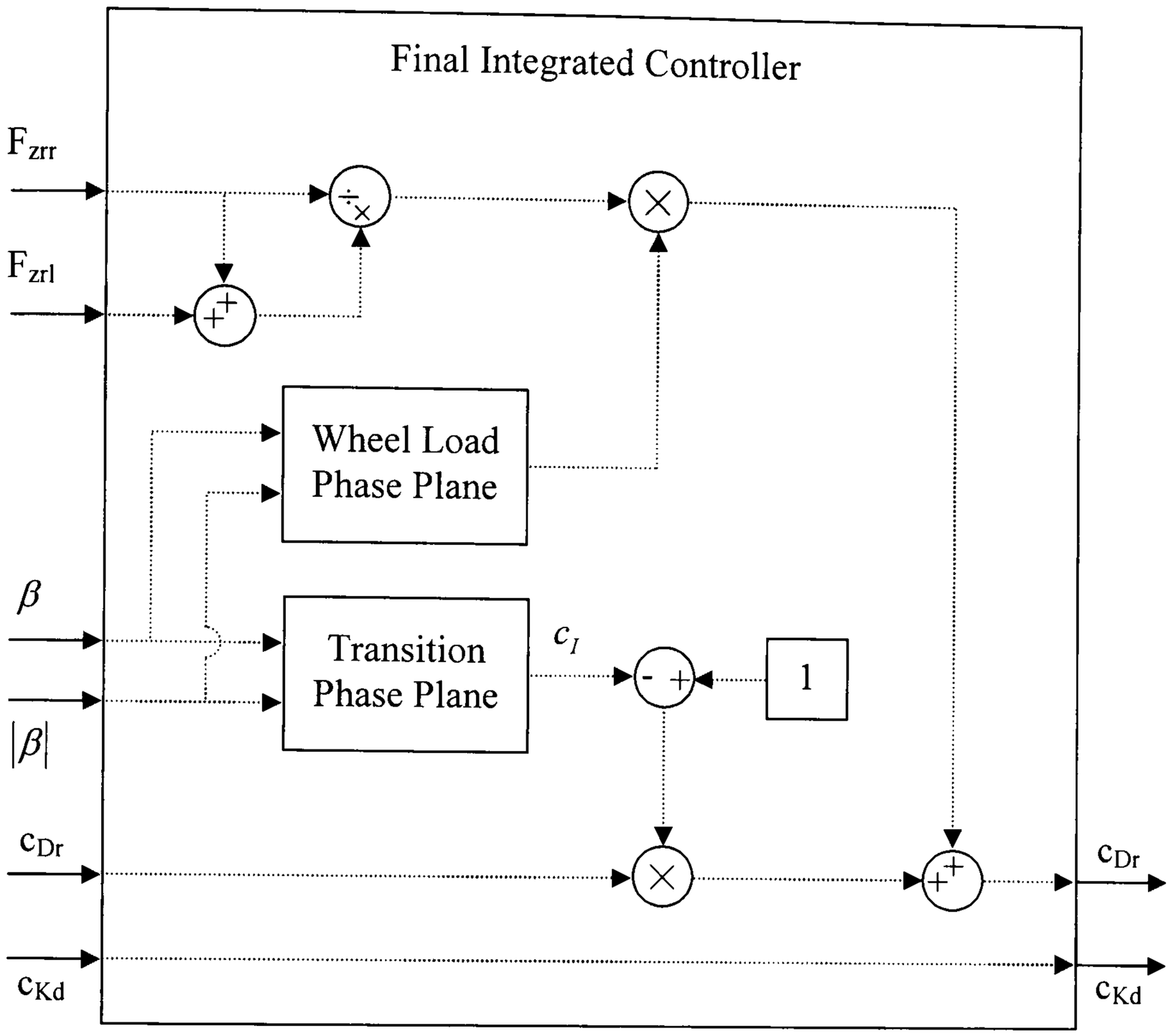

Figure 7.5 Block diagram of the final integration control strategy

7.2.1. Simultaneous Control

The first improvement in the integration strategy is to ensure the two independent controllers are not active at the same time. The initial integration strategy would give sole precedence to the driveability control when c_I is zero and sole precedence to the stability control when c_I is unity. However, any value in between would give a combination of both driveability and stability controllers. This is counterproductive because the controllers have different goals. The driveability control tracks the yaw rate but also increases the sideslip angle as a secondary effect. The stability control aims to reduce the sideslip angle but also decreases the yaw rate. If both controllers are active simultaneously they will work against each other towards conflicting goals. Not only will their control actions be at odds with each other, but energy will be wasted by having both controllers active at the same time. Therefore the final integration strategy must work towards only one control goal at any given time.

7.2.2. Determining Vehicle Stability

The basic strategy in the integrated controller is to switch from the yaw rate tracking control to the stability control when the vehicle approaches its stability limit. This is the same motivation behind the stability controllers. Since the initial integration strategy was designed with the sideslip angle based PID control it was a logical continuation to use a sideslip angle based PID control as the integration strategy. However, this required the use of the adaptive offset to create a "deadzone" where the stability controller would not operate. The result was that although both the integrated control and the stability control base their control outputs on the degree of vehicle stability, they used different methods to determine the vehicle stability. Since the stability control already determines the vehicle stability, it makes sense that the integrated control uses the same strategy.

Since the phase plane stability control was determined to be the best stability strategy in Section 6.2.2, the integrated control will be based on the sideslip angle phase plane as well. Currently the stability control uses a boundary to determine the control action. Inside the control boundary, no stability control is required. Once the vehicle state moves beyond the control boundary, the stability control action is proportional to the distance the state lies from the boundary. To ensure that the two controllers do not conflict with each other, the integrated control must give all precedence to the stability control once the vehicle state moves beyond the control boundary. However, the stability control does not need to be "phased in" since it is never active inside the stability boundary. Therefore the stability control signal, c_{Kd}, does not need to be modified, as shown in the block diagram in Figure 7.5.

Within the control boundary, the driveability control can be active. However, phasing out the driveability control needs to be addressed. Simply cutting off the driveability control at the control boundary would result in a very abrupt and disruptive control. To make the transfer of precedence smoother, a transition zone is created. This is illustrated in Figure 7.6 and shown as the Transition Phase Plane block in Figure 7.5.

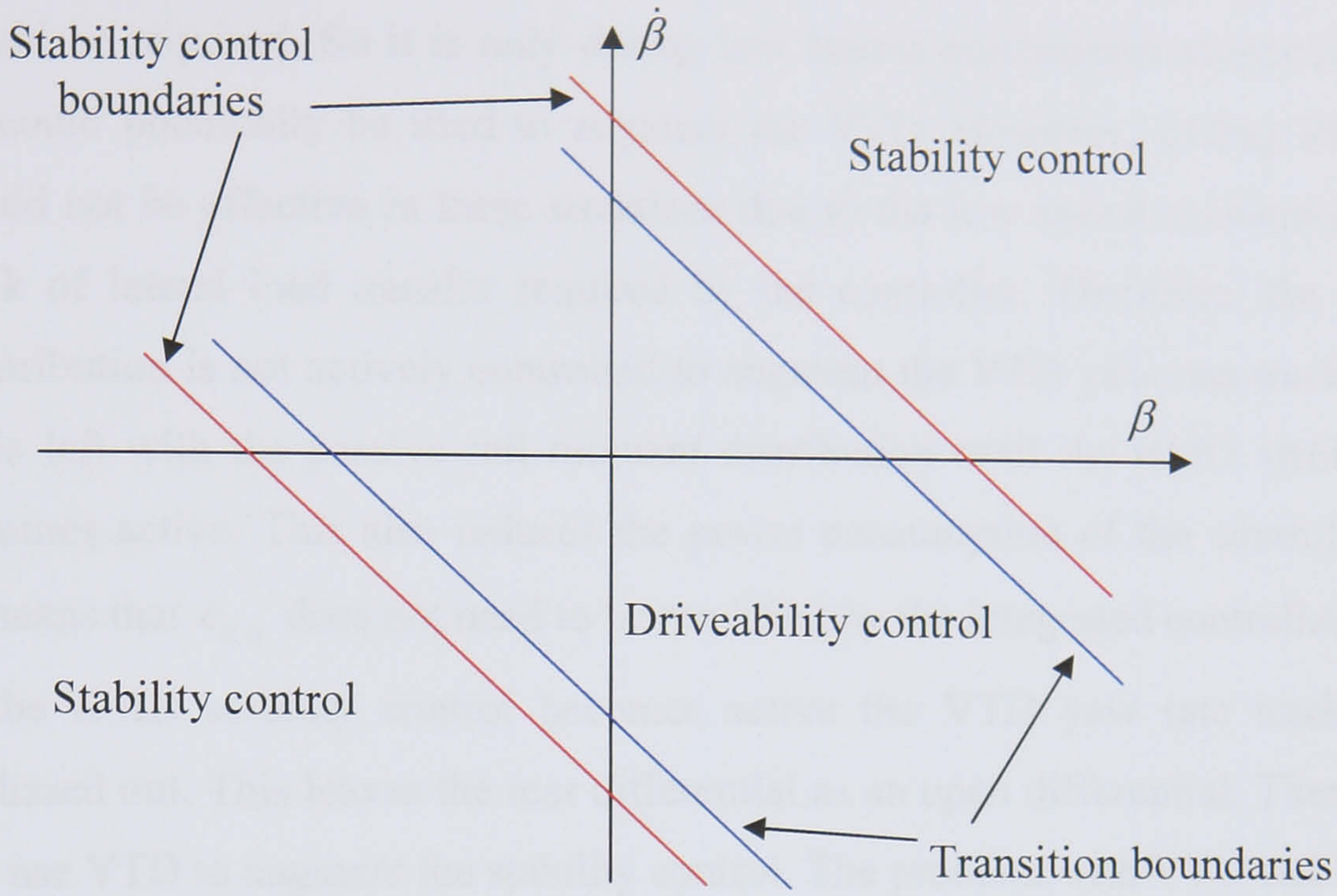

Figure 7.6 Modified sideslip angle phase plane boundaries for the integrated control

A second boundary is created within the stability control boundary and parallel to it. This is the transition boundary given by the blue lines. Inside the transition boundary, c_I is defined as zero and the driveability control operates at its full capability. Once the vehicle state moves beyond the transition boundary, c_I starts increasing and the driveability control is proportionally decreased. As the vehicle state approaches the stability control boundary, shown by the red lines, c_I becomes unity and the driveability control is inactive. Outside the stability control boundaries, c_I remains defined as unity completely negating the driveability control. The integration coefficient, c_I, is used as a coefficient to phase out the driveability control.

7.2.3. Control of Non-Active Systems

The integration strategy switches from the VTD driveability control to the RMD stability control as the vehicle approaches the limits of its stability. This leaves one control system deactivated at all times when it could potentially be used to augment the vehicle dynamics. When the VTD driveability control is active the RMD control could potentially be used to improve the yaw rate tracking. However, the VTD controller already manages to track the yaw rate very well. It is only during rapid steering inputs that the VTD control does not manage to track the yaw rate. If the

vehicle is at higher lateral accelerations and rapid steering inputs occur the stability control would be required. So it is only during low lateral acceleration manoeuvres that RMD could potentially be used to augment the VTD. However, adding RMD control would not be effective in these situations due to the low lateral accelerations and the lack of lateral load transfer required by the controller. Therefore, the roll moment distribution is not actively controlled to augment the VTD yaw rate tracking control. It is left with the passive roll moment distribution until the RMD stability control becomes active. This also reduces the power consumption of the controllers and again means that c_{Kd} does not need to be modified by the integrated controller.

When the RMD stability control becomes active the VTD yaw rate tracking control is phased out. This leaves the rear differential as an open differential. There is potential to use VTD to augment the stability control. The problem with VTD stability controls, as presented in Section 6.2, is that it transfers torque to the inside wheel to stabilise the vehicle. At the same time the inside wheel is unloaded by the lateral load transfer. Transferring torque to the unloaded inside wheel to promote a contra-cornering yaw moment will lead to tyre saturation and a dramatic loss of grip at the inside rear tyre. This destabilises the vehicle as shown in Section 6.2. Leaving the rear differential open with no control action would lead to the same tyre saturation, although not as quickly. The open differential will allow the torque to go to the wheel with least resistance, which is the inside wheel. Therefore, although the torque is not being actively pushed to the inside wheel it will still end up with more torque transferred to it.

To prevent the rear inside tyre from saturating due to the torque input, VTD can distribute the torque proportionally to the wheel load. This control strategy was presented in Section 5.2.1. As an independent control it was not effective but integrated into the full vehicle control strategy it can be effective. Although transferring torque to the outside wheel will promote a pro-cornering yaw moment, there is enough capacity in the RMD stability control to cope with this additional yaw moment. To implement the wheel load control, an additional phase plane boundary is needed to gradually phase it in, shown in Figure 7.7.

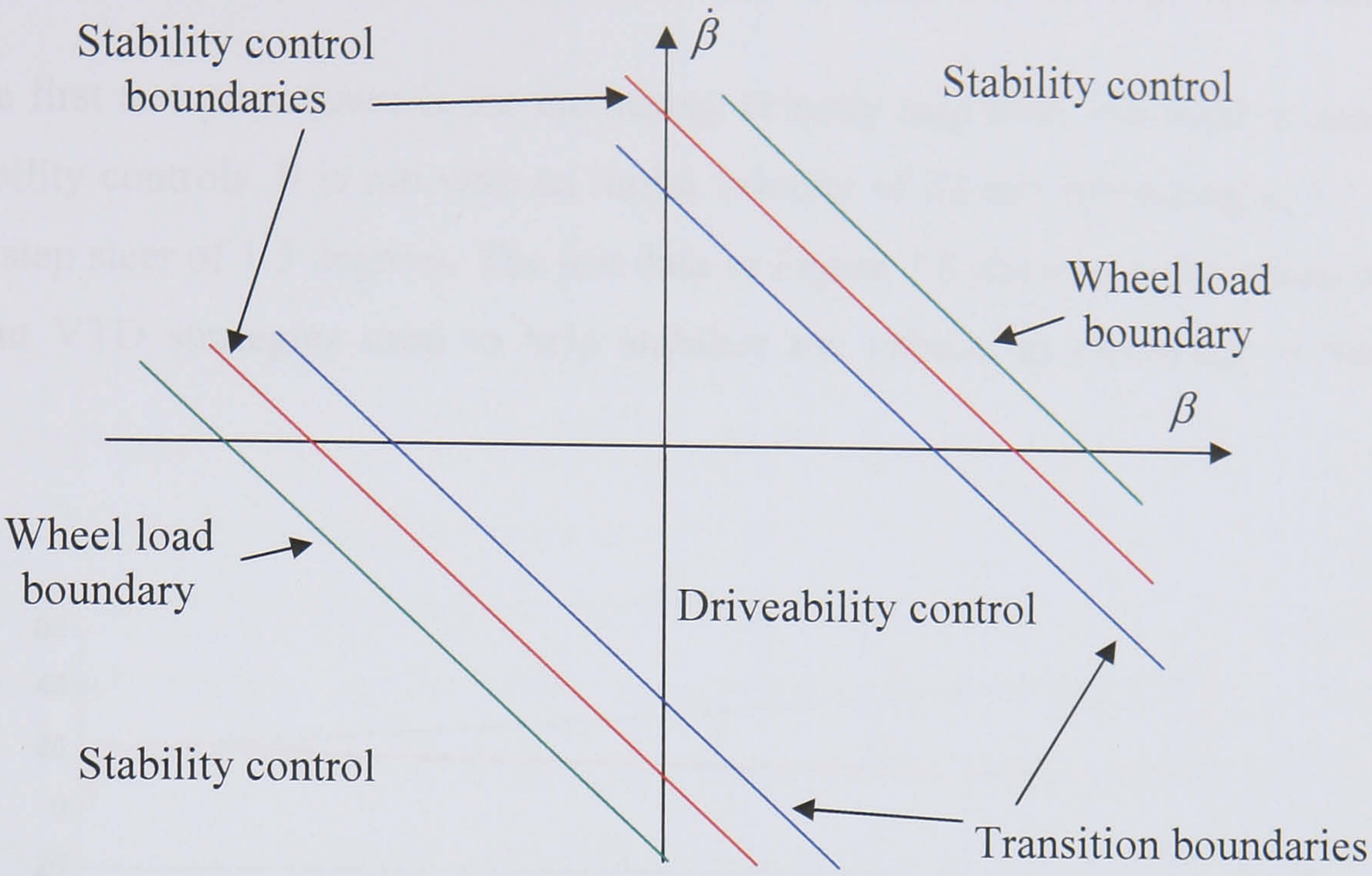

Figure 7.7 Modified sideslip angle phase plane boundaries for multiple integrated control

The green wheel load boundaries show the area where the VTD wheel load control is phased in as the stability control is active. Inside the red stability boundary, the wheel load gain is zero. As the vehicle state passes the stability boundary the wheel load gain increases from zero and becomes unity as the green wheel load boundary is reached. During this time the torque is distributed as a fraction of the actual wheel load distribution. Beyond the green boundary the torque is distributed in direct proportion to the wheel load. The results showing the integration of VTD into the full control strategy are presented in Section 7.3 along with the full results of the integrated controller.

7.3. Final Integration Strategy Results

The final phase plane integration strategy is tested using the same manoeuvres as shown in Chapter 6 to compare all the independent strategies. First, the different VTD strategies implemented to augment the RMD stability control are compared. This is followed by the full results of the final integrated control strategy.

7.3.1. Comparison of the VTD Control Strategies to Augment the Stability Control

The first test manoeuvre is the increasing velocity step steer test used to tune the driveability controls. It is run with an initial velocity of 22 m/s increasing at 1.5 m/s^2 with a step steer of 1.5 degrees. The test data in Figure 7.8 shows a comparison of the different VTD strategies used to help stabilise the vehicle as discussed in Section 7.2.3.

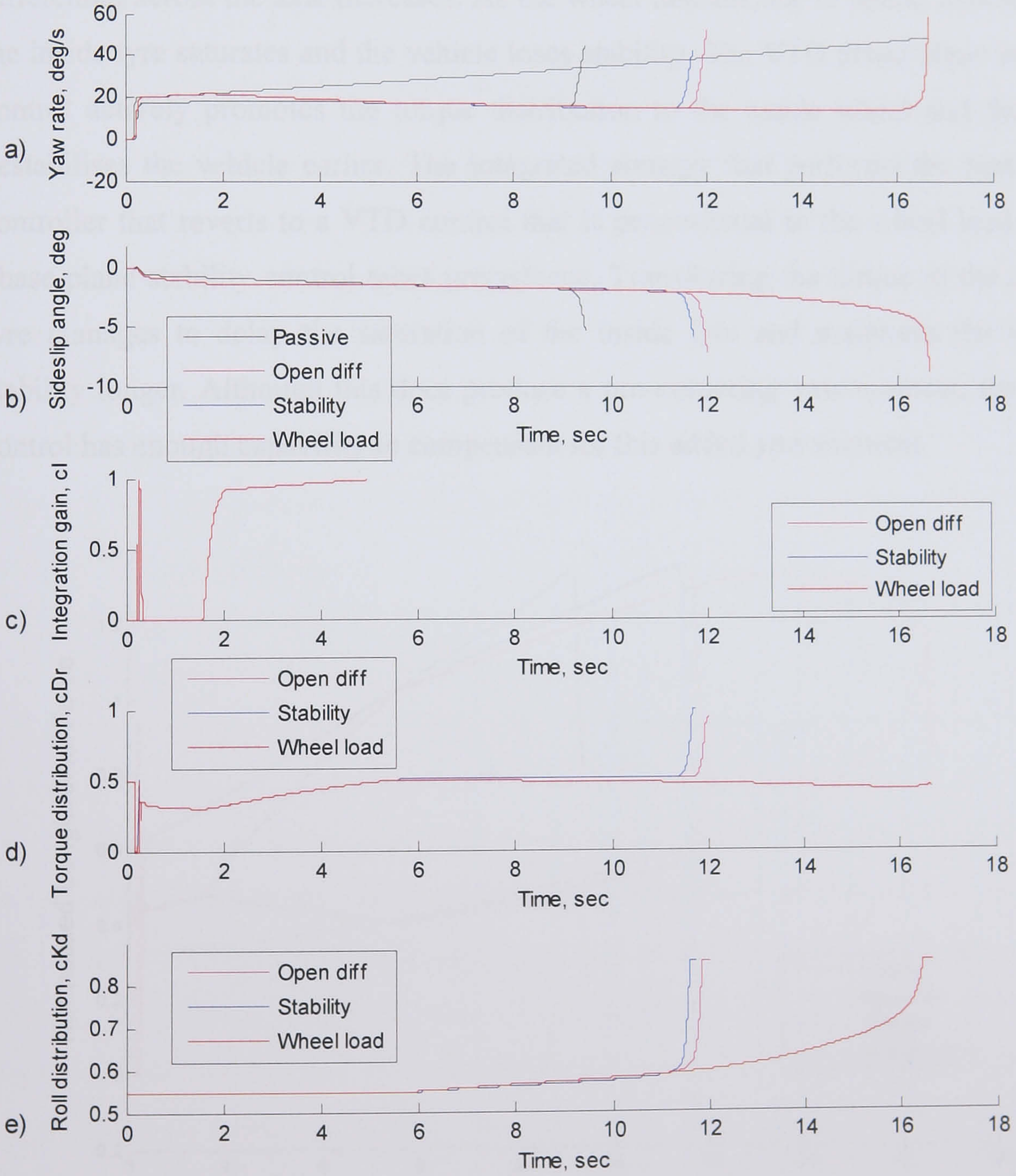

Figure 7.8 Step steer results and VTD strategy selection for the integrated controller, 22 m/s initial velocity, 1.5 m/s^2 acceleration, 1.5 deg steer angle

The results show that the passive vehicle does not follow the reference yaw rate (shown in grey) and loses stability before all the integrated control strategies. The vehicle that reverts to an open differential as the RMD stability control becomes active lasts slightly longer than the strategy that implements the VTD phase plane stability control. These two strategies are very similar in behaviour. As the yaw rate tracking control is phased out the vehicle stabilises but with the increasing speed demand the stability control has to work progressively harder. In the case of the open differential strategy, the torque gets transferred to the inside wheel as the speed differential across the axle increases. As the wheel unloads due to lateral load transfer the inside tyre saturates and the vehicle loses stability. The VTD phase plane stability control actively promotes the torque distribution to the inside wheel and therefore destabilises the vehicle earlier. The integrated strategy that performs the best is the controller that reverts to a VTD control that is proportional to the wheel load as the phase plane stability control takes precedence. Transferring the torque to the outside tyre manages to delay the saturation of the inside tyre and maintains the vehicle stability longer. Although this does produce a pro-cornering yaw moment, the RMD control has enough capability to compensate for this added yaw moment.

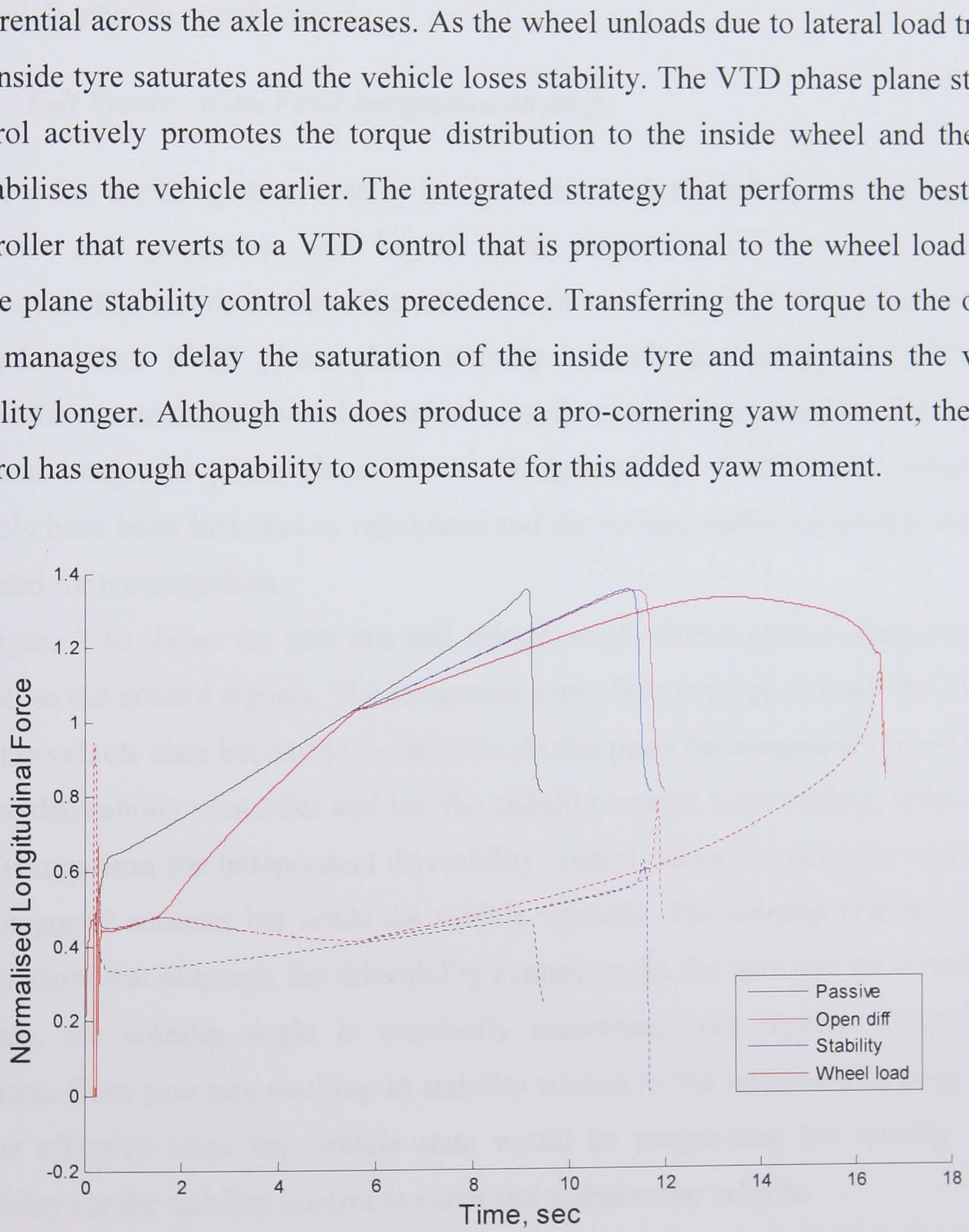

Figure 7.9 Rear tyre saturation for the VTD strategy selection of the integrated controller, 22 m/s initial velocity, 1.5 m/s^2 acceleration, 1.5 deg steer angle (solid lines show the inside tyre, dashed lines show the outside tyre)

The normalised longitudinal forces of the rear tyres are presented in Figure 7.9 to show the tyre saturation. The solid lines represent the rear right, inside tyre while the dotted lines show the rear left, outside tyre. The passive vehicle and the integrated strategies with the open differential and stability control all lose stability as the inside rear tyre saturates. The capability of the saturated tyre to provide any force dramatically decreases causing the loss of stability. In contrast, the integrated controller with the wheel load VTD strategy augmenting the RMD phase plane stability control manages to prevent the inside right tyre from saturating and maintains the vehicle stability much longer.

7.3.2. Full Results of the Final Integration Strategy

Now that the integration strategy has been finalised, the full results are presented. The first test manoeuvre will be the same increasing velocity step steer test manoeuvre. The test data shows the reference yaw rate (in grey), the passive vehicle, the independent RMD phase plane stability control, the independent VTD SM driveability control, the revised initial integrated control (designated by 'Initial') and the final integrated phase plane control (designated by 'Final'). The independent controls have been included as references and the revised initial integrated control is provided for a comparison.

Figure 7.10 shows the yaw rate and sideslip angle time response of the controller as well as the control signals. The integrated controllers manage to track the yaw rate until the vehicle state becomes too unstable. At this point the integrated control phases out the driveability controller and lets the stability control work without interference. As a comparison the independent driveability control tracks the yaw rate longer than the integrated controls but sends the vehicle unstable. The sideslip results in Figure 7.10.b show that although the driveability control tracks the yaw rate for a further 2.5 seconds, the sideslip angle is constantly increasing very rapidly. Delaying the transition from yaw rate tracking to stability control in the integrated strategy would not be effective since the vehicle state would be progressing too quickly toward instability for the stability control to catch and stabilise the vehicle.

The independent stability control is effective at initially stabilising the vehicle. However, it loses stability before the integrated controllers because the differential is just left as an open differential and not controlled. As presented in the previous results

and in Figure 7.8, the open differential allows the driving torque to saturate the inside rear tyre and destabilise the vehicle. The revised initial integrated control strategy lasts longer because as the stability control takes precedence the torque distribution reverts back to a 50% split between the left and right wheels. This is effective at delaying the loss of stability but the final integrated control strategy shows the best performance. This is due to the VTD wheel load control that augments the stability control and delays the saturation of the inside rear tyre.

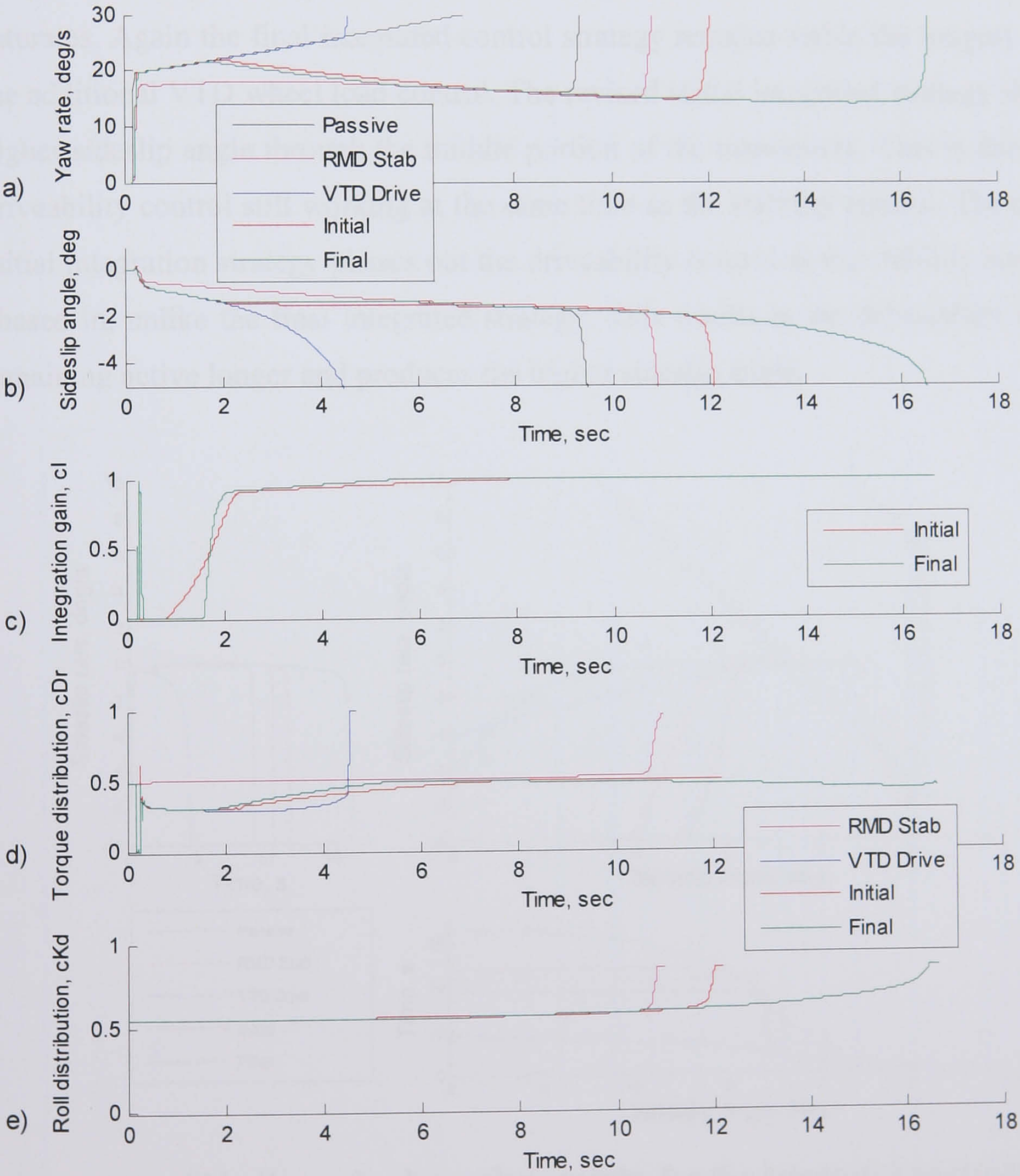

Figure 7.10 Step steer results for the integrated controller, 22 m/s initial velocity, 1.5 m/s^2 acceleration, 1.5 deg steer angle

Figure 7.11 shows the sideslip angle phase plane results. The main plot shows the sideslip rate verses the sideslip angle while the two subsidiary plots show the time response of the sideslip angle and rate. The time response plots have the same scale as the main phase plane plot so the results correspond between the plots. The solid grey lines show the stability control boundary while the dotted grey lines show the transition boundary of the integrated control strategy.

These results reiterate that the independent driveability control loses stability early in the simulation. The passive vehicle, independent stability control and revised initial integrated control strategy all lose stability in quick succession as the rear inside tyre saturates. Again the final integrated control strategy remains stable the longest due to the additional VTD wheel load control. The revised initial integrated strategy shows a higher sideslip angle through the middle portion of the manoeuvre. This is due to the driveability control still working at the same time as the stability control. The revised initial integration strategy phases out the driveability control as the stability control is phased in, unlike the final integrated strategy. This results in the driveability control remaining active longer and produces the higher sideslip angle.

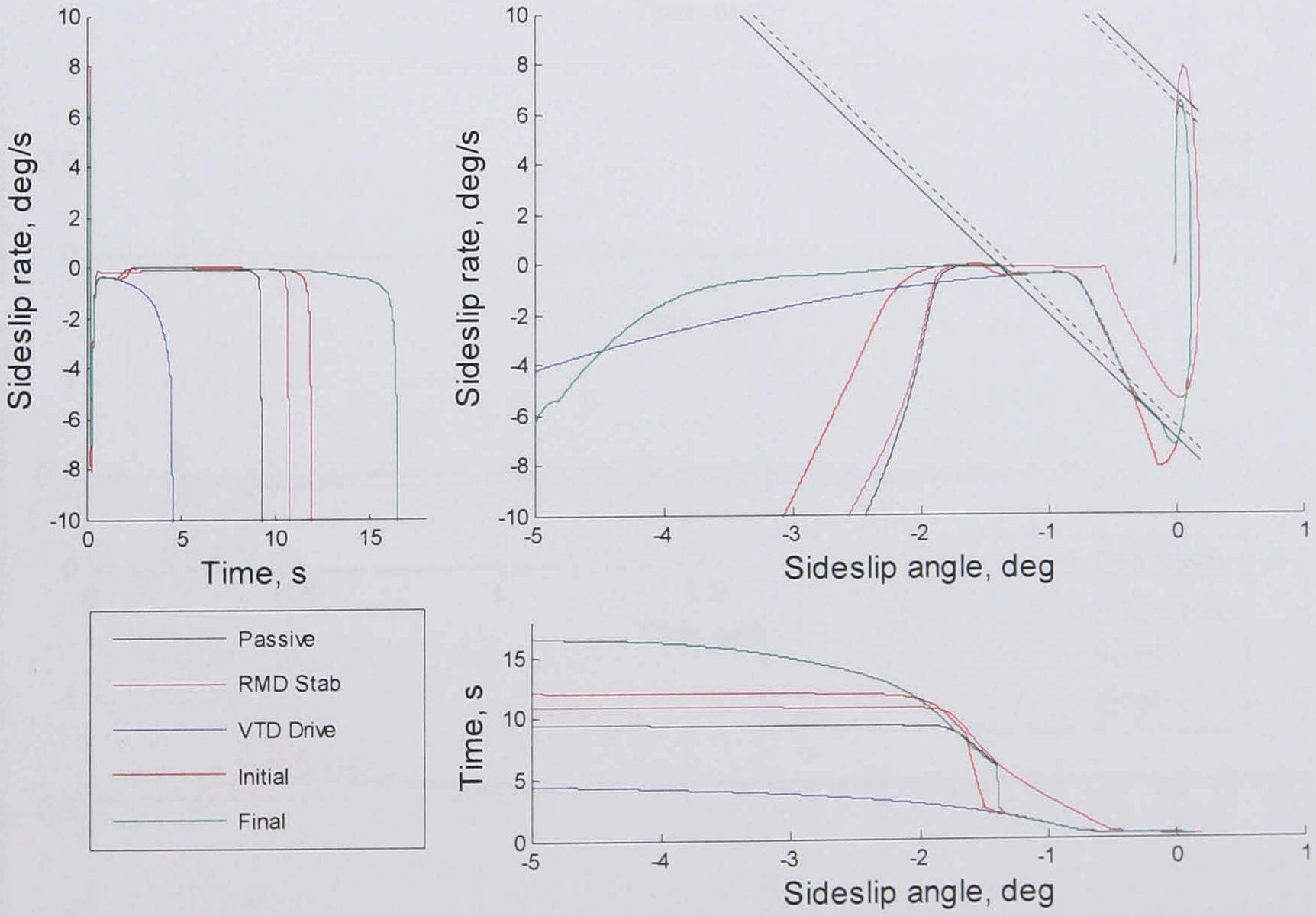

Figure 7.11 Sideslip angle phase plane results for the integrated controller step steer, 22 m/s initial velocity, 1.5 m/s^2 acceleration, 1.5 deg steer angle

The next test manoeuvre shown is the constant velocity step steer test used to tune the stability controllers. It is run at 25 m/s with a step steer angle of 2.5 degrees. Once

again the reference yaw rate (shown in grey) and the revised initial integrated control strategy and independent controllers have been included to provide a reference and comparison. Figure 7.12 shows the yaw rate and sideslip angle results including the control variables while the time response characteristics of the sideslip angle can be seen in Table 7.1. Since this manoeuvre was used to tune the stability controls, it is run on the limit of the vehicle handling. Due to this, it is not surprising that the independent driveability control sends the vehicle unstable very quickly. Likewise the independent stability control stabilises the vehicle effectively as expected.

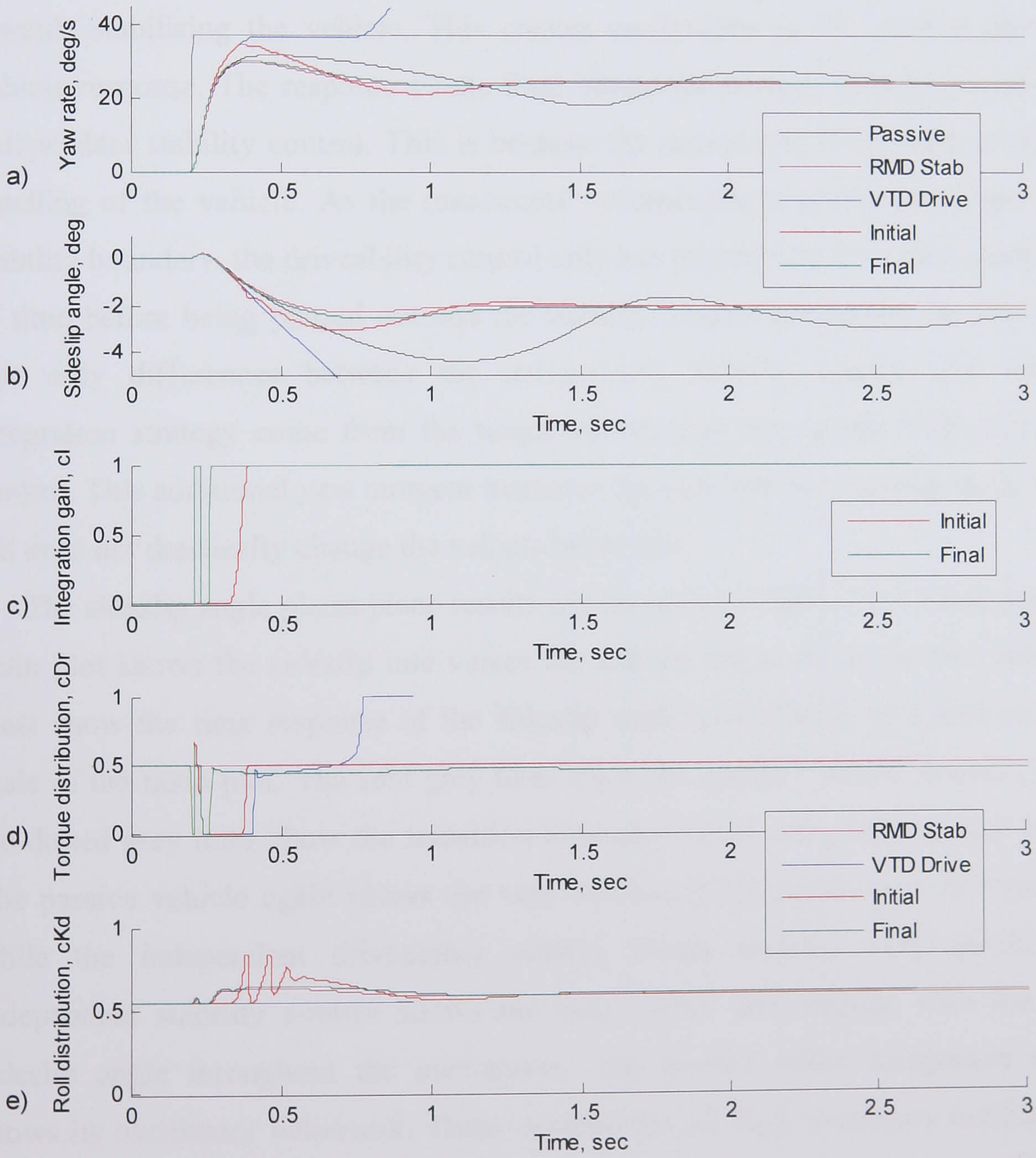

Figure 7.12 Step steer results for the integrated controller, 25 m/s velocity, 2.5 deg steer angle

	Passive	RMD Stab	VTD Drive	Initial	Final
% Overshoot	66.9	12.6	-	50.1	18.0
63% Rise time (s)	0.253	0.218	-	0.175	0.219
10-90% Rise time (s)	0.241	0.212	-	0.147	0.219
1% Settling time (s)	3.63	1.272	-	1.70	1.50

Table 7.1 Step steer sideslip angle results of the integrated controller, 25 m/s initial velocity, 2.5 deg steer angle

The revised initial integrated control manages to follow the reference yaw rate slightly longer than the final integrated control strategy. However, the benefit of this is short lived since the stability control has to force the roll moment distribution more towards stabilising the vehicle. This creates oscillations in the control signal and vehicle response. The response of the final integrated strategy closely resembles the independent stability control. This is because the manoeuvre is so close to the limit handling of the vehicle. As the manoeuvre becomes more severe and closer to the stability boundary, the driveability control only has precedence for a very short period of time before being phased out and the stability control dominates the manoeuvre. The only differences between the independent stability control and the final integration strategy come from the torque distribution due to the VTD wheel load control. This additional yaw moment increases the yaw rate and sideslip angle slightly but does not drastically change the vehicle behaviour.

The sideslip angle phase plane results can be seen in Figure 7.13. Once again, the main plot shows the sideslip rate verses the sideslip angle while the two subsidiary plots show the time response of the sideslip angle and sideslip rate and match the scale of the main plot. The sold grey lines show the stability control boundary while the dotted grey lines show the transition boundary of the integrated control strategy. The passive vehicle again shows the very oscillatory behaviour seen in Figure 7.12 while the independent driveability control looses stability very quickly. The independent stability control shows the most stable performance with the lowest sideslip angle throughout the manoeuvre. The revised initial integration strategy shows its oscillatory behaviour. These oscillations are high frequency oscillations in the sideslip rate that occur at the beginning of the manoeuvre. This is a result of tracking the yaw rate too long and trying to stabilise the vehicle after it has been pushed to a state much further from the stability control boundary. Not only does this

result in the high frequency oscillations but it also produces a longer settling time. The final integrated control strategy is almost as good as the independent stability control and shows a well damped response and only a slightly higher steady state sideslip angle. This higher sideslip angle is once again due to the wheel load VTD control that creates an additional yaw moment.

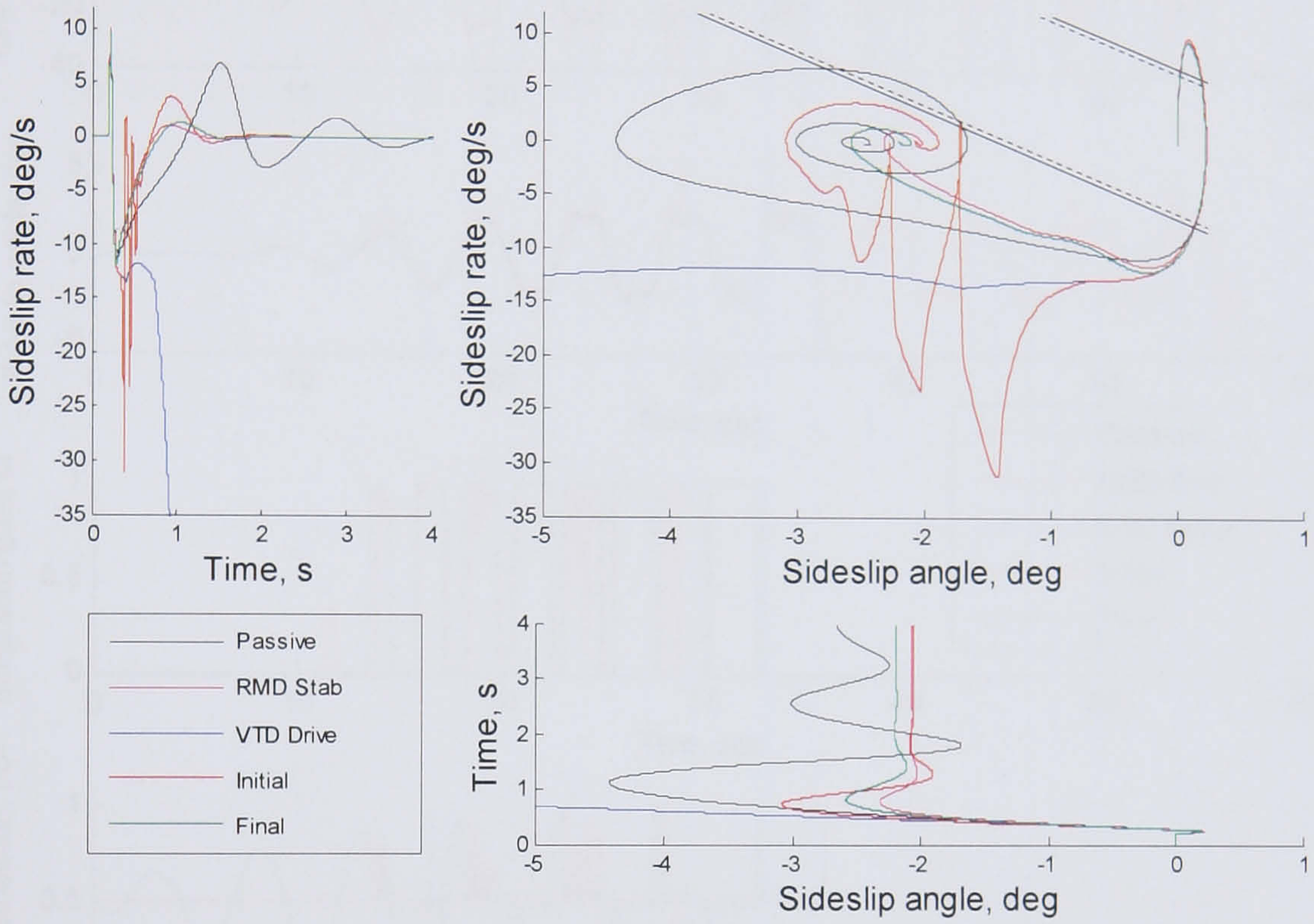

Figure 7.13 Sideslip angle phase plane results for the integrated controller step steer, 25 m/s velocity, 2.5 deg steer angle

The increasing velocity, increasing sinusoidal steer test results are presented in Figure 7.14. Again the yaw rate, sideslip angle and the control inputs are shown with the reference yaw rate in grey. The test is run with an initial velocity of 15 m/s accelerating at 0.5 m/s^2 while the steering angle starts at 1.0 degree and increases at 0.1 deg/s. The independent stability control maintains the vehicle stability the longest, lasting 57 seconds. As the manoeuvre progresses, the response becomes increasingly oscillatory before the final loss of stability. The independent driveability control loses stability the quickest after 16 seconds. This is expected since the control only aims to track the linear reference yaw rate. This reference keeps increasing as the test becomes more severe and its not long before the vehicle is unable to track it without losing stability. The revised initial independent control strategy performs well. It manages to track the reference yaw rate with each sinusoidal cycle. However, the driveability control phases out as the stability control becomes active. This allows the

vehicle to track the yaw rate slightly longer than the final integrated strategy but results in a more oscillatory behaviour.

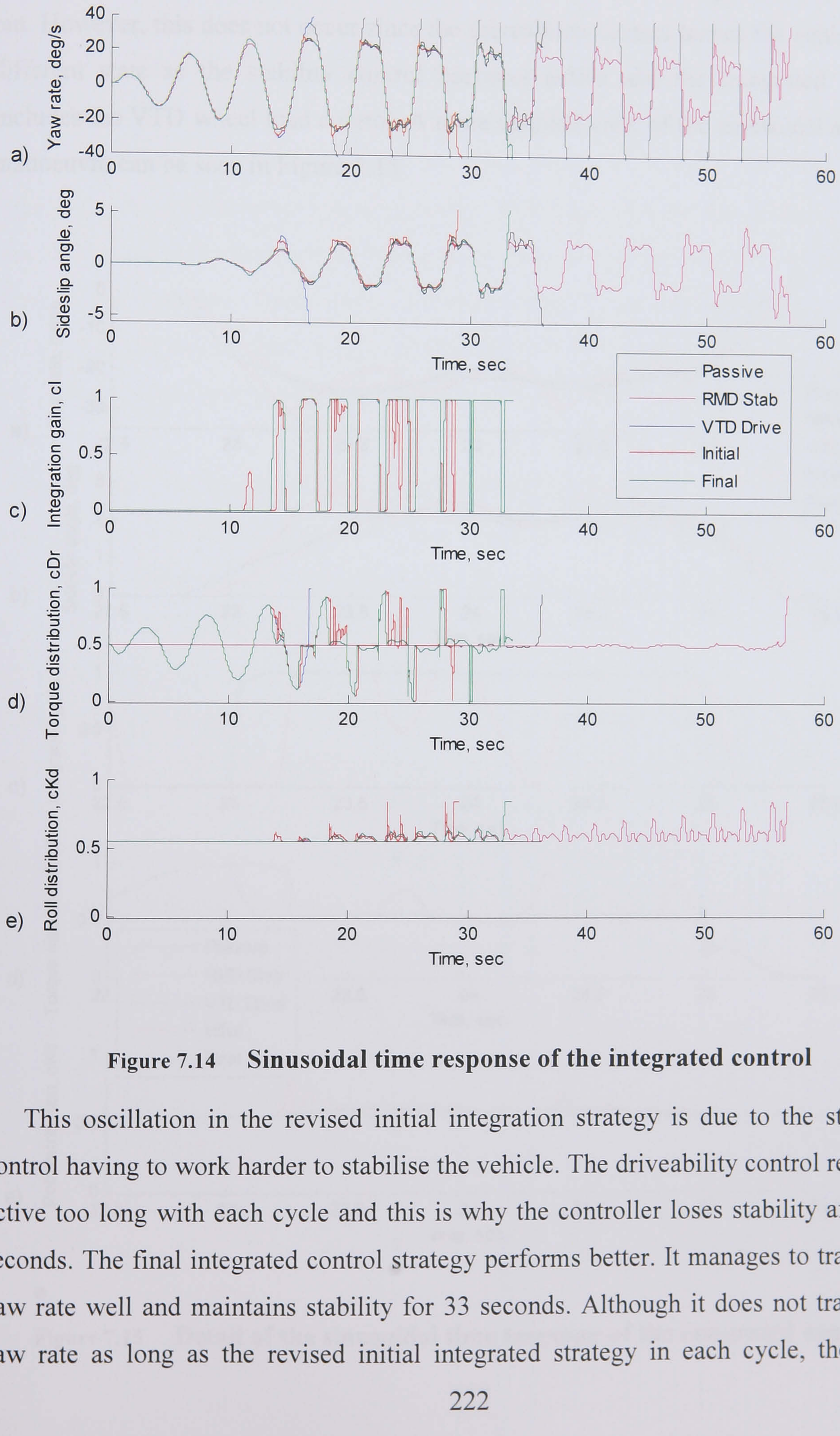

Figure 7.14 Sinusoidal time response of the integrated control

This oscillation in the revised initial integration strategy is due to the stability control having to work harder to stabilise the vehicle. The driveability control remains active too long with each cycle and this is why the controller loses stability after 29 seconds. The final integrated control strategy performs better. It manages to track the yaw rate well and maintains stability for 33 seconds. Although it does not track the yaw rate as long as the revised initial integrated strategy in each cycle, the final

integrated control does not have to work as hard to stabilise the vehicle. This gives a much smoother vehicle response with less oscillation and also allows the vehicle to remain stable longer. It might be expected that the final integrated strategy would follow the independent stability control once the yaw rate tracking control is phased out. However, this does not occur since the driveability control leaves the vehicle in a different state as the stability control becomes active and the integrated control includes the VTD wheel load control. A more detailed view of the sinusoidal steering manoeuvre can be seen in Figure 7.15.

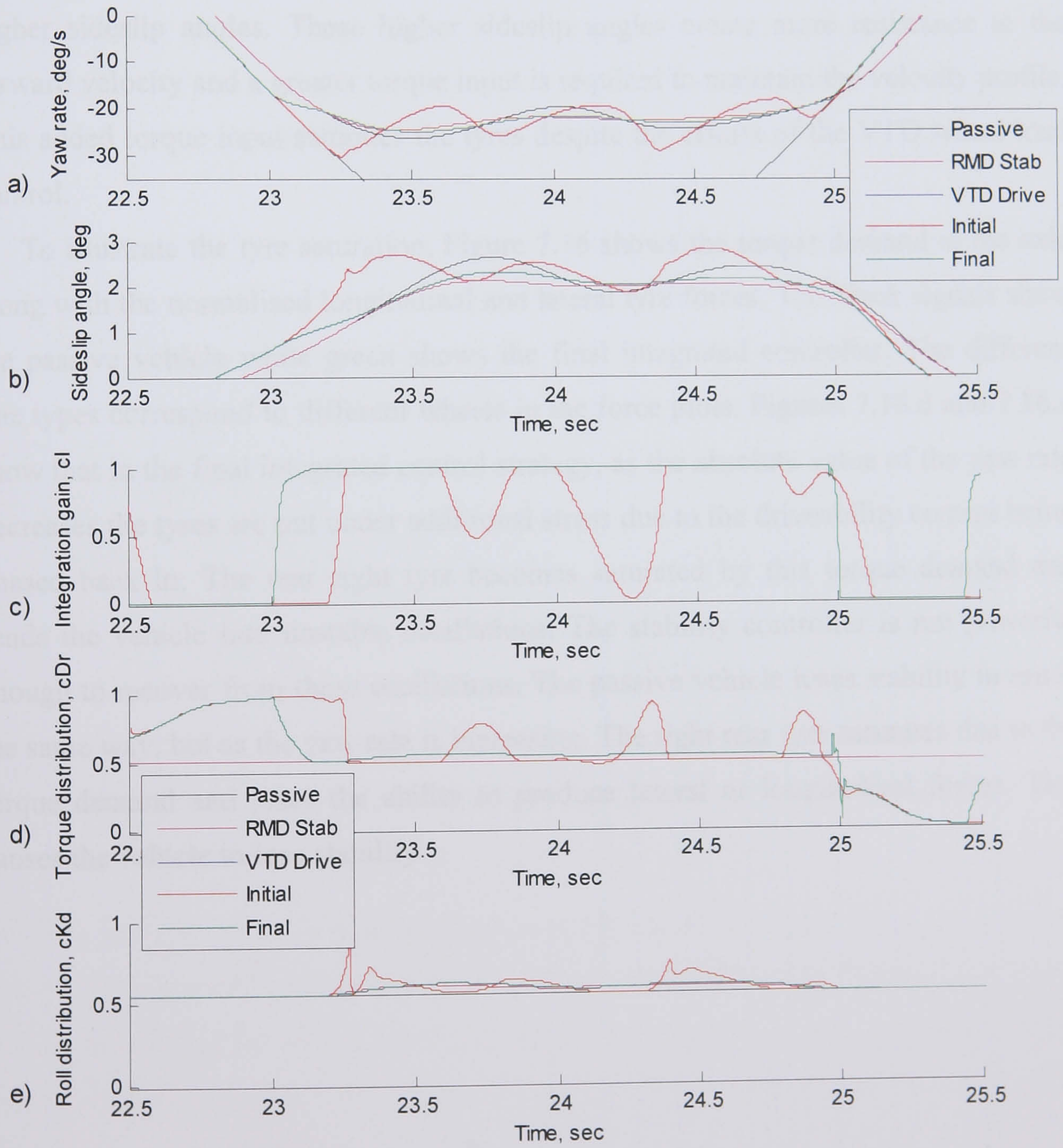

Figure 7.15 Detail of the sinusoidal time response of the integrated control

Figure 7.15 shows the smoother response of the final integrated control strategy. This is due to the controller phasing out the driveability control slightly earlier than the revised initial integrated strategy. Although this means the final integrated strategy does not track the yaw rate quite as long in each cycle, it does result in a smoother response and a more stable vehicle. The passive vehicle manages to maintain stability for one more cycle than the final integrated control strategy. The reason that the vehicle loses stability in both cases is that it is trying to track the velocity profile of the test manoeuvre. As the vehicle becomes more unstable, it takes more torque input to maintain the accelerating velocity profile. This added torque input saturates the tyres. Since the controlled vehicle tracks the reference yaw rate more closely, it has higher sideslip angles. These higher sideslip angles create more resistance to the forward velocity and a greater torque input is required to maintain the velocity profile. This added torque input saturates the tyres despite the efforts of the VTD wheel load control.

To illustrate the tyre saturation, Figure 7.16 shows the torque demand at the axle along with the normalised longitudinal and lateral tyre forces. The black signals show the passive vehicle while green shows the final integrated controller. The different line types correspond to different wheels in the force plots. Figures 7.16.d and 7.16.e show that in the final integrated control strategy, as the absolute value of the yaw rate decreases the tyres are put under additional stress due to the driveability control being phased back in. The rear right tyre becomes saturated by this torque demand and sends the vehicle into unstable oscillations. The stability controller is not powerful enough to recover from these oscillations. The passive vehicle loses stability in much the same way, but as the yaw rate is increasing. The right rear tyre saturates due to the torque demand and loses the ability to produce lateral or longitudinal forces. This causes the vehicle to lose stability.

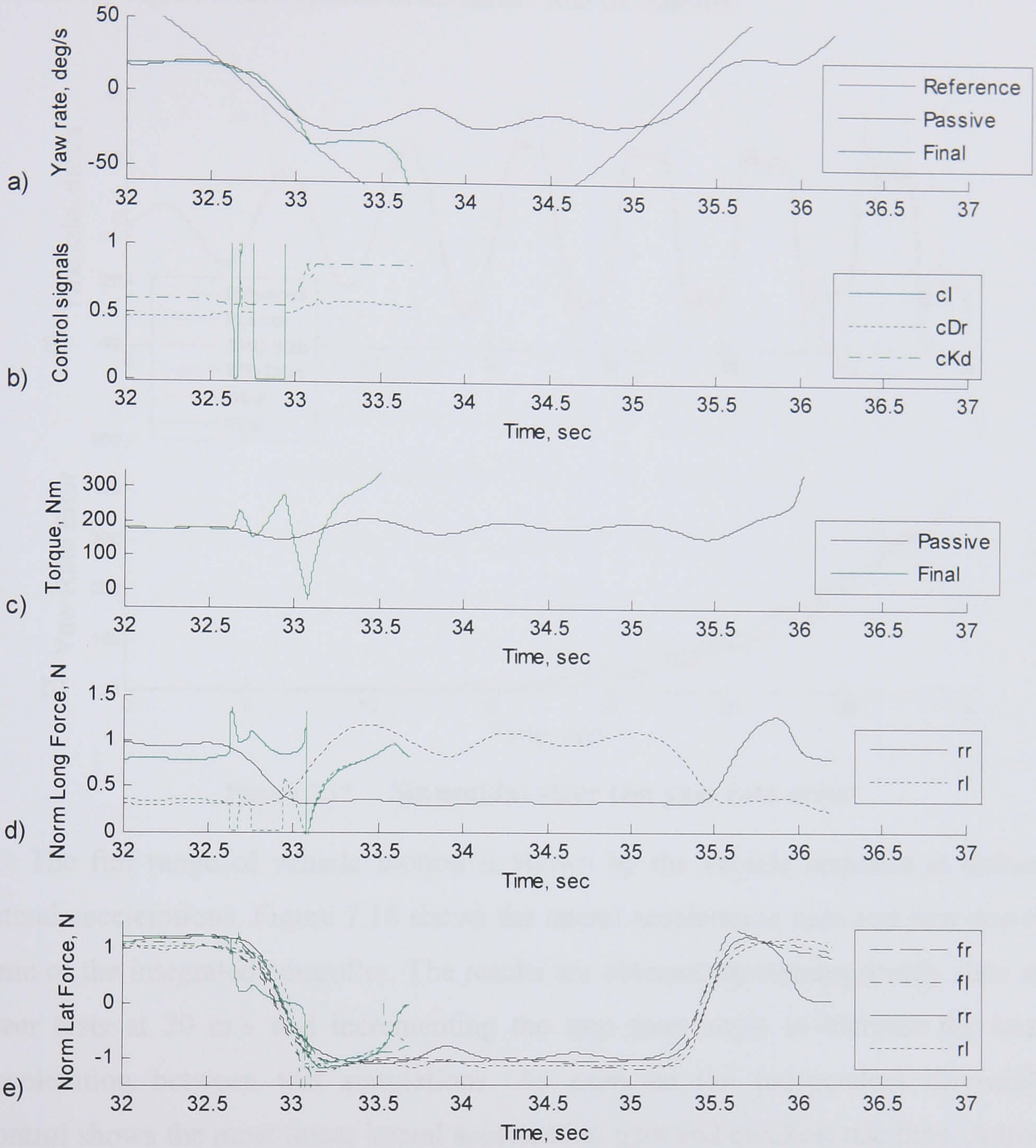

Figure 7.16 Torque demand and normalised longitudinal and lateral tyre forces for the sinusoidal steer test

The yaw rate and yaw rate tracking error are shown in Figure 7.17. The yaw rate error is the sum of the absolute yaw rate error, as presented in Section 6.1. Figure 7.17.b shows that the independent stability control has the largest yaw rate tracking error, which is expected, while the passive vehicle shows only slightly better tracking performance. The final integrated control strategy shows better yaw rate tracking than the passive vehicle. Although the revised initial integrated control strategy shows a

marginal improvement over the final strategy, it accomplishes this with a much more oscillatory signal which results in an earlier loss of stability.

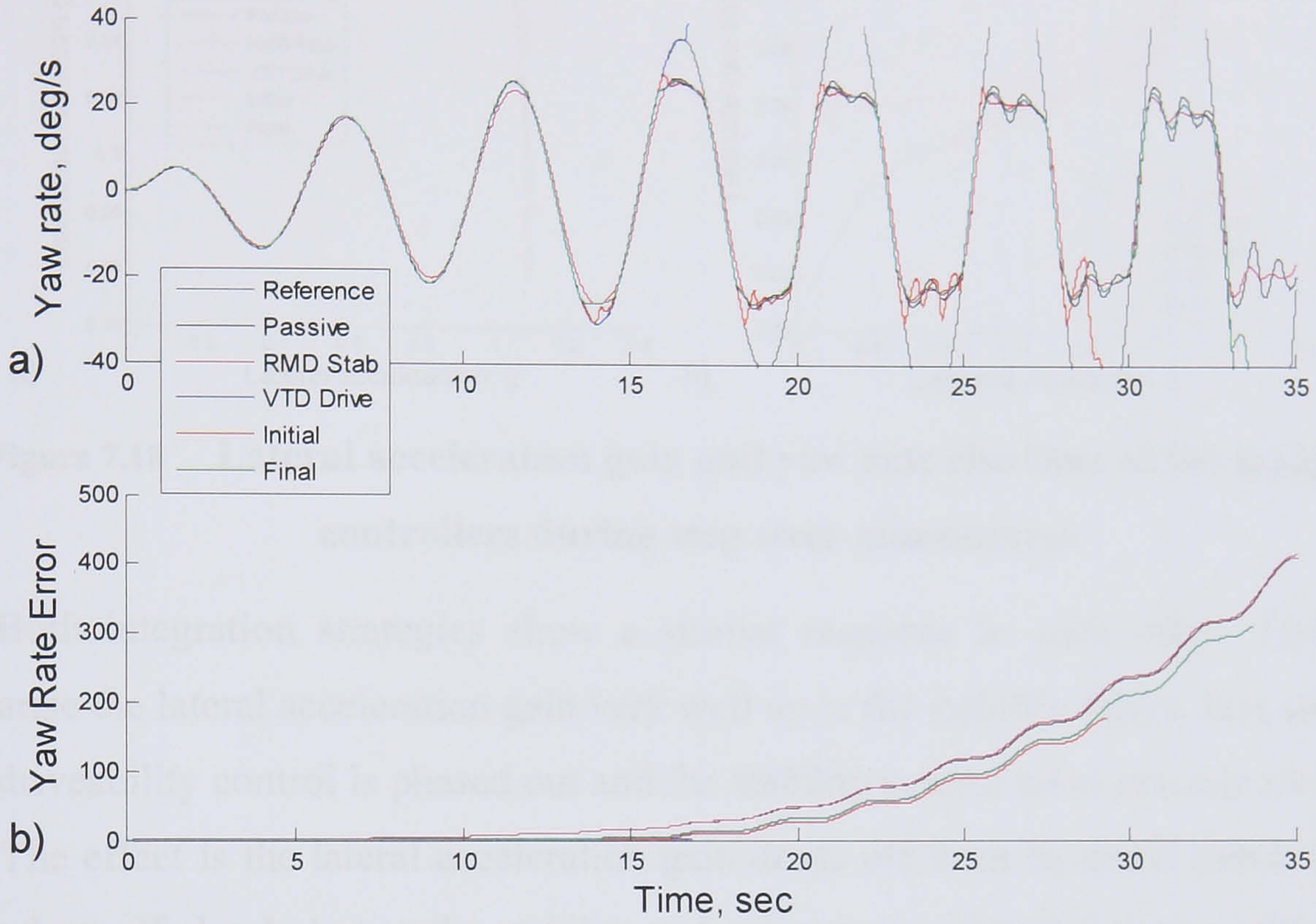

Figure 7.17 Sinusoidal steer test yaw rate error

The full range of vehicle motion is shown by the vehicle response at different lateral accelerations. Figure 7.18 shows the lateral acceleration gain and yaw rate rise time of the integrated controller. The results are obtained by running steady state step steer tests at 20 m/s and incrementing the step steer angle to increase the lateral acceleration between test simulations. As expected the independent driveability control shows the most linear lateral acceleration gain and quickest rise time. A linear lateral acceleration gain demonstrates that the vehicle lateral acceleration rises linearly with increasing steering angle input. This gives the vehicle a linear response that is easy for the driver to predict and reduces the driver work load. However, the driveability controller destabilises the vehicle, as shown in the previous results. The independent stability controller follows the passive vehicle until the higher lateral accelerations. Around 1g, the vehicle state reaches the stability boundary and the lateral acceleration gain greatly decreases.

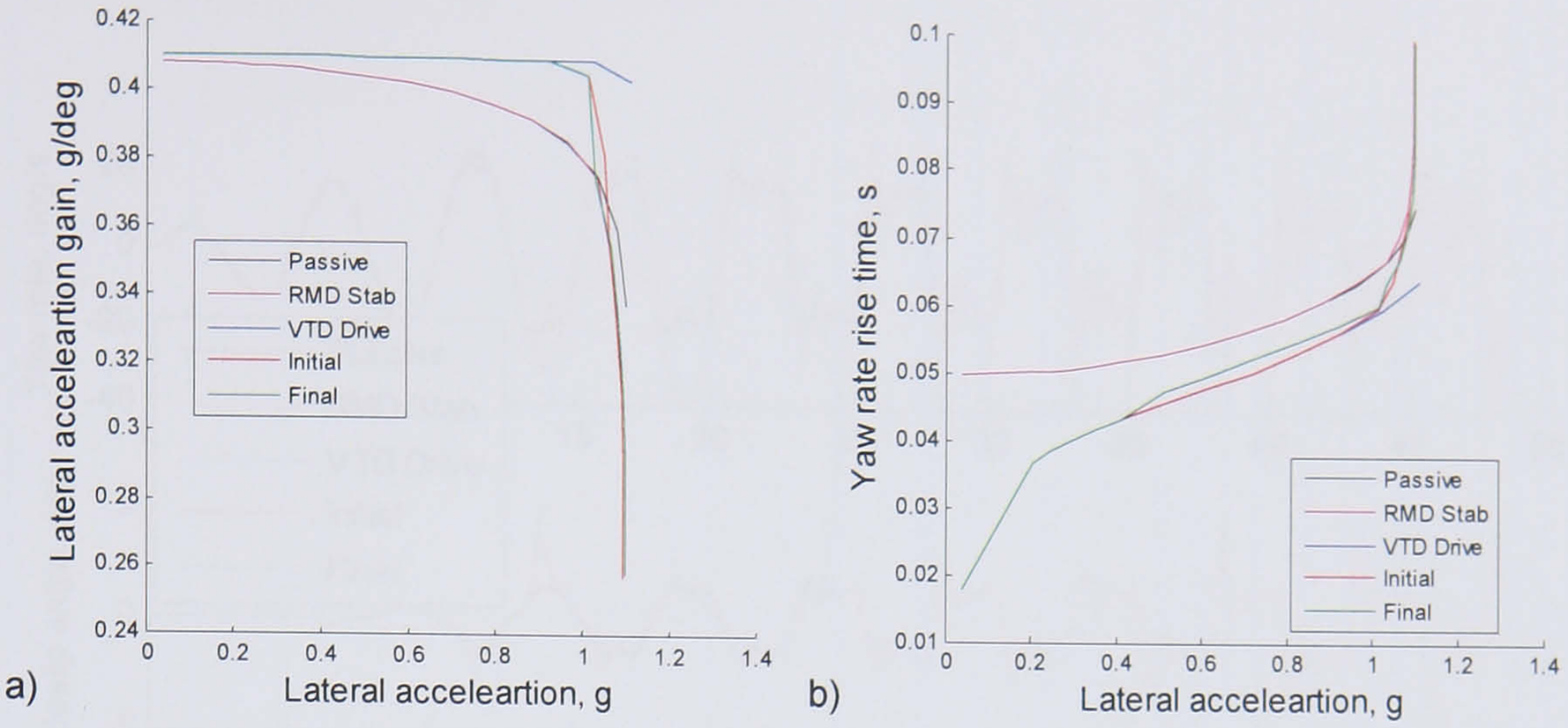

Figure 7.18 Lateral acceleration gain and yaw rate rise time of the integrated controllers during step steer manoeuvres

Both integration strategies show a similar response to each other. They both linearise the lateral acceleration gain very well up to the stability limits. Just after 0.9g the driveability control is phased out and the stability control takes precedence around 1g. The effect is the lateral acceleration gain drops off from its linear trend. Initially they drop off slowly but as the stability control activates they follow the independent stability control. The revised initial integrated strategy shows a slightly slower drop-off in lateral acceleration gain as the stability control activates. This is due to the yaw rate tracking control being active longer as it is phased out. Although it may appear to be advantageous in these results, it promoted vehicle instability as shown in the previous tests.

The yaw rate rise time shows a very similar response. The independent driveability controller has the quickest rise time throughout the simulations but the integrated controllers follow it well until the stability limit is reached. Once more, as the vehicle approaches the stability limit, the integrated controller phases out the yaw rate tracking control and the stability control activates, increasing the rise time.

The final test manoeuvre is the increasing velocity, increasing sinusoidal steer test run on a low friction surface. The manoeuvre is run on a low friction surface to test the robustness of the control strategies. The friction coefficient is set to 0.7 to simulate a wet road surface. The results are presented in Figure 7.19. Again the yaw rate, sideslip angle and the control inputs are shown with the reference yaw rate in grey. The test is run with the same velocity and steer angle profile as the test presented earlier in this section.

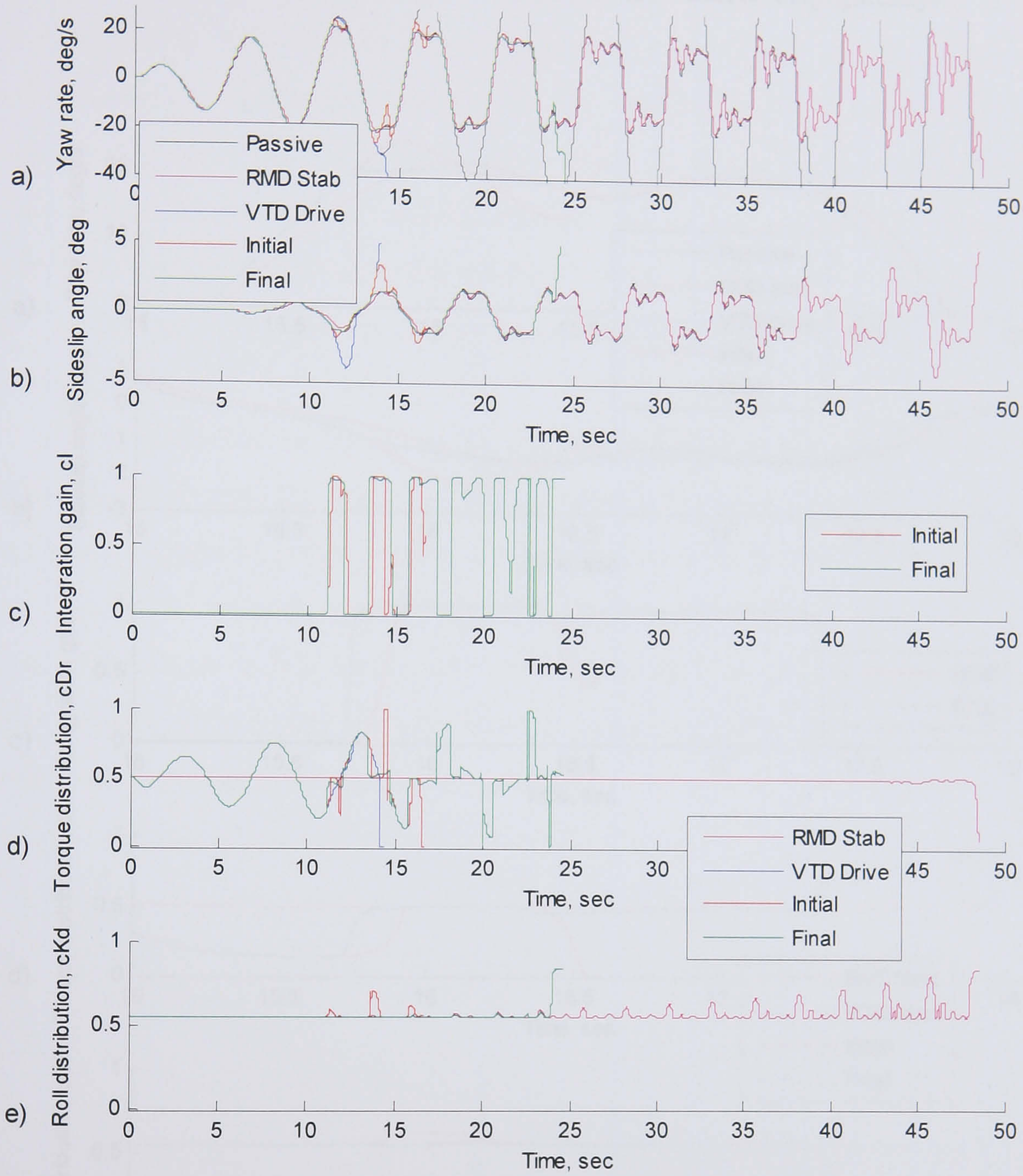

Figure 7.19 Sinusoidal time response of the integrated control on a low friction road surface

The independent stability control manages to stabilise the vehicle the longest, lasting 48 seconds. Although the vehicle does not completely lose stability before 48 seconds, the response becomes increasingly oscillatory. As expected the independent driveability control is very quick to lose stability and does so after 14 seconds. Again, the controller pushes the vehicle to match the linear yaw rate, which is determined by a reference model that is not adapted to the low friction road surface. Therefore the controller still aims to match the same yaw rate that the vehicle would obtain on a

high friction surface. Although this will give the driver the same linear response regardless of the road conditions, it destabilises the vehicle very quickly.

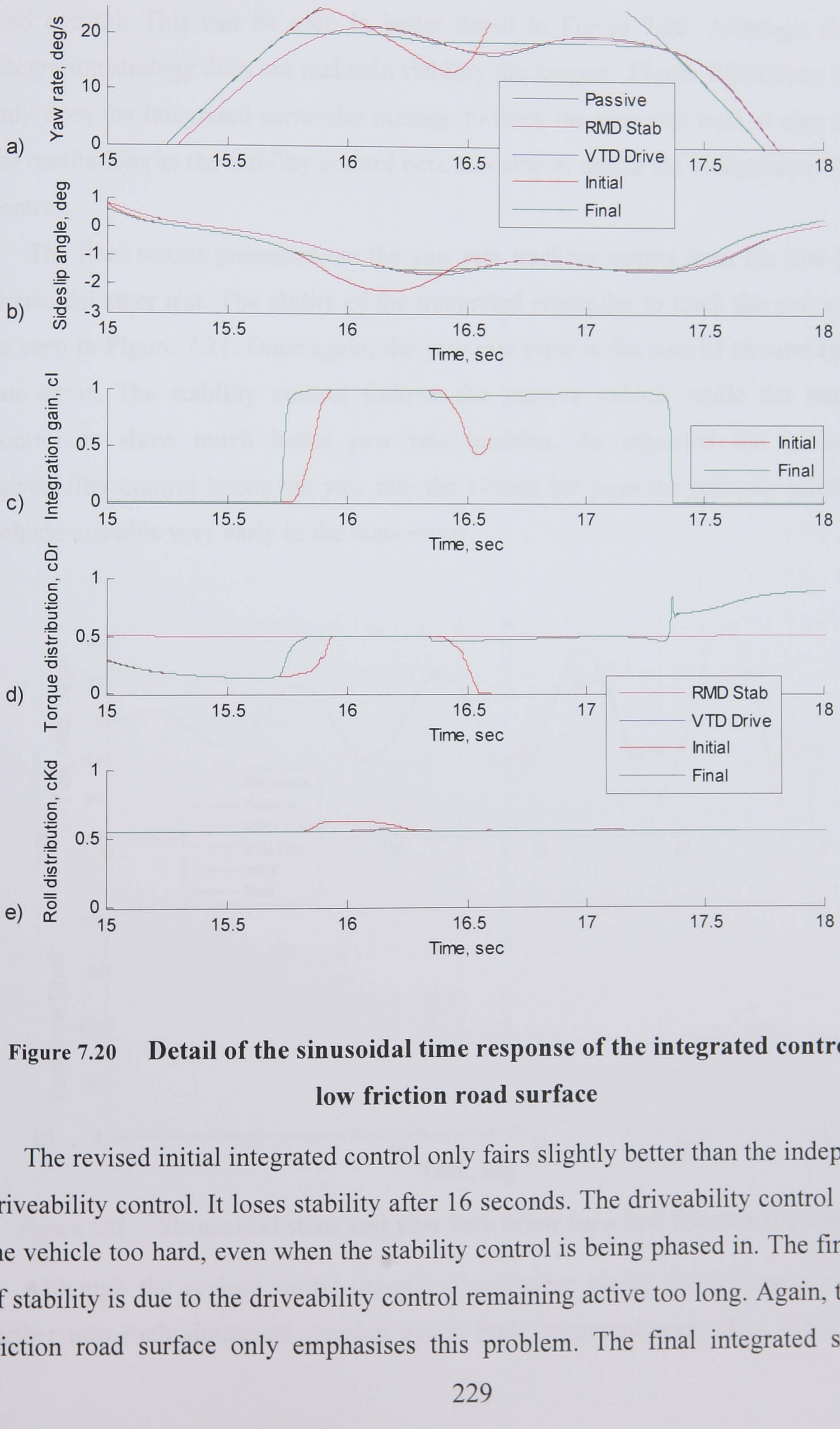

Figure 7.20 Detail of the sinusoidal time response of the integrated control on a low friction road surface

The revised initial integrated control only fairs slightly better than the independent driveability control. It loses stability after 16 seconds. The driveability control pushes the vehicle too hard, even when the stability control is being phased in. The final loss of stability is due to the driveability control remaining active too long. Again, the low friction road surface only emphasises this problem. The final integrated strategy

performs well, managing to maintain vehicle stability until almost 25 seconds. It also achieves this while keeping the yaw rate and sideslip angle oscillations small, unlike the independent stability controller. This is once again due to the driveability control being phased out before the stability limits are reached and the additional VTD wheel load control. This can be seen in better detail in Figure 7.20. Although the final integration strategy does not maintain stability the longest, Figure 7.20 shows that not only does the integrated controller manage to track the yaw rate well, it also reduces the oscillations as the stability control becomes active, unlike the independent stability control.

The final results presented are the yaw rate tracking results from the low friction sinusoidal steer test. The ability of the integrated controller to track the yaw rate can be seen in Figure 7.21. Once again, the yaw rate error is the sum of the absolute yaw rate error. The stability control follows the passive vehicle while the integrated controllers show much better yaw rate tracking. As expected the independent driveability control tracks the yaw rate the closest but pays the price by sending the vehicle unstable very early in the manoeuvre.

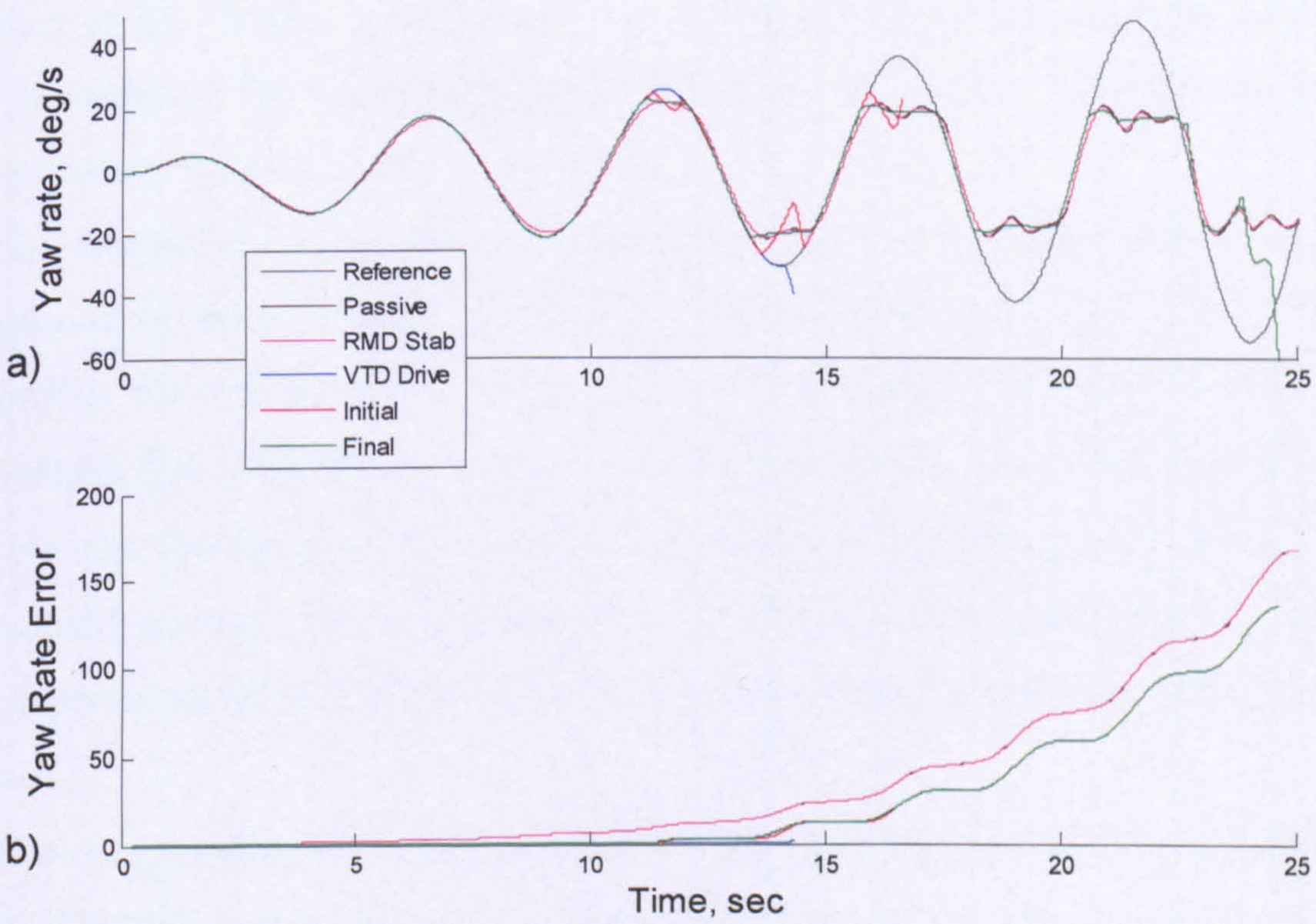

Figure 7.21 Sinusoidal steer test yaw rate error on a low friction road surface

Although the revised initial integrated controller tracks the reference yaw rate further into each sinusoidal steering cycle, both integrated controllers show almost

equal absolute yaw rate error. This is due to the stability control overcompensating in the revised initial integrated control strategy and reducing the yaw rate dramatically. The final integrated strategy removes these oscillations by intervening with the stability control slightly earlier and producing much smoother results. This smoother control action is particularly beneficial on the low friction surface. Figure 7.21.a also shows how far the vehicle behaviour diverges from the reference behaviour indicating that the manoeuvre has become very severe and highly non-linear.

7.4. Integration Strategy Conclusions

The integration strategy has to manage two conflicting control objectives. The first objective is to maintain the vehicle stability and the second objective is to track the reference yaw rate. These two objectives work against each other since stabilising the vehicle by reducing the sideslip behaviour also reduces the yaw rate while tracking the yaw rate increases the sideslip angle. Therefore the basic integration strategy has to be a switching control that determines when each objective should have priority. This prevents both controllers from operating at the same time which not only prevents negative interactions but also conserves energy. As the vehicle operates at low lateral accelerations, the yaw rate tracking driveability control can have precedence. However, as the severity of the manoeuvre increases the stability control needs to take priority.

The integrated control needs to determine where the vehicle state lies and give precedence to the appropriate controller. The phase plane stability control already determines the stability limit of the vehicle and defines a "deadzone" where it does not operate. The integration strategy uses the same method to integrate the controllers. This ensures that the stability control still operates without being compromised by the driveability control. The integration strategy uses the same phase plane boundary to progressively deactivate the driveability control before the stability control becomes active.

The integrated control also takes advantage of the inactive VTD controller while the RMD stability control operates. One of the causes of the loss of vehicle stability is the saturation of the rear inside tyre. It was found that the torque required to maintain the velocity profile would saturate the unloaded inside tyre. Since the yaw rate tracking control is phased out as the vehicle approaches the stability limit, it is

available to help stabilise the vehicle. As the vehicle state progresses beyond the stable limit the torque is distributed in proportion to the vertical tyre forces. This sends more torque to the loaded, outside tyre and helps delay the saturation of the unloaded, inside tyre.

The integrated controller is effective at improving the vehicle performance. It improves the yaw rate tracking up to the vehicle stability limits and then stabilises the vehicle beyond them. The increasing velocity step steer test highlighted this. Initially the vehicle tracks the linear reference yaw rate and gives the driver a predictable linear response to the steering inputs. As the vehicle reaches the stability limits, the yaw rate tracking controller is phased out and the stability control takes precedence. The stability of the vehicle is maintained beyond the passive vehicle and even longer than the vehicle with independent stability control. The integrated control also manages to maintain a smooth response without oscillations in the vehicle behaviour.

The increasing velocity, increasing sinusoidal steer test also showed a good response from the integrated controller. Once again it showed good yaw rate tracking up to the vehicle stability limits. As the vehicle approached the stability limits the yaw rate tracking control gave way to the stability control, which stabilised the vehicle. The transition of the control authority and the performance of the stability control managed to prevent oscillations in the vehicle behaviour. This smoother vehicle response is desirable for a driver. However, the integrated control did not perform flawlessly. In the sinusoidal steer tests the passive vehicle maintained stability longer. This is due to the increasing torque demand that saturates the inside rear tyre. The integrated control also performed worse than the stability control due to the increased yaw rates that the driveability control created and the addition of the VTD wheel load control.

8. Conclusions

Chapter 8 presents the final conclusions of this research and concludes with recommendations for areas of future research.

8.1. Introduction

Advanced chassis control systems are becoming a feature on modern vehicles. The critical literature review highlighted the need for integration strategies of advanced vehicle controls. Some research has been carried out in this field to integrate passenger vehicle safety systems. However, many control strategies only considered the stability of the vehicle without concern for the driving dynamics and only a few were oriented towards a high performance racing environment. One of the most prevalent stability control systems is the brake based dynamic yaw control. Although it manages to maintain vehicle stability well, it has the undesirable effect of intervening in the longitudinal dynamics, slowing down the vehicle during activation. This research aims to provide an integrated control strategy that enhances the driveability of the vehicle while ensuring the stability.

To enhance the vehicle dynamics without interfering with the driver's demands, roll moment distribution and variable torque distribution are chosen. Roll moment distribution becomes more effective as the severity of the manoeuvre increases and the lateral load transfer increases making it ideal for a stability control. Variable torque distribution allows the torque demand from the driver to be used as efficiently as possible. Both these control systems allow improvement in the vehicle dynamics without interfering with the driver's demands. Active steering can provide improved vehicle performance but as the vehicle approaches the limits of handling, it loses its effectiveness. As previously mentioned, brake based systems are very effective at stabilising the vehicle but have a negative impact on the longitudinal dynamics.

8.2. Control Strategy

The aim of improving the driveability of the vehicle is to linearise the yaw rate response to the drivers steering input. A linear response is predictable and therefore

reduces the driver's workload. The independent driveability controllers are all linear reference yaw rate tracking controllers. Tracking a linear reference yaw rate will provide a linear yaw rate response to the steering input. The stability of the vehicle is measured by the sideslip response. A vehicle with a small sideslip angle will have smaller tyre slip angles. This will ensure that the tyres are not close to their saturation limit and leaves potential in the tyres to create lateral forces in response to driver steering inputs. The best independent stability controllers used a sideslip angle phase plane to bound the sideslip response of the vehicle and maintain stability.

8.2.1. Independent Control

Many control algorithms were developed for independent controllers using both roll moment distribution and variable torque distribution. These independent controllers were yaw rate tracking driveability controls and also sideslip angle reducing stability controls. The best driveability controller was the variable torque distribution, yaw rate tracking, sliding mode control. It managed to provide the best yaw rate tracking with a smooth, stable vehicle response. The other control algorithms managed to provide a very similar response. They each gave very similar control demands but used different algorithms to calculate them.

The best stability control was the roll moment distribution, sideslip angle, phase plane control. The reference sideslip angle tracking control was not effective during severe manoeuvres due to the increasing reference sideslip angle. Other control algorithms that would require a reference behaviour, like internal model control or sliding mode control, would also have similar failings. The phase plane approach directly limits the sideslip behaviour, which is the goal of the stability control, and roll moment distribution is ideally suited to the task of stability control due its improved performance with increasing lateral acceleration and its unobtrusive control action.

When these two independent controllers were simply combined conflicting interactions occurred. The two controllers operate at the same time trying to achieve different goals. The driveability control increases the yaw rate, which also increases the sideslip while the stability control aims to reduce the sideslip which also reduces the yaw rate. In addition to these negative interactions the behaviour showed large oscillations and did not provide a smooth vehicle response.

8.2.2. Integrated Control

A key deliverable from this research is the multi-objective integration strategy, combining variable torque distribution and roll moment distribution to improve the vehicle performance while maintaining stability and minimising interactions with the longitudinal dynamics. The integration strategy was created from the combined control results to minimise the negative interactions of the two controllers. The first task was to ensure that the controllers did not operate at the same time while pursuing conflicting goals. The basic integration strategy had to be a switching control. Once the phase plane control was chosen as the stability control, the integration strategy was a logical continuation. Since the stability control already determines when the vehicle reaches the stability limits, it is only natural to use the same criteria to determine the precedence of each control strategy. The switching strategy allows the driveability control to track the reference yaw rate until the stability limits of the vehicle are reached. As the vehicle state approaches the stability limits, the driveability control is phased out and the stability control takes precedence. In addition to this, the variable torque distribution is used to augment the stability control. One of the causes of instability was saturation of the longitudinal tyre dynamics on the unloaded rear wheel. So once the stability limit is reached, the variable torque distribution distributes the torque in proportion to the vertical tyre forces to delay the saturation of the unloaded inside tyre.

The integration strategy works well, especially in the step steer tests. The vehicle tracks the yaw rate until the stability limits are approached. Then the driveability controller is phased out and the stability controller becomes active. The sideslip behaviour of the vehicle is contained and the vehicle is stabilised. The response to the increasing sinusoidal steer test is not quite as good but still shows improved performance. The controller tracks the yaw rate well and also manages to maintain the vehicle stability. The vehicle behaviour is stabilised and the controller provides a smooth vehicle response.

8.3. Future Research

The obvious continuation of this research is to eventually implement the control strategy in a real vehicle. The first step would be to model the control actuators and hardware. This would determine the limits imposed on the control systems and could

require further control tuning to compensate for the actuator dynamics. After modelling the hardware and ensuring the controllers are properly calibrated and tuned, hardware in the loop testing could be carried out to verify the results. The final step would be to implement the complete vehicle control strategy on an actual test vehicle.

There are also opportunities for extending this research in the future. This research focused on roll moment distribution and variable torque distribution. There is scope to integrate other control systems into the complete vehicle control strategy.

8.3.1. Integration strategies

The integration of independent vehicle controllers can be spilt into two separate tasks. The integration of controllers with different goals and the integration of controllers with the same goal. This research focused on the integration independent controllers with different goals. This allowed a complete vehicle control strategy to be created that could improve the vehicle performance over the entire range of vehicle dynamics. In this case the integration will take the form of a switching strategy to give precedence to either control goal. The switching criteria will generally follow from the stability control. On the other hand, the integration of control strategies that work towards the same goal provides opportunities for optimisation. For example, multiple controllers could be optimised to provide the control demand while minimising the actuation energy.

8.3.2. Yaw Rate Tracking in the Integrated Strategy

The yaw rate tracking of the controllers presented is at the limit of what the vehicle is capable of achieving. The use of different control algorithms will probably not make a significant difference. However, there is potential to use different control systems to achieve the same yaw rate tracking goal. An active steering system could be implemented to track the yaw rate. Active steering is effective at the lower lateral accelerations where the yaw rate tracking control takes precedence. Although it is doubtful that an active steering system could achieve better yaw rate tracking than that already achieved, it would give an extra option to the design engineer and would give opportunities for optimisation. An integrated control could be developed which minimised the actuation energy required to meet the yaw rate tracking goal by using both active steering and active torque control. The use of a brake based system would

not be very effective since it would have a negative impact on the longitudinal dynamics of the vehicle.

8.3.3. Sideslip Angle Reduction in the Integrated Strategy

Stability control can always be improved to maintain vehicle stability at more extreme manoeuvres. In this research, roll moment distribution provided a very good stability control. This was augmented by variable torque distribution. But again, like the yaw rate tracking task, additional control systems could be incorporated to give the design engineer more options for an integration strategy. One of the goals in this research was to track the desired velocity. This was one of the main causes of instability due to the torque demand at the rear wheels saturating the tyres. If this requirement to track the vehicle velocity was relaxed, a brake based system could provide additional control power to stabilise the vehicle. Brake based systems could also be effective during decelerating manoeuvres when the brakes are applied. However, active steering would not provide an effective stability control due to its inability to create yaw moments at high lateral accelerations.

References

Abe, M. (1987). "Effects of Traction Force Distribution Control with Additional Rear Wheel Steer on Turning Behavior of 4WD Vehicle." Vehicle System Dynamics 17(Suppl): pp 1-12.

Abe, M. (1992). Roll Moment Distribution Control in Active Suspension for Improvement of Limit Performance of Vehicle Handling. AVEC 1992.

Abe, M. (1998). Vehicle Dynamics and Control for Improving Handling and Active Safety: From 4WS to DYC. Kanagawa Institute of Technology, Department of Mechanical System Engineering.

Abe, M., Y. Kano, et al. (1999). "Improvement of Vehicle Handling Safety with Vehicle Side-Slip Control by Direct Yaw Moment." Vehicle System Dynamics 33(Suppl): pp 665-679.

Abe, M., N. Ohkubo, et al. (1996). "A Direct Yaw Moment Control for Improving Limit Performance of Vehicle Handling - Comparison and Cooperation with 4WS." Vehicle System Dynamics 25(Suppl): pp 3-23.

Cech, I. (2000). "Anti-Roll and Active Roll Suspensions." Vehicle System Dynamics 33: pp 91-106.

Chen, B. and H. Peng (2002). Design of Vehicle Dynamics Control with Rollover Prevention via UMTRI Preview Driver Model. AVEC 2002, 6th Int'l Symposium on Advanced Vehicle Control, Hiroshima, Japan.

Constantine, C. J. and E. H. Law (1994). "The Effects of Roll Control for Passenger Cars During Emergency Maneuvers." SAE Technical Paper Series(940224): pp 31-51.

Cooper, N., W. Manning, et al. (2005). Integration of Active Suspension and Active Driveline to Ensure Stability While Improving Vehicle Dynamics. SAE 2005 World Congress, Detroit, Michigan.

Crolla, D. A. (1991). An Introduction to Vehicle Dynamics. Leeds, Vehicle Dynamics Group Universtiy of Leeds.

Doniselli, C., G. Mastinu, et al. (1994). "Traction Control for Front Wheel Drive Vehicles." Vehicle System Dynamics 23(Suppl): pp 87-104.

Elbeheiry, E. M., Y. F. Zedyada, et al. (2001). "Handling Capabilities of Vehicles in Emergencies Using Coordinated AFS and ARMC Systems." Vehicle System Dynamics 35(3): pp 195-215.

Esmailzadeh, E., G. R. Vossoughi, et al. (2001). "Dynamic Modeling and Analysis of a Four Motorized Wheels Electric Vehicle." Vehicle System Dynamics 35(3): pp 163-194.

Everett, N. R. (2001). Integrated Vehicle Chassis Control. Leeds, PhD Thesis University of Leeds.

Everett, N. R., M. D. Brown, et al. (2000 a). "Investigation of a Roll Control System for an Off-Road Vehicle." SAE Technical Paper Series(2000-01-1646).

Everett, N. R., M. D. Brown, et al. (2000 b). Investigation of the Integration of a Roll Control System and a Traction Force Distribution System for an Off-Road Vehicle. AVEC 2000, 5th Int'l Symposium on Advanced Vehicle Control, Ann Arbor, Michigan.

Ghoneim, Y. A., W. C. Lin, et al. (2000). "Integrated Chassis Control System to Enhance Vehicle Stability." International Journal of Vehicle Design 23(1-2): pp 124-144.

Hac, A. and M. O. Bodie (2002). "Improvements in Vehicle Handling Through Integrated Control of Chassis Systems." International Journal of Vehicle Design 29(1-2): pp 23-50.

He, J. (2005). Integrated vehicle dynamics control using active steering, driveline and braking. Leeds, PhD Thesis University of Leeds.

He, J., D. A. Crolla, et al. (2004). "Integrated Active Steering and Variable Torque Distribution Control for Improving Vehicle Handling and Stability." SAE Technical Paper Series(2004-01-1071).

Heydinger, G. J., W. R. Garrot, et al. (1991). "The Importance of Tire Lag on Simulated Transient Vehicle Response." SAE Technical Paper Series(910235).

Horiuchi, S., K. Okada, et al. (1998). Integrated Control of Four Wheel Steering and Wheel Torques Using Nonlinear Predictive Controller. AVEC 1998.

Horiuchi, S., K. Okada, et al. (1999). "Effects of Integrated Control of Active Four Wheel Steering and Individual Wheel Torque on Vehicle Handling and Stability -A Comparison of Alternative Strategies." Vehicle System Dynamics 33(Suppl): pp 680-691.

Hou, Y., Y. Hu, et al. (2001). "A Study of Tire Lag Property." SAE Technical Paper Series(2001-01-0751).

Hutchkoetter, H. and T. Gassman (2004). "Vehicle Dynamics and Torque Management Devices." SAE Technical Paper Series(2004-01-1058).

Hwang, S. M. and Y. Park (1995). "Active Roll Moment Distribution Based on Predictive Control." International Journal of Vehicle Design 16(1): pp 15-28.

Ikushima, Y. and K. Sawase (1995). "A Study on the Effects of the Active Yaw Moment Control." SAE Technical Paper Series(950303).

Jung, H., B. Kwak, et al. (2000 a). Improved Directional Stability in Traction Control System. AVEC 2000, 5th Int'l Symposium on Advanced Vehicle Control, Ann Arbor, Michigan.

Jung, H., B. Kwak, et al. (2000 b). Development of Traction Control System. FISITA 2000, World Automotive Congress, Seoul, Korea.

Kaelani, Y., N. Sutantura, et al. (2002). Integrated Traction Control with Implementation of Fuzzy Logic Controller. AVEC 2002, 6th Int'l Symposium on Advanced Vehicle Control, Hiroshima, Japan.

Kahrs, J. J. and E. H. Law (1995). "An Investigation of the Effects of Roll Control on Handling and Stability of Passenger Vehicles During Severe Lane Change Maneuvers." SAE Technical Paper Series(950305).

Kin, K., H. Kiryu, et al. (2002). Enhanced Vehicle Stability and Steerability with VSA. AVEC 2002, 6th Int'l Symposium on Advanced Vehicle Control, Hiroshima, Japan.

Kitajima, K. and H. Peng (2000). H Infinity Control fro Integrated Side-Slip, Roll, and Yaw Controls for Ground Vehicles. AVEC 2000, 5th Int'l Symposium on Advanced Vehicle Control, Ann Arbor, Michigan.

Kuriki, N. and Y. Shibahata (1998). Development of Active Torque Transfer System. FISITA 1998, World Automotive Congress, Paris, France.

Kwak, B. and Y. Park (2000 a). Robust Vehicle Stability Controller by Multiple Sliding Mode Control. AVEC 2000, 5th Int'l Symposium on Advanced Vehicle Control, Ann Arbor, Michigan.

Kwak, B., Y. Park, et al. (2000 b). Design of Observer for Vehicle Stability Control System. FISITA 2000, World Automotive Congress, Seoul, Korea.

Lang, R. and U. Walz (1991). Active Roll Reduction. EAEC 3rd Int'l Conference on Vehicle Dynamics and Power Train Engineering, Strasbourg.

Liu, C., V. Monkaba, et al. (2002). "Driveline Torque-Bias-Management Modeling for Vehicle Stability Control." SAE Technical Paper Series(2002-01-1584).

Lugner, P., H. Lanzer, et al. (1987). "4 Wheel Drive with Visco Coupling Elements." Vehicle System Dynamics 17(Suppl): pp 239-251.

Lyon, K., M. Philipp, et al. (1994). "Traction Control for a Formula 1 Race Car: Conceptual Design, Algorithm Development, and Calibration Methodology." SAE Technical Paper Series(942475).

Mastinu, G. (1995). "Integrated Controls and Interactive Multi-Objective Programming for the Improvement of Ride and Handling of Road Vehicles." Smart Vehicles: pp 219-251.

Matsuno, K., R. Nitta, et al. (2000). Development of a New All-Wheel Drive Control System. FISITA 2000, World Automotive Congress, Seoul, Korea.

Milliken, W. F. and D. L. Milliken (1995). Race Car Vehicle Dynamics. Warrendale, PA, Society of Automotive Engineers.

Mokhiamar, O. and M. Abe (2002). "Combined Lateral Force and Yaw Moment Control to Maximize Stability as well as Vehicle Responsiveness During Evasive Maneuvering for Active Vehicle Handling Safety." Vehicle System Dynamics 37(Suppl): pp 246-256.

Motoyama, S., H. Uki, et al. (1993). "Effect of Traction Force Distribution Control on Vehicle Dynamics." Vehicle System Dynamics 22: pp 455-464.

Ono, E., Y. Hattori, et al. (2006). "Vehicle Dynamics Integrated Control for Four-Wheel-Distributed Steering and Four-Wheel-Distributed Traction/Braking Systems." Vehicle System Dynamics 44(2): pp 139-151.

Ottgen, O. and T. Bertram (2002). Influencing Vehicle Handling Through Active Roll Moment Distribution. AVEC 2002, 6th Int'l Symposium on Advanced Vehicle Control, Hiroshima, Japan.

Pacejka, H. B. and I. J. M. Besselink (1997). "Magic Formula Tyre Model with Transient Properties." Vehicle System Dynamics 27(Suppl): pp 234-249.

Park, J. and J. Kroppe (2004). "Dana Torque Vectoring Differential Dynamic Trak." SAE Technical Paper Series(2004-01-2053).

Park, J. H. and C. Y. Kim (1999). "Wheel Slip Control in Traction Control System for Vehicle Stability." Vehicle System Dynamics 31: pp 263-278.

Park, K. and S. Heo (2000). Design of a Control Logic for Improving Vehicle Dynamic Stability. AVEC 2000, 5th Int'l Symposium on Advanced Vehicle Control, Ann Arbor, Michigan.

Rivals, I. and L. Personnaz (1996). Internal Model Control Using Neural Networks. ISIE 1996., Proceedings of the IEEE International Symposium on Industrial Electronics, Warsaw, Poland.

Sakai, S. and Y. Hori (2000). Advanced Vehicle Motion Control of Electric Vehicle Based on the Fast Motor Torque Response. AVEC 2000, 5th Int'l Symposium on Advanced Vehicle Control, Ann Arbor, Michigan.

Samsundar, J. and J. C. Huston (1999). "Lateral Stability Analysis of a 2 Degree-of-Freedom Vehicle Using a Time Lagged Lateral Tire Force Model." SAE Technical Paper Series(1999-01-0791).

Schwarzenbach, J. and K. F. Gill (1992). System Modelling and Control. London, Edward Arnold.

Sharp, R. S., D. Casanova, et al. (2000). "A Mathematical Model for Driver Steering Control, with Design, Tuning and Performance Results." Vehicle System Dynamics 33: pp 289-326.

Sharp, R. S. and D. Pan (1992). "On Active Roll Control for Automobiles." Vehicle System Dynamics 20: pp 566-583.

Shibahata, Y., K. Shimada, et al. (1993). "Improvement of Vehicle Maneuverability by Direct Yaw Moment Control." Vehicle System Dynamics 22: pp 465-481.

Shino, M., P. Raksincharoensak, et al. (2002). Vehicle Handling and Stability Control by Integrated Control of Direct Yaw Moment and Active Steering. AVEC 2002, 6th Int'l Symposium on Advanced Vehicle Control, Hiroshima, Japan.

Shino, M., Y. Wang, et al. (2000). Motion Control of Electric Vehicles Considering Vehicle Stability. AVEC 2000, 5th Int'l Symposium on Advanced Vehicle Control, Ann Arbor, Michigan.

Siegler, B. (2002). Lap Time Simulation for Racing Car Design. Leeds, PhD Thesis University of Leeds.

Smakman, H. (2000 a). Functional Integration of Slip Control with Active Suspension for Improved Lateral Vehicle Dynamics. Munich, Herbert Utz Verlag.

Smakman, H. (2000 b). Functional Integration of Active Suspension with Slip Control for Improved Lateral Vehicle Dynamics. AVEC 2000, 5th Int'l Symposium on Advanced Vehicle Control, Ann Arbor, Michigan.

Tahami, F., S. Farhangi, et al. (2004). "A Fuzzy Logic Direct Yaw-Moment Control System for All-Wheel Drive Electric Vehicles." Vehicle System Dynamics 41(3): pp 203-221.

Tobata, H., K. Fukuyama, et al. (1993). "Advanced Control Methods of Active Suspension." Vehicle System Dynamics 22: pp 347-358.

Van Zanten, A., R. Erhardt, et al. (1996). Control Aspects of the Bosch-VDC. AVEC 1996, International Symposium on Advanced Vehicle Control, Aachen University, Germany.

Wheals, J. C., H. Baker, et al. (2004). "Torque Vectoring AWD Driveline: Design, Simulation, Capabilities and Control." SAE Technical Paper Series(2004-01-0863).

Williams, D. E. and W. M. Haddad (1995). "Nonlinear Control of Roll Moment Distribution to Influence Vehicle Yaw Characteristics." IEEE Transactions on Control Systems Technology 3(1): pp 110-116.

Appendix A

Vehicle Parameters

[Siegler, 2002]

mf = 20.4	front unsprung mass (kg)
mr = 20.4	rear unsprung mass (kg)
mb = 262.9	sprung body mass (kg)
Izz = 200	yaw moment of inertia (kgm^2)
Ixx = 35	roll moment of inertia (kgm^2)
Ixz = 0	coupled roll and yaw moment of inertia (kgm^2)
a = 0.98	length from centre of gravity to front axle (m)
b = 0.82	length from centre of gravity to rear axle (m)
tf = 1.15/2	length of half front trackwidth (m)
tr = 1.10/2	length of half rear trackwidth (m)
h = 0.2974	distance from roll axis to centre of gravity (m)
hcf = 0.025	height of front roll centre (m)
hcr = 0.050	height of rear roll centre (m)
ha = 0.0386	height of reference roll axis (m)
Kphi = 36444	roll stiffness (Nm/rad)
KspringfI = 61.25	front spring stiffness (kN/m)
KspringrI = 70.0	rear spring stiffness (kN/m)
IRf = 0.68	front installation ratio
IRr = 0.68	rear installation ratio
Ptyre = 0.827	tyre pressure above atm (bar)
antirollf = 5000	front antiroll bar roll rate (Nm/rad)
antirollr = 0	rear antiroll bar roll rate (Nm/rad)
Dphi = 1170	roll damping (Nsm/rad)
rw = 0.232	wheel radius (m)
Iw = 0.21	wheel inertia (kgm^2)
Teng = 1800	max available engine torque at wheels (Nm)

Tbrake = 180	max available individual wheel brake torque (Nm)
frontArea = 0.8	frontal area (m^2)
coeffDrag = 1.05	aerodynamic coefficient of drag
rho = 1.22	air density (kg/m^3)

longF_lag = 0.001	longitudinal tyre lag time constant
longF_gain = 1.0	longitudinal tyre lag gain
latF_lag = 0.0163 * exp(-0.0253 * uInput)	lateral tyre lag time constant
latF_gain = 0.75	lateral tyre lag gain

Ktyre = ((50 * Ptyre) + 140) * 1000	tyre rate (N/m)
toeAngle = -0.2775	toe angle offset for tyres

cdm = 0.0	centre diff distribution, 1 is all front distribution
cdf = 0.5	front diff distribution, 1 is all right distribution
cdr = 0.5	rear diff distribution, 1 is all right distribution
cKd = Kphif / (Kphif + Kphir)	0.5438, static roll moment distribution

CfRef = 53000	reference model front cornering stiffness (N/rad)
CrRef = 59500	reference model rear cornering stiffness (N/rad)

Appendix B

Pacejka Tyre Model Parameters

[Siegler, 2002]

Ro = 0.232;

FzoLat = 1445;

FzoLong = 4361;

LMUx = 1.25;

LMUy = 0.5385;

Pcx1 = 1.6116;

Pdx1 = 1.1005;

Pdx2 = -0.0141;

Pex1 = 0.02261;

Pex2 = 0.16482;

Pex3 = 0.21884;

Pex4 = 0;

Pkx1 = 18.385;

Pkx2 = 1.5051;

Pkx3 = 0.29119;

Phx1 = -0.000551;

Phx2 = 0.0001;

Pvx1 = 0;

Pvx2 = 0;

rbx1 = 10.395;

rbx2 = -6.3236;

rcx1 = 0.99326;

rhx1 = -0.0029427;

qsx1 = 0;

qsx2 = 0;

qsx3 = 0;

Pcy1 = 1.676;

Pdy1 = -2.587;

Pdy2 = 0.59325;

Pdy3 = -3.8474;

Pey1 = -0.14887;

Pey2 = 0.56009;

Pey3 = 0.023786;

Pey4 = 4.1175;

Pky1 = -34.238;

Pky2 = 1.0867;

Pky3 = 0.73877;

Phy1 = 0.0058088;

Phy2 = -0.0007589;

Phy3 = 0.10852;

Pvy1 = 0.041154;

Pvy2 = -0.055694;

Pvy3 = -0.72216;

Pvy4 = 0.24275;

rby1 = 6.1187;

rby2 = 2.8069;

rby3 = -0.0091738;

rcy1 = 1.004;

rhy1 = -0.035516;

rvy1 = 0.046621;

rvy2 = 0.048196;

rvy3 = 0.54064;

rvy4 = 11.444;

rvy5 = 1.9;

rvy6 = -10.734;

qbz1 = 8.964;

qbz2 = -1.106;

qbz3 = -0.842;

qbz4 = -0.227;

qbz5 = 0;

qbz9 = 18.47;

qbz10 = 0;

qcz1 = 1.180;

qdz1 = 0.100;

qdz2 = -0.001;

qdz3 = 0.007;

qdz4 = 13.05;

qdz6 = -0.008;

qdz7 = 0.000;

qdz8 = -0.296;

qdz9 = -0.009;

qez1 = -1.609;
qez2 = -0.359;
qez3 = 0;
qez4 = 0.174;
qez5 = -0.896;
qhz1 = 0.007;
qhz2 = -0.002;
qhz3 = 0.147;
qhz4 = 0.004;

Ssz1 = 0.043;
Ssz2 = 0.001;
Ssz3 = 0.731;
Ssz4 = -0.238;

qIay = 0.109;
qIaxz = 0.071;
qIby = 0.696;
qIbxz = 0.357;
qIc = 0.055;

qma = 0.237;
qmb = 0.763;
qmc = 0.108;

qcbx0z = 121.4;
qcby = 40.05;
qccx = 391.9;
qccy = 62.7;

qkbxz = 0.228;
qkby = 0.284;
qkcx = 0.910;
qkcy = 0.910;

qcbT0 = 61.96;
qcbGP = 20.33;
qccP = 55.82;
qkbT = 0.080;
qkbGP = 0.038;
qkcP = 0.834;
qFcx1 = 0.1;

qFcy1 = 0.3;
qFcx2 = 0;
qFcy2 = 0;

qV1 = 7.1e-5;
qV2 = 2.489;
qFz1 = 13.37;
qFz2 = 14.35;

qsy1 = 0.01;
qsy3 = 0;
qsy4 = 0;

qa1 = 0.135;
qa2 = 0.035;
qbvxz = 3.957;
qbvT = 3.957;

Breff = 9;
Dreff = 0.23;
Freff = 0.01;